Implications of Lateral Flow Generation on Land-Surface Scheme Fluxes

by

Kenneth R. Snelgrove

A thesis
presented to the University of Waterloo
in fulfilment of the
thesis requirement for the degree of
Doctor of Philosophy
in
Civil Engineering

Waterloo, Ontario, Canada, 2002

Author's Declaration for Electronic Submission of a Thesis

I hereby declare that I am the sole author of this thesis. This is a true copy of the thesis, including any required final revisions, as accepted by my examiners.

I understand that my thesis may be made electronically available to the public.

Abstract

This thesis details the development and calibration of a model created by coupling a land surface simulation model named CLASS with a hydrologic model named WATFLOOD. The resulting model, known as WatCLASS, is able to serve as a lower boundary for an atmospheric model. In addition, WatCLASS can act independently of an atmospheric model to simulate fluxes of energy and moisture from the land surface, including streamflow. These flux outputs are generated based on conservation equations for both heat and moisture ensuring result continuity. WatCLASS has been tested over both the data rich BOREAS domains at fine scales and the large but data poor domain of the Mackenzie River at a coarse scale. The results, while encouraging, point to errors in the model physics related primarily to soil moisture transport in partially frozen soils and permafrost. Now that a fully coupled model has been developed, there is a need for continued research by refining model processes and test WatCLASS's robustness using new datasets that are beginning to emerge.

Hydrologic models provide a mechanism for the improvement of atmospheric simulation though two important mechanisms. First, atmospheric inputs to the land surface, such as rainfall and temperature, are transformed by vegetation and soil systems into outputs of energy and mass. One of these mass outputs, which have been routinely measured with a high degree of accuracy, is streamflow. Through the use of hydrologic simulations, inputs from atmospheric models may be transformed to streamflow to assess reliability of precipitation and temperature. In this situation, hydrologic models act in an analogous way to a large rain gauge whose surface area is that of a watershed. WatCLASS has been shown to be able to fulfill this task by simulating streamflow from atmospheric forcing data over

multi-year simulation periods and the large domains necessary to allow integration with limited area atmospheric models.

A second, more important, role exists for hydrologic models within atmospheric simulations. The earth's surface acts as a boundary condition for the atmosphere. Besides the output of streamflow, which is not often considered in atmospheric modeling, the earth's surface also outputs fluxes of energy in the form of evaporation, known as latent heat and near surface heating, known as sensible heat. By simulating streamflow and hence soil moisture over the land surface, hydrologic models, when properly enabled with both energy and water balance capabilities, can influence the apportioning of the relative quantities of latent and sensible heat flux that are required by atmospheric models. WatCLASS has shown that by improving streamflow simulations, evaporation amounts are reduced by approximately 70% (1271mm to 740mm) during a three year simulation period in the BOREAS northern old black spruce site (NSA-OBS) as compared to the use of CLASS alone.

To create a model that can act both as a lower boundary for the atmosphere and a hydrologic model, two choices are available. This model can be constructed from scratch with all the caveats and problems associated with proving a new model and having it accepted by the atmospheric community. An alternate mechanism, more likely to be successfully implemented, was chosen for the development of WatCLASS. Here, two proven and well tested models, WATFLOOD and CLASS, were coupled in a phased integration strategy that allowed development to proceed on model components independently. The ultimate goal of this implementation strategy, a fully coupled atmospheric - land surface - hydrologic model, was developed for MC2-CLASS-WATFLOOD. Initial testing of this model, over the Saguenay region of Quebec, has yet to show that adding WATFLOOD to CLASS produces

significant impacts on atmospheric simulation. It is suspected, that this is due to the short term nature of the weather simulation that is dominated by initial conditions imposed on the atmospheric model during the data assimilation cycle.

To model the hydrologic system, using the domain of an atmospheric model, requires that methods be developed to characterize land surface forms that influence hydrologic response. Methods, such as GRU (Grouped Response Unit) developed for WATFLOOD, need to be extended to taken advantage of alternate data forms, such as soil and topography, in a way that allows parameters to be selected *a priori*. Use of GIS (Geographical Information System) and large data bases to assist in development of these relationships has been started here. Some success in creating DEMs (Digital Elevation Models) able to reproduce watershed areas, was achieved. These methods build on existing software implementations to include lake boundaries information as a topographic data source. Other data needs of hydrologic models will build on relationships between land cover, soil, and topography to assist in establishing grouping of these variables required to determine hydrologic similarity. This final aspect of the research is currently in its infancy but provides a platform from which to explore future initiatives.

Original contributions of this thesis are centered on the addition of a lateral flow generation mechanism within a land surface scheme. This addition has shown a positive impact on flux returns to the atmosphere when compared to measured values and also provide increased realism to the model since measured streamflow is reproduced. These contributions have been encapsulated into a computer model known as WatCLASS, which together with the implementation plan, as presented, should lead to future atmospheric simulation improvements.

Acknowledgements

I wish to express my sincere thanks to my supervisors Professor Ric Soulis and Professor Nick Kouwen. Together, you were able to coax me along to realize my goals and produce a body of work of which we can all be proud. While your methods of motivation were very different, the combination of resources and advice you collectively offered have been instrumental in the creation of this thesis and development of WatCLASS.

Many others have played a significant role in the development of WatCLASS. While my name appears on the cover of this thesis, it would not have been possible without the efforts for a number of colleagues. I would especially like to acknowledge the contributions of Ted Whidden, Frank Seglenieks, Clyde McLean and Karen Graham who were instrumental in the putting together the code for WatCLASS and helped build the immense databases required to operate the model. Others from the Hydrologic Modelling Group, including Steve Fassnacht, Todd Neff, Larry Hamlin (deceased), and Allyson Bingeman also provided enlightening ideas and encouragement over the years. I have also had the pleasure of the company of Bruce Davison and Erasmo Rodriguez who have shown great interest in WatCLASS.

I would also like to gratefully acknowledge the sources of funding I received in support of this research include the Government of Newfoundland and Labrador, Faculty of Engineering Graduate Scholarships, and the Ontario Graduate Scholarship for Science and Technology. For the majority of my funding, I would like to thank my supervisors Ric Soulis and Nick Kouwen who saw it fit to support me with their research grants from the Mackenzie GEWEX Study, the Canadian Climate Research Network and the Natural Science and Engineering Research Council of Canada.

Special thanks are also due to Professor Jay Doering, Civil Engineering Department Head and Professor Douglas Ruth, Dean of Engineering at the University of Manitoba for their patience and good-will while I completed the written portion of my degree requirements while on staff at the University of Manitoba.

Most of all, I wish to thank my wife, Lynette, for her love and support. She alone has had to bear to brunt of my mood swings during dead-end research initiatives and put up with the dark side of thesis preparation. I can only hope that there will be many happy years ahead for her and our two children, Stephen and Martha, now that my formal education is complete.

TABLE OF CONTENTS

LIST OF FIGURES

LIST OF TABLES

List of Acronyms

AGCM-III – 3rd Generation of **A**tmospheric Circulation Model
ANUDEM – **A**ustralian National University Digital Elevation Model
API – **A**ntecedent Precipitation Index
ARNO – Hydrologic Model Named for the **A**rno River Basin
ASA – **A**ggregated Simulation **A**reas
ASCII – **A**merican Standard Code for Information Interchange
BATS – Biosphere-**A**tmosphere Transfer Scheme
BC – British Columbia
BOREAS – Boreal Forest Ecosystem Study
CCC – Canadian Climate Centre
CCCma – Canadian Centre for Climate Modeling and **A**nalysis
CCRnet – Canadian Climate Research Network
CDED – Canadian Digital Elevation Data
CH – **C**lapp and Hornberger
CLASS – Canadian Land Surface Scheme
CMC – Canadian Meteorological Center
CRCM – Canadian Regional Climate Model
DEM – Digital Elevation Model
DHSVM – Distributed Hydrology Soil Vegetation Model
DV – Dependent Variable
ECHAM – European Centre – H**A**Mburg
ECMWF – European Centre for Medium Range Weather Forecasting
ENSIM – Environmental Simulation Program
EROS – Earth Resources Observation System
FC – Field Capacity
GCM – Global Circulation Model
GCM-II – Second Generation Climate Model
GEM – Global Environmental Multi-Scale Model
GEWEX – Global Water and Energy Experiment
GFDL – Geophysical Fluid Dynamics Laboratory
GISS – Goddard Institute for Space Studies
GLASS – Global Land-**A**tmosphere System Study
GLUE – Generalized Likelihood Uncertainty Estimation
GRU – Grouped Response Unit
HYDAT – Environment Canada's National Water Data **A**rchive
IAHS – International **A**ssociation of Hydrological Sciences
ID – Independent Variable
IPCC – Intergovernmental Panel on Climate Change
ISBA – Interactions between the Soil, the Biosphere, and the **A**tmosphere
LAI – Leaf **A**rea Index
LSS – Land Surface Schemes
LZS – Lower Zone Storage
MAGS – Mackenzie GEWEX Study

MAP – Meso-Scale **A**lpine Project
MC2 – Canadian Mesoscale Compressible Community Model
MHM – Macroscale Hydrological Model
MMR – Modular Multi-Spectrum Radiation
MODFLOW – Modular Three-Dimensional Finite-Difference Ground-Water Flow Model
MOSES – Met Office Surface Energy Scheme
MPI – Max Plank Institute
MRF – Medium Range Forecast
MSA – Modeling Sub-**A**rea
MSC – Meteorological Service of Canada
NCAR – National Center for **A**tmospheric Research
NCEP – National Centers for Environmental Prediction
NIR – Near Infrared Radiation
NSA – Northern Study **A**rea
NSA-FEN – Northern Fen site
NSA-OJB – Northern Old Jack Pine
NSA-OSB – Northern Old Black Spruce
NSA-YJP – Northern Young Jack Pine
NTDB – Canadian National Topographic Database
NWP – Numerical Weather Prediction
PCI – Geomatics Software Firm Based in Richmond Hill, Ontario
PET – Potential Evapotranspiration
PILPS –Project for Intercomparison of Land-Surface Parameterization Schemes
PLACE – Parameterization for Land-**A**tmosphere-Cloud Exchange
PUB – Prediction in Ungauged Basins
RCM – Regional Climate Model
RFE – Regional Finite Element
RMS – Root Mean Square
SERM – Saskatchewan Environment and Resource Management
SF – Scaling Factor
SiB – Simple Biosphere Model
SIR – Shuttle Imaging Radar
SLURP – Simple Lumped Reservoir Parametric Distributed Watershed Model
SPSS – Statistical Software Package
SSA – Southern Study **A**rea
SSA-FEN – Southern Fen
SSA-OA – Southern Old **A**spen
SSA-OBS – Southern Old Black Spruce
SSA-OJP – Southern Old Jack Pine
SSA-YA – Southern Young **A**spen
SSA-YJP – Southern Young Jack Pine
SVAT – Soil Vegetation **A**tmospheric Transfer Model
SWE – Snow Water Equivalent
SWMM – Stormwater Management Model
TM – Thematic Mapper
TOPLATS – TOPMODEL-Based Land **A**tmosphere Transfer Scheme

TOPMODEL – The Topographic-Based Hydrologic Model
TOPOG – Terrain analysis-based hydrologic modelling package
TOPOGRID – ArcInfo Command which Implements **A**NUDEM Software
USDA – United States Department of **A**griculture
USGS – United States Geological Survey
UTM – Universal Transverse Mercator
UZS – Upper Zone Storage
VG – van Genuchten Model
VIC – Variable Infiltration Capacity
VIS – Visible Radiation
VPD – Vapour Pressure Deficit
WatCLASS – W**A**TFLOOD / CL**A**SS Coupled Model
WATFLOOD –Waterloo Flood Forecasting Model
WATROUTE – Waterloo Routing Model
WMO – World Meteorological Organization
WP – Wilting Point

List of Symbols

$\overline{T}$ – layer average soil temperature in CLASS
$\overline{\chi}$ – layer average volumetric soil moisture in CLASS
$\overline{S}$ – basin average storage deficit from TOPMODEL
$\subseteq$ – horizontal divergence operator
ς – soil moisture dependent thermal conductivity in CLASS
ν, η, ζ – place hold symbols in equation 2-3.
ϑ_1 – period of the diurnal cycle equal to 1 day in force-restore scheme
ψ_w – density of water
A – area of the grid or catchment
a – normalize upslope area in TOPMODEL
a, b – interflow parameters from WatCLASS
a, p – fitted soil texture parameters from ISBA force-restore
A5 – **A**PI coefficient for W**A**TFLOOD
$\mathbf{A}_s$ – saturated area in VIC model
$\mathbf{A}_t$ – total area of the basin in TOPMODEL
B – empirical shape parameter in VIC model
b , c – Clapp and Hornberger soil parameters
c – contour length in TOPMODEL
C_1, C_2 –moisture decay parameters in force restore scheme
C_1, C_2 ,C_3– force-restore parameters from ISBA
C_{1sat}, C_{2ref} – soil dependent constants from ISBA force-restore#
d_1 – upper layer depth in force-restore model
d_2 – total depth of soil in force-restore scheme
D_D – drainage density
d_e – depth above natural depressions
d_i – distance from the surface to the center of the i^{th} layer
dS/dT – change channel storage with respect to time
DUZ - runoff depth per unit area from W**A**TFLOOD
E – actual evaporation from bucket model
e – actual vapour pressure
E_g – surface layer evaporation rate from force-restore scheme
E_o – atmospherically limited evaporation rate from bucket model
e_{sat} – saturated vapour pressure
F – lateral flux of water
f – vertical moisture flux in CLASS
F(t) – cumulative infiltration depth at time, t for Green-Ampt infiltration
f(t) – represents the rate of infiltration at time, t for Green-Ampt infiltration
F_y – horizontal component of soil-water flux
F_z – vertical component of soil-water flux
G – ground heat flux
G(0) – flux of energy entering the surface
G_i – energy flux across a layer boundary (i)

I - inflow to a reach in WATFLOOD
K – saturation dependent hydraulic conductivity of soil
$K(\chi)$– saturation dependent value of the horizontal conductivity
K_* – net short wave radiation
K_o – hydraulic conductivity at the soil surface
K_{sat} – saturated hydraulic conductivity
K_{satH} – horizontal saturated hydraulic conductivity
K_{satV} – vertical saturated hydraulic conductivity
l – length of sink channels
L_* – net long wave radiation
L_v – latent heat of vaporization in CLASS
L_v – the length of the stream valley
m – decay parameter of hydraulic conductivity with depth
m – exponential decay of the transmissivity with depth in TOPMODEL
M – rate of snow melt from WATFLOOD
MF – melt factor from WATFLOOD
n – Manning's roughness coefficient
N – number of sink channels
n and m – van Genuchten parameters related by m=1-1/n
O – outflow from a reach in WATFLOOD
P – atmospheric pressure
P – precipitation rate from force-restore scheme
p(t) – precipitation depth from WATFLOOD's API calculation
PET – potential evapotranspiration
q – specific humidity
Q – total grid square volumetric outflow
Q – vertically integrated flux of specific humidity
q_a – specific humidity
Q_b – volumetric base flow in TOPMODEL
Q_{basin} – basin volumetric runoff
Q_E – latent heat flux
Q_H – sensible heat flux
q_{int} – interflow streamflow contribution per unit area
Q_{int} – total volumetric runoff from interlow
Q_o – maximum volumetric base flow in TOPMODEL
q_{over} – overland flow per unit horizontal area
Q_{over} – overland volumetric flow
R – recharge rate in TOPMODEL
r_a – aerodynamic resistance term in CLASS
r_c – canopy resistance term in CLASS
REC – optimized lateral flow generation parameter from WATFLOOD
REC_1 – WATFLOOD's REC multiplied by the land surface area
RETN – optimized undrainable portion of UZS from WATFLOOD
R_{local} – runoff from the land surface tiles to the stream channels
R_{net} – net all-wave radiation
S – degree of soil saturation (χ/χ_{sat}),

S_0 – maximum storage deficit from ISBA TOPMODEL
$S_{channel}$ – channel storage
SF – K_{sat} scaling factor
S_g – degree of saturation in upper soil layer in force-restore scheme
S_i – storage deficit in i^{th} topographic index bin
S_{land} – land surface moisture storage
t – time
T – transmissivity of soil layer in TOPMODEL
T_a – air temperature for snow melt calculations
T_{base} – snow melt base temperature
T_c – canopy temperature
T_o – saturated transmissivity of soil in TOPMODEL
T_S – skin surface temperature
u – dimensionless measure of basin wetness from WatCLASS
UZS – upper zone storage from WATFLOOD
UZS_{max} – maximum upper zone storage value
v – overland flow velocity
vpd – vapour pressure deficit
w – basin soil storage capacity in VIC model
W – water content in an atmospheric column
w_{max} – maximum basin soil storage capacity in VIC model
÷ – temperature gradient of the saturated vapour pressure curve
÷S – change in water content
$÷_{topo}$ - effective vertical topographic rise in PLACE model
÷Z – soil layer thickness
Θ#4 land surface slope gradient
T – slope of the surface in degrees
ζ – Priestley-Taylor alpha
ζ – surface shortwave albedo
ι – distance between sinks
κ – long wave radiation surface emissivity
λ – soil porosity
λ_e – drainable porosity (χ_{sat} - χ_{fc})
ν – average basin area topographic-soil index
ν – psychrometric constant from Priestley-Taylor ET
ς – average topographic index of the basin
χ_{fc} – field capacity volumetric soil moisture content
χ_{geq} – equilibrium volumetric soil moisture from ISBA force-restore
χ_i – initial moisture content for Green-Ampt infiltration
χ_l – small value used to prevent division by zero results near saturation
χ_r – Brooks and Corey residual moisture content parameter
χ_{sat} – saturated volumetric soil moisture content
χ_{total} – sum of the liquid and frozen portions of soil moisture
χ_{wilt} – wilting point volumetric soil moisture
χ_2 – average volumetric moisture content of force-restore soil

χ_g – volumetric moisture content of upper force-restore layer
χ_{gi} – initial volumetric moisture content of upper soil layer in force-restore scheme
χ_{*} – critical soil moisture from bucket model
χ_{max} – saturation soil moisture content
χ – volumetric soil moisture
ψ_a – density of air
ψ_b - bulk density of the soil
ω – Stefan-Bolzmann constant
ω_h – standard deviation of GCM basin orography
ω_{max} – maximum standard deviation of GCM orography
ω_o – minimum standard deviation of GCM orography
$\ldots_e$ – Brooks and Corey air entry suction
$\ldots_f$ – suction head at the wetting front for Green-Ampt infiltration
$\ldots_i$ – soil suction in the i^{th} layer
$\ldots_{sat}$ – Clapp and Hornberger saturated soil tension parameter

1 Introduction

Complex land surface schemes (LSSs) are becoming more commonplace in today's climate and weather forecast models. As atmospheric models evolve, the requirements for improved representation of their lower boundary will continue to increase as well. Goals for land surface boundary representation are twofold. Of primary importance is the simulation of fluxes to the atmosphere, especially latent and sensible heat fluxes and of secondary importance is the enhancement of the physical realism of the land surface including carbon cycling and river discharges to the oceans (Rosenzweig, 1998). Manabe (1969) has been credited with instituting the first land surface scheme (Carson, 1982) that has become widely known as the "bucket" model. While simple in principle with a single, globally defined 1 m soil layer, a 15 cm water field capacity, and without benefit of a vegetation component, this scheme, when coupled with a crude, 1960s vintage atmospheric model, was able to contrast gross differences between dry deserts and wet tropical forests. This first land surface scheme recognized that the surface of the earth must provide boundary conditions necessary to exchange fluxes of energy, water and momentum with the atmosphere. These requirements remain the same today. Today's LSSs are premised on the physical depiction of the diversity within the planetary vegetation and soil systems. These systems are highly non-linear making them difficult to model. This requires that all available information be synthesized and used in order to evaluate and improve them. One such source of information for LSS evaluation is the streamflow record and one class of models that can be used for LSS improvement are hydrological models.

1.1 Objective

The objective of this thesis is to establish a mechanism whereby realistic streamflow processes may be introduced within atmospheric simulation models. All atmospheric models, including those that implement the bucket model, produce a flux of liquid moisture that one might classify as runoff. This liquid water moisture flux is most often generated as a residual in the land surface water balance after evaporative and storage requirements have been met. This runoff component is usually termed "excess moisture" and is rarely used for further predictive purposes within atmospheric model studies. However, it is this moisture that ultimately generates streamflow in the natural world and this moisture that is the subject of this thesis.

The problem with poor representation of moisture "excess" in atmospheric models lies in its relationship with surface wetness and therefore soil moisture. Errors introduced through the calculation of runoff are likely to impact soil moisture since they are directly connected though the water balance equation, often given as P-E=R+÷S and defined fully in Chapter 4. Generally speaking, simulations that do not produce enough streamflow have soil moistures that are too high. While streamflow error may not be crucial to the success of an atmospheric simulation, the resulting soil moisture errors are. Soil moisture has a substantial impact on many land surface processes and, perhaps of most importance, the partitioning of turbulent energy fluxes between evaporation (latent heat flux) and near surface heating (sensible heat flux). Wetter land surfaces favour increased latent heat production and therefore cooler surface temperatures while dry surfaces promote sensible heating. Within an atmospheric model, this distinction between near surface sensible heating and latent heat release that occurs higher in the atmosphere has important implications for atmospheric circulation and

weather development. Particular examples may be found for convective precipitation generation (Raddatz, 1998), weather prediction (Beljaars *et al*, 1996), and climate simulation (Sellars *et al*., 1997).

Rigorous treatment of streamflow within an atmospheric model will tend to improve soil moisture simulation. The magnitude and timing of streamflow is highly dependent on the antecedent soil moisture conditions prior to rainfall or snowmelt inputs. For example, dry conditions, prior to a rainfall event, will promote increased soil storage and lower runoff. If the timing and magnitude of streamflow can be reproduced in a reasonable way, the resulting soil moisture can be expected to be more accurate as well. Benefits of streamflow simulation for atmospheric models may therefore be summarized as:

1. measured streamflow provides a means for validation of atmospheric simulations through comparison with routed excess moisture. Here, watersheds act as large lysimeters from which streamflow is the integrated response of all atmospheric inputs;

2. improved streamflow simulation will have a positive impact on soil moisture simulations and hence the partitioning of energy inputs into latent and sensible heat fluxes.

The goal of this thesis is to present a mechanism whereby the simulation of streamflow can be incorporated into atmospheric process models. Once implemented, it is anticipated that overall simulation improvements will not only benefit the atmospheric modelling community but also the hydrologic modelling community through improved precipitation forecasts often used as inputs to distributed hydrologic models.

1.2 Motivation

The enhancement of atmospheric schemes to include streamflow processes has been recognized as an important requirement for future atmospheric models and has been called for by a number of agencies.

International organizations have recognized the need for improved hydrology within land surface process models. The Global Water and Energy Experiment (GEWEX), which is a major scientific program of the World Meteorological Organization (WMO), has, as a strategy for improving the understanding of the global energy and water cycles, the "development and validation of appropriate large scale hydrological-surface models that will be coupled with atmospheric models" (GHP, 1998). While numerous GEWEX projects are focused on continental domains, larger global applications such as general circulation models (GCMs) are often "challenged with regards to reproducing and predicting changes in atmospheric wet processes (Morel, 2001)". In fact, the Intergovernmental Panel on Climate Change (IPCC) that assesses the state of climate change research, has stated that "significant problems remain to be solved in the areas of soil moisture processes, runoff prediction, land-use change and the treatment of snow and sub-grid scale heterogeneity" (Albritton and Meira Filho, 2001, p. 51).

GCM wet cycle problems are partially attributable to the large spatial scales required for GCM operation. These scales limit their ability to resolve wet processes such as soil moisture distribution, streamflow generation and convective precipitation all of which have domains of spatial variability much smaller than typically GCMs grid squares. A group of leading international hydrologists (Entekhabi *et al.*, 1999), in calling for a second

International Hydrological Decade, suggests that lateral soil moisture redistribution in complex terrain cannot be captured in current one-dimensional (vertical) LSSs used in many GCMs and numerical weather prediction (NWP) models without significant calibration of empirical parameters. Fortunately, these concerns are currently being addressed. **A** new GEWEX modelling and prediction program known as the Global Land-**A**tmosphere System Study (GL**A**SS) (Polcher, 2001) has been implemented to foster the development of the next generation LSSs. It is anticipated that future LSSs will have "larger importance given to the horizontal complexity of the surface" as a result of GL**A**SS efforts. In addition to greater emphasis on horizontal processes, this new breed of LSS is also expected to i) include carbon budgets to provide atmospheric models with a CO_2 flux and ii) possess new data assimilation capabilities to incorporate remotely sensed data.

While these new measures will greatly assist NWP models and limited area climate models (e.g. Canadian Regional Climate Model (CRCM)), large grid sizes will continue to have an adverse impact on GCMs for some time to come. Large grids are a necessity in GCMs because their long periods of integration, small time steps, and global extent of their spatial domain. Even with promised parameterization of more realistic horizontal land surfaces, there remains the problem of low intensity precipitation within large GCM grids. Sub-grid parameterization of atmospheric processes, such as efforts toward statistically downscaling precipitation within GCMs (e.g. Wilby and Wigley, 2000) and RCMs (e.g. Venugopal *et al*., 1999), may assist in solving the large grid problem by better representing convective precipitation for land surface schemes.

1.3 Approach and Limitations

Coupling of hydrological models with LSSs can provide the improvement in both flux simulations and land surface realism that match the two goals specified by Rosenzweig (1998) described previously. These improvements stem from the perspective that the hydrologist brings to the problem. Dickinson (1992) comments that the climatologist views runoff as the simple residual after evapotranspiration requirements are met while the hydrologist views runoff as a direct result of precipitation with evapotranspiration calculated as a residual. While these statements greatly simplify the role of both groups, the philosophy of the differentiation is clear. The hydrologist utilizes the patterns of measured runoff as the spatially integrated response of a watershed. This response then acts as an information source that provides insight into processes that contribute to streamflow such as snow accumulation and melt, the quantity and distribution of soil moisture, and rate of evapotranspiration.

To derive any such insight into these processes, the hydrologist must have at his disposal spatially and temporally accurate estimates of precipitation. Without good precipitation estimates, it becomes difficult to distinguish between the influence of the process and the error related to precipitation. Complicating this is the inherent difficulty in measuring precipitation, which by its nature is heterogeneous both in time and space. Many hydrologic studies have noted that the greatest source of error resides in the measurement of precipitation (Dirmeyer, 1997) and much effort has been devoted to its determination. The hydrologist's need for accurate precipitation has lead to a synergy with the climatologist who wishes to evaluate their atmospheric models against the streamflow record. As these coupled

models come closer to a true representation of earth-atmosphere interactions, benefits for both groups will be realized.

Differences between the hydrological view of the land surface and the climatological view arise primarily in the horizontal transport of soil water. Many land surface process schemes take a "flat Earth" representation of the land surface and as such often have very simple ideas regarding the mechanisms for runoff generation (Liang *et al*., 1994). While these mechanisms are based on hydrological principles, such as infiltration-excess runoff and drainage through a soil column, their implementation neglects the redistribution of soil water based on land surface slope. As mentioned previously, excess water generated from these simplified flow mechanisms is often output from the model without further analysis. This is in contrast with hydrological models, which have traditionally used topography to aid in partitioning precipitation into soil water storage and runoff. Topographic mechanisms for runoff generation include transport of soil moisture within a landscape for the determination of local areas of surface saturation (e.g. TOPMODEL, Beven and Kirkby, 1979) or as the gradient used for interflow generation from shallow subsurface soil horizons (e.g. WATFLOOD, Kouwen *et al*., 1993). Generated runoff in hydrologic models, unlike LSSs, is further analyzed by considering the role of topography in routing streamflow through a drainage network and ultimately to the ocean.

1.3.1 Spatial Scale and Domain

In coupling hydrologic and atmospheric models, the questions of both spatial scale and domain arise. Here, scale is defined as the representative length at which processes are resolved and domain is the total area over which processes, at their representative scales, are

represented. Both scale and domain may be quite different in atmospheric and hydrologic models and as such provide a limitation in the current study. Suitable scales must be defined so that hydrologic process may be adequately represented within atmospheric domains.

For models of the atmosphere, the domains over which simulations are preformed are most often very large. For example, GCMs and weather prediction models typically operate globally. This global domain is necessary because there are no natural lateral boundaries that can be used to define a particular domain. However, there are exceptions to this since hemispheric atmospheric models exist that operate on an assumption of little exchange across an equatorial boundary. Limited area atmospheric models have been developed to provide high-resolution simulations within smaller domains by providing temporally varying conditions along the domain boundaries. Examples of these models include the Canadian Regional Climate Model (CRCM) (Caya and Laprise, 1999) and the Canadian Mesoscale Compressible Community Model (MC2) (Benoit *et al*. 1997). For these limited area simulations, global models typically used to provide lateral boundary conditions. Processes within the new limited area domain are allowed to evolve based on enhanced high-resolution processes. Even with limits set by imposed boundaries, the domains of interest for atmospheric simulation tend to be very large. This is necessary to allow processes to evolve in the model without undo domination by the prescribed boundary conditions. Examples of recent Canadian atmospheric model studies in which WATFLOOD has participated include the:

1. Saguenay flood study (Lin *et al*., 2002) that modelled a large portion of eastern North America with MC2 in order to focus its high-resolution capabilities on a heavy rainfall event in eastern Quebec.

2. Modelling of the Mackenzie River watershed for the Mackenzie GEWEX Study (MAGS) required the domain for the CRCM to be set over a large polar region extending into northern Asia (MacKay *et al*, 2002, submitted).

3. Evaluation of rainfall generation with MC2 against radar and streamflow observations in southern Ontario required a large domain over central North America be used to establish a nested domain (Benoit *et al*., 2000).

These large domain requirements contrast sharply with the hydrologic system. Hydrologic study domains have well defined boundaries that surround areas known as watersheds. Across watershed boundaries virtually no flux of energy or moisture occurs except for river channel output. Groundwater outflow, for large basins and well defined topography, also tends to follow watershed boundaries. These boundaries are most often determined based on the topography of a region and its pattern of stream channels. Because these boundaries are easily identified, studies of watershed processes typically are confined to small areas over which components of the water balance can be physically measured with relatively high accuracy. Larger watershed domains, approaching those of atmospheric models, may be employed by selecting gauging locations farther downstream. However, in selecting larger watersheds, limitations are imposed due to the lack of measured data. Also, greater heterogeneity within watershed properties is introduced that often begins to overwhelm hydrologic modelling efforts.

For this study, which has as its goal the coupling of atmospheric and hydrologic models, a trade-off has to be made between the scale of the processes that are to be represented in the model and the domain over which they are to be applied. Typically, the scale of atmospheric processes represented in weather and climate models range from 10^0 km (thunderstorms and

local winds) to 10^2 km (jet streams and anticyclones) for meso-and macro-scale processes (Oke, 1987, p.4). Smaller scale processes, such as local turbulence, are parameterized as sub-grid processes.

Much smaller scales, on the other hand, characterize hydrologic systems, with soil moisture variability and the precise definition of flow paths being quite variable within a range of 1 m (Beven, 2001, p. 2). One cannot reasonably represent hydrologic processes at this scale over domains used in limited area atmospheric models due to both lack of available data and computational constraints. This trade off between domain and scale requires the preservation of those processes that are most important in the hydrologic system. For this application it is important to:

1. Capture the spatial and temporal distribution of atmospheric forcing over the land surface. Of these forcing variables, precipitation dominates hydrologic simulation. Precipitation also has a high degree of variability when compared to more conservative atmospheric fields such as temperature and humidity.

2. Represent the characteristic hillslopes in a region by providing a perceptual model that expresses our ideas of how watersheds transform rainfall inputs into runoff.

Fortunately, limited area atmospheric models, discussed previously, and macroscale hydrologic models (MHMs) are classes of atmospheric and hydrologic models where similarity in scale and domain meet. One example of an MHM is the WATFLOOD hydrologic model (Kouwen *et al.*, 1993). This model is used to form the basis of this thesis. Examples of other MHMs will be discussed in greater depth in Chapter 2. WATFLOOD is particularly well suited for combining with an atmospheric model since it has been used extensively to model hydrologic processes at scales ranging between 2 km to 50 km. Within

this range of scale, both meteorological processes and hydrologic processes that contribute to first order stream generation may be represented.

1.3.2 Process Representation

Representation of streamflow within atmospheric models requires an expanded vision beyond the traditional hydrologist's and climatologist's view of the world as outlined above by Dickinson (1992). Hydrologists normally employ water balance techniques to generate streamflow and often increase or decrease evaporation amounts, within reasonable limits, to suit. Generally, this is done without regard to energy conservation equations. Rainfall, in excess of that required to satisfy streamflow requirements, is simply made to vanish though a number of techniques including: (i) raising the alpha coefficient in the Priestly-Taylor evaporation scheme or (ii) altering a calibration parameter used to control evaporation in an air temperature based model. These techniques, which may violate conservation of energy principles, are equivalent to the practice in climatology of discarding "excess" moisture from the water balance and violating mass conservation principles from which streamflow is applied.

Within this thesis, constraints are imposed so that both water and energy conservation equations are incorporated. This added constraint requires that sites with both measured evaporation and streamflow be used. Because both the inputs and the outputs of energy and water are fixed, system solutions are forced to more adequately represent the storages of energy and water within the land surface. These manifest themselves as changes in soil temperature and ice/water phase changes (plus other minor surface vegetation changes) for energy storage and soil moisture, snow pack, and canopy moisture changes for water

conservation. Ultimately, if model inputs have been measured reasonably well and constraints are imposed on the model outputs, then through suitable adjustment of controlling parameters, modelling efforts should reproduce the state of system storage. If these storages are well represented, then it can reasonably be presumed that these models are representative of the system as a whole.

1.3.3 Scaling Strategy and Parameter Identification

Much has been written regarding the scaling of hydrological parameters. Most researchers recognize that very fine scale process measurements may not be representative of landscapes as a whole. Views differ on the degree that hydrological parameters can be aggregated. Wood (1997), for example, shows that averaging of soil moisture measurements over a number of land surface types significantly smoothes seasonal evaporation amounts. Noilhan *et al*. (1997), taking the opposite view point, demonstrated that averaging makes little difference to the effective evaporative fluxes contributed by individual components of the land surface.

This difference in views of how to capture the essence of the physical system, in a simple fashion, is also present for hydrologic modelling. There are many hydrologic models, each with its own assumptions, strengths and weaknesses. Beven (2001, p. ix) states that the word 'plethora' springs to mind when the number of hydrologic models that currently exist is considered. The reason for such a wide variety of models is that mathematical solutions of the hydrologic system are likely beyond our capability given current [large scale] measurement techniques (Beven, 2001, p. 2). Undaunted by the commentary of Beven regarding the likelihood of success in modelling the hydrologic system, the task at hand is to

implement the theories of a hydrologic model so they may be incorporated in a LSS to predict streamflow.

Here, rather then entering the debate, a scaling strategy is adopted that has been effectively used by both hydrologists and climatologists. This strategy is based on the identification of land surface covers with similar physical characteristics (for example, land cover type) and the assumption that each individual component in the land surface mosaic behaves in a similar fashion for given inputs of energy and water. By making this similarity assumption, individual elements may be grouped together into large homogeneous areas for which only one calculation is required to describe its response. Since position of individual elements within the computation unit is no longer of importance, the limitation on size of area that may be grouped together becomes dependent only on the homogeneity of the input forcing data. This grouping methodology is known as the Grouped Response Unit (GRU) (Kouwen *et al*., 1993) approach by hydrologists and the Mosaic method (Avissar and Pielke, 1989) by climatologists. Issues related to the scaling of GRU from 2 km to 50 km are reserved for Chapter 3 where model development is considered.

1.4 Base Model Description

In designing a runoff generation model for a land surface scheme (LSS) the goal is to capture the essence of the streamflow generation phenomena. Factors influencing the character of streamflow can be divided into two major categories, those that affect the storage and release of moisture from the land surface and those that shape the accumulation of runoff in stream channels through hydraulic routing. The emphasis here is on the first of these that controls the partitioning of net moisture inputs into storage and runoff. Hillslope hydrologic

investigations have revealed that streamflow response is composed of response elements that range over a continuum of velocities (Dingman, 2002, p.439; Beven, 2001, p.97). These ranges generate the classical hydrograph shape with a sharp fast rise and slow gradual decline. Hydrologic models attempt to capture this classic response and their variants by simulating moisture fluxes in and out of storage elements that most often include leaf interception storage, surface storage, and various soil water stores. Moisture inputs to the system, derived through rainfall or snowmelt, are transferred between the storage elements and ultimately leave the system as evaporation or runoff. The transfer rates between the storage elements are controlled by physical processes, which are both spatially heterogeneous and non-linear. Given the complexity in the natural system, which often seems infinite, generation of streamflow is likely to be far more complex than models used for its simulation. Fortunately, mass conservation constrains hydrologic solutions. Models in hydrology may therefore attempt to capture the essence of the physical system by experimenting with water movement through conceptual elements of storage. Through experimentation, the proper proportion of fast and slow watershed responses may be determined that best fits measured streamflow.

For this thesis the hydrologic model WATFLOOD will be coupled with the Canadian Land Surface Scheme (CLASS). Underlying principles from WATFLOOD, such as lateral flow generation, and the GRU approach will be integrated into the energy and water balance methods of CLASS.

1.4.1 WATFLOOD

WATFLOOD (Kouwen *et al*., 1993) began development in 1972 at the University of Waterloo as a flood forecast model. Since then various components such as snowmelt and re-distribution (Donald *et al*., 1995; Hamlin, 1996), and evapotranspiration (Neff, 1996) have been introduced in the model. Others have experimented with additional processes such as sublimation (Whidden, 1999). These changes have allowed WATFLOOD to operate as a continuous model for multi-year simulation. The WATFLOOD modelling emphasis has been on capturing the essential elements of the water balance calculation using a minimum of computational effort.

WATFLOOD is based on two underlying conceptualizations of the watershed. The first is the division of runoff generation into surface runoff, interflow, and base flow. Surface runoff, which rarely occurs, is generated by an infiltration excess mechanism controlled by an implementation of the Green-Ampt like Philip formula (Philip, 1954). Interflow, WATFLOOD's dominant storm flow mechanism, is generated by modelling a variable depth shallow aquifer whose response is controlled by a linear relation with land surface slope and water content. Finally, long-term base flow is generated from a deeper storage reservoir whose outflow is controlled by a simple two-parameter power law formulation. This lower reservoir, known as lower zone storage (LZS), is fed by drainage of the upper shallow aquifer, known as upper zone storage (UZS). The moisture content states of UZS and LZS ultimately control the partitioning of rainfall inputs into fast, medium, and slow response streamflow inputs.

The second conceptualization of the watershed by WATFLOOD is based on the grouped response unit (GRU) approach (Tao and Kouwen, 1989; Kouwen *et al*., 1993). The GRU approach operates by gathering together pixels of similar hydrologic response and performing a single calculation to determine their response. Hydrologic similarity, used to assess group membership, is based solely on the land cover type and is most often determined from classified satellite imagery. This method of grouping is not unlike that of the TOPMODEL (Beven, 1986), which relies on a combined distribution of topography and soil type to determine an index of hydrologic similarity. Rather than the TOPMODEL's topographic-soil index, WATFLOOD relies on a land cover surrogate of hydrologic similarity. This is accomplished by presupposing that like vegetation preferentially occurs in regions of similar soil type and topographic condition. Based on this implicit relationship between vegetation and a basin physiography, a set of effective soil parameters are chosen that control the rate of moisture flow between the various model stores (e.g. UZS to LZS).

Reliance on a land cover surrogate for determining soil parameters has the advantage of drawing on an increasing pool of observations. However, this method has the disadvantage of having no means of determining the soil based parameters values a priori. To determine the distribution of parameters for each GRU, WATFLOOD employs a guided optimization scheme to select effective parameters based on the percentage of a land cover within a watershed and its influence on the hydrograph response. Past knowledge, multiple stream gauge locations, each dominated by a particular land cover, and long periods of calibration, incorporating multiple events, all contribute to the parameter selection process.

Fundamental concepts of the GRU approach stem from methods developed for analysis of urban hydrologic systems. In many models of urban storm drainage (e.g. Stormwater Management Model (SWMM), Huber and Dickinson, 1988) the land surface is divided into separate impervious and pervious areas. It is well known that impervious areas have a markedly different rainfall-runoff response from their pervious area counterparts with much higher runoff volumes and shorter lag times between the commencement of rainfall and runoff. Maintaining separate, cover dependent, calculations allow the impact of impervious area runoff to be captured even when the proportion of the total basin area is small. Use of an alternate lumped parameter approach, which produces effective runoff coefficients by blending the impact of pervious and impervious areas, will tend to mask the impact of impervious runoff, especially as its contributing area decreases. In addition, calibrated runoff parameters from the blending method would be unique for each modelling area and thus not transferable.

A concept similar to the GRU approach has become more prevalent in atmospheric modelling. These concepts, developed independently from the GRU approach (Kouwen, personal communication, 2001), are known by names such as mosaic, tile, or patchwork approaches and have been often attributed to Avissar and Pielke (1989). In this atmospheric context, similar land surface vegetation types are grouped together to calculate fluxes of mass and energy to the atmosphere. Locations of individual elements within a computational tile become unimportant because of the dominance of vertical transfer from the land surface when compared to horizontal fluxes between land cover types. Simple averaging of these vertical fluxes (rather than the parameters) may then be performed owing to the integrating effect of turbulence within the atmospheric boundary layer. These integrated values are used

to determine the grid averaged flux returned to the atmospheric model. An alternate approach (analogous to parameter lumping in hydrological modelling) is the assumption of grid homogeneity based on dominant land cover or parameter aggregation. Avissar and Pielke (1989) advocate the mosaic approach over homogeneous assumptions partially because of its ability to define conditions within land cover patches that have practical application in areas such as agriculture. It was noted that effective parameters may perform equally well for simple heterogeneous surfaces but as the range of response for the various sub-grid classes increases, the mosaic approach was expected to improve grid average flux calculations.

Integrated within the GRU concept is the use of large areas from which pixels of like vegetation are drawn to determine groupings. These areas, normally 4 to 2500 km^2, are limited in size by climatic and hydraulic routing considerations. WATFLOOD traditionally uses square grid areas each of which contain a number of land cover groupings and a stream channel routing element. Another GRU based hydrologic model, SLURP (Kite and Kouwen, 1992), uses sub-watershed elements known as aggregated simulation areas (ASAs) to group like land covers. Regardless of whether square grids or irregular polygons are used, there is an assumption of constant climatic forcing over each set of GRUs. This limits WATFLOOD's grid size primarily because of the spatial variability of hourly rainfall inputs used for runoff calculations. This spatial length scale corresponds reasonably well with World Meteorological Organization (WMO, 1970) recommendation for rain gauge network density of one rain gauge per 600-900 km^2 in flat areas with temperate climates. SLURP, on the other hand, with a daily time step, often uses much larger computational ASAs. For example, SLURP modelling of the Mackenzie River basin (Kite *et al.*, 1993) utilize sub-

basin ASAs whose largest size was 145,000 km^2, which, even for daily computations, far exceeds WMO implied spatial extent of a constant rainfall assumption.

A second limitation on the upper bound of WATFLOOD's grid size is based on hydraulic routing considerations. Routing in the natural environment is composed of headwater streams of order zero, which feed larger streams of higher order. Overlaying a gridded pattern of squares over this system yields two sets of streams: (i) those sub-grid routing elements that are contained within a single grid, and (ii) those main channel elements that transfer flow from grid to grid. Only one routing element per grid square is used to represent streamflow in WATFLOOD and these are used for main channel elements. Sub-grid element travel times and hence distance are assumed to be small in comparison with main channel elements and therefore limits overall grid size. Generation of runoff within a GRU is delivered instantaneously to the upstream end of the main channel routing element at the end of each time step. Upstream entry of runoff insures that at least some sub-grid routing delay is included by forcing local inputs to travel together with upstream contributions through the length of a grid square. While increased flow depth tends to decrease main stem travel times, in comparison to sub-grid channels, a compensating effect is introduced due to the increased steepness of smaller sub-grid channels. Other routing schemes, including the PILPS-2c (Arkansas-Red) routing scheme of Lohmann *et al*. (1996), utilize explicit sub-grid routing such as unit hydrograph theory to specifically account for sub-grid routing delays. By limiting the maximum grid size in WATFLOOD, these added calibration requirements are not required.

The lower limit of the WATFLOOD grid size is based on the assumption of grid independence. Grid independence implies that no soil water is transferred laterally between grid elements and that the only connection between grids is the stream channel network. Since no inter-grid soil water transfers are modelled, the grid sizes must be large enough to drain a typical hillslope which lies between a drainage divide and a sub-grid river channel. Typical zero order stream drainage density range from two streams per kilometre to 100 streams per kilometre (Dingman, 2002, p.433). This requires that the smallest WATFLOOD grid be larger than one kilometre. Higher drainage density networks would permit the use of a smaller grid size. However, the effect of more frequent stream channel occurrence is incorporated in the model by altering the typical hillslope flow path length. This length scale parameter may be derived from topographic maps by determining the total length of stream channel per unit land surface area. However, due to the dominance of lateral soil conductivity in determining travel time to a routing element, its effect is not explicitly defined within WATFLOOD. Instead, average travel length, often referred to in terms of watershed width or time of concentration, is incorporated with the lateral soil conductivity in an optimized parameter named REC. While not explicit, the presumption that WATFLOOD grid elements include a non-ephemeral stream underlies the minimum computational grid size.

A powerful claim of the GRU approach is its ability to transfer parameters calibrated for one area to other areas based solely on land cover description. While this claim has yet to be definitively proven, it is anticipated that climatic zone consideration may need to be incorporated in assessing hydrologic similarity. While vegetation within a climatic zone may tend toward regions of similar soil and topographic conditions, this same vegetation may tend

toward a different soil-topography combination under different conditions of moisture and temperature. For example, spruce forest within the BOREAS project's northern study area (NSA) lie over clay type soils in wet conditions. However, within the southern study area (SSA) sandy conditions are dominant where spruce forests grow. These soil conditions indicate a much different hydrologic response mechanism requiring different parameter values. Work towards a universal hydrologic parameter data set is continuing and positive results are beginning to emerge for southern Ontario watersheds.

1.4.2 CLASS

The Canadian Land Surface Scheme (CLASS) (Verseghy, 1991; Verseghy *et al*, 1993) is typical of the many land surface schemes that exist today. These schemes are used to model the lower boundary of atmospheric models. A number of these models are currently undergoing trial intercomparisons under the Project for Intercomparison of Land-Surface Parameterization Schemes (PILPS). Under this program, between 20 and 30 land surface schemes have participated in tests using various ecosystem conditions, time scales and domain sizes.

The CLASS model development has been undertaken to replace the 'bucket' land surface scheme currently used in the Canadian Climate Centre's (CCC) second generation GCM. The CLASS addition represents a more physically based representation of land surface processes and includes the following major features:

- Gradient based heat and moisture transfer through three distinct soil layers
- Infiltration calculations using the Green-Ampt approximation

- Snow cover accumulation and depletion represented as a separate 'soil-like' layer
- Incorporation of seasonally varying vegetation characteristics
- Parameterization of distinct vegetation types into a 'composite canopy'
- Energy and moisture exchange between the surface and the atmosphere
- Grid calculations over four separate sub-areas: bare soil, snow covered soil, vegetation cover and snow covered vegetation.

For this study, the CLASS model represents an important link with atmospheric models. A requirement for many land surface models is to exchange fluxes of heat, moisture, and momentum with the atmosphere. Hydrologic models, such as WATFLOOD, make no provision to provide such exchanges and as a result are not suitable to provide boundary conditions for an atmospheric model. By coupling CLASS with WATFLOOD, the essence of hydrologic models may be incorporated with an atmospheric model.

1.5 Thesis Hypothesis and Objectives

The subject of this thesis is broad and touches on many topics from data handling techniques to detailed discussions of soil physics properties. Because of this breadth, it is necessary to provide a central thesis focus by establishing a hypothesis. Introduction of streamflow hydrologic processes into atmospheric models will be accomplished by incorporating the GRU concept and elements of streamflow generation from WATFLOOD within the structure of the CLASS land surface model. By combining these elements into a single model, this thesis aims to test the following:

> Constraining the land surface moisture budget by providing pathways necessary for the reproduction of measured

> streamflow hydrographs will have a positive influence on the partitioning of land surface energy between latent and sensible heat flux generation.

Without an adequate streamflow generation mechanism, it is anticipated that soil surface conditions will remain wet for extended periods. This increased wetness will result in a greater potential for the production of latent heat that is controlled by the gradient developed between land surface moisture and moisture in the overlying atmosphere. Higher surface wetness values will tend to increase this gradient and result in higher portions of available energy being transformed into evaporation. This is demonstrated in Chapter 4.

In addition to the central hypothesis theme, two other objectives, related to the hypothesis, must be examined in order to establish a fully coupled hydrologic-land surface process model. These are:

1. Demonstration that grouping of responses from individual GRU contributions will yield measured hydrographs. Modelling results evaluated against measured evaporation will show that the response from an individual point is sufficient to prove the thesis hypothesis. However, because evaporation measurements are influenced by spatial heterogeneity, it is also necessary to compare simulation results with measured hydrographs. In this case, hydrographs are used as surrogate measures of evaporation because spatial evaporation measurements are not available. This is demonstrated in Chapter 5.

2. Demonstration of the methodology for spatial domains coincident with atmospheric models. The eventual goal of this research is the improvement of atmospheric models through introduction of hydrologic simulation. Objective 1, above, will be demonstrated for two small, intensively monitored watersheds. In order to demonstrate the potential of the method within an atmospheric model, results must be

presented over domains approaching those of atmospheric models. This is demonstrated in Chapter 6.

1.6 Description of Thesis

Following some background for the establishment of the problem of streamflow generation within atmospheric models in Chapter 2, the remainder of this thesis will focus on establishing a framework within which streamflow processes can be readily applied within components of atmospheric models. In addition, the coupled WATFLOOD-CLASS model will be tested against field data to demonstrate the application of the approach.

Following the background in Chapter 2, Chapter 3 will describe the linkage strategy and methodology used in the establishment of the coupled land surface / hydrologic model known as WatCLASS. This model is one of a number of the WATFLOOD based models that have been developed at the University of Waterloo and a strategy for their implementation within field studies will be presented briefly.

Chapters 4 and 5 will apply the WatCLASS model at various scales within the Boreal Forest Ecosystem Study (BOREAS). Tower scale studies will be used to derive parameters that control the generation of streamflow within WatCLASS and these will be applied to the study area watershed scales to reproduce the measured hydrographs. Essential to this study is the existence of both simultaneous measurement of streamflow and evaporation. Only because of this extensive data set, which closes the land surface energy and moisture budgets, can the hypothesis for this thesis be tested.

Application of the model to other data sets will be presented in Chapter 6. One limitation of the small domain testing, as with the BOREAS data set, is the transference of parameters to larger domains used within atmospheric models. The Mackenzie River basin will be used to test the WatCLASS coupling over a large domain. This Mackenzie River modelling effort is seen as an introduction to further study that is required with land surface representation in atmospheric modelling.

The discussion in Chapter 7 will focus on the lessons learned from the coupling of hydrologic and land surface models, and the direction of future research to best address the differences that remain between modelled and measured streamflow. A majority of these differences are related to the constraints imposed by maintaining an energy balance within the land surface system. Energy storage within the CLASS model soil layers is required to regulate spring and fall air temperatures and to maintain a balance between frozen and liquid moisture. However, this balance between frozen and liquid soil moisture complicates the physical processes used in distributed hydrologic models and results presented may offer some insight into directions for future field campaigns and modelling efforts.

2 Literature Review

Literature pertinent to this thesis is reviewed here to provide a sample of similar studies that have been done to date. Incorporation of hydrologic processes in atmospheric models is currently receiving considerable attention in scientific journals. It is timely to review a selection of this work in order to put the current study in perspective with other efforts.

2.1 Hydrology in Land Surface Schemes

Prior to describing the proposed land surface - hydrologic model coupling, other runoff generation mechanisms used within LSSs are presented. This review is intended to highlight broad categories of runoff production that have participated in the various phases of the Project for Intercomparison of Land Surface Schemes (PILPS) (Henderson-Sellers *et al*., 1993). As mentioned previously, current land surface schemes (LSSs) often have simplified hydrology used to remove excess moisture from the soil column without specific regard for streamflow generation. The schemes in this category may be classified generally as either i) sloped or ii) flat.

A majority of LSSs have been designed specifically for GCM and NWP applications. However, another class of model, known as the macroscale hydrologic model (MHM), has been designed for large scale streamflow generation application. These MHMs possess many of the attributes found in LSSs with a number including energy balance closures. Non-closure of the surface energy budget is much less of a restriction when considering streamflow generation only since processes such as evapotranspiration (ET) and snowmelt, which depend jointly on both energy and water mechanisms, may be tuned without the

constraint imposed by available energy. While these models offer valuable insight into processes that control streamflow, they will not be considered in this review. Examples of MHMs which provide both energy and water balance closure include TOPLATS (Famiglietti and Wood, 1994) and VIC-2L (Liang *et al*., 1994). These MHMs have been built on traditional hydrological models (TOPMODEL and the Xinanjiang model, respectively) and have been updated to function as LSSs with the addition of vegetation influences and energy balance closures. While these hydrologic adaptations have simplified vertical processes when compared to traditional LSSs, they offer increased realism in their depiction of horizontal processes especially those responsible for the generation of streamflow.

A third class of model, which couple a MHM with a traditional LSS, are also beginning to emerge. These models will be reviewed as well.

2.1.1 Historical Perspective

Bucket Model

Manabe (1969) has been credited with the introduction of interactive hydrologic land surface schemes (Carson, 1982). This scheme and its derivatives have subsequently become known as the 'bucket model'. Soil moisture in this model is contained within a single, 1m soil layer. Manabe (1969) justifies this choice by stating that the majority of soil roots are contained within 1m of the land surface and that the range of moisture change in both the 0-0.5m and 0.5-1.0m soil horizons are comparable. Evaporation from this soil column (E) is scaled linearly from the atmospherically limited, wet surface, evaporation rate (E_o) by the relation:

$$E = E_0 \qquad \text{for } \chi \geq \chi_k$$

$$E = E_0 \frac{\chi}{\chi_k} \qquad \text{for } \chi < \chi_k$$

Equation 2-1

Selection of the critical soil moisture value (χ_*) in equation 2-1 was suggested as ¾ of field capacity soil moisture and was based on Russian literature attributed to Budyko as cited by Manabe (1969). Current theories of soil moisture control on transpiration, based on Jarvis type stomatal resistance formation (e.g. Stewart, 1988), in fact might be simplified to a linear trend from some point beyond field capacity without significant error. While no explicit vegetation exists in the bucket model, there is a clear intention to allow root zone soil moisture to evaporate above that available to bare soil alone. Further analysis, however, has revealed that vegetative control on evapotranspiration is far more complex than depicted in the bucket model.

Runoff from a bucket model is generated only when soil moisture is increased beyond field capacity which was globally specified as 15cm of liquid water within the 100cm soil layer. Soil moisture in excess of 15% by volume is designated as runoff without any time evolutionary decay. Wood *et al.* (1992) compared measured streamflows against both the variable infiltration capacity (VIC) model and the bucket model during an evaluation of VIC for possible inclusion in the Geophysical Fluid Dynamics Laboratory (GFDL) GCM. The bucket model when forced with measured precipitation and potential evapotranspiration (PET) provided reasonable runoff statistics for 30-day aggregated time series. However, the variability in daily values was much too large and produced either very high or zero runoff amounts. This result suggests that the bucket model's 15cm capacity produces acceptable long term ET to PET ratios and was likely the motivation for the χ_k parameter selection.

Sellers (1992) suggests that the 'boom or bust' representation of the land surface hydrology from the bucket model provided partial motivation for the creation of the original biophysically realistic LSSs namely BATS (Dickinson, 1984) and SiB (Sellars *et al*., 1986).

Force-Restore Runoff

Carson (1982), in his review of climate model land surface schemes, suggested that the Deardorff (1978) force-restore soil moisture scheme was beginning to replace the bucket model scheme in many of the GCMs of the day. The primary motivation for this change was the improved representation of the diurnal cycle in the new two-layer system which could not be represented with a single layer bucket model.

Deardorff (1978) created the force-restore land surface scheme primarily to improve the representation of ground heat flux. To accomplish this, the soil column was divided into two layers, a thin upper layer that would respond to the diurnal cycle of temperature and radiation changes, and a thick lower layer that would respond slowly to seasonal variations. The upper layer responds quickly to heat flux exchange with the atmosphere and is buffered through an energy diffusion process to/from the lower layer. For long simulations, the temperature of the lower layer evolves slowly due to its increased thickness. This rate of change is set based on the depth of the annual temperature wave propagation.

Soil moisture in the force restore scheme is treated in an analogous fashion. Precipitation rate (P) minus surface layer evaporation rate (E_g) drives the two layer scheme which wets/dries a thin 10cm upper soil layer. Moisture inputs to the upper layer are buffered by a diffusive link with a thicker 50cm lower layer by the following relations:

$$\frac{\partial \chi_g}{\partial t} = \frac{C_1}{\psi_w d_1}(P - E_g) - \frac{C_2}{\vartheta_1}(\chi_g - \chi_2) \quad \text{(a)}$$

$$\text{for } 0 < \chi < \chi_{max} \qquad \text{Equation 2-2}$$

$$\frac{\partial \chi_2}{\partial t} = \frac{1}{\psi_w d_2}(P - E_g) \quad \text{(b)}$$

The total depth of the column is d_2 with the upper layer depth expressed as d_1. From Equation 2-2(b), it is apparent that during normal conditions when soil is below saturation ($\chi < \chi_{max}$) all excess precipitation ($P-E_g$) enters the soil column. The proportion of moisture contained in the thin upper layer (χ_g) is controlled by Equation 2-2(a) whose second term describes the gradual decline in the upper soil moisture toward the column average moisture content, χ_2. This second term is often referred to as the restore term. The empirical parameter, C_2 is a non-dimensional decay rate equal to 0.9 and ϑ_1 is the period of the diurnal cycle equal to 1 day. The first term of Equation 2-2(a) controls the rate at which excess precipitation wets the upper soil layer. It is referred to as the forcing term. Like C_2, the C_1 parameter is empirical and is set to 14 for dry soils ($S_g < 0.15$), 0.5 for wet soils ($S_g > 0.75$) and varying linearly between 14 and 0.5 values depending on the upper layer degree of saturation, $S_g = \chi_g / \chi_{max}$. All of these parameters are derived from the work of Jackson (1973) using Adelanto loam soil. This empirical relation for C_1 suggests that wet soils change moisture content at a slower rate than a corresponding dry soil, which is concurrent with expected infiltration behavior. Runoff from the force restore method occurs once either the upper layer or total soil column exceeds χ_{max}. Precipitation excess ($P-E_g$) that fails to saturate the upper layer and which is not used to increase its moisture content is effectively added to the lower soil layer. This simulates flow through upper layer to the lower layer. However, the actual mechanism is a direct transfer of $P-E_g$ to the lower layer without any

gradient transfer mechanism governed by Richard's Equation. The remaining variable, ψ_w is the density of water.

The great benefit of Deardoff's force restore scheme is the simplicity of its solution. The scheme describes a system of linear differential equations that can be solved explicitly. For the case of constant value of C_1 and initial conditions, $\{\chi_g(0) = \chi_{gi} ; \chi_2(0) = \chi_{2i}\}$, the solution is given as:

$$\chi_g(t) = \chi_{2i} + \frac{\nu + \zeta + \eta\chi_{2i}}{\eta}\left(1 - e^{-\eta t}\right) + \chi_{gi} e^{-\eta t}$$

$$\chi_g(t) = \chi_{2i}$$

Equation 2-3

where :

$$\nu = \frac{1}{\psi_w d_2}\left(P - E_g\right), \quad \zeta = \frac{C_1}{\psi_w d_1}\left(P - E_g\right), \quad \eta = \frac{C_2}{\vartheta_1}$$

A similar solution can be determined using the linear varying rather then constant value of C_1. However, the solution remains exact and contains a number of extra terms.

By adding a thin upper layer, the force restore scheme is able to provide an improved simulation of soil surface humidity and temperature to the atmosphere over that of the bucket model. This is realized by allowing upper layer soil layers to dry out and therefore reduce total evaporation. The force restore scheme also captures some of the essential hydrologic processes neglected by the bucket model including surface saturation runoff, restrictive infiltration capacity resulting from increased soil moisture, and redistribution of excess surface moisture to deeper soils.

Although a step forward over the bucket model, the force-restore scheme still has a number of deficiencies including i) no facility for bottom drainage, ii) only a single saturated surface runoff mechanism, and iii) no mechanism for adding soil dependent coefficients. Each of these shortcomings have been addressed by the model named "Interactions between the Soil, the Biosphere and the Atmosphere" also known as ISBA. The ISBA land surface scheme extends the force restore scheme and is discussed in more detail below.

2.1.2 Current Schemes

Sloped LSS Hydrology

A number of LSSs use land surface slope as a driving force to remove moisture from the land surface in layered soil scheme. It has been recognized that land surface slope plays a major role in hydrologic models and that the ability to simulate streamflow is a desirable attribute for a climate model. A sloping surface allows Darcy's law to be split into two components:

$$F_z = 4K\left(\frac{d\ldots}{dz}2\cos(\mathrm{T})\right\}$$

$$F_y = 4K\sin(\mathrm{T})$$

Equation 2-4

where z represents the vertical distance below the surface, y is the horizontal coordinate perpendicular to z, K is the saturation dependent conductivity of the soil layer and T is the slope of the surface in degrees. This formulation allows a horizontal flux, F_y to be determined across the grid square of interest and is illustrated in Figure 2-1. To remove water from a large grid square a concept of sinks is introduced such that each sink intercepts

water at a regular interval along the lateral flow path. The total grid square outflow (Q) generated by a soil layer of thickness (÷Z) may be determined as:

$$Q \mid N(F_y l \div Z) \qquad \text{Equation 2-5}$$

where N is the number of sink channels of length, *l*. The number channels may be related to the average distance between sinks, ι and the area of the grid, **A** since, N=w/ ι5 This is combined with w=**A**/ *l* to give N=**A**/(*l* ι) which when substituted in Equation 2-5 allows the flow of water (Q) leaving the grid square of area (**A**) to be calculated as follows:

$$\frac{Q}{\mathbf{A}} \mid F_y \frac{\div Z}{\iota} \qquad \text{Equation 2-6}$$

This derivation follows that of Rozenzweig (1998) for the LSS known as Model II-LS which was designed for the Goddard Institute for Space Studies (GISS) GCM. This model uses global slope estimates extracted from a one degree spatial resolution data base compiled by Zobler (1986). Only one of three slope classes (0-8%, 8-30%, or >30%) is assigned to each grid box in this data set. The sink distance, ι, represents the mean inter-stream distance, which is currently set to 10m for all grid boxes in the GISS GCM.

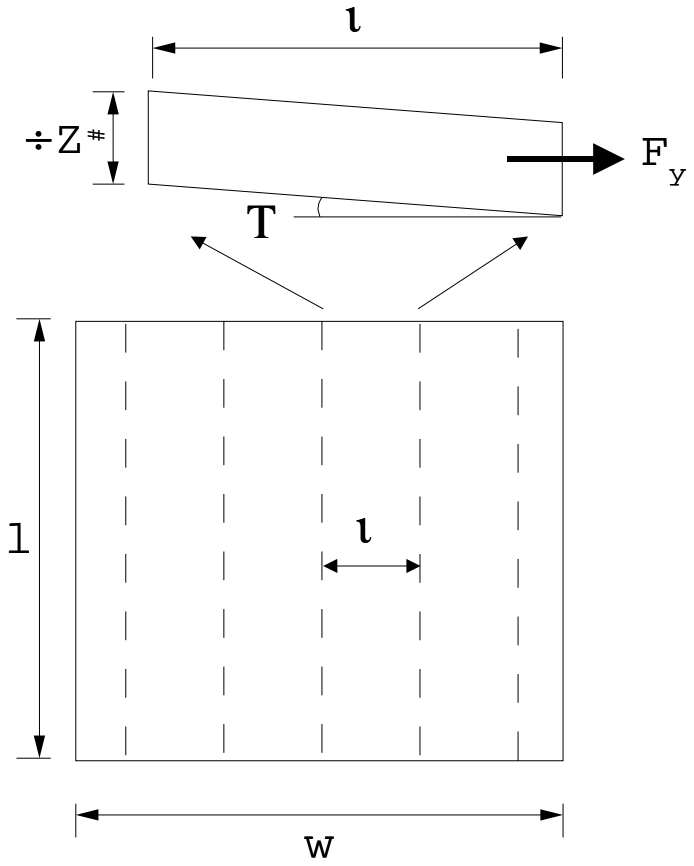

Figure 2-1 : Representation of drainage within the GISS land surface scheme

The Parameterization for Land-Atmosphere-Cloud Exchange (PLACE) LSS (Wetzel and Boone, 1995) also considers the relief of the terrain in calculating horizontal runoff. Rather than considering only the slope of the land surface, PLACE calculates sin(T) for each layer considering both the local relief, the thickness of the soil layer and the soil suction in the calculation as:

$$\sin(T) = rise / l \qquad where: \quad rise = \left(\ldots_i + d_i \right) \frac{\div_{topo}}{2} \qquad \text{Equation 2-7}$$

Here, the effective vertical topographic rise ($\div_{topo}$) is reduced by the distance from the surface to the center of the i^{th} layer (d_i) and the soil suction ($\ldots_i$) within the layer that becomes

increasingly negative with reduced soil moisture. Negative values of 'rise' are considered to be zero. Wetzel and Boone (1995) suggest values of $\div_{topo}$= 20m and ι = 500m for moderately rolling plains of the United States.

Variable Source Area Schemes

A popular scheme for representing runoff from the land surface is derived from the Xinanjiang model developed in China in 1973 (Zhao, 1992). This model bases the volume of runoff from a precipitation event on the current infiltration capacity of the soil. The proportion of the precipitation that does not runoff increases the soil moisture reservoir which in turn decreases the infiltration capacity of the soil. At the extremes, saturation values of soil water storage coincide with runoff equal to precipitation and field capacity soil moisture is tied to zero runoff production. While the Xinanjiang model is composed of additional flow separation, routing, and evaporation components, the heart of the model is the runoff generation mechanism that relates the current water storage of the soil non-linearly to the saturated area of a river basin. This empirical relation also forms the basis of two other runoff generation parameterizations for LSSs namely the variable infiltration capacity (VIC) water balance model (Wood *et al*., 1992), and the ARNO scheme (Dumenil and Todini, 1992), name after the basin in Italy where it was developed.

Saturated area (A_s) in each of these three schemes is determined by a simple non-linear soil moisture storage (w) relation as:

$$\frac{A_s}{A} = \left(\frac{w}{w_{max}}\right)^B \qquad \text{Equation 2-8}$$

where the A_s is normalized by the total catchment area (A), w is normalized by the maximum basin soil storage capacity (w_{max}) and B is an empirical shape parameter. The shape parameter is determined by calibration in both the Xinanjiang model and the VIC model. However, the ARNO scheme has related its B parameter to the characteristic land surface slope for each GCM grid square (h) as follows:

$$B = \left(\frac{\omega_h - \omega_o}{\omega_h - \omega_{max}} \right) \qquad \text{Equation 2-9}$$

where ω_o is the minimum and ω_{max} is the maximum value of standard deviation of orography from the GCM topographic data sets. The minimum and maximum values of ω, however, are GCM resolution dependent. Dumenil and Todini (1992) speculate that while topography may explain some of the variability in B, it is known that other factors, such as soil type influence its value. Values of B may vary from lower runoff production values of 0.001 to values in excess of 1.0. It should be noted that the value of B is dependent on spatial scale with large grids having larger values. This scale dependence is partially an attempt to compensate for the spatial variability of rainfall (Zhao and Liu, 1995).

Operation of each of the VIC/ ARNO/ Xinanjiang schemes is similar in that rainfall is partitioned into runoff and storage. The Xinanjiang model assumes that the combined runoff components of surface runoff, interflow, and base flow are all derived from this single calculation. Subsequently these components are separated and routed through the soil system separately. Both the VIC and ARNO schemes assume a grouped 'fast' response is determined by the rainfall partitioning and a subsequent calculation of the stored soil moisture is

preformed to produce base flow. Separation of precipitation into storage and runoff is best illustrated graphically in Figure 2-2.

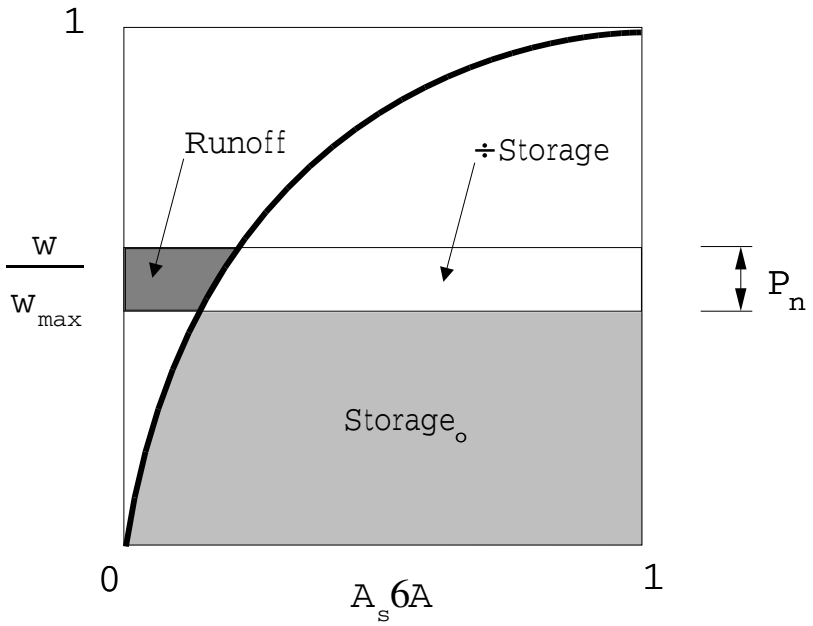

Figure 2-2 : VIC runoff generation representation (after: Wood *et al*.. 1992)

Initially, the total volume of basin storage is represented by the area under the curve marked $Storage_o$. A precipitation event (P_n), normalized by w_{max}, occurs. The dark, shaded area is designated as Runoff and the remainder increases the basin storage by the amount (P-Runoff = ÷Storage). Total basin storage is increased by precipitation and snowmelt inputs, and decreased by evaporation and base flow generation (separate base flow calculations are considered in the ARNO and VIC models, only). Impervious area and water bodies that contribute directly to runoff may be incorporated by designating a portion of the area as permanently saturated and shifting the ordinate of zero saturated area to the right. The impact of adding impervious area (A_{imp}) and changing the value of B are shown schematically in Figure 2-3.

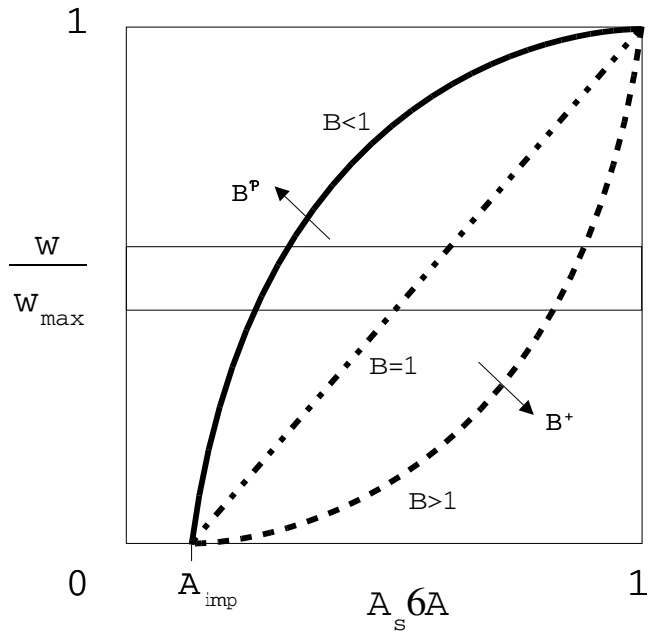

Figure 2-3 : Impact of parameter changes in VIC model runoff (after: Zhoa, 1992)

The VIC / ARNO schemes have become popular within LSSs. ARNO is used in the German, Max Plank Institute (MPI) GCM LSS known as ECHAM (short for European Center - HAMburg) (Dumenil and Todini, 1992), the French ISBA scheme (Habets *et al*., 1999), and forms the basis for the VIC-2L MHM (Liang *et al*., 1994). The ARNO scheme also is the basis for the ARNO hydrologic model (Todeni, 1996). Differences between VIC-2L and the ARNO hydrologic model lie primarily in the scale of their application. VIC-2L is normally applied to continental (Wood *et al*., 1997) and global scales (Nijssen *et al*., 2001) using a square grid implementation while the ARNO model is applied to head water basin scales subdivided using a sub-basin approach.

TOPMODEL Based Schemes

The TOPMODEL (Beven and Kirkby, 1979) was designed to simulate the distributed predictions of runoff and saturated area based on an analysis of the catchment topography.

The model was originally designed as a hillslope model whose scales would reflect precise flow pathways including the effect of convergence and divergence of flow lines as well as changes in slope angle within the hillslope. These assumptions required that resolution of digital elevation data (DEM) to be less than 50m (Beven *et al*., 1995) since it is the subtlety in the local changes in the topography that determines where the model water table will intersect the surface. DEM data that is large in relation to a typical hillslope length will fail to capture the location of saturated areas required for the models storm flow response.

The essence of the model lies in the use of an index used to determine a grid cells wetting potential. The index, known as the topographic index, is given as ln (a / tan T) where 'a' is the area upslope of the grid element normalized by the DEM resolution (or more traditionally the contour length) and tan T is the slope of the grid cell determined from its eight neighbors. Index values are high for flat grid cells with large upslope areas such as those at the base of concave hillslopes and low for steep slopes near topographic divides. An underlying assumption of the model is that all grids with similar topographic index values will behave in a hydrologically similar fashion and so can be grouped together for calculation proposes. Calculations proceed under an assumption of constant rainfall (an added spatially limiting factor) to redistribute soil water over the hillslope as:

$$S_i = \bar{S} + m\left(\varsigma - \ln\left(\frac{a}{\tan T}\right)\right) \qquad \text{Equation 2-10}$$

The storage deficit, S_i of any grid element (or more precisely any 'group' of hydrologically similar elements) is adjusted from the basin average storage deficit, $\bar{S}$ by the difference in the natural log of the topographic index of the grid and the average topographic index of the

basin (ς). The coefficient 'm' represents an exponential decay in the transmissivity (T) (hydraulic conductivity (K) per unit depth [L^2T^{-1}]) from its saturated value (T_o) for basin soils with increased soil water deficit given as:

$$T \mid T_o e^{4S/m} \qquad \text{Equation 2-11}$$

Beven *et al*. (1995) describes the 'm' parameter as the effective depth of the catchment soil profile with larger values increasing active soil depth. The storage deficit equation, (Equation 2-10) assumes a constant soil type over the hillslope. However, more recent model innovations (Beven, 1986) allow a spatial soil distribution and use of an alternate form of the index called the soil-topographic index.

Hillslope runoff is generated by a number of mechanisms that have evolved with the development of the model. An infiltration excess (Hortonian) overland flow mechanism has been added in addition to the saturation excess (Dunne type) overland flow which produces runoff when precipitation fills the local saturation deficit, S_i. An additional runoff mechanism, known as return flow, is generated when a positive saturation deficit is calculated for a grid cell. The model has also evolved to include moisture stores that allow unsaturated transfer of infiltrated water to the saturated zone. These moisture stores provide a mechanism for calculating actual ET from potential calculations when unsaturated storage amounts falls below soil moisture field capacity. Outflow from the saturated zone is termed base flow (Q_b) and calculated using the basin average storage deficit as:

$$Q_b \mid Q_o e^{4\bar{S}/m} \qquad \text{Equation 2-12}$$

where Q_o is the maximum base flow generated when there is a zero storage deficit as derived from the area averaged soil-topographic index. While termed base flow, when low saturation deficits interact with high conductivity surface soils, as determined from Equation 2-12, one might regard this as a storm flow component (known here in as interflow).

It is important to note that TOPMODEL equations are derived from first principles, given a number of assumptions regarding hillslope hydrological processes. This is in contrast to the VIC/ARNO method that fits an empirical function to the determination of saturated area. This VIC/ARNO relation includes not only the spatial variability of topography and soils, as in TOPMODEL, but also the variability of vegetation and rainfall. Like the VIC/ARNO method, TOPMODEL relies on the determination of saturated area to generate a storm flow responses. Rather than an empirical function, TOPMODEL determines the saturated area explicitly by the intersection of the water table (expressed as a S_i) with the hillslope surface.

A number of efforts have been initiated to extend the resolution of TOPMODEL to MHM scales. These include TOPLATS (Famiglietti and Wood, 1994) and a coupling of TOPMODEL and ISBA land surface scheme (Habets and Saulnier, 2001). Both of these schemes rely on the TOPMODEL framework for the determination of saturated area and hence the partitioning of rainfall into fast and slow response.

TOPLATS

The TOPLATS model, described by Famiglietti and Wood (1994), has built onto the TOPMODEL framework a collection of moisture stores and new energy balance calculations. These additions have essentially created a new LSS but one which has yet to be incorporated into an atmospheric model framework. For small basin applications, TOPLATS

maintains a separate calculation for each DEM based pixel in the watershed. Each pixel has vertical water and energy balance calculations applied to determine local runoff and recharge. Local recharge is then redistributed based on the topographic-soil index method (derived below) which is similar to that given by Equation 2-10. From this redistribution, local depth to the water table and its impact on soil moisture and evaporation can be determined. Small scale pixel representation allows each land surface to be represented uniquely.

A break from this approach is made for marcoscale processes required for large domain problems. At this larger scale, TOPLATS groups hydrologic similarity based on a statistical representation of the topographic-soil index. Here, the statistical distribution of the index is sub-divided into discreet computational elements. By this method, soil water from each saturated zone is essentially coupled together so that moisture is transferred from element to element within the distribution. These water transfers are not done explicitly as in the DHSVM model (Wigmosta *et al*., 1994) where a finite difference mechanism is employed to transfer soil moisture using Darcy's Law, but rather the topographic-soil index is used to distribute the mean soil water deficit throughout the watershed. This procedure preserves the fine scale representation of topography necessary to satisfy TOPMODEL assumptions but loses the representation of the vegetation in doing so. Grid averaged vegetation parameters are used for the scheme since grouping is based on topographic-soil uniqueness. A deliberate choice between a detailed representation of vegetation and topography has been made within TOPLATS which favors topography. This represents an opposite viewpoint from the modeling philosophy presented in this thesis.

To understand more fully the implications of TOPLATS assumptions, a derivation of the soil-topographic index is given below which follows closely that of Hornberger *et al*. (1998, p. 214). Given an element of soil from a hillslope, two equations can be used to describe moisture flow through it. The first is based on simple continuity and the second based on Darcy's Law:

$$Q = RA \qquad\qquad Q = Tc\tan\beta$$

Equation 2-13

Continuity *Darcy's Law*

where R is the recharge rate, A is the surface area of the element, and c is the contour length through which the section drains. These equations are combined under an assumption of steady-state conditions to give:

$$RA = Tc\tan\beta \qquad \text{Equation 2-14}$$

Given the exponential decline of conductivity with saturation deficit, defined by Equation 2-11, an expression in terms of the saturation deficit can be obtained as:

$$\bar{S} = -m\ln\left(\frac{RA}{T_o c\tan\beta}\right) \qquad \text{Equation 2-15}$$

The basin average soil moisture deficit can also be expressed taking the area average value as:

$$\bar{S} = \frac{1}{A_t}\sum_i -m\ln\left(\frac{RA}{T_o c\tan\beta}\right) \qquad \text{Equation 2-16}$$

where A_t is the total area of the basin. Early versions of the model assumed that R, T_o, and m where constant over the basin meaning they could be removed from the summation and eliminated by subtraction with those derived at a point. If soil properties (T_o) are given non-constant values over the basin and an upstream area per unit contour length is defined as a=A/c then the equation for a point, given by Equation 2-15 can be subtracted from area averaged form, Equation 2-16, to yield:

$$S - \bar{S} = m \ln\left(\frac{RA}{T_o c \tan\beta}\right) - \frac{1}{A_t}\sum_i m \ln\left(\frac{RA}{T_o c \tan\beta}\right)$$

Equation 2-17

$$S - \bar{S} = m\left(\nu - \ln\left(\frac{a}{T_o \tan\beta}\right)\right)$$

where $\ln(a/T_o \tan(\beta))$ is the topographic-soil index for a grid element and ν is the average basin area topographic-soil index. Sauliner *et al*. (1997) have also expressed the same equation with non-constant values of 'm', the effective soil depth, in a similar fashion. Using Equation 2-17, TOPLATS redistributes soil water down-slope without the need to explicitly define fluxes from cell to cell. An alternate formulation of this expression is given as an equivalent water table depth under an assumption that soil moisture over field capacity drains rapidly to form a water table.

Distribution of the soil-topographic index in TOPLATS is determined based on a three parameter gamma distribution. This distribution is divided into discreetly binned ranges and separate hydrologic calculations are performed for each bin. Typically, seven or eight class bins from the soil-topographic index distribution are used with each class given the same spatially averaged vegetation parameters and forcing dataset. The only difference between

each of the classes in an atmospheric model grid cell is the depth of the water table which is dynamically redistributed based on the TOPMODEL equations.

ISBA - TOPMODEL

Habets and Saulnier (2001) describe a linkage between the TOPMODEL and the ISBA land surface scheme. Previously, Habets *et al*. (1999) adapted ISBA to use the ARNO scheme for determination of saturated area by using the empirical storage versus saturated area relation, described previously. This ARNO based method was tested within the Rhone basin (Etchevers et al., 2001). However, the topographic index provides a more physically based approach to the determination of saturated area. Rather than building a LSS structure for TOPMODEL as is done by TOPLATS, ISBA-TOPMODEL has extracted only the concept of saturated area determination and applied this to the existing ISBA scheme.

The IBSA LSS (Noilhan and Planton, 1989) is built upon the force-restore scheme of Deardorff (1978) described previously. A downside to the wider use of the force-restore scheme has been the difficulty in describing the parameters C_1 (forcing term) and C_2 (restore term) for different soil textures. These parameters are used to control the distribution of soil moisture between the upper and lower layers. Unlike many other LSS that have implemented Richard's equation solutions for soil water flow (such as CLASS, SiB, and MOSES), the force-restore parameters cannot be directly linked to soil physics concepts.

Noilhan and Planton (1989) devised a scheme to estimate the C_1 and C_2 parameters for various soil textures by fitting force-restore behavior to that of a reference model. This reference model consists of a twenty-six layer scheme that resolves temperature and soil moisture based on the Fourier and Darcy equations. A fitting approach is used to calculate

C_2 and is used to check the forcing term, C_1 which is derived from a diffusion approximation of Richard's equation with a specified sinusoidally varying surface forcing boundary. The results are equations for both parameters in terms of the current moisture content and are given as:

$$C_1 = C_{1sat}\left(\frac{\chi_{sat}}{\chi_g}\right)^{b/2+1} \qquad C_2 = C_{2ref}\left(\frac{\chi_2}{\chi_{sat} - \chi_2 + \chi_l}\right) \qquad \text{Equation 2-18}$$

where 'b' is the Clapp and Hornberger soil disconnectivity index, C_{1sat} and C_{2ref} are specified ordinal values for 11 soil texture classes and χ_l is a small value used to prevent division by zero results near saturation. In addition to calculated values of C_1 and C_2 based on soil type, it was recognized that the upper layer soil moisture should restore to a value based on a balance between gravity forces and capillary forces rather than the average column soil moisture (χ_2). A polynomial fit was used to determine this equilibrium soil moisture restore value based on the χ_2 as:

$$\chi_{geq} = \chi_{sat}\left(\frac{\chi_2}{\chi_{sat}} - a\left(\frac{\chi_2}{\chi_{sat}}\right)^p - a\left(\frac{\chi_2}{\chi_{sat}}\right)^p\right) \qquad \text{Equation 2-19}$$

where 'a' and 'p' are fitted parameters based on the on ordinal soil texture descriptions.

Early versions of the model were intended for short range forecasts (less than a few days) where χ_g and χ_2 are initialized based on observations. However, extended time integrations produced excessively large soil moisture results. This required the addition of a lower layer drainage function to simulate base flow production. Mahfouf and Noiliah (1996) added this

base flow formulation to the original Deardorff (1978) equations that restores, over time, the lower layer soil moisture to field capacity as follows:

$$\frac{\partial \chi_g}{\partial t} = \frac{C_1}{\psi_w d_1}(P - E_g) - \frac{C_2}{\vartheta_1}(\chi_g - \chi_{geq}) \quad \text{for } 0 < \chi < \chi_{max} \qquad \text{Equation 2-20}$$

$$\frac{\partial \chi_2}{\partial t} = \frac{1}{\psi_w d_2}(P - E_g) - \frac{C_3}{\vartheta_1}\max(0, (\chi_2 - \chi_{fc}))$$

where χ_{fc} is field capacity defined for this purpose as the soil moisture where the hydraulic conductivity falls to 0.1 mm day^{-1} and C_3 is a soil type dependent constant estimated by fitting the force-restore drainage scheme to a simplified Richard's equation solution. This fitted function is given as:

$$C_3 = \frac{5.32(\text{Clay Fraction})^{1.042}}{d_2} \qquad \text{Equation 2-21}$$

Clearly, ISBA's force-restore scheme relies heavily on the empirical derivation of the constants C_1, C_2, and C_3 developed specifically for ISBA. Other land surface schemes, which use a Richard's equation solution of unsaturated flow, benefit from the large body of literature that exists for their parameterization. Introduction of the non-linear force parameter (C_1) also creates a non-linear system of differential equations which creates a more complicated solution when compared to Deardorff's (1978) original linear system. An additional downside of the method is that while behaving well for average moisture conditions for which it was calibrated, inferior results are produced for extreme wet or dry conditions. While there are some disadvantages to the use of the ISBA scheme, atmospheric models that traditionally rely on Deardorff's force-restore method can benefit from a wider

variety of soil type specifications and an improved prediction of soil moisture due to χ_2 recovery toward field capacity. This is the case for the Canadian GEM model which has recently implemented the ISBA LSS operationally.

Implementation of TOPMODEL within ISBA uses the cell average moisture content (χ_2) to predict the saturated area fraction based on the topographic index. The average storage deficit ($\overline{S}$) is determined by calculating the depth of water equivalent soil moisture between the current value (χ_2) and the saturated value (χ_{sat}) as:

$$\overline{S} = (\chi_{sat} - \chi_2) d_2 \qquad \text{Equation 2-22}$$

The maximum storage deficit is also required to derive the effective soil depth 'm' and is simply determined as the difference between the wilting point moisture (χ_{wilt}) and the saturated moisture content as:

$$S_o = (\chi_{sat} - \chi_{wilt}) d_2 \qquad \text{Equation 2-23}$$

Habets and Saulnier (2001) state that the parameter 'm' which linearly links the difference in local and average topographic index with the difference in local and average soil moisture deficit can be defined as $m = S_o/4$. They argue that, for an exponentially decreasing transmissivity with depth, 98% of the total transmissivity of an infinitely deep soil column is contained within four times m, the effective depth.

Testing of the scheme has been performed for each 8x8 km grid cell of the Ardeche Basin located in north-east France by determining the topographic index for each cell within a 75m spatial resolution DEM and determining the area averaged value of the topographic index (ς)

for each 8x8 km grid. A simple subtraction is made from the value of $\overline{S}$, determined each time step from the ISBA soil moisture, to calculate the number of the 75m grid cells which are saturated ($S_i > 0$). This can be determined by rearranging Equation 2-10 in the form:

$$S_i = m\left(\varsigma - \ln\left(\frac{a}{\tan\beta}\right)\right) - \overline{S} \qquad \text{Equation 2-24}$$

where ς the average averaged topographic index is calculated as:

$$\varsigma = \frac{1}{A_t}\sum_i \ln\left(\frac{a}{\tan\beta}\right)_i \qquad \text{Equation 2-25}$$

The number of saturated DEM cells is then used to calculate the fractional saturated area and hence the fraction of precipitation which becomes direct surface runoff. Note that no return flow, defined as the depth of water above saturation, is calculated from excess positive values of S_i and base flow is calculated from the ISBA force-restore methods rather than from the TOPMODEL formulation. This new method is very similar in practice to the implementation of ARNO method within ISBA but has the advantage of explicitly representing the spatial variability of topography and could be adapted to include soils information using the topographic-soil index if such detailed information was made available.

2.2 Chapter Summary

The discussion above has highlighted two basic methods through which quick flow hydrological processes are implemented within atmospheric simulations. These basic groupings are:

1. Lateral flow through a soil layer based on Darcy's Law and flow through porous media theory. This method is used by the GFDL GCM and the PLACE land surface scheme.

2. Determination of the portion of the watershed area that exists in a saturated state and calculation of the quick flow response based on over land runoff from the catchment. Two methods have been used for the calculation of saturated area: i) TOPMODEL theory which explicitly determines the saturated area based on the intersection of the water table with the land surface topographic features and ii) empirically using VIC/ ARNO/ Xinanjiang based functions which relate saturated area to average basin wetness through a calibration exercise. Both these methods have been implemented in the ISBA land surface scheme and other models such as the UK Met Office Surface Energy Scheme (MOSES) are implementing the VIC/ ARNO/ Xinanjiang approach (Blyth, 2001).

In the next Chapter, the methodology used to implement WATFLOOD within the CLASS land surface scheme is examined. WatCLASS, as the coupled model is known, shares much in common with the GISS GCM implementation with respect to its categorization as a aquifer flow model. However, horizontal conductivity in upper soil layers is enhanced due to

the presence of macropores and other lateral conductivity enhancements. This flow enhancement borrows much from TOPMODEL theory.

It is interesting to consider that the determination of moisture flux travel distance during a time step (a length) in a shallow aquifer model multiplied by the length of stream channel to which it is contributing (a width) is not dissimilar to the determination of the portion of saturated area of a watershed in any one time step (area = length * width). While the conceptual view of shallow aquifer flow and saturated area determination differs somewhat, the spatial area of the watershed that contributes to quick flow and the ultimate response to rainfall inputs are likely to be very similar. The only real difference between the two model forms is in the determination of whether water interacts with soil or simply runs off the surface. This does not have immediate impacts for soil moisture simulation in land surface models but may become important in determining sediment and chemical migration from the land surface as atmospherically based modeling grows into other forms of environmental prediction.

3 Model Development

The purpose of this chapter is to present the theory used in the development of the WatCLASS model. WatCLASS has been designed to include features from each of its parent models, WATFLOOD and CLASS. These components allow the simulation of streamflow through a water budget mechanism using lateral flow generation derived from WATFLOOD and land surface energy fluxes from its energy budget supplied by CLASS. Tight coupling between water and energy dependent processes, such as evaporation and ground ice, provide the greatest potential for improving prediction. However, these same interactions also cause the greatest difficulty within the model since the detailed physics of energy and water interactions in the earth-atmosphere interface has yet to be detailed in full and is often rooted in empirical relationships. Here, the introduction of streamflow generation, which have been shown to be successful in WATFLOOD, are introduced to CLASS to assess its implications for land surface scheme modelling.

3.1 Motivation

In addition to the overarching motive for development of coupled land surface and hydrologic models, presented in Chapter 1, there are more practical motivations for developing a model such as WatCLASS. These motives are drawn from more immediate needs of the two modelling groups which contribute to this modelling effort. For the hydrologist, a great source of modelling uncertainty lies in the spatial and temporal uncertainty of precipitation inputs to the hydrologic model. Given perfect precipitation inputs, the task of streamflow prediction would be made much less onerous. For the atmospheric scientist, there is also uncertainty regarding the inputs of land surface heat and

moisture to the atmospheric model which are functions of surface wetness. Without accurate land surface boundary conditions, the atmospheric scientist is very unlikely to be able to predict patterns of weather and land surface climates which include precipitation.

The prediction of streamflow is based, in part, on the accuracy of precipitation and the prediction of precipitation is based, in part, on the behaviour of the land surface which includes the generation of streamflow. The motivation therefore is a cyclical process of continual improvement where precipitation simulation advances, resulting from better simulation of land surface fluxes, reduces the error associated with streamflow forecasts and around again to improved precipitation through a soil moisture simulation mechanism. This process is an integrated one which provides not only an validation data source to the atmospheric modeller through streamflow prediction but a built-in mechanism for improving the simulation of soil moisture.

3.2 Coupling Methodology

To couple WATFLOOD, CLASS and atmospheric models in a coherent structure that provides feedback to each part, a phased implementation is required. Theories regulating the generation of streamflow have been developed, yet to implement them directly into an atmospheric model is a daunting challenge. Therefore it is necessary to provide a mechanism of component model assembly to ease the process of integration and solidify new concepts prior to implementation within the fully coupled model.

In addition to logistical requirements for model integration, the WATFLOOD to CLASS coupling requires some modification to WATFLOOD's interflow generation mechanism to accommodate the range in soil properties available within CLASS. This involves the

relaxation of the WATFLOOD linear interflow model with a more generalized power function relation which is more suited to CLASS's soil parameterizations. Here, rather than assuming constant soil porosity and variable 'field capacity' which enables WATFLOOD to use a linear drainage simplification, the reverse situation is used instead. For WatCLASS, variable soil properties and a constant 'field capacity' (based on a suction head specification) are used. This principle is in keeping with practices developed for soil physics and modern theories of stomatal evaporative control.

3.2.1 Model Integration

To realize the goal of a coupled atmospheric-hydrologic model, a phased integration strategy was required. Without a phased approach, direct coupling of hydrologic processes would proceed in a haphazard fashion without benefit of the development of model components within controlled environments. Aims of the current strategy are to:

1. Use existing models that have computationally similar modelling environments in order to ease integration.

2. Set an appropriate division of tasks that is compatible with existing model development and allows smooth transition to an eventual coupled model product.

3. Evaluate the coupled model and develop controlling parameters using a variety of land surface types and for extended simulation periods.

4. Use physical hydrologic principles to control the partitioning of soil water on both the wet and dry sides of field capacity.

Models selected for the integration of atmospheric and hydrologic models in Canada have evolved over a number of projects. Initially, under a project sponsored by the Land-Air node of the Canadian Climate Research Network (CCRnet), the CLASS land surface scheme was

combined with the WATFLOOD hydrologic model. This first attempt at model integration was accomplished by replacing the vertical water balance and degree-day energy parameterizations within WATFLOOD with a point version of the CLASS model (Snelgrove, 1996). This project allowed conceptual differences between the model structures to be explored and for 'proof of concept' runs to be performed. Initial runs, over selected southern Ontario watersheds, showed that the CLASS water balance could generate realistic streamflow hydrographs when an interflow mechanism was provided (Soulis *et al*., 2000). Adding CLASS to the WATFLOOD structure (rather then visa versa) allowed CLASS to remain as a simple 'black box' which acted simply as a plug-in to WATFLOOD. This eased code integration and allowed initial runs to be performed with only limited knowledge of CLASS water and energy balance mechanisms.

Later projects, including the Saguenay flood study (Lin *et al*, 2002) and follow-on Land-Air node efforts required that lateral flow generation concepts from WATFLOOD be integrated into the CLASS structure; in effect, the reverse of the previous effort. This reversal in modelling philosophy was necessary because CLASS already existed within atmospheric models and WATFLOOD did not. Stronger atmospheric model ties stem from the origin of CLASS which was developed as a land surface scheme for the Canadian GCM. WATFLOOD alone could not be easily incorporated within an atmospheric model because it lacks the necessary energy balance calculations to function as an atmospheric model boundary condition. Rather than overhauling WATFLOOD to act as a land surface scheme, which was the approach taken by both TOPLATS and VIC-2L discussed previously, it was more practical and useful to extract important hydrologic concepts from WATFLOOD and include them in CLASS structure. The essence of this transfer was the inclusion of

streamflow generation mechanisms from WATFLOOD including surface runoff, interflow, and baseflow generation and implementing these deep within the structure of CLASS such that they would impact both the water and energy processes. As discussed in Chapter 2, other land surface schemes, including MOSES and ISBA are utilizing similar strategies with other hydrologic modelling forms.

Other transfers required to complete the integration of CLASS and WATFLOOD included i) the elimination of parameter blending used by CLASS and its replacement with the GRU concept, and ii) the addition of the WATFLOOD streamflow routing algorithms. Figure 3.1 illustrates these additions. Coding of these additions from WATFLOOD theory to the CLASS structure are attributable to Whidden (1999) based on the previous work of Snelgrove (1996). These developments have led to the stand-alone hydrological model known as WatCLASS and a version of the CLASS model with a controlled lateral runoff generation mechanism.

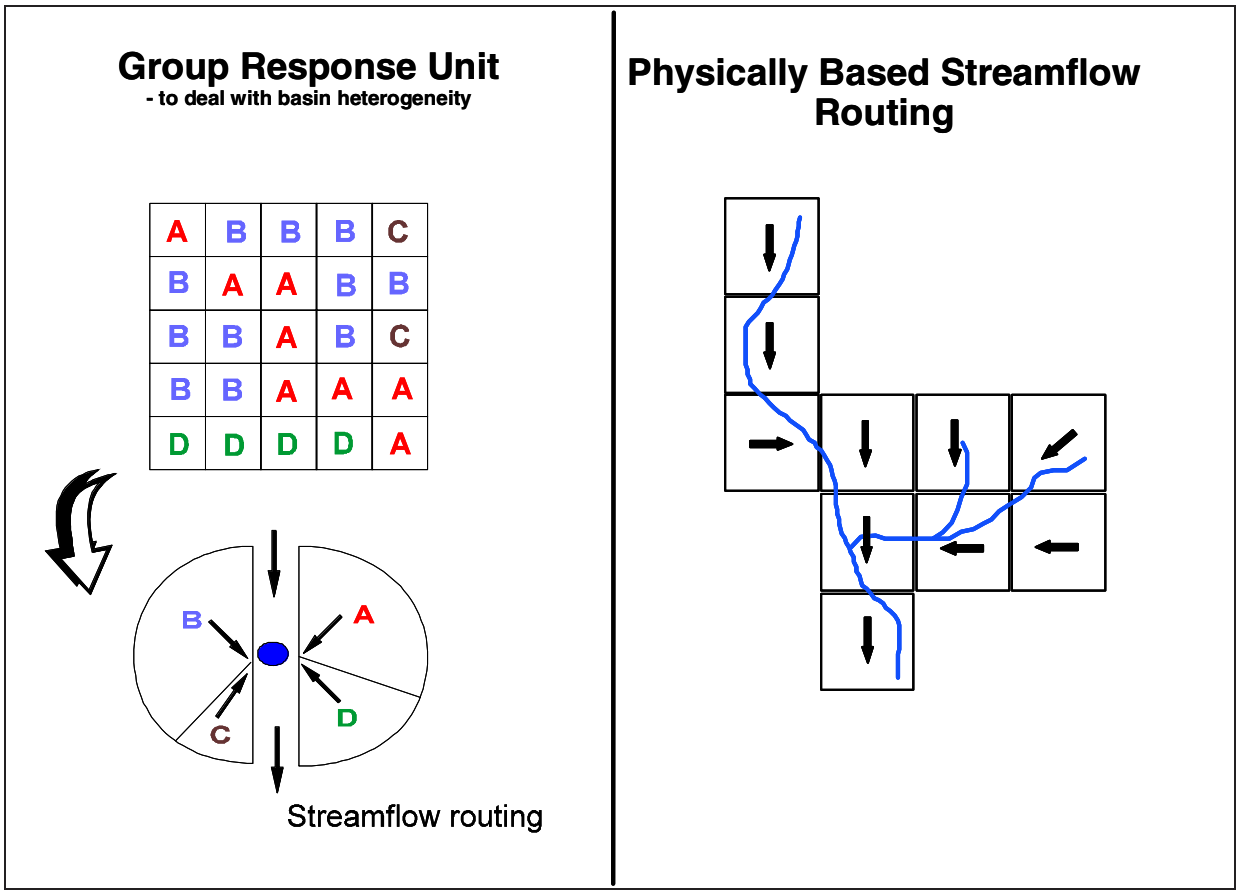

Figure 3-1 : Conceptualization of the GRU method with land cover factions grouped into 4 computational elements from the original 25 components (after: Donald, 1995) and routing of streamflow through grid squares making up a sub-watershed.

Level I Modelling

WatCLASS development has paralleled other Canadian coupling efforts. These efforts have been centered on the integration of CLASS within various atmospheric models including the Canadian GCM which has incorporated CLASS in the third generation of the atmospheric circulation model (AGCM-III) (McFarlane *et al*, 2001), the Canadian regional climate model (RCM) which has included CLASS for experiments over the Mackenzie River basin (MacKay *et al*., 2002), the Meso-Scale Community Climate model (MC2) which includes CLASS as a land surface scheme option (Lin *et al*., 2002) for short term, limited area forecasts, and the Canadian global forecast model (Delage and Verseghy, 1995) which has

experimented with CLASS as a future land surface scheme. Experimentation and implementation of CLASS within atmospheric models allows issues related to atmospheric - land surface coupling to be resolved concurrently with the implementation of hydrologic processes from WATFLOOD. This phase of model integration where a modern land surface scheme interacts with the lower boundary of an atmospheric model is referred to here as Level I coupling.

Level II modelling

This 'levels' concept of model development has other hierarchical designations as well. The coupling of a hydrologic model with a land surface scheme, of which WatCLASS is an example, is known as a Level II model. Here, the generation of runoff in a manner which satisfies streamflow requirements has a two-way or coupled effect with land surface scheme soil moisture and therefore an impact on the surface energy balance. For Level II modelling, measured surface forcing fields including precipitation, radiation, wind speed, humidity, pressure, and temperature are used as driver datasets in place of a coupling with an atmospheric model. In this way, alternate forms of forcing data including atmospheric model archives and radar precipitation estimates maybe used together with or in place of measured gauge data. The use of the Level II model allows identification of controlling hydrologic parameter based on high quality measured forcing datasets that are not influenced by biases and errors associated with concurrent atmospheric model simulation.

A logistical benefit is also gained by separating the Level II model from the atmospheric model. This is because large area, long time period simulation, necessary to develop Level II parameters, using atmospheric models often requires the use of large super computer platforms that were not available for this project. Level II models, while still requiring

significant computing resources, can be run on more readily available high-power workstations.

Other benefits may be derived from Level II models beyond strictly water and energy studies. Application studies in such areas as agriculture, environmental impact assessment, and reservoir operation may also be performed in a similar manner to traditional hydrologic model studies. These application studies will assist in the further development of the WatCLASS Level II model by posing interesting research questions which require new and innovative ways of thinking about the hydrologic system. These questions may also help guide and give direction to future projects involving field data collection. Simpler methods may now yield superior results. However, developing models of increased complexity is required in order to gain insight into hydrological processes. This may well and should lead back to simpler modelling forms but not without enhancing our understanding of the system processes.

Level III Modelling

The ultimate integration of atmospheric, land surface, and hydrologic models is referred to as Level III modelling. Within this phase of modelling, fluxes of heat and water vapour from the land surface are altered by soil moisture changes due to the addition of hydrological model control. These changes impact atmospheric energetics and may prove to increase climate model accuracy and weather prediction skill. Early indicators of these potential impacts are evident from Level I coupling results. Arora and Boer (2002) have shown that stomatal resistance functions used by CLASS tend to decrease atmospheric water vapour content and improve model simulations, including precipitation amounts, in the current

version of the Canadian GCM. This improvement, over previous versions of the Canadian GCM, has been attributed to the addition of CLASS.

Work toward full Level III modelling in Canada has been initially directed toward short period weather forecast modelling. Here, WatCLASS was coupled with the MC2 atmospheric model for simulation of the large 1996 flood event which occurred over the Saguenay region of Quebec. The MC2-CLASS-WATFLOOD Level III model, developed during this study, was able to reproduce the measured hydrographs responsible for the devastating flooding. However, the short duration of the weather prediction simulation (only 48 hours) was dominated by the influence of initial atmospheric conditions. These initial conditions were generated by operational data assimilation methods and their influence masks the role of the altered land surface in influencing the atmospheric simulation. Longer periods of integration with a focus on climate rather than weather prediction are required to make definitive statements concerning the implications of improved hydrology on atmospheric simulations. Experiments of this type are currently underway with a RCM based implementation of the Level III model over the Mackenzie River basin. The remainder of this thesis will focus on the lower boundary supplied to atmospheric models through Level II simulation leaving Level III results for future research.

Level 0 Modelling

A modelling level designation has also given to interactions of atmospheric models with traditional hydrologic models. This model development level allows one-way transfer of surface forcing data from an atmospheric model to a hydrologic model for the purpose of atmospheric model evaluation and is referred to as Level 0 modelling. Yarnal *et al*. (2000) refers to one-way modelling as 'linkage', reserving the word 'coupling' and the phase 'coupled

model' to two-way interactions or in the present case each of Level I, II, and III models. While Level 0 modelling offers no direct feedback to the atmospheric model, its use as a tool for evaluation of atmospheric model output has been often demonstrated. In this situation, a calibrated hydrologic model acts effectively as a large rain gauge whose surface area is that of a watershed. **A**nalysis of the resulting hydrologic model streamflow output allows interpretation of the distribution and timing of atmospheric model precipitation and to a lesser extent radiation and temperature fields which influence evaporation. Examples of W**A**TFLOOD participation in such studies are numerous and include southern Ontario evaluation of MC2 precipitation and radar rainfall estimates (Benoit *et al.*, 2000), simulation of reservoir inflows for British Colombia (BC) Hydro (Bingeman, 2001) using boundary layer model precipitation and weather prediction storm maxima, and near real time flood forecast prediction from a number of atmospheric model simulations for the Meso-Scale **A**lpine Project (M**A**P) for the European **A**lps (Benoit *et al.*, 2002).

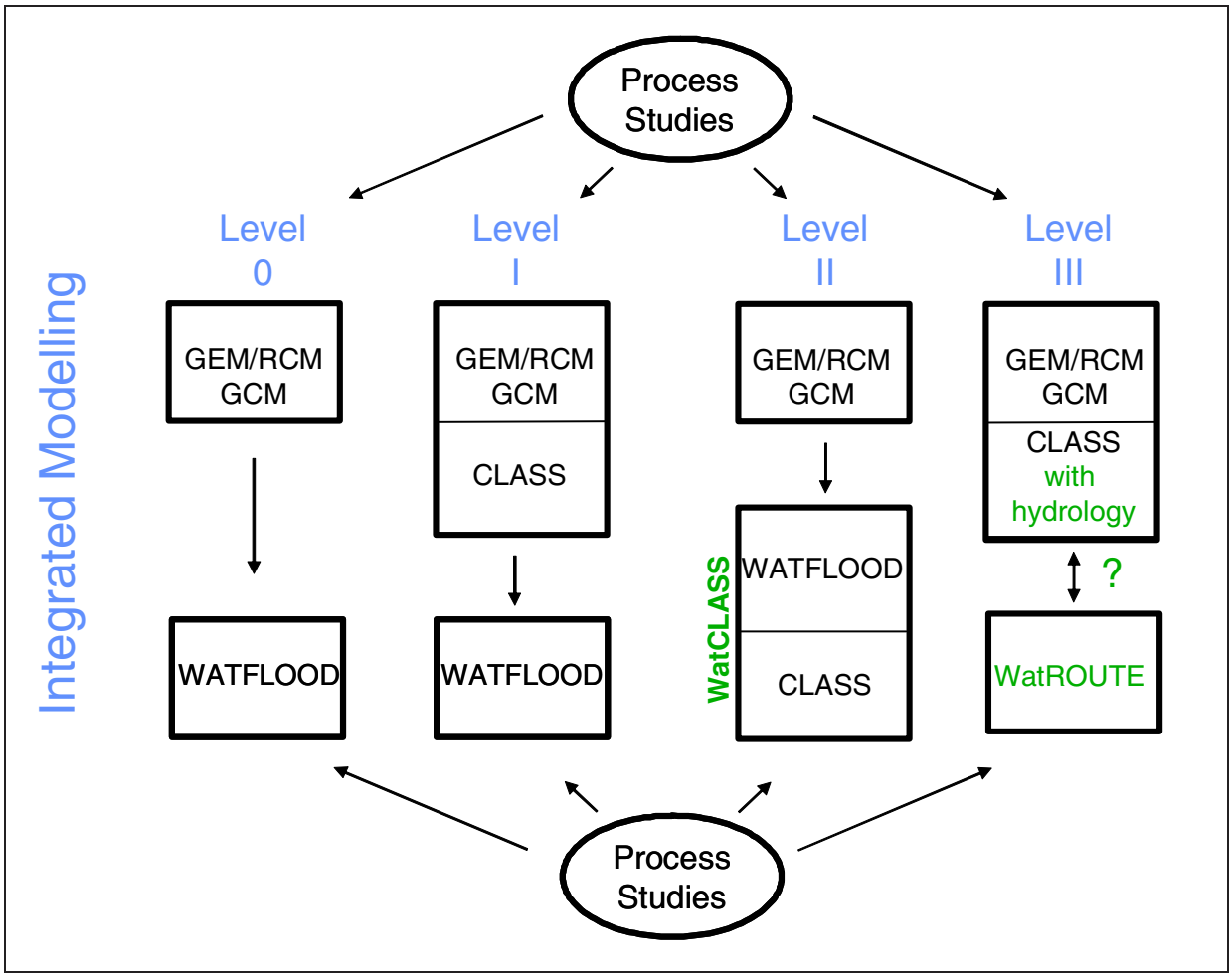

Figure 3-2: Levels coupling strategy for integration of hydrology within atmospheric models. Arrows depict points of model linkage while coupling is shown as joined boxes.

Figure 3.2 depicts the coupling strategy used to develop the Level II model so that it may be introduced naturally into the Level III structure. The figure shows the Level III model linked rather than coupled to a streamflow routing model, known as WatROUTE. The question mark (?) indicates that a possible coupling between streamflow routing and land surface hydrology may be developed in the future. Currently, runoff generated from surface, interflow, and baseflow sources are assumed to enter the stream channel where they no longer interact with land surface processes. This assumes that streams act only as sinks for land surface moisture. However, a number of situations, including streamflow through arid

regions, agricultural irrigation, and flooding due to limited stream channel capacity result in streamflow losses and additions to the land surface. The impacts of flooding, while devastating to those directly impacted, are often short term and limited area events which would not significantly affect the surface boundary of an atmospheric model. However, there have been situations in areas of low topographic relief and severe flood conditions, such as the Red River flood of 1997, where the natural land surface was transformed from dark bare soil to a large water body that remained for an extend period of time. These processes are not currently represented in WatCLASS or existing Level III models and would be an interesting future research topic because of the coupling required between stream channel hydraulics and land surface processes.

Figure 3-2 also shows process studies feeding into all modelling levels indicating that each model level is under continued development. Some interesting areas of this development work for WATFLOOD and WatCLASS include (i) the representation of wetland water sources and sinks, (ii) the influence of frozen ground on soil water movement in WatCLASS, (iii) the linkage of WATFLOOD with other land surface schemes such as ISBA, and (iv) the development of pollutant mass balances for modelling the fate and transport of other constituents.

In practice, WatCLASS serves as a complementary model to WATFLOOD by allowing detailed soil process and energy balance investigations to be carried out with WatCLASS following an initial water balance analysis with WATFLOOD. This is similar to the dual modes of operation available within the VIC-2L model (Liang *et al*., 1994) in which energy based processes are modelled either with full energy balance methods or with parameterized energy processes using temperature based surrogates. Important for the use of WatCLASS,

is the decreased computational time offered by WATFLOOD, which runs approximately two orders of magnitudes faster than WatCLASS. Decreased computation time allows many of the streamflow hydraulic and land surface hydrologic parameter selections to be made using optimization methods contained within WATFLOOD. Initial investigations using WATFLOOD also allow the quality of the input data, especially precipitation, to be evaluated prior to commencing with the extra computational burden and model complexity introduced by WatCLASS. Once determined for a calibrated WATFLOOD watershed, many of the parameters and characteristics of the drainage layer data base may be transferred directly to WatCLASS. An example of this includes the use of the automatic watershed delineation program MAPMAKER (Seglenieks, 1998), which sets up streamflow routing directions, aggregates internal land slopes, and develops land class distributions from remote sensing data. Important parameters transferred directly to WatCLASS from WATFLOOD include those which control base flow, overland flow, and streamflow routing.

Solution Uniqueness

Solution uniqueness must also be considered when developing the WatCLASS model and its parameters. Beven (2001, p. 19) states that estimation of parameters from measured data alone is generally not possible due to limitations of current measurement techniques. This requires that some parameter estimation technique be employed to determine their value based on a goodness of fit between measured and modelled streamflow or other suitable data set. In addition, Beven (2001, p. 21) argues that, because the hydrologic problem is ill-posed, there will be many parameter sets that give equally good fits to the data and that a final parameter selection must be considered purely arbitrary. Beven uses the termed 'equifinality' to describe a group of parameters and models which are 'behavioural' or

believable. Recognizing this equifinality, Beven (2001, p. 234) proposes that a generalized likelihood uncertainty estimation (GLUE) be used to estimate the uncertainty associated with each combination of parameter set and model formulation. This method requires that a set of equifinal results be generated from Monte Carlo experiments. Data from these experiments is all retained for uncertainty analysis.

While the concept of determining modelling confidence intervals is appealing, the computational constraints imposed by the many Monte Carlo simulations would be excessive for WatCLASS. Instead, for the present analysis, extended multi-year simulations are conducted over a variety of land cover types. Use of long integration periods reduces the dependence on initial conditions so that rainfall antecedent conditions are predicted based on the physics of drainage and evaporation in the model. Additionally, a strategy of parameter disaggregation is employed to increase parameter dependence on measurable properties of the watershed so that the variability of the remaining unexplained parameters is reduced.

Field Capacity

The goal of this research is to bring the essence of physical hydrologic processes to a land surface scheme and, through the LSS connections with atmospheric models, onward to influence climate and weather prediction simulations. Changes introduced to CLASS may be considered with respect to field capacity soil moisture. The concept of 'field capacity' has been found to have great utility but remains a poorly defined term. The original concept was established to differentiate between rapidly draining gravitational water and water held in the soil column by capillary force and was initially reviewed by Veilhmeyer and Hendrickson (1950). Field capacity has practical significance for hydrologists since it defines a soil moisture content below which runoff generating processes no longer produce significant

streamflow contributions. Unfortunately, there is no definite point where gravitational flow from a soil column suddenly stops since current unsaturated flow theory shows that the vertical redistribution of soil moistures continues to decrease as drainage approaches zero asymptotically. This has lead to many definitions of field capacity which often conflict with one another. These definitions range from the soil moisture remaining after a soil, which has been thoroughly wetted, has been allowed to drain for 2 or 3 days (Veilhmeyer and Hendrickson, 1952) to that of Bear (1972, p.438) who concludes that no clear definition can be applied except to use the ultimate irreducible soil moisture content (χ_r). This later definition, along with that of Hillel (1998), essentially concludes that the term is poorly defined and has no real physical interpretation.

While the meaning of the term 'field capacity' has been debated, many researchers still use the term to describe the soil moisture value at which moisture flow through the soil column becomes very low. Below field capacity, evaporation alone dominates the hydrologic regime and flow generation algorithms become unimportant. Above field capacity, drainage and fast runoff processes dominate soil moisture change over relatively short time intervals when compared to evaporative losses. This distinctive separation between evaporative and runoff dominated processes focuses attention on field capacity and the rate at which processes move toward or away from some threshold value.

Complicating matters for LSSs is an overlap and a co-dependence between evaporation and runoff which manifests itself as soil moisture. Below field capacity evaporation begins to decrease as soil moisture decreases and above field capacity the rate of runoff increases as soil moisture increases. In a balanced scenario, parameters controlling runoff would reduce

soil moisture to field capacity at just the time that vegetation begins to be stressed by soil moisture reductions. In the same light, parameters controlling evaporation would reduce soil moisture just enough so that rainfall additions to soil moisture induce a runoff response that would match streamflow hydrographs. Unbalanced situations, which leave soil moisture above field capacity due to poor parameterization of vertical drainage and/or horizontal runoff, lead to higher evaporation rates, cooler surface temperatures, and poor partitioning of the incoming energy. Thus, the key to joint simulation of evaporation and runoff, in a balanced response, is to focus both on a "field capacity based" soil moisture.

To develop a model that can better predict the onset of field capacity conditions requires datasets that contain simultaneous measurements of both evaporation and streamflow. New experiments which seek to understand land surface processes are collecting data to address this need. One such experiment that has both measured runoff and evaporation data is known as the Boreal Ecosystem-**A**tmospheric Study (BOREAS) (Sellers *et al*., 1995) and forms the basis on which this thesis is developed.

3.2.2 Scaling Strategy

Much has been written about scaling of the hydrologic system (eg. Michaud and Shuttleworth, 1996) and experiments including the BOREAS project (Sellers *et al*., 1995) have been designed to make assessments of the loss of information that occurs in moving from point scale to plot scale and onward to regional scales that are represented within GCM grid squares. No new approach to scaling is developed here but instead parameters that include scale are introduced that allow flow generation mechanics to maintain relative scale independence.

The question of scale is further reduced by adopting the existing strategy used by WATFLOOD that has been successful in reproducing streamflow from a grid based system with elements that range in size from 4 km^2 to 2500 km^2. Here it is accepted that information loss occurs as the domain of the solution area increases and the resolution of inputs to the system degrades. Some of these degrading influences, which are sources of modelling error, include the decrease in average land surface slope introduced through the use of coarse topographic information and the loss of land class information from significant but spatially discontinuous features of the landscape, such as wetlands, that are underrepresented in coarse resolution remote sensing imagery. However, by maintaining a maximum size of 2500 km^2 (50x50 km grid) much of the variability in the atmospheric forcing data is captured. What is employed here is the GRU concept, described in Chapter 1 and illustrated in Figure 3.1, which captures much of the spatial heterogeneity of the hydrologic system; provided that variability of the original input data sources have not been previously lost by other "averaging" techniques.

For streamflow generation within a large grid square, a sub-grid representation of the micro-stream channel network is implicitly included. This captures the behaviour of the characteristic hillslopes that contribute to the larger system. Because of the sub-grid nature of these streams, individual hillslopes that exist in the natural world do not exist within the model. Instead, their characteristic outflow response is determined by the portion of time water remains in the fast stream channel portion of the sub-grid compared with time in the slower sub-grid soil matrix. This is determined for any size grid by preserving the length of the typical valley hillslope in a similar fashion to the sink distance used by Rozenzweig (1998) in the GISS GCM that is shown in Figure 2-1. However, rather than using a fixed

distance of 10m as the sink distance for all grid squares, a geomorphologic property of a watershed known as drainage density, D_D is used instead. By utilizing drainage density, relative differences between terrain features in large watersheds can be used to disaggregate the physiographically controlled drainage density portion of a calibration parameter. Without this type of disaggregation, transferability of controlling parameters between watersheds would be reduced. Determination of drainage density and typical values for the BOREAS watersheds are presented in Chapter 5.

Sampling strategies may be devised to provide increased input data confidence. An example of such a technique might be to augment a coarse resolution DEM with finer resolution samples for greater accuracy in determining the land surface slope. However, until methods for dealing with heterogeneity of the land surface are devised, errors will continue to be captured and compensated for by model parameters.

3.3 Process Enhancement

The coupling of CLASS and WATFLOOD to form WatCLASS requires that changes to the CLASS generation of runoff be made to be more consistent with WATFLOOD methods. The essence of this change is presented in the Figure 3.3. The original CLASS soil structure allowed only instant surface runoff and Darcy drainage. When WATFLOOD algorithms are introduced, a new flow generation mechanism from shallow soil layers, termed interflow, is introduced together with a controlled surface runoff generation mechanism. Both of these are influenced by the representative land surface slope of the grid square.

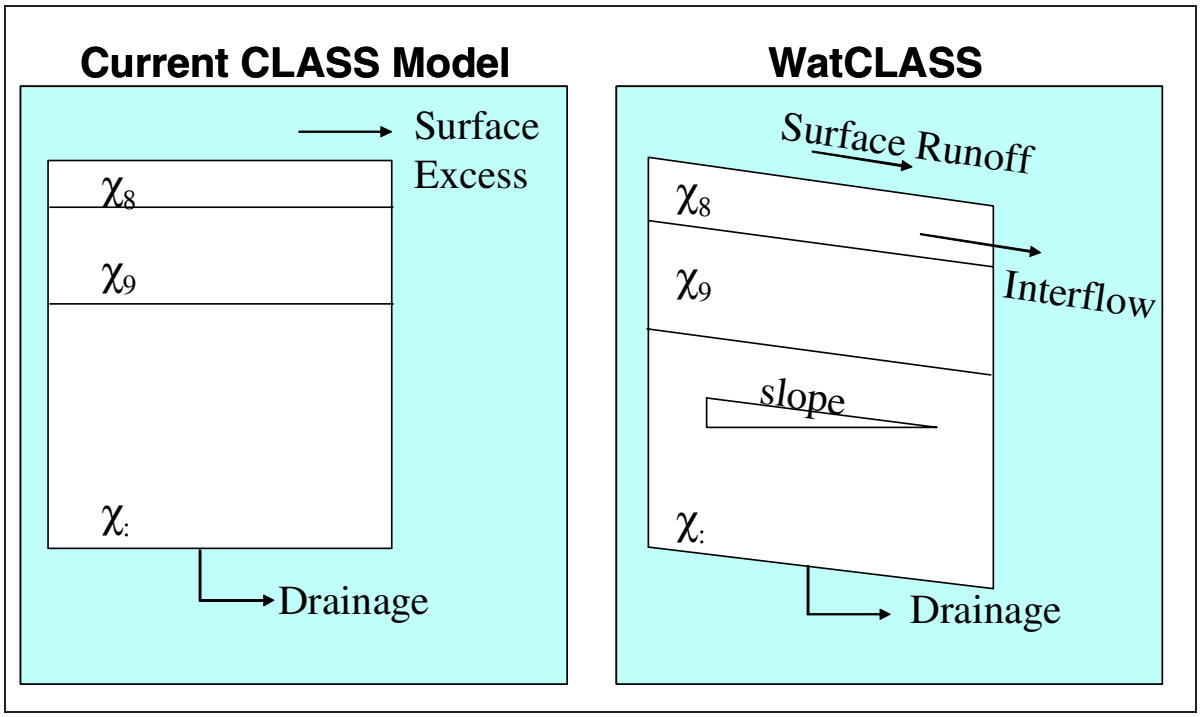

Figure 3-3 : Essence of the WATFLOOD addition for runoff generation to the CLASS soil profile.

3.3.1 Interflow

The majority of the storm water generation in WATFLOOD is generated through an intermediate mechanism known as interflow. Beven (2001, p. 4) describes the earliest stage of model development as a perceptual model. Within this stage, the ideas of the flow generation processes are imagined or envisioned prior to deciding on the governing equations or development of numerical techniques that will be used to solve the equations. A perceptual model of the interflow mechanism used within WATFLOOD consists of flow through shallow upper soil horizons whose lateral conductivity is enhanced when compared to its vertical conductivity. High conductivity surface soils together with a gradient supplied by local topography enable this storm flow pathway to enter a stream channel. Evidence supporting an enhanced lateral flow mechanisms lie both in direct observational evidence and through indirect evidence obtained by streamflow hydrographs analysis.

Direct evidence of enhanced lateral flow mechanisms have been reported in the literature. Some of these mechanisms include: (1) existence large soil pores and cracks known as macropores (Beven and Germann, 1982), (2) gravitationally induced soil consolidation which increases bulk density and decreases conductivity with depth, (3) natural soil development processes which erode and transport fine soil particles to depth forming flow obstructions (Money, 1972, p. 156), (4) increases in soil porosity due to the expansion of frozen water in soil pores, (5) soil particle anisotropy which tend to orientate their largest dimension horizontally (Bear, 1972, p.124), (6) earlier thawing of upper soil layers during spring melt periods (Quinton *et al*., 2000), (7) dynamic anisotropy which occurs during rainfall events initially increasing upper soil wetness and hence lateral conductivity (McCord *et al*., 1991), and (8) funnelled flow where a fine soil overlaying a coarser soil will direct flow laterally along the layer boundary (Walter *et al*., 2000). These physical processes each lead to an enhancement of lateral conductivity but are not individually modelled within WATFLOOD. Instead their combined influence on streamflow generation is determined through calibration.

Indirect evidence supporting the existence of an interflow mechanism stems from the analysis of streamflow hydrographs. The analysis by Freeze (1974) indicates that a perceptual model of a subsurface, saturated storm flow mechanism alone could not feasibly deliver the runoff rates necessary to match observed hydrographs. This has led to other models of storm water generation. Another, once popular, perceptual model has lost favour in more recent times. The theory of a dominant infiltration excess overland flow mechanism was originally proposed by Horton (1933) and has since become known as Hortonian overland flow. This theory is based on generation of surface sheet flow from rainfall which exceeded the infiltration capacity of soil. However, lack of observational evidence has led to

greater acceptance of alternate flow mechanisms (Beven, 2001, p. 12; Dingman, 2002, p. 408). While Hortonian flow is likely not a dominant mechanism, its role during large rainfall events can be very important, especially for flood forecasting.

Other perceptual models exist to explain observed runoff. These have been summarized by Beven (2001, p. 13) and are the basis of many macro-scale hydrologic models. Perhaps the most well known of these are the variable saturated area models of which TOPMODEL, TOPLATS and VIC-2L are examples. As mentioned in Chapter 2, these models use average basin wetness as an index to determine the saturated portion of the watershed and hence the area capable of producing saturation excess overland flow.

Rather than saturated area, WATFLOOD uses a linear response function to generate interflow from within the soil profile. This shallow aquifer flow is generated by:

$$DUZ \mid REC \mid UZS\ 4\ RETN 0\ \Theta \qquad \text{Equation 3-1}$$

where REC is an optimizable lateral flow generation parameter that includes preferential flow effects due to macropores and RETN represents the portion of upper zone storage (UZS) that cannot be drained but is free the evaporate. Gradient energy in the form of land surface slope (Θ) provides the driving force for the system. The RETN term is synonymous to a field capacity like term in unsaturated flow theory. However, in practice, WATFLOOD uses a constant porosity, equal to 0.3, for the soils of all land classes which prevents direct use of literature based field capacity values. A linear assumption also requires a variable RETN value be used so that the hydraulic response of true soils, which is highly non-linear, may be captured. Constant porosity and fitting flexibility therefore require that RETN be optimized to obtain satisfactory streamflow hydrographs. Numerous results from

WATFLOOD have shown that Equation 3-1 can be extremely useful in capturing the essence of streamflow hydrology. In this equation, DUZ [LT^{-1}] is the runoff depth per unit area and REC may be regarded simply as the percentage of available storage (UZS-RETN) [L] that is withdrawn during a particular time step. The REC parameter includes constant conversion factors for the time step length (typically one hour) [T^{-1}]. The total runoff Q_{int} [L^3T^{-1}], is determined by multiplying DUZ by the computational modelling area [L^2]. The form of this equation, however, is similar to more analytical ones used to describe the flow through a fixed depth shallow aquifer. A number of these theories have been developed including those by Beven (1982), Sloan and Moore (1984), Hurley and Pantelis (1985), Stagnitti *et al*. (1986), Steenhuis *et al*. (1988), Sanford *et al*., (1993) and Steenhuis *et al*. (1999). However, unlike WATFLOOD, all of these models have some non-linear relation with soil moisture.

Shallow aquifer models mentioned above are categorized using both their underlying flow equations and their simplifying assumptions. Underlying equations from which they are developed are either derived from Richard's equation (Richards, 1931) or the Boussinseq (1877) approach. These are combined with simplifying assumptions in order to solve the underlying non-linear differential equations. These assumptions are either approximations of the physical system to allow analytical solutions or numerical approximations used to solve the equations iteratively. Many of these models have been tested against experimental data gathered from Coweeta Hydrological Laboratory (Hewlett and Hibbert, 1963) where a sloping concrete tough was filled with soil, continually wetted to produce steady state conditions and then allowed to drain under conditions of zero evaporation.

Soulis *et al*. (2000) have also developed a sloping aquifer model very similar to the one presented by Beven (1982). In both these solutions, soil moisture remains above field

capacity and soil suction terms within Richard's equation can be neglected. This allows for a closed form solution using the method of characteristics. Variability of hydraulic conductivity with soil moisture, $K(\chi)$, is decreased by including the effect of an exponentially decreasing value of saturated value of hydraulic conductivity, K_{sat}, with depth.

The objective here is to use a simple unsaturated flow model that incorporates measurable geophysical characteristics of the land surface. By including more measured data into the model framework, it is hoped that the dependence of results on model calibration may be reduced. As mentioned previously, the total elimination of calibration and the *a priori* selection of controlling parameters are unrealistic at this point in time. However, by introducing, in a physically realistic way, the character of the land surface within the modelling structure it is anticipated that over time the magnitude of unexplained parameter variability will be lowered.

The model of shallow aquifer flow introduced by Soulis *et al*. (2000) differs somewhat from the implicit and numerical solutions of previous authors since the implicit solution of the shallow aquifer model has been forced to fit a simpler explicit power law. This fit is achieved by integrating the difference between the implicit solution and the power law solution and setting this result to zero. The parameters that migrate to the power law, through the integration, represent a minimization of the error between the two models over the dynamic range of soil moisture from field capacity to saturation. The form of the resulting simple power law is given as:

$$q_{\text{int}} \mid a/u0^{\gamma} \qquad \text{Equation 3-2}$$

where q_{int} is the interflow contribution to streamflow per unit land surface area and 'a' is a parameter. Both q_{int} and 'a' have dimensions [L/T]; 'u' is some dimensionless measure of basin wetness and 'b' is a dimensionless parameter. Soulis *et al*. (2000) have shown that the power law maintains the behaviour of a shallow aquifer formulation but, because the solution is explicit, it makes its use in a land surface scheme more attractive. Details of the development of the shallow aquifer model and the integration process for parameter transfer are beyond the scope of this thesis. However, the implementation of the power law formation for land surface schemes, and its relation to the WATFLOOD interflow scheme are present below.

The interflow equation for WATFLOOD can be rewritten to have the same basic form as equation 3-2 by dividing through by the land surface area, and normalizing the effective wetness (UZS-RETN) of the basin by some maximum amount as follows:

$$q_{\text{int}} = REC_1 \left(\frac{UZS - RETN}{UZS_{\max} - RETN} \right)^{\Theta} \qquad \text{for UZS} \le \text{UZS}_{\max} \qquad \text{Equation 3-3}$$

where q_{int} equals Q_{int}/ **A** and REC_1 is the original value of REC multiplied by the land surface area, **A** and a maximum value of effective basin storage, (UZS_{max}-RETN). This alternate WATFLOOD interflow formulation is somewhat flawed since the concept of a maximum upper zone storage value, UZS_{max} is not included in WATFLOOD theory. Rather, WATFLOOD does not restrict the growth of UZS since no artificial boundaries such as soil layers are required for WATFLOOD operation. Virtually all land surface schemes, with the exception of ISBA, use soil layering to generate soil moisture gradients and fluxes of soil water. To allow WATFLOOD theory to operate inside a land surface scheme, a slight

departure from the original theory must be made. Here, a maximum UZS storage value must be considered so that it may be related to maximum soil moisture content of a layer, χ_{sat} also known as soil moisture saturation.

An additional caveat to using equation 3-3 directly in land surface schemes relates to the use of the RETN term in WATFLOOD. To fit measured hydrographs, WATFLOOD allows the value of RETN to float to an optimum value which separates evaporative and drainage dominated storage changes. Allowing this value to float would not be consistent with stomatal and soil physics parameterization in a land surface scheme. Instead, for integration within CLASS, this parameter is fixed to the field capacity soil moisture (χ_{fc}) that will be defined here as the soil moisture at which a tension head value of -340cm is developed. As discussed previously, this is not the only definition of field capacity but is an often measured value in soil classification tests Dingman (2002, p.235). To allow this transformation to occur within WatCLASS an unknown "b" power is introduced to replace the value of b=1 in equation 3-3. This change from a fixed value of "b" to a variable one does not introduce any new parameters in the WatCLASS formulation since the value of RETN now disappears from the relation in favour of the fixed quantity, field capacity soil moisture (χ_{fc}).

The change in response characteristic is shown schematically by Figure 3-4. The linear portion of the curve shows the typical WATFLOOD response to increasing soil moisture deficit which decreases interflow linearly until a value equivalent to RETN is reached. The non-linear curves of the plot show two forms of WatCLASS response which decrease in a smooth curve until a soil moisture deficit, equivalent to field capacity, is reached. To allow parameter transfer between the two model forms, Soulis *et al*. (2000) advocates equating the

area under the curve of each function. Accepting that this integration method of parameter transfer is valid, one can see how a change in "b" could replicate the WATFLOOD response.

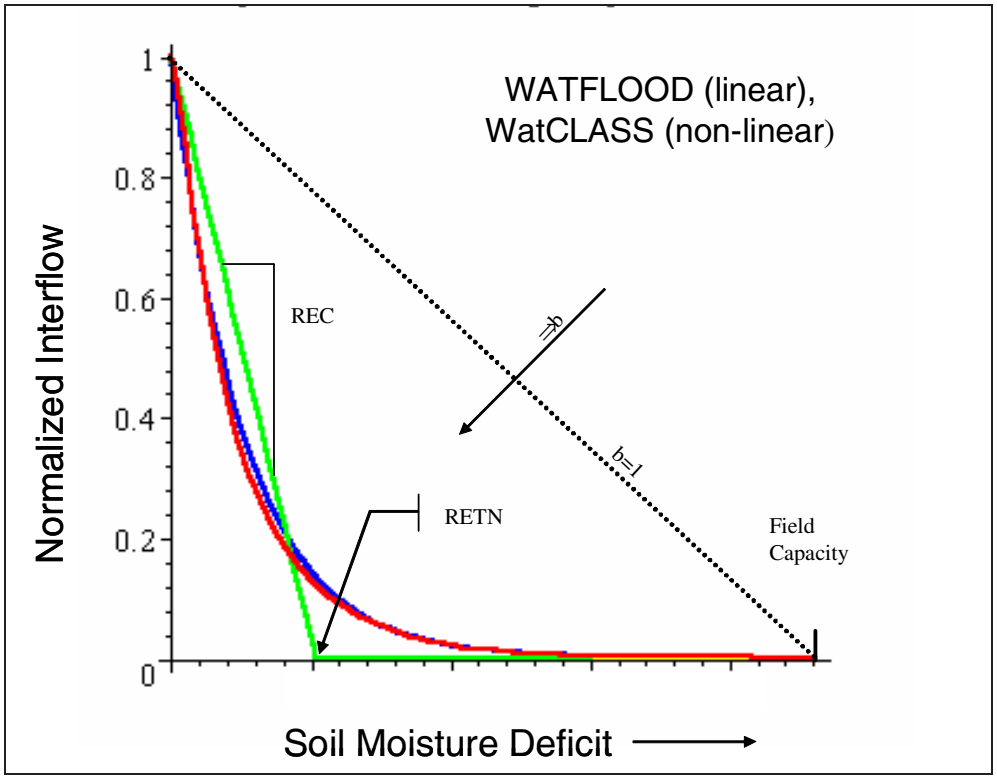

Figure 3-4 : Schematic representation of WATFLOOD and WatCLASS interflow. Values of field capacity less than RETN require positive values of 'b' to match the WATFLOOD response. WatCLASS interflow for b=1 is shown as a dashed line for reference.

The form of equation 3-3 is also similar to unsaturated flow theory developed for the GISS GCM (Rozenzweig, 1998) and the PLACE (Weztel and Boone, 1995) model discussed in Chapter 2. Equation 2-6 can be written as:

$$q_{\text{int}} \mid 2D_D K(\chi) \div Z\Theta \qquad \text{Equation 3-4}$$

where the distance between sinks, ι is replaced by a drainage density D_D and F_y, the flux of runoff from a shallow aquifer of unit width, is replaced by the saturation dependent value of the horizontal conductivity, K(χ) and ÷Z remains the soil layer thickness. Drainage density,

D_D is defined by Dingman (2002, p. 433) as the total length of streams draining an area divided by that area. This gives $D_D=1/2\iota$ with the value 2 indicating that there are two sides to each stream channel. The problem with this formulation in equation 3-4 is that no distinction is made between the values of horizontal and vertical of the hydraulic conductivity. Previous discussion has established that an enhanced lateral conductivity due to macropores and other features in upper soil layers does exist. However, using this formulation alone and substituting the normally used Clapp and Hornberger (1978) relation $K(\chi)=K_{sat}(\chi\#\chi_{sat})^c$ into equation 3-4 would result in:

$$q_{\text{int}} \mid 2D_D K_{sat} \left\{ \frac{\chi}{\chi_{sat}} \right\}^c \div Z\, 1\, \Theta \qquad \text{Equation 3-5}$$

This result would be sufficient for soil moisture values lower than field capacity. However, values of 'c' for normal soils range between 10 for sand to 25 for clay. This would yield, for soil moisture values lower than saturation (i.e. $\chi\#\chi_{sat} < 1$), a large penalty since this ratio would be raised to the large power 'c' making the value of the soil moisture scaling term very small. In addition, as discussed in Chapter 4, the Clapp and Hornberger relation as used in the majority of land surface schemes is not valid for soil moistures approaching saturation.

It is interesting to note that the form equation 3-5 is very similar to that of both the WATFLOOD interflow equation 3-3 and the simple power law equation 3-2 proposed for WatCLASS. There is some measure of basin wetness (u) raised to a power, $(u)^b$, and a number of terms that when combined form the multiplier 'a' in equation 3-2. Replacing the moisture deficit term in equation 3-5 with terms valid for soil moisture values greater than field capacity, we arrive at the final interflow equation used for WatCLASS:

$$q_{\text{int}} = 2D_D K_{satH} \left(\frac{\chi - \chi_{fc}}{\chi_{sat} - \chi_{fc}} \right)^b \cdot Z \cdot \Theta \qquad \text{Equation 3-6}$$

While equation 3-6 gives a form of equation that is similar to that used by WATFLOOD and that used by the GISS model, Soulis *et al*. (2000) present a method to determine values of the 'b' parameter and value of the K_{satH}, the horizontal saturated hydraulic conductivity. The vertical value of saturated hydraulic conductivity, K_{satV} for consolidated soils has been well studied and tables exist to determine both their mean value and variability based on soil texture and soil moisture characteristic (eg. Clapp and Hornberger, 1978). K_{satH}, on the other hand, is poorly known and is complicated by the fact that saturated conductivities decrease with depth due to the reductions in marcopores and soil cracking, discussed above. Beven (1986) has speculated that values of hydraulic conductivity decrease with depth assuming an exponential decay with depth. This conductivity model was presented in Chapter 2 and will be investigated further in Chapter 4.

3.3.2 Surface Runoff

The relationship for surface runoff is more straightforward and extracted from WATFLOOD directly. In most environments it occurs rarely, only after extreme rainfall events or when infiltration is impeded by ground ice. CLASS has a well-developed generation scheme for determining surface ponding but no method to determine the rate of runoff. This is well represented in WATFLOOD by Manning's equation, which is the momentum equation applied to open channel flow. The form for a wide channel is:

$$v = \frac{1}{n} d_e^{2/3} \Theta^{1/2} \qquad \text{Equation 3-7}$$

where v is overland flow velocity, d_e is effective depth (depth above natural depressions), Θ is land surface slope, and n is Manning's roughness coefficient.

The depth of flow at the stream edge will depend on how much of the slope is contributing to overland flow and how much concentration is occurring. Since the two factors offset each other, we assume the best estimate of depth of flow at the stream bank is the average effective depth. Therefore the flow entering a stream segment is

$$Q_{over} = \frac{1}{n} d_e^{5/3} \Theta^{1/2} L_v \qquad \text{Equation 3-8}$$

where Q_{over} is overland flow (m^3/s) and L_v is the length of the stream valley. In terms of flow per unit horizontal area, q_{over} the concept of sink distance, ι is introduced in the same fashion as the interflow calculation to give:

$$q_{over} = Q_{over} / L_V \iota = \frac{2 D_d}{n} d_e^{5/3} \Theta^{1/2} \qquad \text{Equation 3-9}$$

3.3.3 Baseflow

Soil moisture that flows through the three CLASS soil layers is used to generate a base flow contribution to the streamflow system. To be consistent with the WATFLOOD methodology, only one base flow reservoir is used per grid square. This differs from the interflow and the surface runoff streamflow components which generate a separate moisture stream for each land cover grouping in a grid square. To accommodate the land classes for

surface runoff and interflow, state variables for prognostic variables such as soil moisture and temperature are maintained for each grid and land class combination in the watershed.

A separate index in the WatCLASS source code is created to accumulate the base flow contribution of the CLASS soil column. This amount is then controlled by the WATFLOOD base flow generation power law formulation which has the form:

$$Q_{base} \mid LLZS / LZS0^{PWR} \qquad \text{Equation 3-10}$$

Values of PWR in this empirical formulation are typically between 2 and 3. Calibration of these parameters is most often accomplished by comparing simulated and modelled hydrographs on a semi-log plot.

This power law form is very similar to the interflow formulation presented previously. Other models including the VIC-2L and ARNO models use similar methods for controlling baseflow. However, rather than a simple power function these models divide base flow generation into a linear portion for low values of storage and a non-linear portion for high storage amounts. This separation of a linear and non-linear portion requires the estimation of extra parameters for the VIC and ARNO formulations. Mousavi and Kouwen (2002) have compared the WATFLOOD power law formulation with results from the MODFLOW groundwater model and show that very little difference in streamflow contributions between the two model forms exist. This result shows that the empirical power law formulation is able to capture the essence of the groundwater flow to streams. MODFLOW and other groundwater models are used for answering questions related to groundwater distribution within the watershed as well as the influence of wells and local topography on groundwater flow.

Generation of baseflow and its linkage with groundwater modelling is a subject of increasing importance. Efforts at the University of Waterloo are currently underway to link groundwater models with surface hydrology models such as WATFLOOD and WatCLASS to determine the influence of surface hydrology on the distribution of groundwater recharge. Knowing this spatial distribution has important consequences for the determination of the piezometric heads in an aquifer system which has application in the transport of contaminants and the protection of ground water resources.

3.4 Structure of WatCLASS Code

Section 3.3 has outlined the underpinnings of theory changes that were made to the CLASS model in order to include WATFLOOD streamflow generation. The following sections build on descriptions of CLASS and WATFLOOD presented in Chapter 1 and presents some of the main theory used in the each model. Also provided is a functional framework of the code structure for each of the three models. This will provide the necessary backdrop for those wishing to extend WatCLASS in the future.

Presentation of the modelling framework is given by Figure 3-5, Figure 3-7, and Figure 3-11 as process flow charts for WATFLOOD, CLASS, and WatCLASS. These flow charts are highly simplified and are intended to give a pictorial representation of the major structural changes made for WatCLASS. The figures are broken down into initialization stages and a number of time dependent groupings. The functional groupings of each box have been altered slightly from the structure of subroutines in the respective Fortran codes. This has been done for the purpose of chart reuse to provide a clearer picture of the changes made to CLASS to create WatCLASS.

3.4.1 WATFLOOD Code

Major processes represented within WATFLOOD are shown in Figure 3-5. Initialization of WATFLOOD is done with a set of ASCII files that are generated with WATFLOOD auxiliary programs or third party software. Figure 3-1, presented previously, depicts how basins are structured from a series of grid squares and how functional elements of these grids are broken down into GRU based land covers and streamflow routing elements. WATFLOOD also provides a set of self-initialization routines that determine the appropriate quantity of moisture to include in lower zone storage (LZS) and stream channels based on initial base flow observations made at stream gauging location. Other moisture stores including i) initial snowpack, ii) upper zone storage, iii) antecedent precipitation index based soil moisture are initialized from separate spatially distributed ASCII files.

Once initialized, WATFLOOD steps through time on an hourly basis and reads spatially distributed inputs of precipitation, temperature, and net radiation. There a many options associated with the forms of input data including features to distribute coarse temporal resolution temperature and precipitation over time. These and other options are beyond the scope of this discussion and the reader is referred to the WATFLOOD user's guide for further reference (Kouwen, 2001).

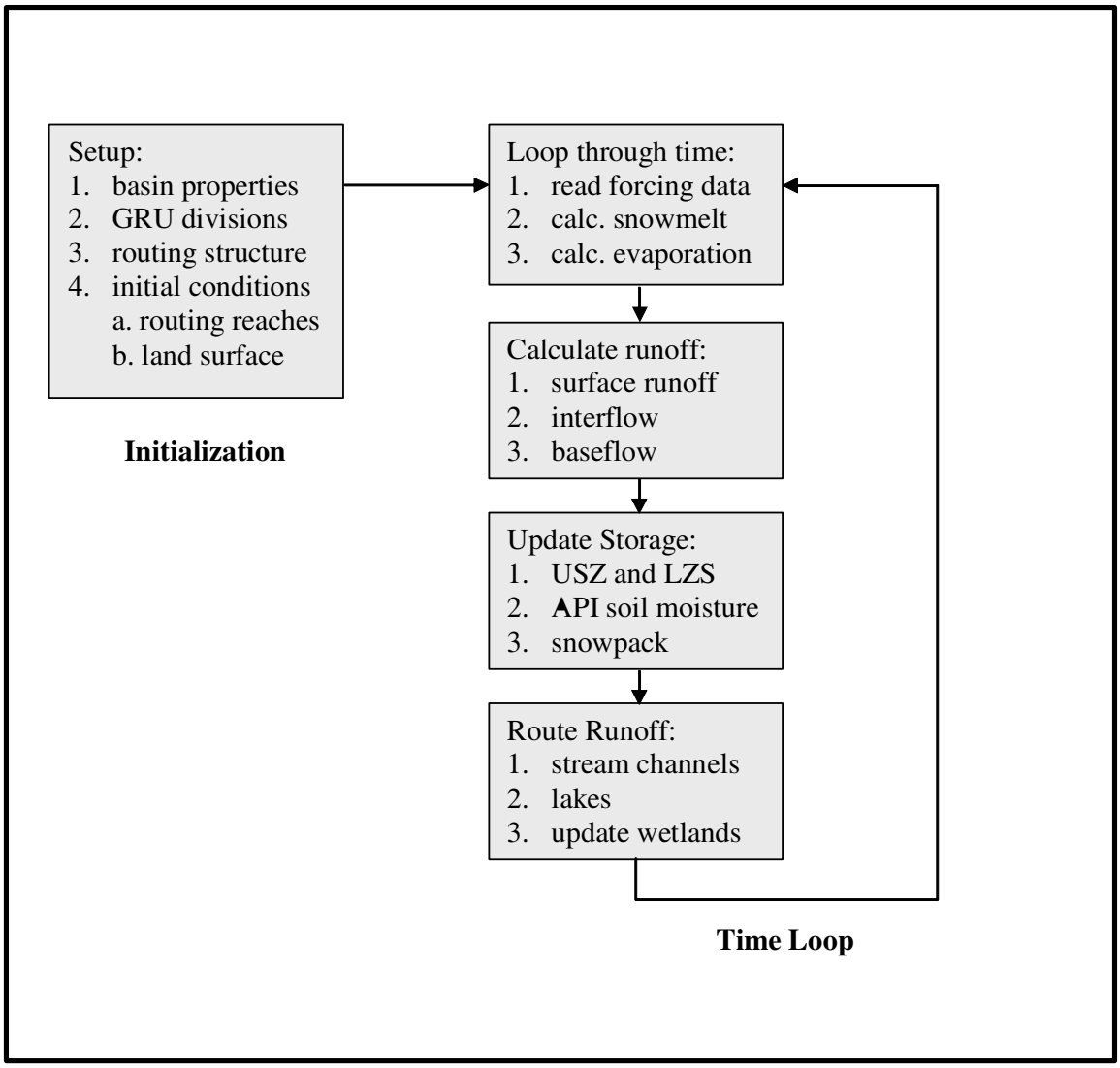

Figure 3-5 : WATFLOOD process flow chart.

Evapotranspiration

WATFLOOD supports three evapotranspiration (ET) algorithms based on a review of current techniques and their implementation by Neff (1996). These include potential evaporation algorithms based on a) pan evaporation measurements, b) Hargreaves temperature based model (Hargreaves and Samani, 1982), and c) Priestly-Taylor radiation based equation (Priestley and Taylor, 1972). Shuttleworth (1993) advises against the use of temperature based evaporation estimates except where temperature is the only archived field. For

BOREAS and Mackenzie simulations presented in this thesis, both radiation and temperature are available from measurements and model outputs. Therefore, the Priestly-Taylor scheme was used.

The Priestly-Taylor evaporation scheme is a simplification of the Penman combination equation (Dingman, 2002, p. 310). Penman's approach has become popular because of its innovative idea for combining energy and diffusion estimates of evaporation to eliminate the need for a surface skin temperature. At larger scales, over well watered surfaces, air moving over the ground eventually comes into equilibrium with the surface moisture source (Dingman, 2002, p.310). This would have the effect of eliminating any vapour pressure gradients between the surface and the air and hence the diffusive terms in Penman's equation. Priestley and Taylor (1972) determined that, given well-watered conditions, energy terms dominate over diffusive terms in an almost constant 4 to 1 ratio. They proposed a simplified form of the Penman equation giving potential evaporation (PET) as:

$$PET = \zeta \left(\frac{\div}{\div + \nu} \right) (K_* + L_* - G) \qquad \text{Equation 3-11}$$

where $\div$ is the temperature gradient of the saturated vapour pressure curve, ν is the psychrometric constant which is sensitive to atmospheric pressure, K_* is the net shortwave radiation, L_* is the net long wave radiation, G is the ground heat flux and ζ is known as the Priestley-Taylor alpha given as 1.26 (i.e. approximately a 4 to 1 ratio).

Snow Processes

Snowmelt is often the dominant feature of streamflow hydrographs in Canada and represents the runoff from the previous winter's cumulative precipitation. Because of its importance in the prediction of peak annual flows, both snow accumulation and melt algorithms where added early in the development of WATFLOOD based on the work of Donald *et al*. (1995). WATFLOOD accumulates snow in a separate model layer, redistributes it from areas of low vegetation to high, ripens the pack to a pre-melt condition and subsequently melts out the snow layer as a patchy array of snow cover and no-snow cover areas.

Melt of the ripened snowpack is based on the well know temperature index model given as:

$$M \mid MF /T_a \; 4 \; T_{base} 0 \qquad \text{Equation 3-12}$$

where MF is the melt factor that determines the rate of snow melt (M) per degree of air temperature rise, T_a in a linear relation. The base temperature, T_{base} represents a threshold temperature that must be overcome to initiate snow melt and is often determined through calibration. While very simple, calibrated temperature index models provide exceptionally good results when compared to full energy balance snow melt calculations used by more complex models (Dingman, 2002, p.211).

Runoff Calculations

Runoff calculations to determine: (1) surface flow, (2) interflow, and (3) base flow used by WATFLOOD are integral to the development of WatCLASS and are presented in detail in Section 3.3.

Water Balance Updating

Maintained from time step to time step is the quantity of water in each of WATFLOOD's moisture reservoirs. These include: (a) the vegetation canopy, (b) surface depressions, (c) an upper soil layer, (d) a deeper soil layer, (e) an intermediate, unsaturated soil layer, (f) surface snow storage, and (g) channel storage. Mechanics of land surface runoff generation lie primarily in the partitioning of upper (zone) soil storage (UZS) into evaporation, interflow and contributions to lower (zone) soil storage (LZS). This is shown diagrammatically in Figure 3-6.

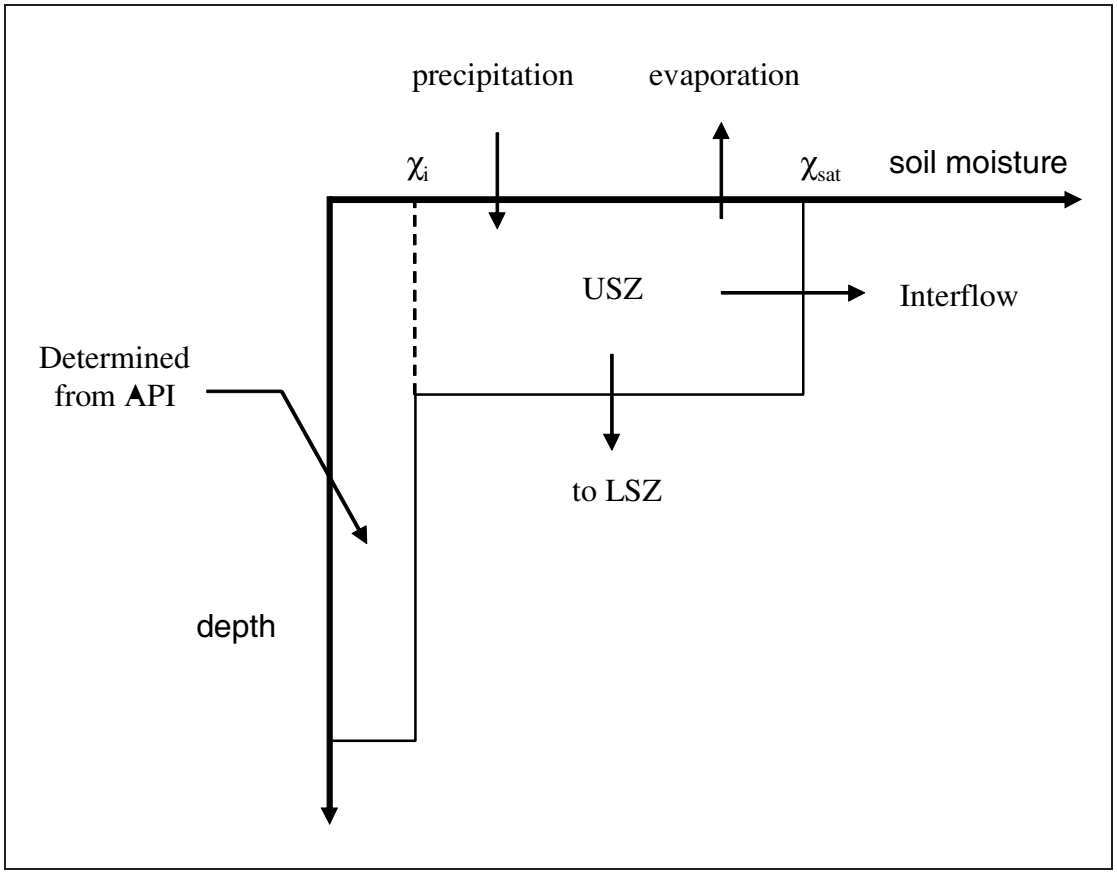

Figure 3-6 : Water balance model used by WATFLOOD.

Rainfall, after overcoming available canopy storage, drips to the soil surface where it becomes available for infiltration. Infiltration calculations are performed using the Green-Ampt theory (Mein and Larson, 1973) given as:

$$f(t) = K_{sat}\left(1 + \frac{\ldots_f (\lambda - \chi_i)}{F(t)}\right) \qquad \text{Equation 3-13}$$

where f(t) represents the rate of infiltration at time t, K_{sat} is an optimizable saturated hydrologic conductivity term, $\ldots_f$ is the suction head at the wetting front, (λ-χ_i) is the initial soil moisture deficit calculated from the porosity, λ and χ_i, the initial moisture content, and F(t) is the cumulative infiltration volume at t. This is very similar to the equation of Philip (1954) cited by WATFLOOD except for the addition of ponded water head at the soil surface which is added to wetting front suction.

Within WATFLOOD, unsaturated soil moisture from the model's intermediate layer is not explicitly included in the water balance. This requires modifications to Green-Ampt theory to allow recovery of infiltration capacity between storm water inputs. Firstly, soil moisture below the wetting front, χ_i is determined empirically from an antecedent precipitation index (API) adapted from Linsley et al. (1982, p.242). This index describes the decline in soil moisture with time that is refreshed periodically by precipitation, p(t), as:

$$\chi_i(t + \div t) = A5(\chi_i(t)) + p(t)/100 \qquad \text{Equation 3-14}$$

Values of the coefficient, A5 are constrained to values between 0.985 and 0.998 which correspond to the normal range expressed by Linsley *et al*. (1982, p.243) translated to hourly time steps. Use of χ_i in WATFLOOD represents a complete and separate soil water balance.

However, its use is restricted to the determination of the intermediate layer soil moisture for infiltration calculations and does not enter into water balance calculations used for streamflow determination. A second modification to Green-Ampt infiltration extends its use in both dry and wet periods. This is achieved by using WATFLOOD's UZS to track the cumulative infiltration depth, F(t). Figure 3-6 shows that UZS can be increased by infiltration and decreased by evaporation, drainage to LZS, and the interflow contribution to streamflow. This has the effect of moving the wetting front upward during dry conditions to recover infiltration capacity and downward during wet periods thus limiting infiltration capacity. These extensions eliminate the need for tracking soil moisture decay during dry periods through the use of multi-layered soil systems and finite difference implementations of Darcy's Law. Modifications to Green-Ampt allow WATFLOOD to capture the essence of storm water infiltration and infiltration capacity recovery with a minimum of computational expense.

Streamflow Routing

One of the major strengths of WATFLOOD is its emphasis on stream channel routing. As mentioned previously, surface processes within WATFLOOD are grouped by similar land cover. These groupings are assumed to act independently and do not interact with one another. Tying these independent groupings together is stream channel routing that allows upstream elements to influence flow through their downstream neighbours and ultimately contribute to the streamflow measured at basin outlets.

Routing theory in WATFLOOD is a hybrid routing scheme involving elements of hydrologic routing and hydraulic routing as discussed by Fread (1993). Flow calculations are governed by the simplified hydrologic continuity equation:

$$I - O = \frac{dS}{dt} \qquad \text{Equation 3-15}$$

where I is inflow to the reach, O is the outflow from the reach and the differential describes the change in channel storage, S with time, t. While hydrologic routing models are normally calibrated empirically by relating O and I to S using measured hydrographs, WATFLOOD uses the kinematic approximation of the momentum equation normally used in hydraulic routing schemes together with geomorphological channel properties to relate outflow, O, to storage, S.

WATFLOOD also allows routing through lakes. In this situation, stream channel contributions increase lake surface water elevation. This elevation is then used to determine lake outflow and therefore the contribution to the next downstream stream channel. For large lakes, dynamics effects such as wind set-up may influence lake elevations at the outlet. In these circumstances, WATFLOOD has provision to generate output for more advanced dynamic wave routing schemes.

Wetland routing is the latest addition to WATFLOOD. This feature allows interchange of moisture between the stream channel network and the adjacent wetland. The use and implications of the wetland routing option are centered on its ability to provide increased model storage to supplement evaporation demands. Issues related to the use of wetland routing are discussed in section 6.2.

3.4.2 CLASS Code

Major processes represented within CLASS are shown in Figure 3-7. Initialization of CLASS is done with a set of ASCII files whose values must be determined from the physiographic nature of the land surface. Details of this task and data required for these files are presented in Section 4.2. CLASS, in standalone form, is equipped to operate only over a single point.

Once initialized, CLASS steps through time using time steps of maximum length 30 minutes. Longer time steps result in numeric instabilities in the finite difference solutions used within CLASS. In addition to precipitation and temperature inputs required by WATFLOOD, CLASS requires inputs of both incoming long and short wave radiation, plus humidity, temperature and wind speed measured from the same reference height, and surface pressure. These forcing inputs are normally supplied to CLASS from an atmospheric model to which it is normally attached. However, in stand alone mode, time series of these data must be supplied for each of these forcing variables. This limits the application of CLASS to detailed process study experiments where these variables have been measured.

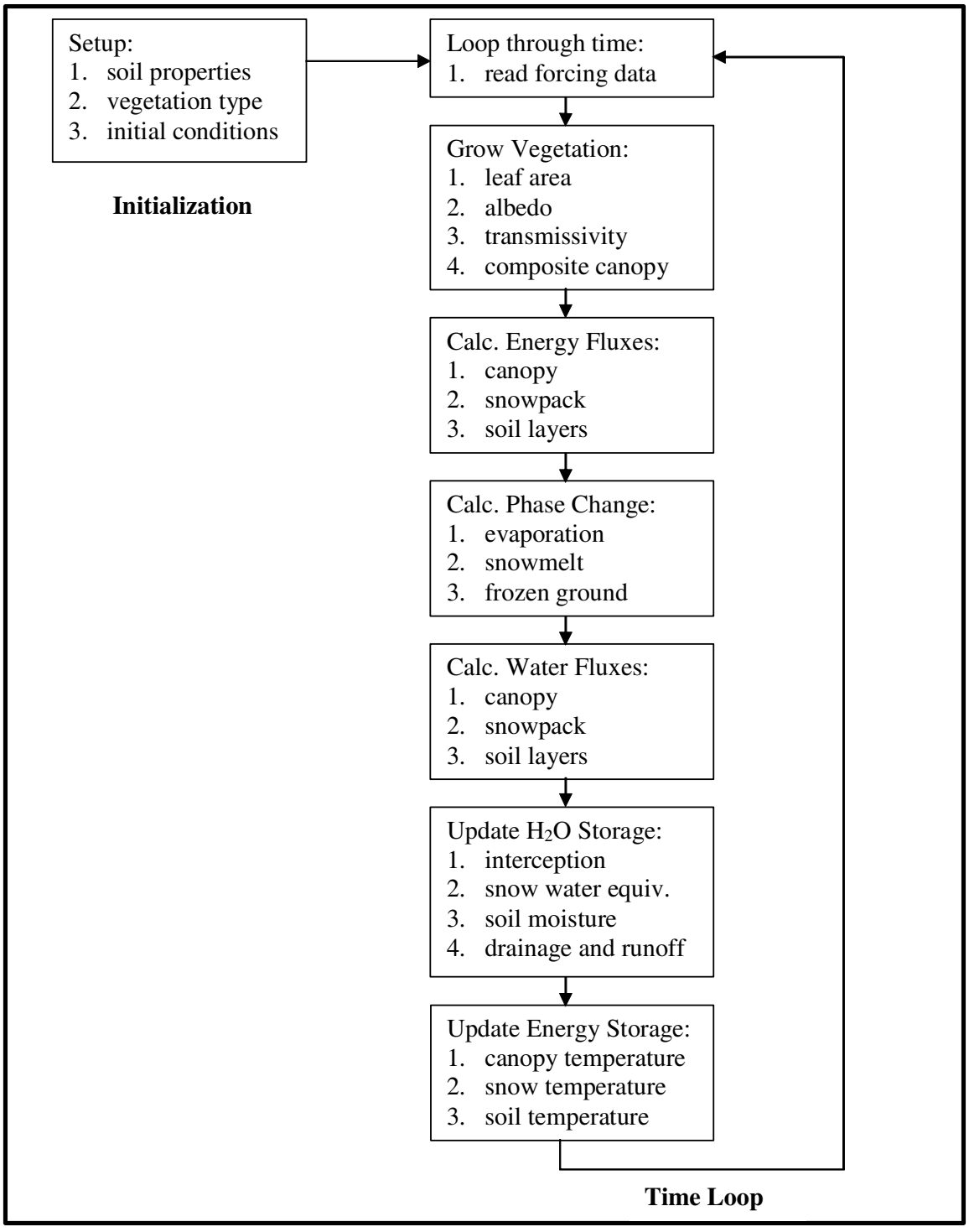

Figure 3-7 : CLASS process flow chart.

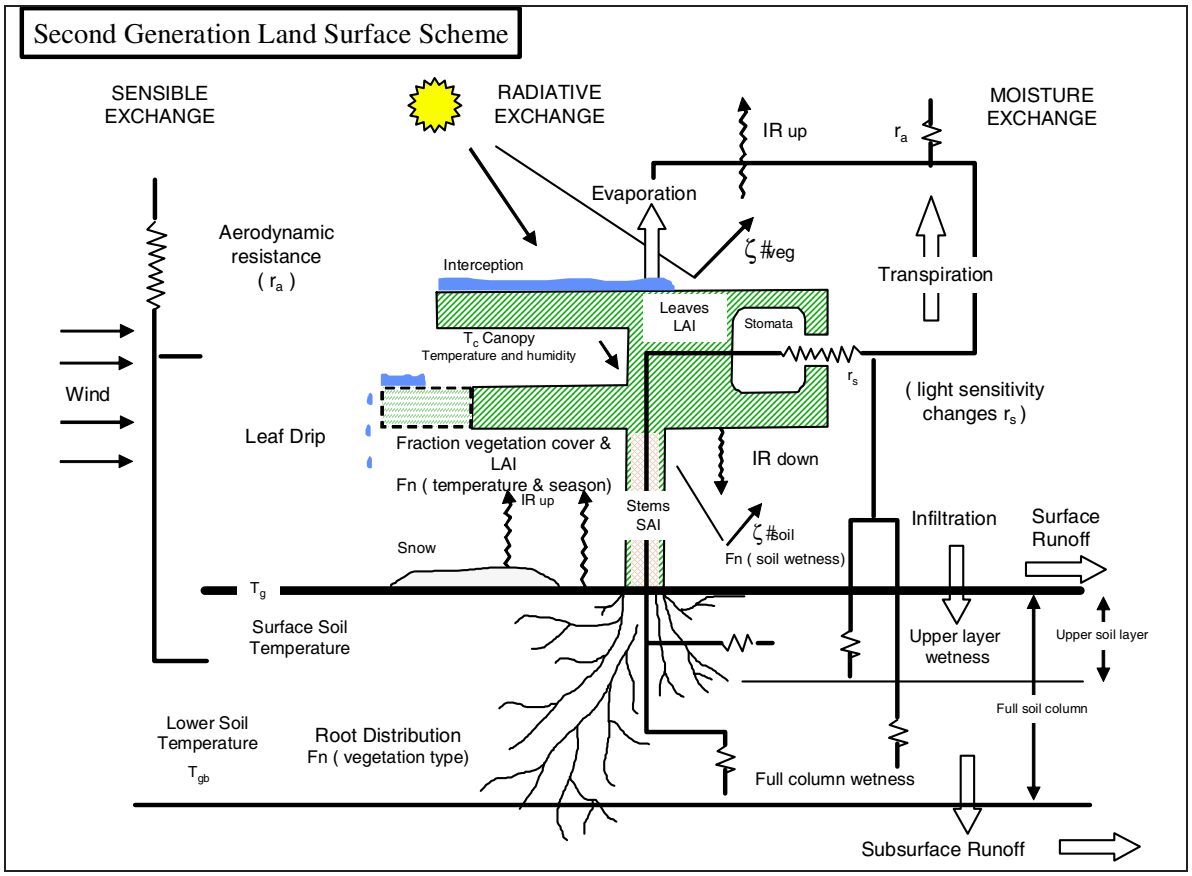

Figure 3-8 : Schematic of processes represented within a LSS such as CLASS (from Sellers *et al.* (1997)).

As time advances, CLASS simulates the motion of energy and water through the terrestrial environment. There are many such processes simulated by CLASS and these are represented schematically in Figure 3-8. This figure is representative of many land surface schemes similar to CLASS and has been adapted from Sellers *et al.* (1997).

Vegetation Characteristics

As mentioned above, baseline characteristics associated with vegetation are first entered in an initialization step. Following initialization, the character of the vegetation is permitted to evolve in response to environmental conditions. For instance, reflectivity of vegetation is influenced by the degree of snow cover or, for deciduous trees and crops, the time of year. Changes in leaf area, measured as a ratio of leaf surface area to ground surface area, are

expressed as the leaf area index (LAI). The LAI influences both the reflectivity of radiation and transmission of radiation through the canopy. For instance, solar radiation penetrates the canopy under the influence of Beer's Law:

$$\vartheta = \exp(-\rho \cdot LAI)$$

where ϑ is the transmissivity, ρ in a species dependent extinction factor. CLASS manages (i) near-infrared bands, and (ii) visible bands of short wave radiation as well as (iii) longwave radiation and calculates transmissivity and reflectivity amounts for each of these bands separately.

Vegetation also controls transpiration. This is done primarily through the response of plant stoma to environmental stresses including: (i) low soil moisture, (ii) extremes in light levels, and (iii) high vapour pressure deficits. These transpiration controls are of great importance to this thesis since they providing the response mechanism relating runoff and evaporation. These are discussed in greater detail in Section 4.2.4.

As it is currently implemented in the Canadian GCM, CLASS adjusts the LAI of plants based on the time of year and their location along a band of longitude. This is done by means of a simple look-up table. Plant species are distributed into coniferous and deciduous forests, low vegetation, and grass. Each of these is permitted to respond in different ways to environmental stimuli and their proportionate properties are lumped together during each time step to generate a 'composite canopy' used for subsequent energy balance calculations.

Energy Flux Calculations

Using properties established for soil, snowpack, and vegetation layers, energy balance calculations are performed next. These determine the flux of energy though each of the soil layers, the snowpack and the canopy. However, at this point no attempt is made to update any of the layer temperatures or ice contents (i.e. energy storage). These energy storage calculations are stepped ahead only after moisture balance quantities have been established.

Energy fluxes are determined by summing component contributions along a flat horizontal plane that is assumed to have zero thickness and therefore no heat storage capacity. Within CLASS, this energy balance is either taken at either i) the soil surface, ii) the snow surface or iii) the equivalent height of the vegetation canopy depending on which of these features are present. Without a storage term the surface energy balance equation reduces to:

$$K_* \; 2 \; L_* \; 2 \; Q_H \; 2 \; Q_E \; 4 \; G(0) \; | \; 0 \qquad \text{Equation 3-16}$$

where K_* is the net short wave radiation, L_* is the net long wave radiation, Q_H is the sensible heat flux, and Q_E is the latent heat flux. The resulting flux balance equation also yields a term, G(0) that is the flux of energy entering either the canopy, the snow mass or the bare ground surface. The equation is solved by relating each of the terms in Equation 3-16 to the surface temperature ($T_{surface}$) of the thin plane and iterating until the left hand side is equal to zero. Figure 3-9 depicts the situation for a bare ground surface.

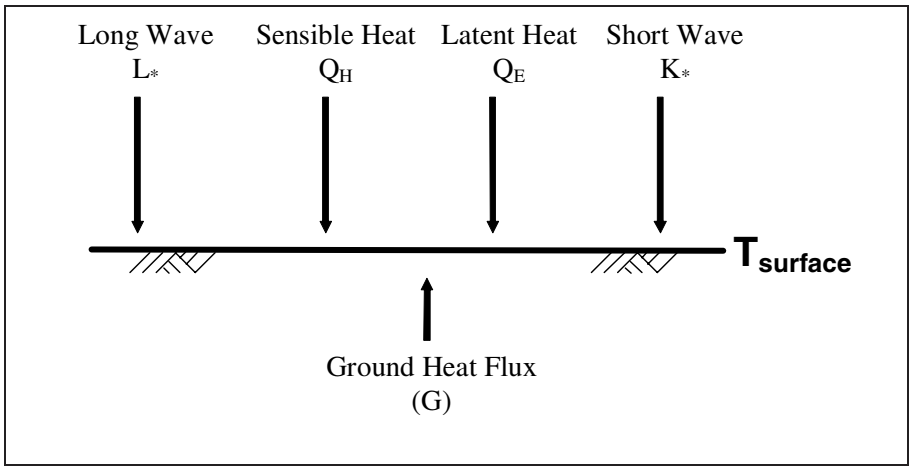

Figure 3-9 : Surface energy balance for bare ground surface

To evaluate the flux of energy across each layer boundary, the flux-gradient relation in one-dimension is used. This equation has the form:

$$G_i \mid 4\varsigma_i \left.\frac{dT}{dz}\right|_i \qquad \text{Equation 3-17}$$

Equation 3-17 states that the energy flux (G) across each layer boundary, i, is controlled by the gradient of temperature, dT/dz, evaluated at the i^{th} boundary, multiplied by the soil moisture dependent thermal conductivity for each soil layer, ς. The lowest soil boundary is assumed to be a no flux boundary, therefore, G (bottom) is assumed to be zero.

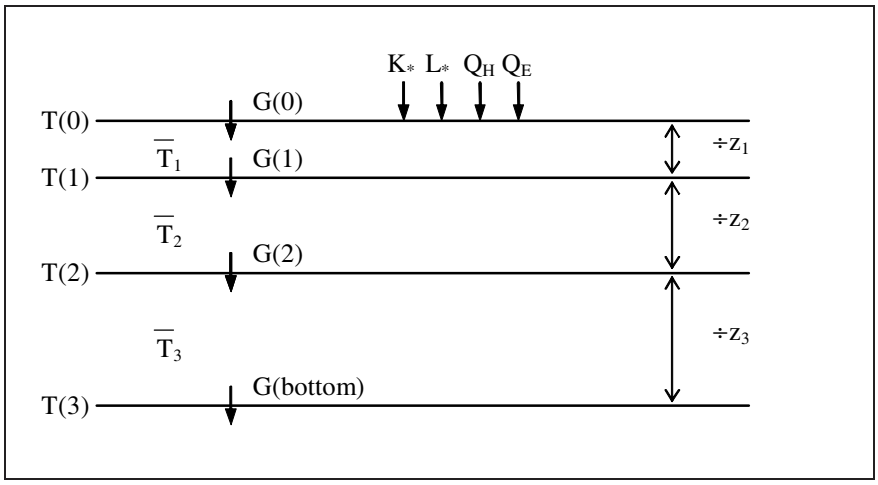

Figure 3-10 : Soil layer energy flux calculations.

Figure 3-10 represents the simple case with only three soil layers. An added snow layer is treated simply by including it as an additional soil layer within the finite difference solution. However, vegetation adds an extra degree of complication requiring a transfer of energy from the canopy to the ground surface. This involves the determination of both canopy and soil surface skin temperatures in an iterative scheme.

With fluxes though each of the soil, snow and canopy layers known, phase change calculations may be determined. Note that the evaporation phase change (Q_E) is derived from the surface energy balance calculations given in Equation 3-16.

Phase Change

Because of this importance to the surface water balance, soil moisture phase changes and snow melt are performed next. Phase change calculations involve the determination of the heat necessary to bring the individual layer temperatures to 0^oC. This is followed by conversion of any remaining energy into either melt or formation of ice within the snowpack and soil layers. At this point, the determination of final soil layer temperatures is not important and this step is used only to provide an estimate of the amount of moisture that will

be available for water balance calculations. The final soil temperatures and ice contents will only be stepped ahead once the soil moisture dependent heat capacity of each layer has been determined. This two step process is used instead of a fully implicit solution because of computational constraints.

Snow simulation in CLASS is influenced by time dependent components. Many of the properties of snow such as thermal conductivity, heat capacity, and albedo are permitted to change as snowpacks age, darken and densify.

Water Balance Determination

Rainfall, snowmelt, and thawed soil moisture serve as liquid water inputs to CLASS. In a similar fashion to gradient based energy flux calculations, moisture is moved through the CLASS soil layers. The one-dimensional unsaturated Darcian flow equation is given by:

$$f_i = K_i\left(1 - \frac{d\psi}{dz}\Big|_i\right) \qquad \text{Equation 3-18}$$

Equation 3-18 is very similar to the energy flux equation given above by equation 3-17. Here, the moisture flux (f) across each layer boundary, i, is controlled by the gradient of suction head, $d\psi/dz$, plus elevation head (i.e. the +1 term), evaluated at the i^{th} boundary, multiplied by the soil moisture dependent hydraulic conductivity of each soil layer, K. The lowest soil boundary is assumed to be a zero suction head boundary ($d\psi/dz=0$), therefore, f(bottom) is set equal to K. Methods for determining the moisture dependent values of K and …are discussed extensively in Chapter 4.

Differing from energy calculation is the treatment of the upper boundary condition. The energy balance equation provides the solution for the skin surface temperature (T(0)) boundary condition. However, no similar solution is available for the moisture flux equation due to the potential for surface ponding. Instead, excess moisture, ponded at the surface, is permitted to infiltrate into the soil column using the Green-Ampt infiltration method, described previously for WATFLOOD. Once surface moisture has infiltrated, the upper unsaturated boundary condition (..(0)) is set by extrapolating the suction value of the two upper soil layers to the surface. While crude, this boundary condition is used within equation 3-18 and the finite difference solution proceeds.

Update Layer Temperature and Moisture

Given fluxes of energy (G) and moisture (*f*) through the soil layer system, conservation equations are used to update the soil layer temperatures and moistures. These are given as:

$$\bar{\chi}(t+1) = \bar{\chi}(t) + [f(i-1,t) - f(i,t)]\frac{\Delta t}{\Delta z_i} \qquad \text{Equation 3-19}$$

for moisture and for energy as:

$$\bar{T}(t+1) = \bar{T}(t) + [G(i-1,t) - G(i,t)]\frac{\Delta t}{C_i \Delta z_i} \pm S_i \qquad \text{Equation 3-20}$$

where C_i is the heat capacities of the individual layers (i.e. the energy required to raise a soil of unit thickness one degree in temperature) and S_i are sources and sinks of energy due to phase change or advection of energy. The overbar symbols represent soil moisture and soil temperature layer average values that are known as state variables within CLASS. As mentioned previously, the order in which these calculations are performed is important. This

is because of the strong dependence of C_i on soil moisture content. This dependence necessitates that moisture updating proceed prior to temperature updating.

3.4.3 WatCLASS Coupled Code

Elements of the coupling of WATFLOOD and CLASS that form WatCLASS are present in Figure 3-11. These have been discussed previously in Section 3.3. However, the schematic highlights how the WATFLOOD additions are integrated within the CLASS code. Addition of WATFLOOD initialization routines provides a watershed structure to WatCLASS and extends CLASS beyond a single point model. Implementation of the WATFLOOD GRU method also circumvents the need for the creation of a 'composite canopy' and permits gridded fractions of any soil / land cover combination to maintain individual water and energy balances. For WatCLASS, this means that proportional output responses are aggregated to generate output. This differs from CLASS alone, which blends parameters to form a composite canopy and a single response.

Within time varying computations, the WATFLOOD calculation of streamflow contributions are determined prior to the stepping ahead of the CLASS soil temperature. Highlights of changes to runoff are the suspension of the CLASS methods and the addition of WATFLOOD routines with modifications necessary for soil moisture based interflow generation. Tight integration of these routines within CLASS permits runoff induced changes in soil moisture to influence the thermal heat capacity of soil layers. When soil temperatures are finally updated within WatCLASS they reflect these heat capacity alterations.

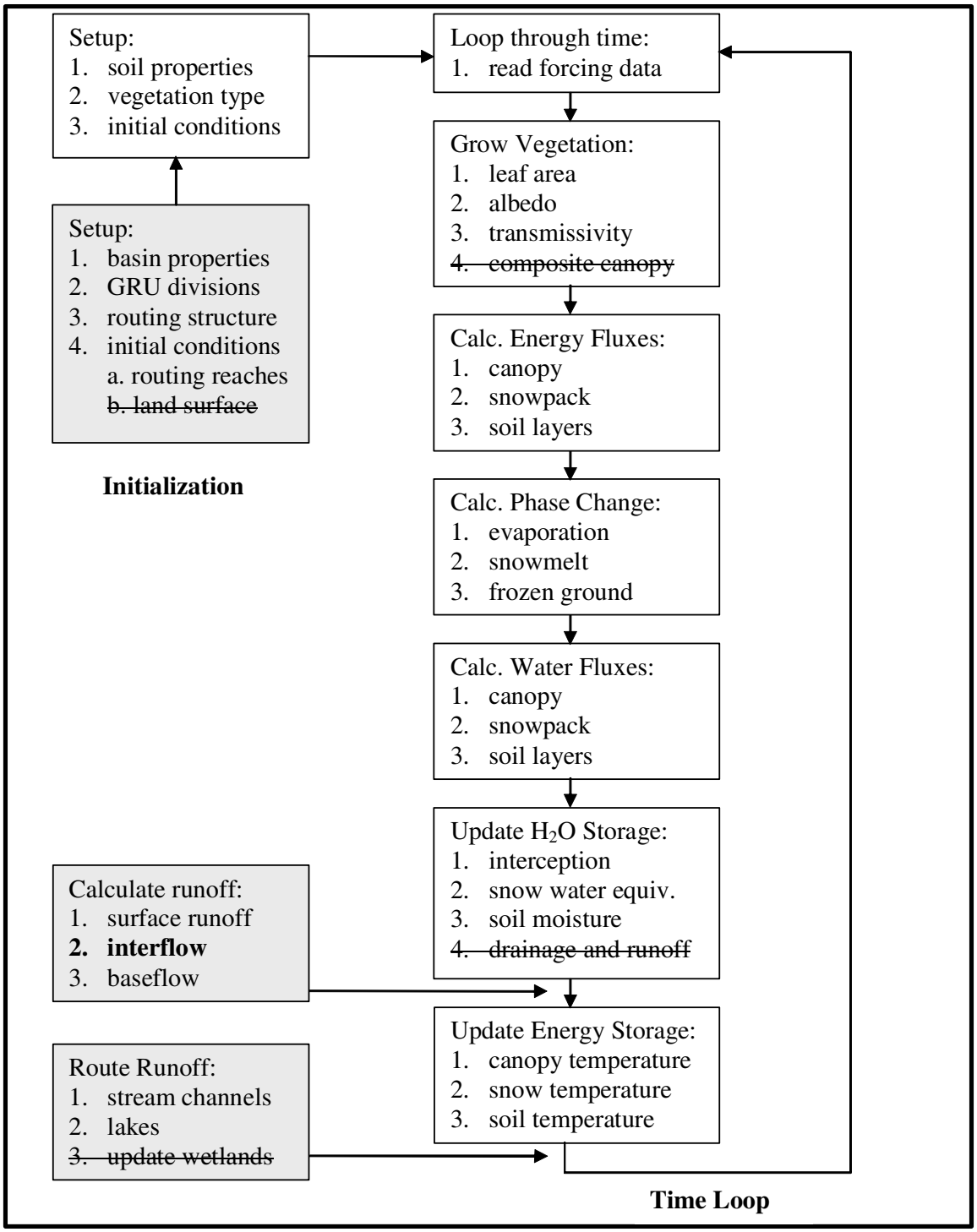

Figure 3-11 : WatCLASS process flow chart. Note, additions to CLASS from WATFLOOD are in dark shading, deletions are stroked out and changes are bolded.

Finally, at the end of the time step, the runoff from WatCLASS is routed through the WATFLOOD stream channel network. Alternatively, these moisture fluxes can be stored in a flat file structure to be routed later by WATROUTE (Arora *et al.*, 2001) or an alternate streamflow routing routine.

3.5 Chapter Summary

This chapter has presented an overview of the concepts and theory that have been used to develop WatCLASS. The basis of the development is the porting of WATFLOOD runoff generation concepts to the CLASS structure together with the GRU concept and streamflow routing. However, some modification to WATFLOOD interflow theory was required to conform to fixed depth soil layers and variable soil texture used in CLASS.

Implementation of runoff generation in an atmospheric model requires that parameters be developed for the interflow, surface runoff and base flow mechanisms using measured data. This can be accomplished using the Level II model directly. In the next Chapter, we use WatCLASS in point mode to determine the impact of generating runoff on the partitioning of turbulent fluxes.

4 BOREAS Study Results

4.1 Introduction

The Boreal Ecosystem-Atmosphere Study (BOREAS) was designed as a large field experiment to measure interactions between the northern boreal forest biome and atmosphere. The goal of the experiment was to determine how climate change might ultimately impact this environment (Sellers *et al*., 1995). Field experiments where conducted over the years 1994-1996 with intensive observation periods occurring in years 1994 and 1996. Important to the work in this thesis are: i) the diversity of data collected, ii) the time long period over which continuous data was collected, and iii) the large number of terrain types represented by coordinated data collection efforts. Combined, these factors permit emerging model studies to reflect the nature of boreal forest environment. Length of the data set is very important. Shorter experimental datasets would allow results to be unduly biased by assumptions of initial conditions or allow model error to be forced into some unmeasured component quantity of the water or energy balance.

The domain of the experiment consisted of a 1000km x 1000km area located in the central and northern portions of Saskatchewan and Manitoba known as the transect area. Within this large region, two detailed study areas were identified and located near the northern and southern limits of the boreal forest. These areas are known as the Northern Study Area (NSA) and the Southern Study Area (SSA) each approximately 100km x 100km. Located within each study area are a number of intensive observational plots, identifiable by the location of flux measurement towers, which are situated within large patches of relatively homogeneous land cover chosen to be representative of that biome. This scaled

observational framework is particularly well suited to WATFLOOD and the GRU concept because the responses from each landscape can be captured using individual model response units and used to collectively generate a streamflow response. Figures 4-1, 4-2, 4-3 and 4-4 show the location of the BOREAS transect and study areas together with the locations of the individual tower locations.

Figure 4-1 : BOREAS Study Region, NSA, and SSA locations. (From: BOREAS Web Site, 1999)

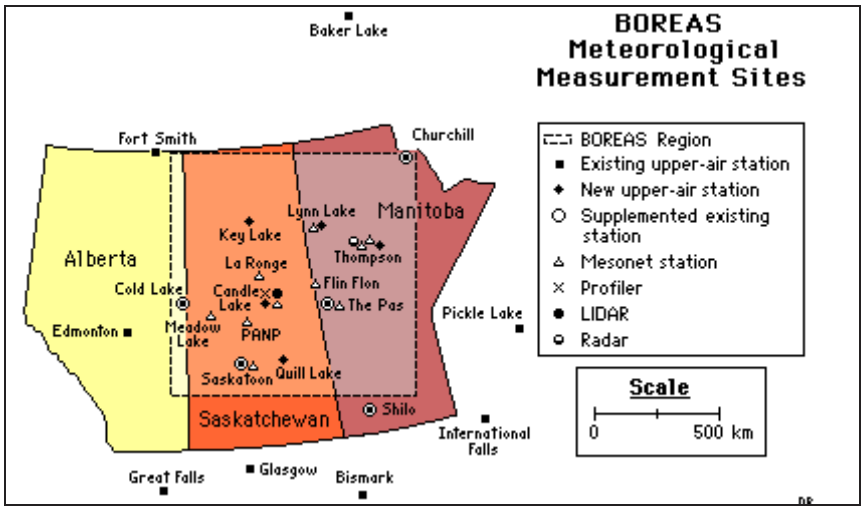

Figure 4-2 : BOREAS 1000x1000km study region. (From: BOREAS Web Site, 1999)

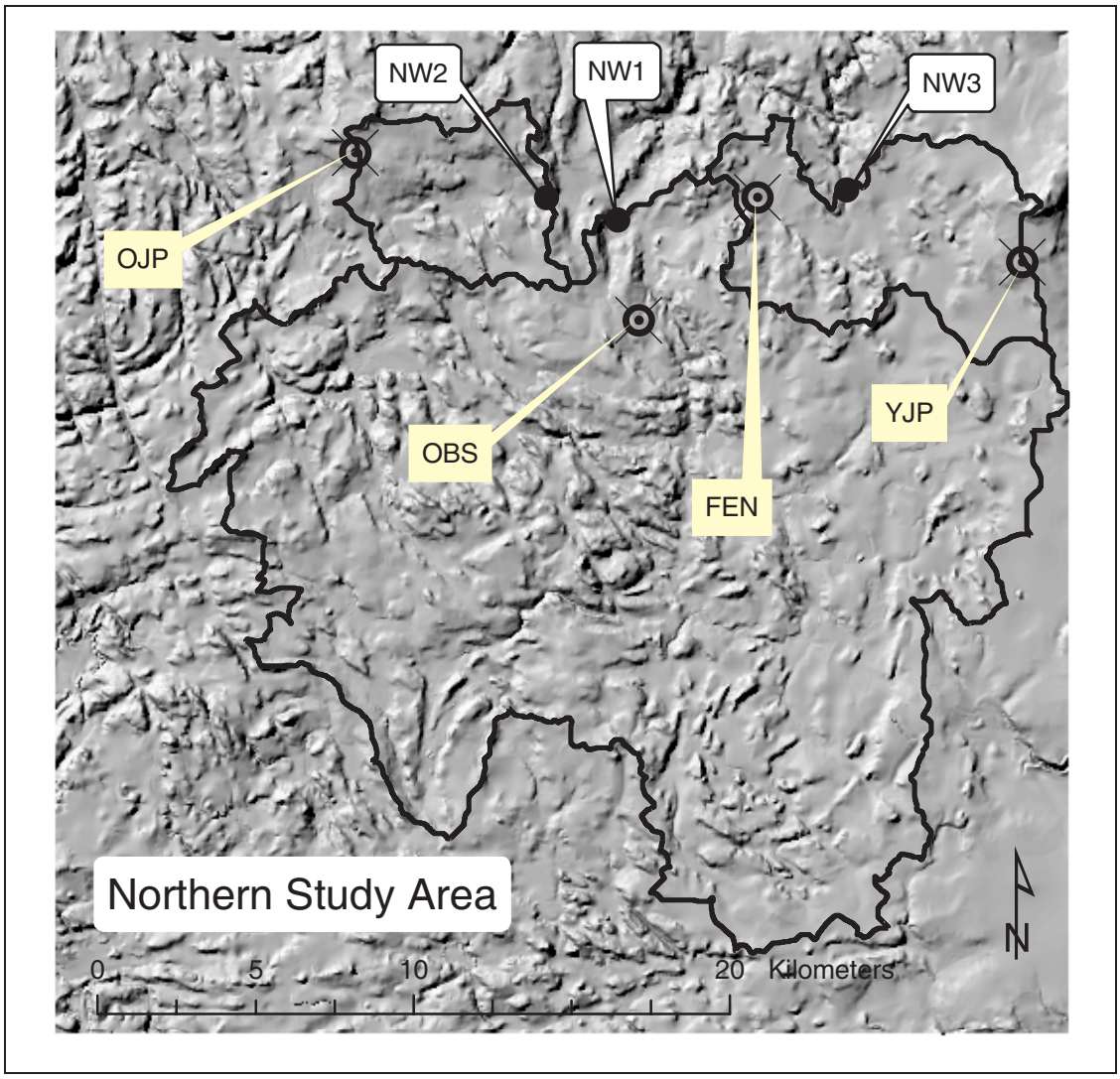

Figure 4-3 : Shaded relief map of NSA watershed and locations of streamflow gauges and flux tower sites

Figure 4-3 and 4-4 show shaded relief maps of the NSA and SSA, respectively. These maps where generated from contour and stream channel data using ANUDEM software, which is outlined in Chapter 5. Included in each map are flux towers sites (OBS, OJP, etc) and locations where streamflow data was measured (SW1, NW1, etc). Also shown for each stream gauge location is its upstream watershed boundary, which is given as a solid black line. Scale bars and north arrows have been included for reference.

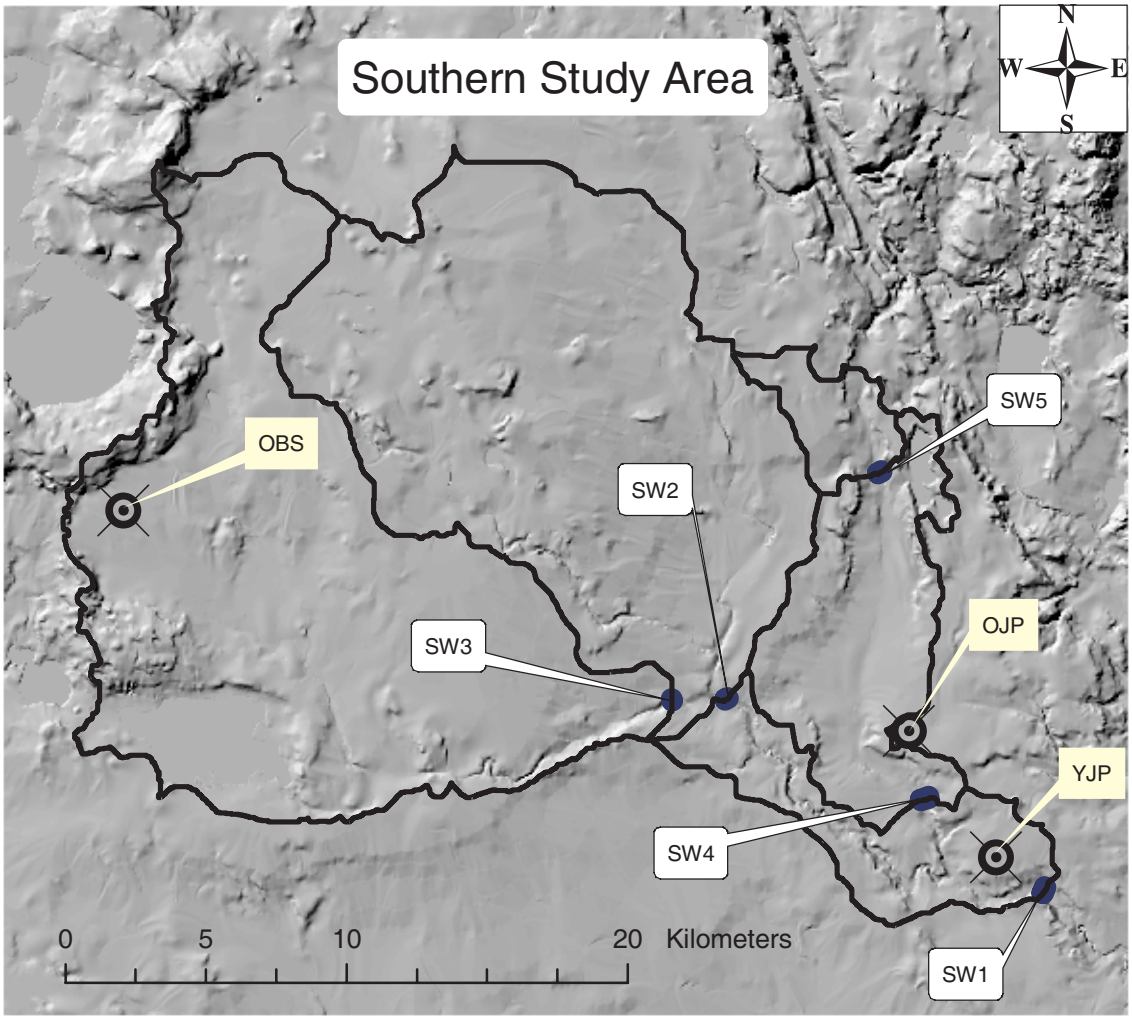

Figure 4-4 : Shaded relief map of SSA watershed and locations of streamflow gauges and flux tower sites

Inherent in the plan of the BOREAS experiment was a desire to address scale related issues. Measurements were conducted at three scale levels: (i) the tower scale, (ii) the study area scale (NSA & SSA), and (iii) the regional scale (transect). It was anticipated that detailed process representations developed from tower studies could be transferred to the study areas. The scale study areas coincide with the resolution of limited area numerical weather prediction (NWP) models. From study area results, supported by additional remote sensing measurements, it was anticipated that parameterizations could be developed for GCMs at the

regional scale. The discussion in this chapter will focus on the first of these scales with WatCLASS results compared with results from tower based measurements. Chapter 5 will examine study area domains and Chapter 6 will address large area domains required for atmospheric modelling using the Mackenzie GEWEX Study (MAGS) as a test case.

Reasons for not modelling the larger BOREAS transect domain at this time are the poor results that have been obtained to date using WATFLOOD (Whidden, 1999). These results do not reflect inadequacies in the model but rather the lack of attention given to this region when compared to the MAGS region. Factors complicating BOREAS transect modelling include (i) the high degree of streamflow regulation imposed for hydro-electric power production and the associated loss of land surface response that results, (ii) the lack of measured forcing and validation data in this remote region for Canada, and (iii) the limited use of WATFLOOD in the region which means that suitable hydraulic and land surface parameters are not available. In keeping with the modelling strategy presented previously, it is first necessary to initiate and develop many of parameters (primarily routing parameters) with the WATFLOOD model prior to implementing WatCLASS. Without first adequately representing the dynamics associated with the water balance using WATFLOOD, the addition of greater modelling complexity imposed by adding energy balance components is unlikely to succeed.

Others have previously pioneered the use of WATFLOOD in the BOREAS study area to allow modelling with WatCLASS to proceed. Neff (1996) and Whidden (1999) have established that rainfall, temperature, and net radiation measured for the NSA and SSA areas are adequate for the generation of streamflow. This has been accomplished by manipulating the water balance of each basin while constraining the result with surrogates of energy

processes including temperature for snow melt and net radiation for evaporation. These previous efforts have also established the drainage layer database from which WatCLASS can define watershed properties. Also important to this study is the previous assembly of much of the forcing data required to drive the model.

4.2 Point Scale Results – Micro-Meteorological Model Scale

The goal of this section is to show the influence of including runoff calculations on evaporation amounts produced by a land surface scheme. To do this, WATFLOOD is used to spatially disaggregate the observed streamflow into its point source contributions; in effect the reverse of normal hydrologic modelling where a calibrated model is used to predict streamflow. This process and its implications are explained further in Chapter 6 but essentially the hydrologic model is forced, through an optimization process, to fit measured hydrographs and the individual point runoff amounts that correspond with tower locations are extracted and assumed for this exercise to be measured data. By proceeding in this manner, each of the variables from the water balance equation are measured and the parameters necessary for WatCLASS can be extracted.

The tower sites that are investigated are located inside watershed boundaries that are coincident with the study areas. For the NSA these include the Northern Old Black Spruce forest (NSA-OBS), the Young Jack Pine site (NSA-YJP) and the Northern Fen site (NSA-FEN). The SSA flux towers were also used in this analysis and these include the Southern Old Black Spruce site (SSA-OBS), the Southern Young Jack Pine (SSA-YJP) and Southern Old Jack Pine (SSA-OJP). A number of tower sites lay outside the watershed boundary but within the study areas and include the two aspen sites old (SSA-OA) and young (SSA-YA),

the fen site (SSA-FEN) and the northern old jack pine (NSA-OJP). Figures 4-3 and 4-4 show the locations of these tower sites.

4.2.1 Vegetation and Soil Parameters

The CLASS model requires that a number of vegetation and soil parameters be determined prior to simulations. Luckily, many of these parameters have been measured as part of the BOREAS experiment. These are required to define how the canopy and soil respond to energy and water inputs. Many of these plant properties have been extracted from the BOREAS literature and data base and are summarized in Table 4-1. Of these, rooting depth and albedo require further explanation.

Table 4-1 : Canopy Properties for BOREAS Tower Locations

Tower Site	Roughness Length ln(m)	Canopy Mass (kg/m^2)	Leaf Area Index (Max)	Leaf Area Index (Min)
NSA-OBS	0.405	5.52	2.86	2.45
NSA-FEN	-2.996	2.00	2.00	0.00
NSA-YJP	-1.204	2.20	1.46	1.46
SSA-OBS	0.405	4.51	4.20	4.00
SSA-FEN	-2.996	2.00	2.00	0.00
SSA-OJP	0.405	3.40	2.50	2.30

Note: see table 4.3 for albedo values and next section for rooting depth information

Rooting Depth

Determination of rooting depth is an important consideration when using the CLASS model and one in which the choice can have a significant impact on results. CLASS is equipped with three horizontal soil layers (see figure 3-3), the depths of which are set, from top to bottom, at 0.10m, 0.25m and 3.75m. This deepest third layer was designed to act as a

thermal sink for soil temperature and ice content which varies seasonally to regulate surface temperature. The third layer depth was chosen to coincide with a zero energy flux boundary at the bottom of the layer. Hydrologic calculations have been superimposed on this layered system with the lowest boundary condition changed from its energy counterpart to provide a unit head gradient (dh/dz=-1). This allows drainage from the layer to be determined based on the moisture content of the layer alone. For this deepest layer, the potential for moisture storage is large. A change in soil moisture from field capacity (340 cm H_20 tension) to the wilting point (15,000 cm H_2O tension) in the third soil layer would be equivalent to 430 mm of water given a sandy loam soil. Allowing a rooting depth specification greater than 0.35 m (i.e. layer1 + layer2) permits virtually unrestricted assess to third soil layer moisture and allows plants access to the equivalent of the average annual BOREAS precipitation (approximately 450 mm per year). CLASS does enforce preferential removal of soil moisture from upper soil layers, owing to an exponential distribution of root mass with depth. However, specifying a rooting depth of 0.351 m will allow plant access to each of the three moisture reservoirs and have soil moisture based transpiration resistance calculated from the layer with the lowest soil moisture tension.

Specification of a rooting depth of less than 0.35 m seems contrary to published values of root depth, which often extend to 4 and 5m. However, a majority of plants' active roots are located very close to the soil surface with deeper roots acting only as anchor roots (Moore *et al*., 2000). In the boreal forest environment, active black spruce rooting depth is specified as 0.30 m (Betts *et al*., 1999) and jack pine roots slightly deeper at 0.45 m (Moore *et al*., 2000) making the specification of a 0.35 m maximum rooting depth much more palatable than a true, slightly deeper measure. It should also be noted that limiting tree roots to remain within

the upper two layers does not preclude transpiration of soil moisture from the third layer. Gradients of total head, which normally point downward, can reverse when low soil moisture in the upper layers cause soil suction values to overcome the gravitational based elevation head. This reversal would generate an upward flux of water from the third layer to supply transpiration demands. Changing this situation so that more realistic rooting depths could be used would require the addition of a fourth, variable depth soil layer. This has been implemented in other LSSs such as MOSES (Cox *et al*., 1999) but requires the estimation of another, poorly defined vegetation parameter. This change could be made in CLASS within its current forward difference soil moisture calculation scheme. However, such a change would be a major one for the model and require the entire user base to retune their results to accommodate the change.

Albedo

Specification of shortwave reflectance in CLASS is done by entering the maximum fully leafed midday reflectance of the land surface vegetation. This reflectance value must be made for both the visible (400-700nm) and the near infrared (700-3000nm) bands of the radiative spectrum. Within these wavelength ranges, reflectivity may vary substantially and depend largely on the nature of the reflecting surface. Albedo (ζ) is defined as the $K\Leftarrow \not\Rightarrow K\Rightarrow$ where K is the total short wave radiation from 150 nm – 3000 nm (Oke, 1987, p. 11). However, very little energy is contained in ultraviolet wavelengths (<400nm) owing to ozone absorption in the upper atmosphere. Of the remaining short wave energy, approximately one-half is contained in the visible portion of the spectrum (Oke, 1987, p. 22).

Published values of albedo are not often available in both the visible (VIS) and near infrared (NIR) ranges which makes it difficult to determine appropriate values to use with CLASS. Fortunately, the BOREAS project has a set of measured reflectance values obtained from a helicopter platform using a Modular Multispectrum Radiometer (MMR) (Loechel *et al*., 1997). The helicopter platform allowed a large field of view (~80m) over which reflectance values were averaged. The radiometer was designed to match the spectrum of LandSat TM frequencies which span much of the shortwave spectrum. However, the MMR only samples a portion of the entire short range spectrum in the seven channel ranges. Table 4-2 gives the list of spectral band ranges, the reflectance, and the percentage of the total measured energy within each band averaged over all sites measured in the BOREAS study area.

Table 4-2 : MMR results for all BOREAS sites (Loechel *et al*., 1997)

Band	***MMR1***	***MMR2***	***MMR3***	***MMR4***	***MMR5***	***MMR6***	***MMR7***
Range (nm)	450-520	510-520	630-680	750-880	1170-1330	1570-1800	2080-2370
Average Reflectivity	1.9%	3.2%	3.0%	19.1%	20.2%	12.5%	5.4%
Radiance	9%	12%	9%	40%	16%	5%	1%

Table 4-3 gives the albedo values generated for the various tower sites using the MMR results. To determine albedo values for CLASS, channels 1, 2, 3 where combined for the (VIS) visible portion and channels 4, 5, 6, 7 where combined for the infrared (NIR) portion. Combining reflectance values was done using their average value weighted by the observed radiance from each channel. Table 4-3 (last column) also presents full short wave spectrum albedo values determined from BOREAS mesonet towers as measured by Betts and Ball (1997). These values appear to be lower than MMR average values since they were

determined over a larger portion of the diurnal and annual cycle. MMR values were determined only at times close to solar noon and for fully leafed conditions, which are more appropriate for CLASS. Albedo correction for changes in the solar zenith angle, vegetation growth stage, and snow cover are handled by CLASS algorithms.

Table 4-3 : Visible and near infrared albedo values for selected BOREAS tower sites

Site	*Visible Albedo*	*Near Infrared Albedo*	*Average Albedo*	*Comparible Albedo Ranges (Betts and Ball, 1997)*
NSA-FEN	3.5	16.9	10.2	-
NSA-OBS	2.4	14.0	8.2	8.1
NSA-OJP	3.5	17.0	10.2	8.6
NSA-YJP	4.2	18.6	11.4	8.6
SSA-OA	2.2	30.9	16.5	15.6
SSA-YA	3.2	33.4	18.3	15.6
SSA-FEN	3.3	15.8	9.5	-
SSA-OBS	2.1	13.7	7.9	8.1
SSA-OJP	3.5	15.1	9.3	8.6
SSA-YJP	2.8	18.0	10.4	8.6

Soil Parameters

Soil parameters used by CLASS are generated though a look-up table based on sand and clay content indices as well as some specialized soil types. Special cases are used to define solid rock ($K_{sat} = 0$), glacier ice ($\chi_{sat} = 1$), and peat soil ($\chi_{sat} = 0.8$). The CLASS index values for mineral soils are calculated based on simple normalization functions as follows:

$$Sand\ Index = \min\left(\frac{\%sand - 17}{5},\ 15\right)$$

Equation 4-1

$$Clay\ Index = \min\left(\frac{\%clay\ 2\ 2}{5},\ 12\right)$$

Index values are rounded to the nearest integer and used to select appropriate soil parameters. Essentially, these equations provide 15 bin ranges of 5% each for sand contents ranging from 22% to 93% and 12 bin ranges of 5% each for clay contents ranging from 3% to 58%. A separate index is maintained for organic matter content that is only used to determine soil thermal properties and has no influence on hydraulic properties.

General soil parameterization used to define unsaturated soil properties for Richard's equation (K(χ) and ..(χ)) are based on a simplified fit of measured moisture characteristics and the Burdine (1953) description of unsaturated flow conductivity in porous media. Equation 4-2, which describes this soil model, was originally proposed by Campbell (1974) as a simplification to the Brooks and Corey (1964) model.

$$\ldots | \ldots_{sat} (S)^{4b} \qquad K | K_{sat} (S)^{c} \qquad \text{Equation 4-2}$$

where S is the degree of soil saturation (χ/χ_{sat}), the parameters 'b' and 'c' are related to pore space properties of the soil. Both $..._{sat}$ and K_{sat}, are the supposed saturated values of tension and hydraulic conductivity respectively, but are determined by the extrapolation of fitted soil curves to a saturated condition and do not represent the saturated values of these quantities. Brooks and Corey had provided a physical interpretation of $..._{sat}$ as the air entry suction ($..._e$) or the value of soil suction that would be found at the top of the capillary fringe in saturated soils. To allow its use, Brooks and Corey required the introduction of an additional residual moisture content parameter (χ_r) in the determination of S as follows:

$$S | \left(\frac{\chi 4 \chi_r}{\chi_{sat} 4 \chi_r} \right) \qquad \text{Equation 4-3}$$

This parameter introduces a sharp discontinuity in the function at χ_r and requires the estimation of this additional parameter. The simplification of Campbell (1974) cautions that departures from measured tension values in the wet range (> -10 kPa) should be expected.

The work of Campbell (1974) was followed by Clapp and Hornberger (1978) who used a power law equation to generate texture based parameters. Campbell had originally provided analysis for only four soil samples. Clapp and Hornberger (1978) extended this data base and estimated parameters 'b', χ_{sat} , K_{sat}, and $\ldots_{sat}$ in terms of soil texture through statistical analysis of 1446 soils. Cuenca *et al*. (1996) points out that this large sample base has lead to its widespread use in atmospheric modelling including the well known SiB (Sellers *et al*., 1986) and BATS (Dickinson *et al*., 1993) land surface schemes.

Clapp and Hornberger (1978) suggest values of 'b', χ_{sat} ,K_{sat}, and $\ldots_{sat}$ only in terms of soil texture designations within the U.S. Department of Agriculture (USDA) soil texture triangle. This ordinal data base is generally not sufficient for modelling purposes. To extend the functionality of the Clapp and Hornberger (1978) parameters, Cosby *et al*. (1984) introduced continuous functions with sand, silt, and clay fractions as independent variables to estimate parameters. Particle size fractions were chosen simply as mid-point texture values within the soil triangle classes using the original Clapp and Hornberger data base. Even with the error this size fraction estimate introduced, Cosby *et al*. (1984) were able to show, through a series of statistical tests, that the mean value of the soil parameters as well as their variances could be estimated using soil texture alone. Two alternate formulations were given by Cosby *et al*. (1984). The first form uses two components of the particle size distribution with the third deemed to be included in the regression since the sum of sand, silt, and clay fractions was

assumed to be 100%. The second formulation is presented in terms of a single dominant component of either sand or clay content. The functional form is a simple linear model as follows:

$$Parameter \mid Intercept\ 2 \sum_{n \mid 1}^{1 or 2} variable * slope_n \qquad (4\text{-}4)$$

Table 4-4 gives the mean values (variances not shown) of the parameters for each of the two Cosby models:

Table 4-4 : Cosby soil parameter estimates (from Cosby *et al*., 1984)

	Two-Component Model			***One-Component Model***		
Parameter	***Intercept***	***Variable***	***Slope***	***Intercept***	***Variable***	***Slope***
B	3.10	%clay	0.157	2.91	%clay	0.159
		%sand	-0.003			
log ψ_{sat}	1.54	%sand	-0.0095	1.88	%sand	-0.0131
		%silt	0.0063			
log K_{sat}	-0.60	%sand	0.0126	-0.884	%sand	0.0153
		%clay	-0.0064			
χ_{sat}	50.5	%sand	-0.142	48.9	%sand	-0.126
		%clay	-0.037			

CLASS uses the 'one-component' model of Cosby *et al*. (1984) and the power law relation developed by Campbell but the question arises as to: 'How well do these functions work for the BOREAS soils?'

Detailed soils data are available from the BOREAS project. Three BOREAS sub-project groups determined the physical characterization soils for the project. These include TE-1

(terrestrial ecology) for SSA soils characterization and mapping (Anderson, 1998), TE-20 for NSA soils characterization and mapping (Veldhuis, 1995) and HYD-1 (hydrology) for the determination of soil hydraulic properties (Cuenca, 1997). These data sets provide soil moisture characteristics and hydraulic properties for soils at the various tower sites within the study areas. The purpose of the remainder of this section is to relate these soil properties to the CLASS soil parameterization.

Use of the Campbell (1974) power function form of the moisture characteristic and hydraulic conductivity presented in equation 4-2 inevitably leads to the criticism of its failure to provide realistic results for wet conditions beyond -10 kPa tension. To overcome this restriction, van Genuchten (1980) suggested the use of a function whose values and first derivatives where smooth and continuous over the entire range of soil moisture values. Cuenca *et al*. (1997) provides estimates for the van Genuchten (1980) soil moisture characteristic model fitted to BOREAS tower site soils. This function takes the following form:

$$S = \left[1 + \left(\psi / \psi_e\right)^n\right]^{-m} \qquad K = K_{sat} \sqrt{S} \left[1 - \left(1 - S^{1/m}\right)^m\right]^2 \qquad \text{Equation 4-5}$$

where S is the effective saturation which includes χ_r as in equation 4-3, n and m are parameters related by m=1-1/n and $1/\zeta$ is often taken as the Brooks and Corey air entry suction value, ψ_e. Also presented is the unsaturated hydraulic conductivity (K) relation that is determined from the soil moisture characteristic equation and scaled with the saturated conductivity value, K_{sat}. The van Genuchten moisture characteristic function matches the behaviour of the Brooks and Corey model with an equal number of parameters but has the advantage of defining, more realistically, soil moisture values at low suctions. Added

complexity, however, in estimating van Genuchten model parameters require non-linear curve fitting models. Schemes such as RETC (van Genuchten *et al*., 1991) exist for this purpose, however, the proliferation of Clapp and Hornberger type models make their wide spread use unlikely in the short term. Cuenca *et al*. (1996) point out that the van Genuchten formulation have received considerable attention in the soil science community but is virtually unused in land surface process modelling.

Table 4-5 below reproduces the van Genuchten parameters developed by Cuenca and are used here to represent "measured" soil conditions. Separate analysis of TE-1 and TE-20 soils lab data indicates that the Cuenca *et al*. (1997) derived parameters accurately reflect measured soil properties.

Table 4-5 : van Genuchten soil parameters for BOREAS tower sites (from Cuenca *et al*., (1997))

	NSA			***SSA***			
Property	***OJP***	***YJP***	***OBS***	***OJP***	***YJP***	***OA***	***OBS***
Texture	Sand	Sand	Clay	Sand	Sand	Silt loam	Sandy loam
Bulk Density (g/cm3)	1.45	1.45	1.3	1.45	1.19	1.37	1.39
K_{sat} (cm/day)	77	191	46	146	186	25	79
N	1.35	1.48	1.15	1.56	1.38	1.22	1.28
86ζ (cm^{-1})	11.5	10.5	66.7	12.8	14.5	47.6	29.4
χ_r	0.01	0.03	0.17	0.03	0.03	0.05	0.01
χ_{sat}	0.21	0.30	0.65	0.40	0.32	0.51	0.51

Rather than adapting CLASS to use van Genuchten theory, it is more advantageous at this point to adapt Campbell type parameters to fit soil observations. Figure 4-5 shows the moisture characteristic and the unsaturated conductivity curves for the clay soil of the NSA-OBS and the sandy soil of the NSA-YJP based on parameters from Table 4-5. Shown

additionally on the moisture characteristic portion of Figure 4-5 are horizontal lines representing soil suction values of significant interest. From top to bottom, these are the wilting point (WP) (15,000 cm), field capacity (FC) (340 cm), and field moisture 10th (100 cm), presented here as positive values for ease of plotting. The moisture characteristic plays two important roles in land surface models. First, it determines the degree of soil moisture regulation on plant transpiration through its influence on stomatal resistance. For example, in NSA-OBS clay soil, wilting will commence at soil moistures lower than 34% while moisture above field capacity at 54% offers no resistance to transpiration. These values are very different for the NSA-YJP sandy soil. Sands for the NSA-YJP have wilting point and field capacity soil moistures of 4% and 8%, respectively. These values indicate a large range in the available evaporative storage capacities of these two systems with spruce forests on clay soil having a 20% differential between field capacity and the wilting point (54%-34%) and jack pine forests on sandy soil have only a 4% (8%-4%) difference.

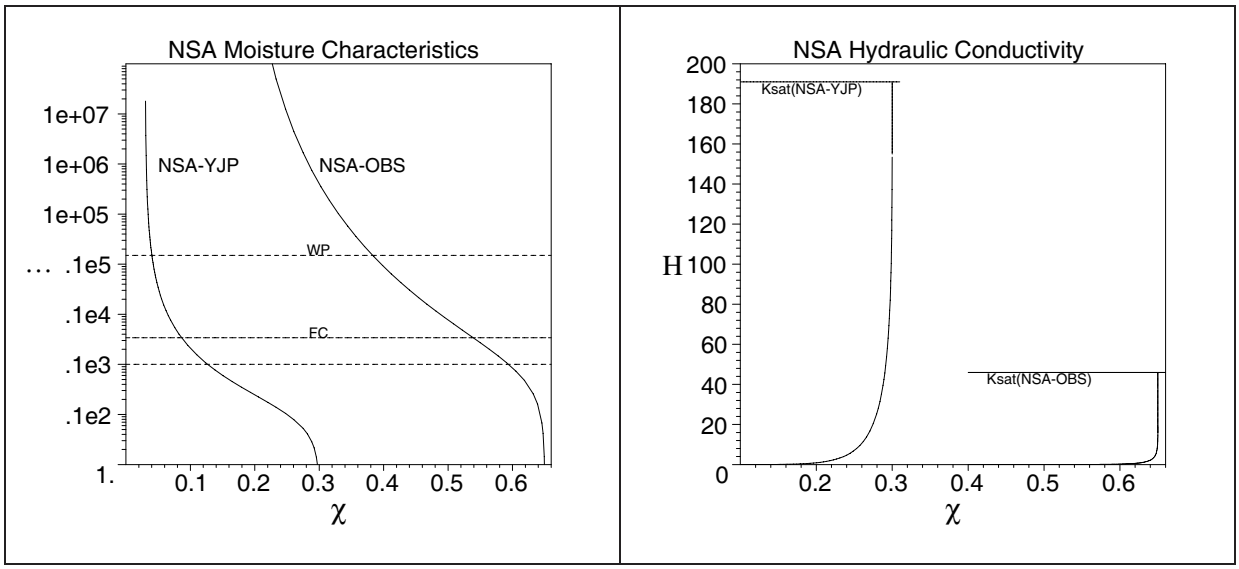

Figure 4-5 : Moisture characteristic and unsaturated hydraulic conductivity for extreme soil conditions found in the BOREAS NSA. Soil suction is in units of cm. and hydraulic conductivity (K) in units of cm/day. Saturated values of hydraulic conductivity are indicated by a horizontal line. Wilting point (WP), field capacity (FC) and soil moisture 10th are shown as horizontal lines.

A second role of the moisture characteristic is its basis for determining the shape of the unsaturated hydraulic conductivity profile. Unsaturated hydraulic conductivity is very difficult and costly to measure. In contrast, the moisture characteristic is much easier to measure in the laboratory. As a result hydraulic conductivity models, such as those used in equations 4-2 and 4-5, have been derived based on (i) the theory of fluid flow though a capillary tube, (ii) a measured moisture characteristic, and (iii) a single hydraulic conductivity measurement, often determined at saturation and called the "matching factor" (Childs and Collis-George, 1950). Examples of hydraulic conductivity models include those of Burdine (1953) and Mualem (1976) which have become popular in unsaturated flow modelling due to Brooks and Corey (1964) and van Genuchten (1980), respectively. These capillary models are based on an analogy of flow through a set of small tubes which visually would resemble a scaled down box of various diameter drinking straws. These tubes are

either cut and randomly rejoined, or made to follow through tortuous pathways in an effort to idealize the model to actual soil conditions. Water drains more quickly through the larger diameter tubes than through the smaller tubes. Summing up the contribution from each full tube of water determines the hydraulic conductivity. This is where the relation to the moisture characteristic becomes important. In order to determine the diameter of the largest tube that is filled with water at a given soil moisture content, the moisture characteristic curve is used. This curve relates soil tension value to moisture content. Tube diameters for conductivity models are then determined by relating these to soil tension using the theory for capillary rise in tubes. By integrating the moisture characteristic function from zero to the measured soil moisture, the entire distribution of full flowing tubes is exactly known. When this distribution is scaled to real soils by combining the conductivity model with a single "matching factor" measurement, the entire range of unsaturated hydraulic conductivity may be determined. Hence, the importance of the moisture characteristic in determining hydraulic conductivity. More details of the theories and development history of soil water movement are presented in Appendix A of this thesis.

The unsaturated hydraulic conductivity curves presented in Figure 4-5 show the implications of moisture characteristic response for limiting conductivity values ($K < 0.1$ cm/day). This occurs for moisture contents less than 58% for clay and 15% for sand. In both these cases, the soil moisture 10^{th} suction value, defined above as the soil moisture where tension equals 100 cm of water, more closely represents this limiting value than does the field capacity (FC) value. Also important to note is the limited practical significance of the saturated hydraulic conductivity value (marked by a short horizontal line in Figure 4-5). Conductivity values drops by more than 80% for soil moisture reductions of only 1% below saturation. A semi-

log version of hydraulic conductivity plot is presented in Figure 4-6. This serves to illustrate that hydraulic conductivity theory does not cut-off soil water flux at low soil moistures but reduces it almost exponentially toward zero.

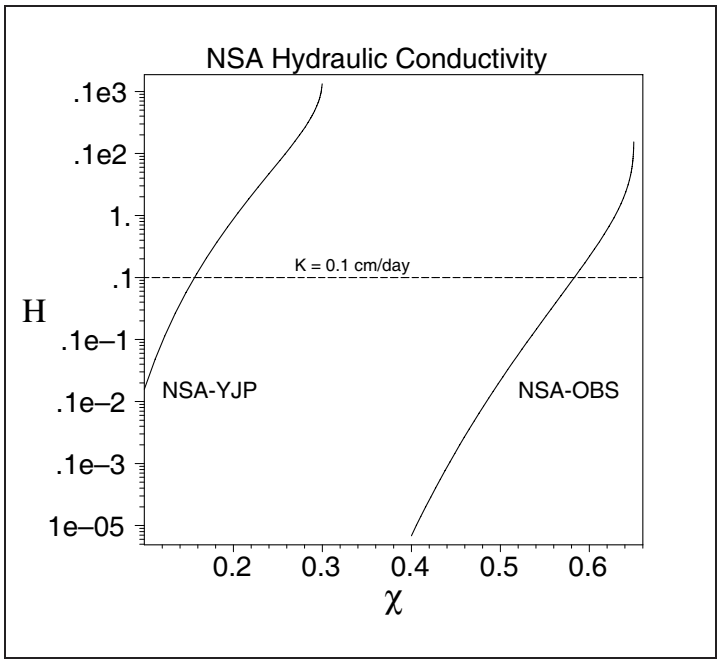

Figure 4-6 : NSA soil conductivity on a semi log plot with K in units of (cm/day). A low conductivity value of 0.1 cm/day is included to show the difference in soil moisture regimes for the two systems.

Measured grain size analysis averaged for all NSA-OBS test pits analysed by Veldhuis (1995) show grain size fractions of 2%, 11% and 87% respectively for sand, silt, and clay contents. These percentages are outside the range of grain size application for CLASS parameter estimates given by Equation 4-1. The most clay like soil that could be represented with CLASS, from Equation 4-1, would have a sand index of 1 and a clay index of 12 which would represent sand and clay contents of 22% and 58%, respectively. Based on this description alone, it would appear that CLASS is not suitable for these environmental conditions.

If only the ranges of realistic application are considered, which are defined here as soil moistures between the wilting point and saturation, CLASS parameters can be forced to fit the observed soil hydraulic conditions. Figure 4-7 illustrates an example of such a fitting exercise for the NSA-OBS clay soils.

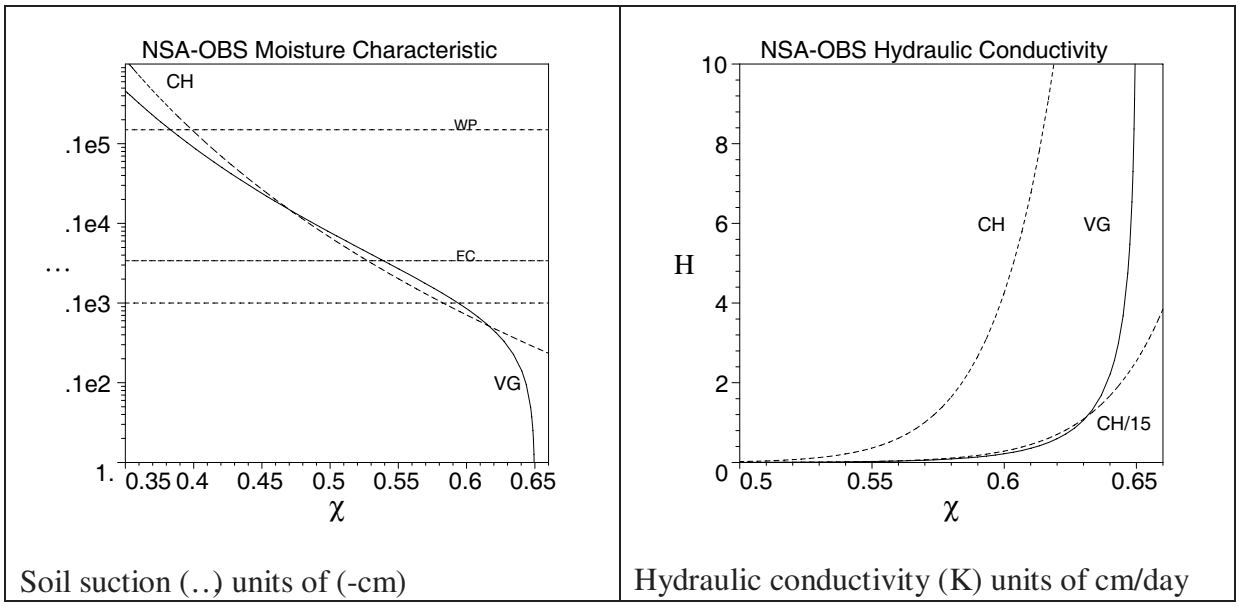

Figure 4-7 : Result of fitting Campbell / Clapp and Hornberger (CH) parameters to van Genuchten (VG) model developed for the NSA-OBS. Soil suction (..) is in units of cm. and hydraulic conductivity (K) in units of cm/day.

The procedure followed to obtain the fitted result includes: i) substitute Cosby equations into Campbell equations, and ii) selection of a Cosby clay fraction which matched the Clapp and Hornberger slope to the slope of the van Genuchten (VG) model between the wilting point (WP) and field capacity (FC). These steps alone were unable to produce acceptable results for any measure of sand content and iii) required that Clapp and Hornberger soil moisture be scaled to van Genuchten curves by the amount of residual soil moisture content, χ_r. Once scaled, iv) the sand content could be selected to provide a reasonable fit to the van Genuchten

model. Generally, the clay fraction changed the curvature of the moisture characteristic and the sand content moved the function to the right or left to produce the fitted relation.

It should be reiterated that this procedure for fitting the van Genuchten and Clapp and Hornberger models has been done because CLASS has been developed using Clapp and Hornberger and the data available are measured using van Genuchten. A preferable solution would be to alter CLASS soil physics to accept van Genuchten parameters. However, this would require a major re-tooling of CLASS which would create a model with better soil physics but hinder its acceptance as a candidate for Level III modelling. The goal here is to introduce WATFLOOD hydrology within atmospheric models and the best method of achieving this is to leave CLASS as intact as possible. These fitting methods would not be readily accepted within the soil science community but they provide a means here for testing WatCLASS with measured BOREAS data.

The fit obtained for the NSA-OBS moisture characteristic is limited somewhat by constraints of sand and clay end points in CLASS but reasonably represents the soil moisture – tension relationship between the wilting point (WP) and field capacity (FC). This fit, however, sharply diverges at very wet soil moisture values, illustrating the inherent and well documented limitation of the Clapp and Hornberger family of models. The final form of the Clapp and Hornberger model used here combines the Cosby equations to produce:

$$\ldots | \; A(\chi 4 \chi_r)^B$$

where :

$$A | \; \exp(4.33 4 0.0302(\%sand)) * (0.489 4 0.00126(\%sand))^B$$

$$B | \; (2.91 2 0.159(\%clay))$$

Equation 4-6

The best fit values for the NSA-OBS moisture characteristic are %sand = 22 and %clay = 35. This corresponds to CLASS index values of 1 and 7.4 for sand and clay, respectively. It is important to note the inclusion of the χ_r term in the equation 4-7. Scaling soil moistures in CLASS by this amount allows the Clapp and Hornberger model to properly match the dynamic range of soil moisture variation without introducing new soil physics theory to CLASS. Examination of Table 4-4 shows that the maximum value of χ_{sat} that can be obtained from Cosby parameters is 48.9%. NSA-OBS clays have measured χ_{sat} value of 65% which requires that an extra parameter be added to scale soil moistures. To compare CLASS simulated soil moisture to field measured soil moisture content requires the addition of an appropriate residual moisture content term.

While the use of the residual soil moisture term allows the dynamic range of soil moisture to be properly modelled, energy balance issues associated with this extra soil moisture are not adequately represented. These processes including thermal conductivity, latent heat of fusion generated through frost generation, and specific heat values, all of which have lower total moisture contents than would be found in BOREAS soils.

Fitting of the unsaturated hydraulic conductivity profiles was not considered concurrently with moisture characteristic parameter selection. As described previously, unsaturated conductivity theory depends primarily on the moisture characteristic of a soil. This fitted function, when combined with an appropriate tube flow theory, is scaled using the "matching value" conductivity. In CLASS, Cosby parameters are used to determine the K_{sat} "matching value". Cosby-derived K_{sat} values produce the Clapp and Hornberger curve in Figure 4-7. This hydraulic conductivity profile is much higher than van Genuchten model results which

are based on unsaturated conductivity measurements performed by Cuenca *et al*. (1997). The selection of a new "matching value" determined by dividing Cosby K_{sat} by 15 (marked as CH/15 in the Figure 4-7) shows that if the shape of the moisture characteristic is preserved, the shape of the unsaturated hydraulic conductivity profile can be matched. Naturally, wet range limitations inherent in the Clapp and Hornberger moisture characteristic translate to poor fits in the wet range of the unsaturated zone. The final equation used for the unsaturated conductivity:

$$K = \frac{A}{SF}(\chi - \chi_r)^B$$

where :

$$A = \exp(42.04 - 0.0352(\%sand)) * (0.489 - 0.00126(\%sand))^{-B} \qquad \text{Equation 4-7}$$

$$B = (8.82 - 0.318(\%clay))$$

$$SF = K_{sat} \text{ scaling factor}$$

The K_{sat} scaling factor (SF) is selected to match conductivity values within 2% of saturation. This is deemed to be appropriate for CLASS since soil moistures are restricted from obtaining fully saturated condition for infiltration calculations owing to the inevitability of trapped air pockets in the soil matrix. There has been concern expressed about the use of K_{sat} as an appropriate "matching factor" because of the influence of marcopores on its value which has not been adequately represented in either van Genuchten or Clapp and Hornberger conductivity models. Table 4-6 gives CLASS soil parameters for all BOREAS soils analysed by Cuenca *et al*. (1997).

Table 4-6 : CLASS parameters for BOREAS soils

	NSA			*SSA*			
Property	***OJP***	***YJP***	***OBS***	***OJP***	***YJP***	***OA***	***OBS***
Texture	Sand	Sand	Clay	Sand	Sand	Silt loam	Sandy loam
Sand Index	15	15	1	15	15	1.2	4.6
Clay Index	1	1	7.4	1	1	2.6	1
Organic Content			5				
SF	0.25	1.25	15	7	0.75	7	6
χ_r	-0.01	-0.03	0.17	0.0	0.03	0.05	0.01

This visual fitting process could be generalized so that any van Genuchten fitted soil can be generalized to CLASS parameters. However, many of the BOREAS soils are at the extreme limits for sand and clay contents which required selection of χ_r that differed from the values determined by Cuenca *et al*. (1997). Fits obtained for NSA-OJP, NSA-YJP, SSA-OJP all required lower values of χ_r to match van Genuchten moisture characteristic curves making a general mathematical solution of lesser value.

Soil Profile Measurement

Field work conducted by Cuenca *et al* (1997) consisted of measurements of conductivity at specified soil moistures using a tension infiltrometer. These were conducted near the top of the mineral soil surface (15 cm depth) and represent the topmost "A" horizon. Soil lab data from BOREAS groups TE-1 (SSA) and TE-20 (NSA) show that deeper soil horizons have similar moisture characteristic curve shapes and that absolute ranges of moisture content between field capacity and the wilting point is similar at all depths. Deeper soils tend to have higher bulk densities and this can be used to determine the "matching factor" conductivity for deeper soil depths.

A majority of the water carrying pores occur at soil moistures higher than field capacity. Ahuja *et al*. (1984), using Carman-Kozeny hydraulic conductivity theory, has determined that the saturated hydraulic conductivity relations can be determined by scaling the value of effective porosity using a power law relation. Rawls *et al*. (1998) extended this theory to include the 'b' parameter from Clapp and Hornberger as a non-linear power. The form of relation is:

$$K_{sat} \mid C\lambda_e^{(3+1/b)} \qquad \text{Equation 4-8}$$

where λ_e is the difference between soil porosity and the soil moisture field capacity (χ_{sat} - %FC) and C is a fitted scaling factor whose best fit was determined by Rawls *et al*. (1998) to be 3860 cm/day. Here, the porosity term will be replaced by $1-\psi_b/\psi_s$ where ψ_b is the bulk density of the soil and ψ_b is the density of the soil particles assumed to be 2650 kg/m^3. Both TE-1 and TE-20 data provide field capacity soil moisture as weight measurement which can be converted to volumetric moisture by multiplying by the soil specific gravity. Table 4-7 gives an example of the depth decay of bulk density for the NSA-OBS clay (test pit #2) and K_{sat} values determined from Equation 4-8. The final column in the table scale the measured K_{sat} (46 cm/day at 15 cm depth) from the distribution obtained using Equation 4-8.

Table 4-7 : NSA-OBS saturated hydrologic conductivity profile

Depth Range (cm)	***Mid Layer Depth (cm)***	***Bulk Density (kg/m^3)***	***Effective Porosity***	***Ksat from equation 4-8***	***Scaled to Cuenca***
0-7	3.5	790	42	370	210
7-14	10.5	1030	26	90	50
14-32	25.5	1060	24	80	46
62-86	74	1350	10	6	3.4

It is desirable to transfer these data to the mid-points of CLASS layers or to use these data for modelling. A well known description of depth varying hydraulic conductivity has been presented by Beven (1986), in which conductivity is expressed as an exponentially declining function of depth in the form:

$$K \mid K_o \exp(4D/m) \qquad \text{Equation 4-9}$$

where D is the depth below the surface, K_o is the conductivity at the soil surface and 'm' is a decay parameter, known as the 'effective depth' that determines the decay of hydraulic conductivity with depth. Figure 4-8 shows an example of this function fitted to the derived conductivity data on a semi-log plot. Rather than perform a least squares fit using all the data, the data point at 10.5 cm was disregarded and the plot fit by eye, giving parameters of K_o = 220 cm/day and m = 18 cm. Fitted parameters for other tower sites are presented in Table 4-8.

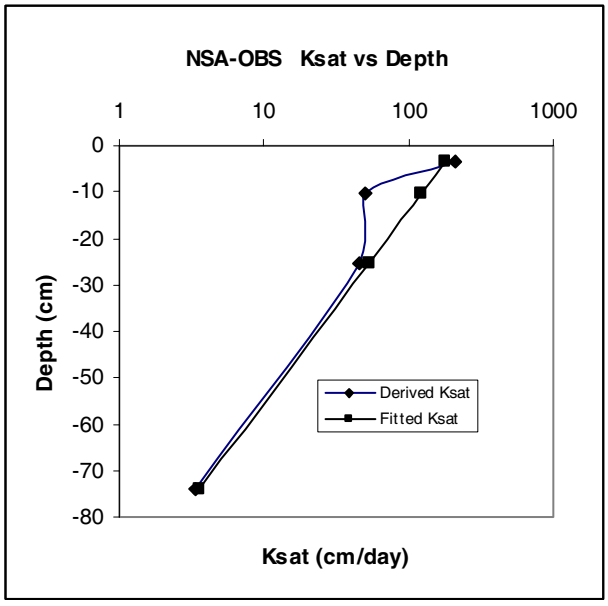

Figure 4-8 : NSA-OBS saturated hydraulic conductivity vs. depth relation derived from bulk density measurements and equation 4-8 by Rawls. Fitted TOPMODEL function shown with squares.

High values of 'm' presented in Table 4-8 indicate slowly changing values of conductivity with depth. Sandy soils in the BOREAS study sites exhibit this property of virtual K_{sat} uniformity with depth while other soils (NSA-OBS, SSA-OA and SSA-OBS) have much larger variability in soil conductivity with depth. Some caution should be used with these derived conductivity values as there have been no depth-based measurements of K_{sat} from the BOREAS soils to support the predictive nature of Equation 4-8. K_{sat} values derived here are based solely on measured bulk density and field capacity values.

Table 4-8 : TOPMODEL parameters developed for BOREAS soils.

	NSA			*SSA*			
Property	***OJP***	***YJP***	***OBS***	***OJP***	***YJP***	***OA***	***OBS***
Texture	Sand	Sand	Clay	Sand	Sand	Silt loam	Sandy loam
K_{sat} (Cuenca)	77	191	46	146	186	25	79
K_o (cm/d)	170	200	220	150	240	120	160
m (cm)	100	500	18	400	100	12	5

Wetland Soils

A large portion of both the NSA and SSA are covered by wetland soils. Wetland soils are known as peat and are composed of dead plant materials which have accumulated over long periods of time. Deeper peat soils have undergone greater degrees of decomposition and as a result have very different hydraulic properties. Unfortunately, there are little data in the BOREAS archive describing the nature of peat soils. This requires an examination of literature on the topic.

Letts *et al*. (2000) have summarized much of the available literature on the moisture characteristic and hydraulic conductivity of peat soils and have adapted these to parameters

in CLASS formats. Two parameterizations are presented: one set for van Genuchten theory and another for the Clapp and Hornberger type formulation. Plots of these functions are presented for the Fibric, Hemic and Sapric layers of peat analysed by Letts and are presented in Figure 4-9. It is obvious from the plot that Letts has attempted to match the wet end of the moisture characteristic with their Clapp and Hornberger parameters. This produces an unsatisfactory result since fitting this portion of the moisture characteristic is beyond the capabilities of the Clapp and Hornberger model. The right hand portion of the plot shows the result of improved fitting of parameters to a Clapp and Hornberger type model. Again, as with mineral soils, a scaling coefficient is used to include impact of the van Genuchten residual moisture content χ_r. Use of the scaling soil moisture has the effect only to shift the moisture characteristic curve to the right or left and changes the degree of saturation equation from $S= \chi \# \chi_{sat}$ to $S= (\chi-\chi_r) / \chi_{sat}$.

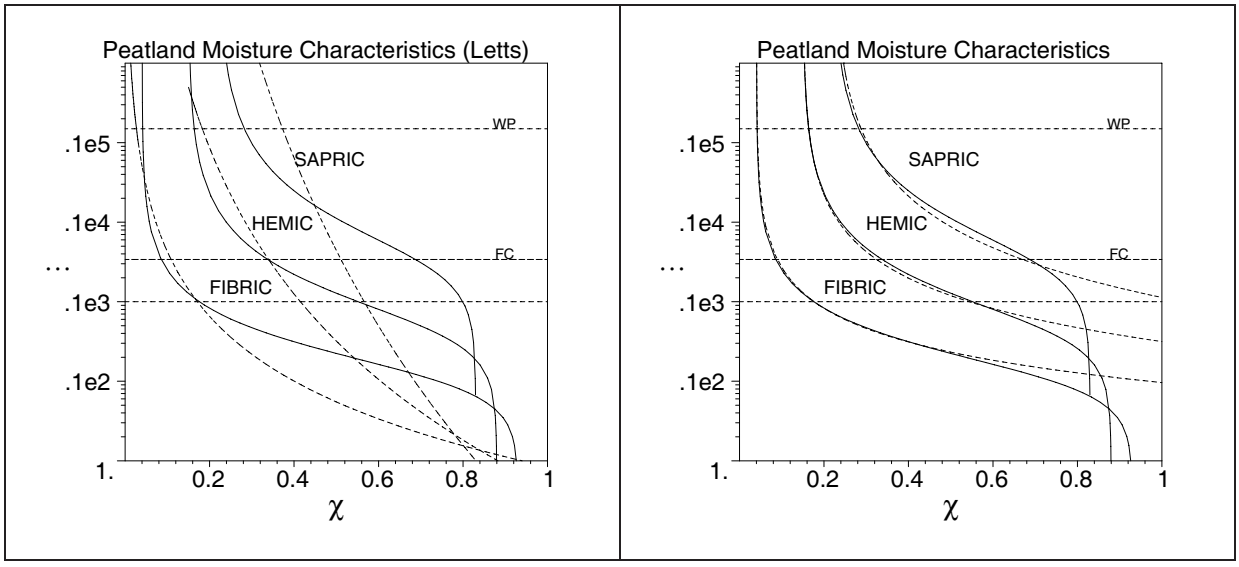

Figure 4-9 : Moisture characteristic curves for peat soils of varying degrees of decomposition. Clapp and Hornberger parameters are presented with dashed lines and van Genuchten parameters with solid lines. The plot on the left shows the models as presented by Letts *et al.* (2000) and the plot on the right shows an alternate fit.

Table 4-9 below gives revised Clapp and Hornberger parameters based on fits obtained for three peat categories analyzed by Letts *et al*. (2000). It is important to note here the assumption that the Clapp and Hornberger fits obtained by Letts were intended to best represent of the data collected in their review. The adjustments made here are merely an attempt to correct the representation of Clapp and Hornberger parameterization and do not reflect any new fitting to the original source data.

Table 4-9 : Clapp and Hornberger type peat soil parameters

	Letts			***Corrected***		
Property	***Fibric***	***Hemic***	***Sapric***	***Fibric***	***Hemic***	***Sapric***
b	2.7	6.1	12.0	1.2	1.5	2.0
ψ_{sat} (cm)	1.03	1.02	1.02	10	30	100
χ_{sat}	0.93	0.88	0.83	0.93	0.88	0.83
K_{sat} (cm/day)	2420	17.3	0.86	2420	17.3	0.86
SF	1	1	1	1.5	1	0.4
χ_r	0	0	0	0.04	0.15	0.22

4.2.2 Forcing Data

To drive the point scale model, atmospheric forcing data are required. These data were assembled as part of the BOREAS Follow-On Project for the NSA-FEN, NSA-OBS and SSA-OBS and SSA-OA (Nijssen and Lettenmaier, 2001) and represent a continuous hourly data record from 1-Jan-1994 through 1-Dec-1996. Missing tower data was filled-in by a systematic method based on near-by stations. Final quality control checks were performed, such as zeroing negative vapour pressure deficits. Figure 4-10 below shows daily average values of the seven atmospheric forcing derived for the NSA-OBS tower. This continuous, three-year data set was used to run the CLASS model.

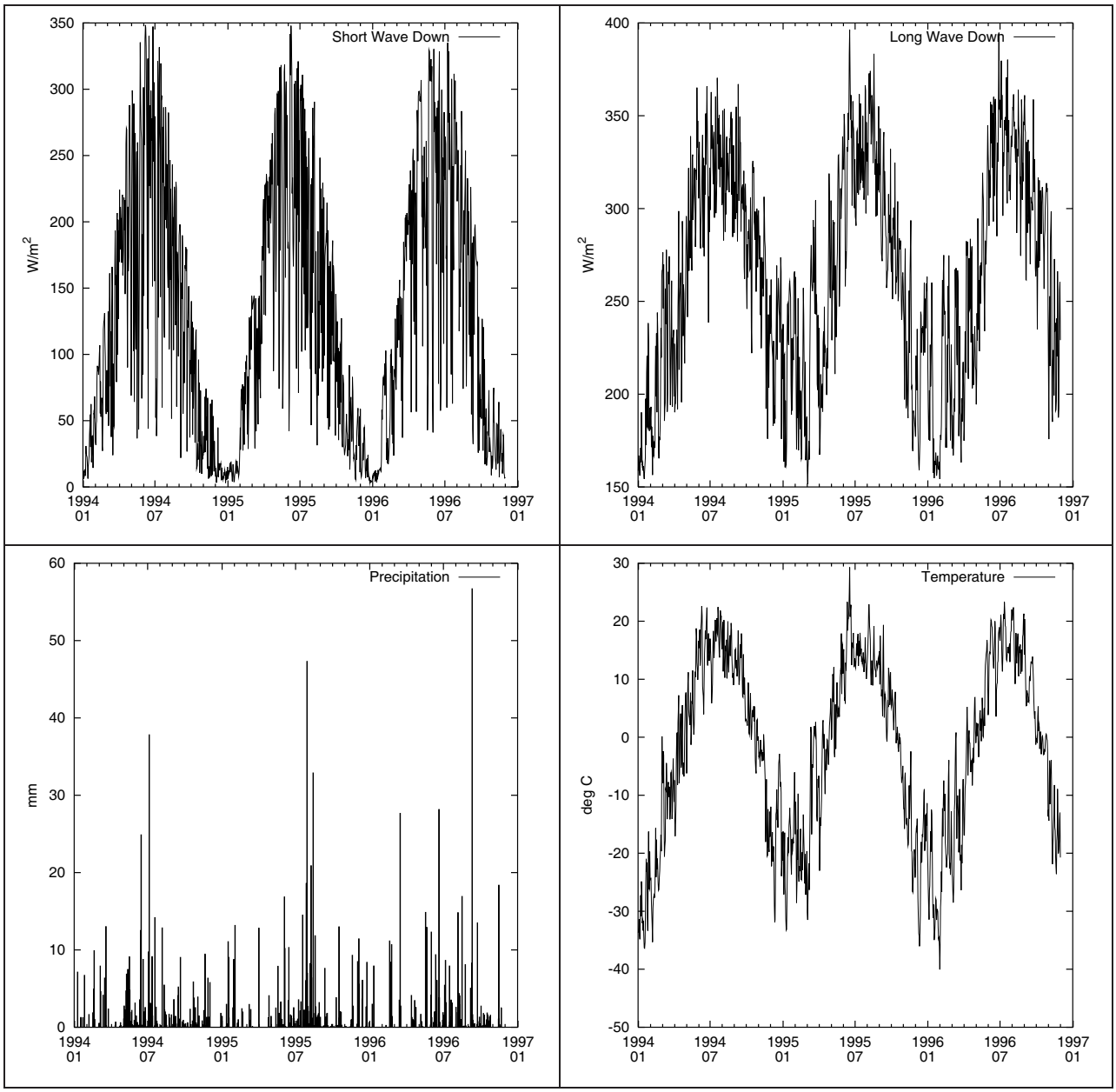

Figure 4-10 : NSA-OBS forcing data used with CLASS.

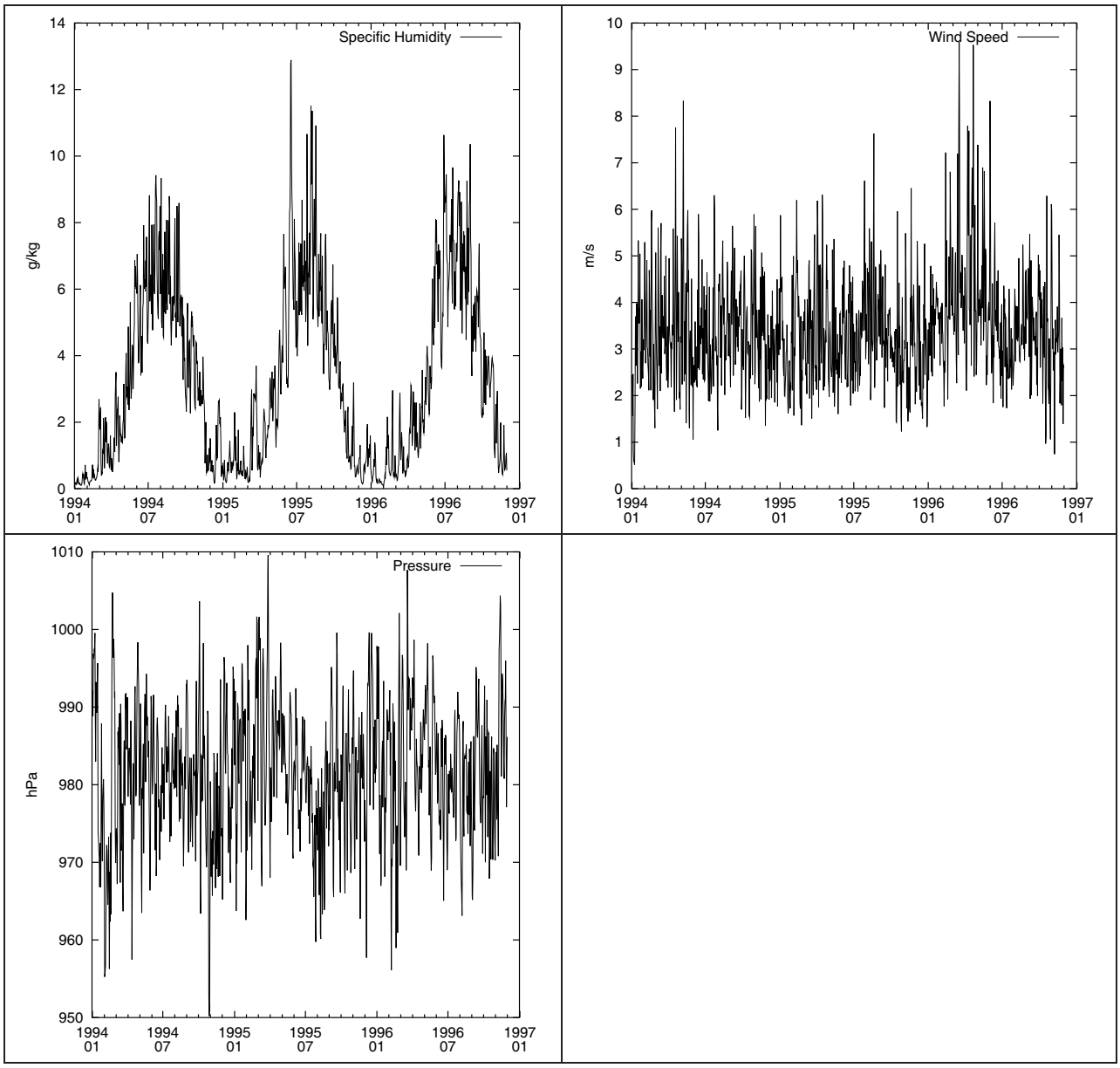

Figure 4-10 (cont): NSA-OBS forcing data used with CLASS.

Care must be taken when generating humidity inputs for CLASS, especially for low humidity values encountered during the winter. CLASS requires input of "specific humidity" which is defined as the mass of water vapour per unit mass of moist air (units of kg/kg). Humidity is rarely specified in this form and most often requires conversion from another format based on a measure of how far current atmospheric moisture deviates from the saturated value. Some of these measures include: (i) relative humidity, the ratio actual humidity to saturated

humidity, (ii) vapour deficit, the difference between saturated humidity and actual humidity and (iii) dew point temperature, the temperature an air parcel must be brought to reach saturation. BOREAS follow-on data were presented as a vapour pressure deficit (vpd) where the pressure measurement is the partial pressure of water vapour in the atmosphere. This can be determined by the following relation:

$$vpd = e_{sat} - e \qquad \text{Equation 4-10}$$

where vpd is the vapour pressure deficit, e_{sat} is the saturated vapour pressure and e is the actual vapour pressure all of which are in the same pressure unit. Given a vpd, the actual vapour pressure, required to determine specific humidity, can be determined by a simple subtraction of e_{sat} from vpd. Saturated vapour pressure is a function of air temperature and can be determined by the empirical Clausius-Clapeyron equation (Dingman, 2002, p. 586) as:

$$e_{sat} = 611\exp\left(\frac{17.27\,T}{237.3 + T}\right) \qquad \text{for } T \geq 0\ ^{\circ}C \qquad \text{Equation 4-11}$$

where T is degree Celsius (^{o}C) and e_{sat} is in Pascals (Pa). This equation is used for air temperatures greater than freezing. Below freezing the relation differs slightly and becomes (see: Oke, 1987, p. 394):

$$e_{sat} = 611\exp\left(\frac{21.87\,T}{265.5 + T}\right) \qquad \text{for } T < 0\ ^{\circ}C \qquad \text{Equation 4-12}$$

This low temperature relation is rarely presented in textbooks and results in lower saturated vapour pressures when compared to its above zero degree counterpart. A mismatch in the generation of saturated humidity for CLASS can lead to prolonged downward gradients of moisture for extended periods during the winter and results in very large accumulations of

snow on the land surface owing to a near continuous condensation process. Other researchers (Lefleur, personal communication, 1999) have described this symptom while using CLASS and the answer appears to lie in the generation of saturated humidity for temperatures lower then 0^{o}C. Finally, specific humidity (q) can be calculated knowing that the ratio of the molar weight of air to water vapour is 0.622 and can be calculated as:

$$q \mid \frac{0.622 \ f e}{P 4 e \ f(1 4 0.622)} \qquad \text{Equation 4-13}$$

were 'P' is the atmospheric pressure in the same units as 'e' vapour pressure.

4.2.3 Runoff Data

No measurement of runoff from plot size areas representing the tower foot prints where made during the BOREAS project. Runoff was measured only at the outlets of the study area watersheds. To examine the water balance at the tower scale, some measure of runoff is required. Whidden (1999) used the WATFLOOD hydrologic model to reproduce measured streamflow hydrographs for BOREAS area. However, while doing an exceptional job in matching observed hydrographs, some liberties were taken in the prediction of evaporation when compared to tower measurements and in the accumulation of model storage over time. None-the-less, prediction of streamflow at a gauge location requires that WATFLOOD generate a gridded time series of point runoff which is routed to the basin outlet through a stream network. Point values of this gridded time series, selected to coincide with a tower site, represent a surrogate of local runoff. While not measured values, the WATFLOOD model is used here as a spatial disaggregator to determine local runoff. Figure 4-11 presents output from WATFLOOD representing the NSA-OBS tower site (Whidden, 1999) and shows

cumulative quantities of precipitation (P=1385mm), evapotranspiration (E=777mm), runoff (R=462mm), and land surface storage (÷S=146mm) over the 35 month period of the BOREAS experiment.

It is worthwhile to mention at this point that in addition to being a good estimate of runoff that the evapotranspiration (ET) value of 777 mm compared well to the tower based measurement of 735 mm which is presented later. However, diurnal ET values generated from WATFLOOD using the Priestly-Taylor model tend to be biased high for midday values when compared to tower data.

The cumulative plots in Figure 4-11 will be used as the primary diagnostic tool for the remainder of this section. These plots show how the rainfall is partitioned into its components and reveal data inconsistencies that are not evident from the time series based hydrographs. For example, storage appears to be trending upward during the WATFLOOD simulation. It should be noted that the storage amount given in each cumulative plot that follows is a relative instantaneous storage amount and is used to make an assessment of the change in storage over time rather than give the amount of moisture in the various model stores. For WatCLASS plots, this relative storage amount is initialized at 1000 mm that is chosen as a convenient starting point for assessment.

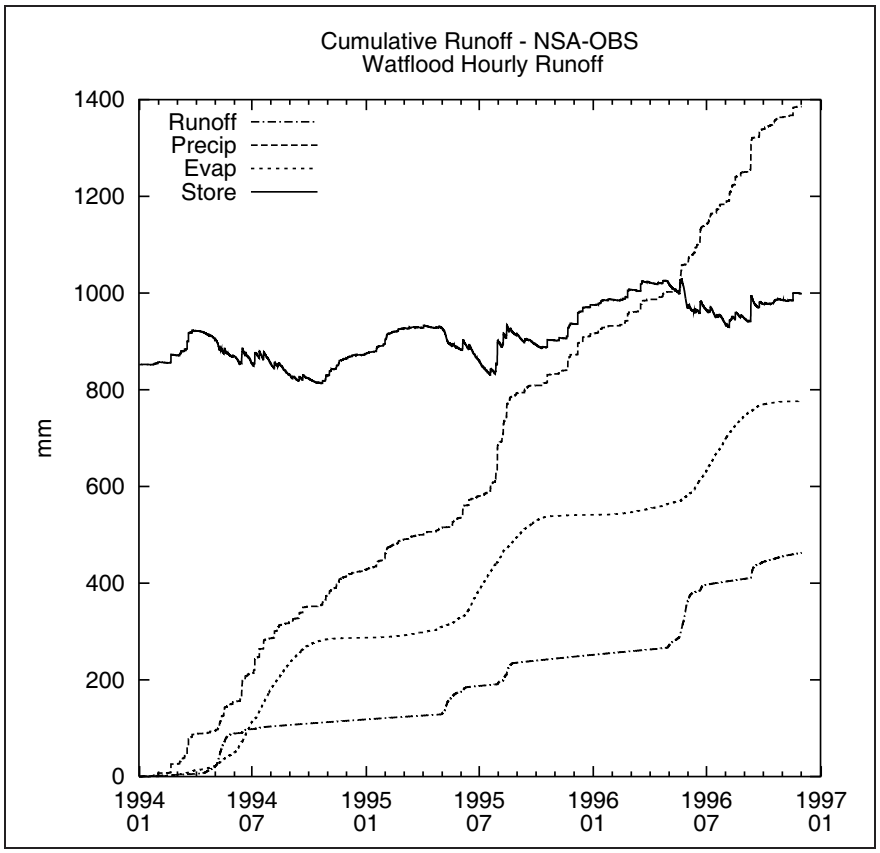

Figure 4-11 : WATFLOOD water balance plot for the NSA-OBS

4.2.4 Site Specific Results

The purpose of this section is to illustrate the impact of the introduction of runoff generation mechanisms within CLASS. These mechanisms control a slowly responding base flow reservoir which is supplied by drainage from the bottom of the CLASS soil column, interflow generated from the upper soil layer, and surface runoff influenced by Manning's equation. CLASS, with runoff generation fully implemented, shall be referred to as WatCLASS. Testing of the model shall proceed in stages with (i) CLASS alone run with root penetration into the third soil layer, (ii) WatCLASS alone with runoff generation mechanisms in place, and (iii) WatCLASS with changes made to canopy resistance functions. To test these schemes, results will be presented from the NSA-OBS only. This

site is selected because it contains the most complete record (by far!) of flux measurement for the three year period.

CLASS in stand alone mode represents version 2.6 of the model together with a number of bug fixes issued over the intervening period. Also added to this version is the improved runoff generation code which may be switched on and off by a 0/1 switch that has been added in a parameter control file known as BENCH.INI. Vegetation and soil parameters have been set to measured values described in the previous sections with the exception that rooting depth has been set to allow penetration into the third soil layer (rooting depth parameter = 351 mm). CLASS documentation recommends that roots for coniferous trees be set to rooting depth of 1000 mm. The depth of 351 mm has been selected to show the sensitivity of this parameter at layer boundaries. Initial conditions for soil moisture have been set to 32.5% which represents an equivalent soil moisture of 49.5% when residual soil moisture (χ_r = 17%) is added. No ice content has been specified at this point for the January 1 start of the simulation and the soil ice content is permitted to develop over the remainder of this first winter period. However, soil temperatures have been initialized to -13,-12 and 0^{o}C for each of the three soils, from top to bottom, respectively to match air temperatures from this period in the top most layers and to ensure that no excess energy in the third layer exists. An initial snow equivalent amount of 38 mm has also been added after Whidden (1999) which is based on limited observational evidence but was found to be required to generate the spring hydrograph for WATFLOOD. This set up represents CLASS in its current operating mode within the Canadian GCM together with a measured set of controlling parameters.

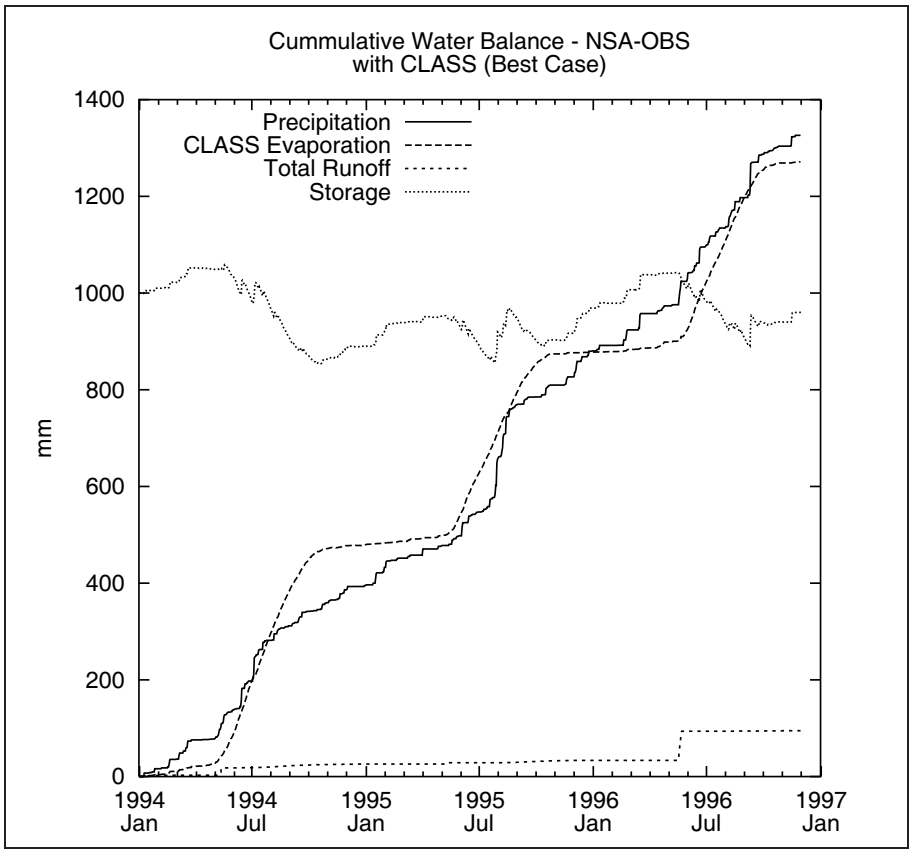

Figure 4-12 : CLASS base case run with NSA-OBS parameters

Figure 4-12 represents the cumulative water balance from this base case scenario. Contrasting this result with WATFLOOD results presented in Figure 4-11 shows major differences in the redistribution of precipitation inputs over the three year period. Most striking is a reduction in runoff (R=95mm) and increase in evaporation (E=1271mm). In fact, virtually all rainfall evaporates. The reduction in storage over the period (÷S=-40mm), in fact, is not very different from the total runoff. It should be noted that the precipitation data set used here (P=1326mm) differs by approximately 60 mm from that used by Whidden (1999) but this slight difference would not account for the large change in runoff.

It is theorized that without a storm runoff generation process and tree root access to the large third layer reservoir of soil moisture, enhanced evaporation suppresses runoff generation.

Restricting access to the third soil layer by reducing rooting depth from 0.351 m to 0.349 m reduces the evaporation by 165 mm to 1106 mm. However, runoff only increased by 48 mm to 143 mm. Other mechanisms are required to improve the partitioning of precipitation.

Examination of evaporative control mechanisms for CLASS shows that soil moisture is used to restrict transpiration of plants. Other evaporative controls include incoming radiation, air temperature, and atmospheric humidity that are formulated in a Jarvis-Stewart type scheme (Verseghy *et al*., 1993). In CLASS, the rate of evaporation is controlled by the gradient between atmospheric humidity and surface saturation humidity that is scaled by land surface and atmospheric resistance terms. Negative gradients produce condensation while larger positive gradients promote increased land surface evaporation. The form of the CLASS evaporation equation is:

$$Q_E = \frac{L_v \rho_a (q_a - q_{sat}(\overline{T}_c))}{r_a + r_c} \qquad \text{Equation 4-14}$$

where L_v is a constant latent heat of vaporization term, the density of air ρ_a varies slightly with atmospheric pressure and q_a is the specific humidity in the atmosphere used to calculate the moisture gradient with the land surface. The land surface is assumed to be always at a saturated specific humidity level which depends on the canopy temperature T_c. Canopy temperature is determined by an energy balance approach solved iteratively through exchanges of energy between the atmosphere, canopy, and soil surfaces all of which are represented as functions of temperature. The atmospheric and canopy resistance terms r_c and r_a are used to scale the gradient and produce a moisture flux. When free water is present in the canopy, r_c drops to zero and intercepted moisture is allowed to evaporate at the potential

rate controlled only by atmospheric factors including boundary layer stability and wind speed. When r_a alone controls evaporation, CLASS is determining, in effect, how quickly the overlying air can move moisture away from the surface. This is a costly calculation and CLASS spends over 60% of is computational time calculating the r_a term as it iterates on the surface temperature solution of the surface energy balance.

The r_a term is critical in determining potential evaporation, however, once free water is removed from vegetative surfaces the canopy resistance, r_c quickly begins to dominate. Under r_c dominance, the land surface supply of moisture for evaporation is restricted rather than the atmospheric limiting case discussed previously. Stewart (1988) reports r_a values ranging from 3- 9 sm^{-1} and r_c values of 100-500 sm^{-1}. Chamber studies have shown that leaf stomatal guard cells respond to conserve moisture when unfavourable environmental conditions such as high light levels, extreme air temperature, low atmospheric humidity, and low leaf water content exist. CLASS incorporates these functions, with a soil moisture suction substituted as a surrogate for leaf water content, in a Jarvis-Stewart formulation as follows:

$$
\begin{aligned}
& r_s = r_{s\min} f_1(K\downarrow) f_2(vpd) f_3(\psi_s) \\
& \textit{where}: \\
& f_1(K\downarrow) = \max(1,\ 500/K\downarrow + 1.5), \\
& f_2(vpd) = \max(1,\ vpd/5), \\
& f_3(\psi_s) = \max(1,\ \psi_s/40)
\end{aligned}
\qquad \text{Equation 4-15}
$$

where $K\downarrow$ is the incoming solar radiation in W/m^2, vpd is the vapour pressure deficit in kPa, and ψ_s is the soil suction measured in meters taken from the soil layer containing roots whose moisture level has the lowest capillary rise. In addition to these environmental variables,

CLASS also has an on/off switch increasing r_c to 5000 sm^{-1} when air temperature falls outside the range 0 to 40°C. This effectively stops transpiration. Each of the resistance functions listed (f_n) are strictly empirical and have been reported with a wide variety of functional forms in the literature.

It is obvious from Figure 4-12 that the current evaporation scheme is clearly not satisfactory for the NSA-OBS, even after careful estimation of plant and soil parameters from BOREAS measured data. The WATFLOOD estimation of evaporation, at approximately 780 mm (which will be shown later to be relatively accurate estimate), is much less than the CLASS estimate of 1100 mm. Examining the WATFLOOD result further indicates that 460 mm of runoff was likely generated from this area to produce a reasonable streamflow hydrograph. Adapting CLASS to generate the WATFLOOD runoff by means of interflow generation produces the results in Figure 4-13.

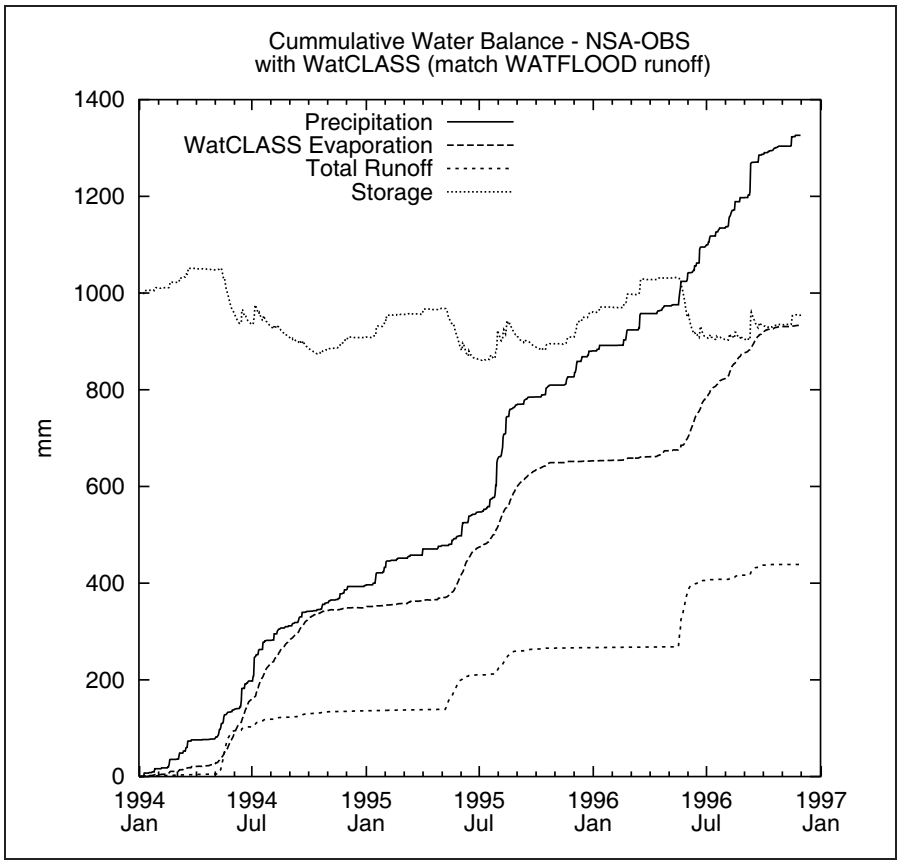

Figure 4-13 : WatCLASS result with interflow tuned to the production of WATFLOOD runoff.

This represents WatCLASS tuned to produce approximately the same runoff volume of WATFLOOD. (Interflow parameters $a=3.5 \times 10^{-3}$ m^2/sec and $b=1.5$). Runoff generation results in a reduction of evaporation to 933mm and runoff increased to 439mm. However, evaporation still remains more than 150 mm greater than the WATFLOOD estimate. Storage has also decreased slightly over the period dropping by 46 mm. This drop in storage is a large change from the WATFLOOD result which had seen an increase of 146 mm. In this WatCLASS simulation, runoff has been generated at a considerable expense in storage change and without the required reduction in evaporation. Figure 4-13 shows the cumulative generation of runoff from this run compared with the WATFLOOD estimate. Flow generation here is dominated by interflow with only a small fraction generated as base flow.

The slope of the cumulative runoff plot indicates the instantaneous flow that would be observed as a streamflow contribution. Comparing the WatCLASS slope in the fall and winter period with WATFLOOD shows a significant decrease in base flow contribution and higher spring melt and summer storm contribution. Selecting interflow parameters for WatCLASS to match WATFLOOD runoff volume, restricts flow to the lowest soil layer by diverting too much of the spring runoff and heavy rainfall through the interflow layer. This results in base flow reduction and provides an illustration of how the dynamics of the streamflow response can give insight into the behaviour of the soil moisture response.

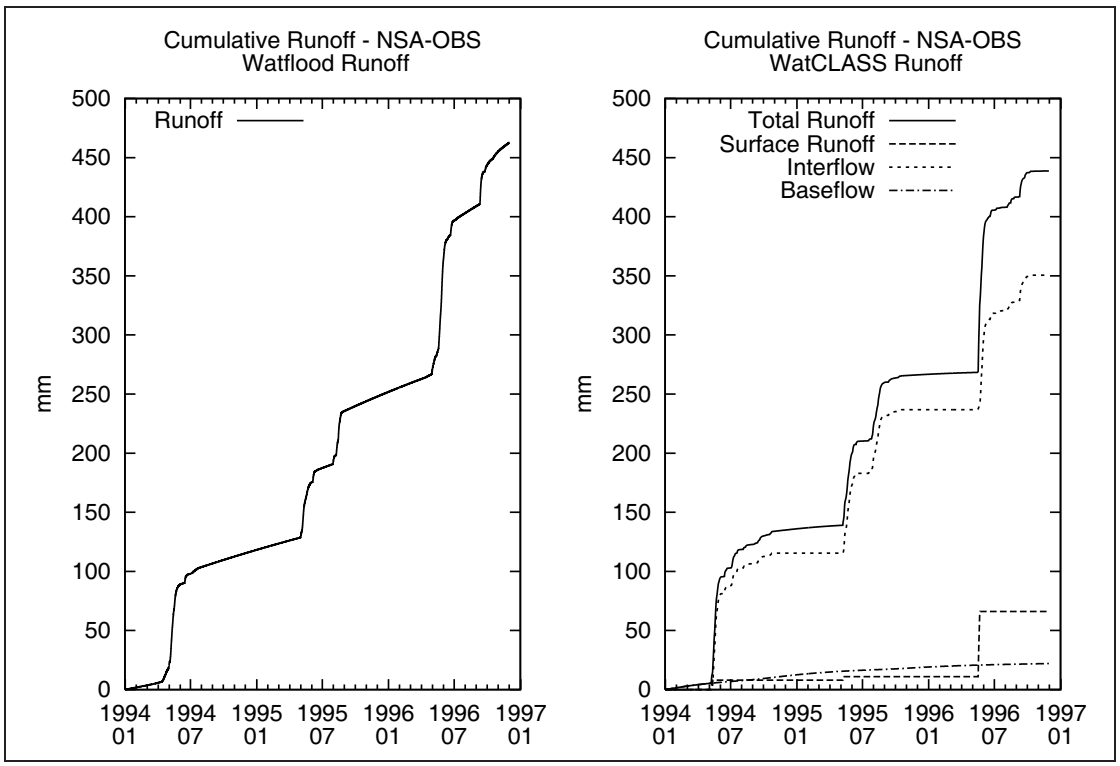

Figure 4-14 : Comparison of runoff generation between WATFLOOD and WatCLASS for the matching runoff experiment.

Increased storm runoff alone has not been effective in reproducing the required water balance. Total runoff volumes can be met but at the expense of runoff timing, storage changes, and poorly simulated evaporation. For the NSA-OBS, low canopy resistance

simulations are responsible for high evaporation. Examining Equation 4-15 shows that increased resistance to soil moisture does not begin until soil moisture tension reaches 4,000 cm. Higher soil moisture levels have no impact on evaporation.

Stewart (1988) who first tested the Jarvis-Stewart evaporation technique found that increased canopy resistance started at soil moisture deficits beginning at field capacity (340 cm). This first model, developed for the Thetford pine forest, a sandy soil area in southern England, found that resistance increased from zero to its maximum value over a range of 8.4% soil moisture change. Assuming here that this maximum resistance corresponds to the wilting point (15,000 cm) and zero resistance to field capacity, a Campbell moisture characteristic model can be fitted if we choose a typical values for both 'b' and porosity in Equation 4-2 as b = 4 and χ_{sat} = 0.36, respectively which a typical for sand. This yields a $\ldots_{sat}$ value of 7.2 cm which is within the accepted range for sand predicted by Clapp and Hornberger (1978). Using this model and substituting it into the Stewart (1988) original soil moisture deficit formulation gives:

$$f_3(\ldots) \mid (1 4 0.00119 \exp(11.1 4 15.1(\ldots)^{4 1/4}))^{41} \qquad \text{Equation 4-16}$$

where …is in meters. More recently, Lhomme (2001) has suggested a much simpler form for the soil tension canopy resistance term as $f_3(\ldots)=(1-\ldots/\ldots_{max})^{-1}$ where $\ldots_{max}$ is the maximum suction value where transpiration ceases. While Lhomme (2001) recommends a value of 260 m for $\ldots_{max}$, a value of 150 m corresponding to the wilting point fits with the assumption used throughout this thesis. Each of these expressions is plotted in Figure 4-15 showing both resistance and conductance (1/f) formats. Resistance and conductance formats are shown here since they are popular in the literature. Note here, that both the Lhomme and Stewart

approaches yield very similar results while the CLASS result, given by Equation 4-15, does not capture increased resistance at low soil moisture because of the step function used in its formulation of $f_3(..)$.

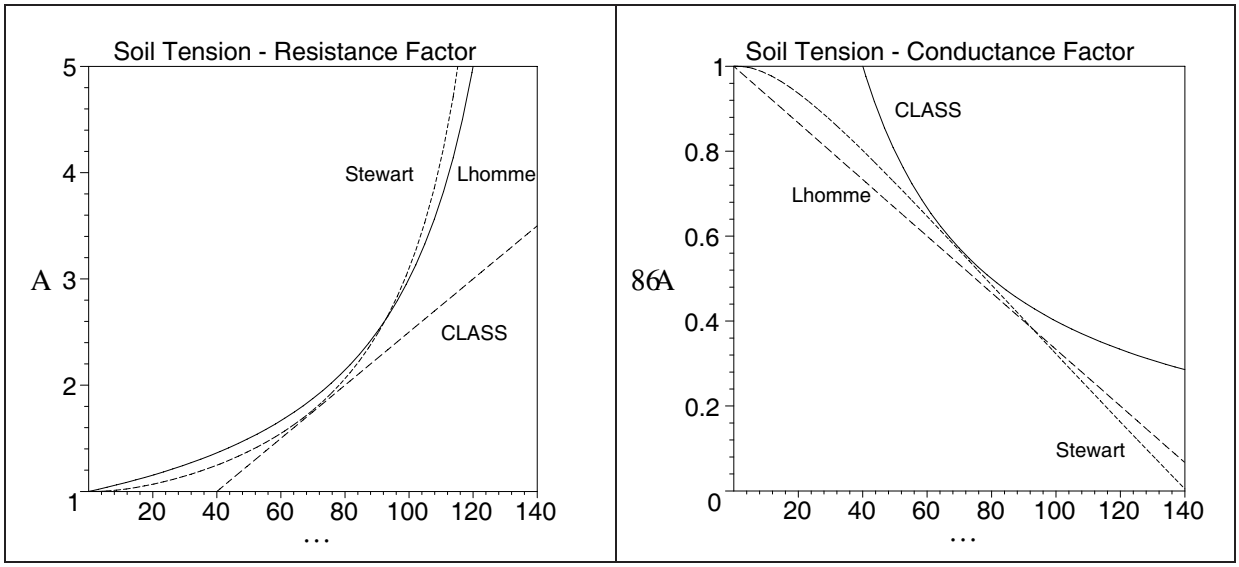

Figure 4-15 : Stewart and Lhomme soil tension based resistance and conductance functions plotted against the soil tension measured in meters.

The Lhomme (2001) formulation was substituted in the CLASS r_c computation. However, this addition resulted in little water balance change suggesting that the small increases in canopy resistance factors had little impact on evaporation reduction.

In order to add a greater understanding to this problem, all dependent variables (soil tension, radiation, and humidity) must be weighted against the resulting evaporation output using an optimization approach. Betts *et al.* (1999) have initiated this process by developing a linear regression model of r_c against various environmental measures. The Betts *et al*. (1999) result is curious in that no correlation was found with measured soil moisture but a strong correlation was found with an alternate, fictitious moisture reservoir. Characteristics of this reservoir include a loss of 1 cm per day when no rainfall occurred and recharge to a

maximum of 5 cm when sufficient rainfall was observed. This is similar to a simplified form of the antecedent precipitation index (API) (Dingman, 2002, p.444). It is speculated that the minimum observed soil moisture for 40% (generated from data supplied by Cuenca by combining two layers of soil moisture measurement) was thought to be too high to warrant consideration. However, for this heavy clay soil a moisture content of 40% translates to tension of approximately 10,000 cm which should have a significant impact on canopy resistance.

Going farther with this analysis is beyond the scope of the current research. A simple solution, for now, is to add an unexplained canopy resistance factor of 2.0 to the general resistance model to achieve desired result. The use of this factor of 2.0 has the effect of doubling $r_{c\ min}$ from a value of 50, used by CLASS, to 100 sm^{-1}. Betts *et al*. (1999) have shown that relationships exist between canopy resistance and other environmental factors such as wind speed and diffusivity of incoming radiation that are not included in the CLASS formulation given in Equation 4-15. Establishing these relationships in a general Jarvis-Stewart model format is a requirement for further research.

No clear definition of $r_{c\ min}$ has been found and is currently set at a value of 50 sm^{-1} for all CLASS vegetation types. Individual leaf resistance values can be measured in the laboratory under ideal environmental conditions. However, leaves in the lab are very different from leaves in the forest since forest leaves are not all exposed to the same light conditions, humidity levels, and height above the ground level. These effects are known collectively as the shelter factor (Dingman, 2002, p298). Values of $r_{c\ min}$ also depend on the complexity of the model used to estimate the resistance terms. Stewart (1988) presented two different models of canopy resistance with the first using four environmental factors which resulted in

an $r_{c\ min}$ value of 45 sm^{-1} and the second with no environmental variables which required an average $r_{c\ min}$ of 135 sm^{-1}. Each model likely explains the average annual evaporation but the more complex version is required to explain the seasonal and hourly variability.

The impact of doubling $r_{c\ min}$ is presented in Figure 4-16. Here the water balance for the NSA-OBS is presented as before. However, now the measured evaporation from the NSA-OBS flux tower is included as well. Tower measurements do not provide a complete record over the 35 month time period and model evaporation is used to fill in 244 days of the total 1064 days of the time series. Periods of missing tower evaporation are represented by a horizontal line in the figure with solid portions indicating missing dates. A majority of missing data occurs early in 1994 before the NSA-OBS tower was established and during winter periods when evaporation was very low. As a result a great majority of the total is observed evaporation. It is felt that this 'data filling' approach is reasonable especially since the trend of the two measures is approximately equal (as confirmed by the plot). Totals for the period indicate evaporation at 740 mm (measured 735 mm), runoff at 505 mm, and change in storage at +80 mm.

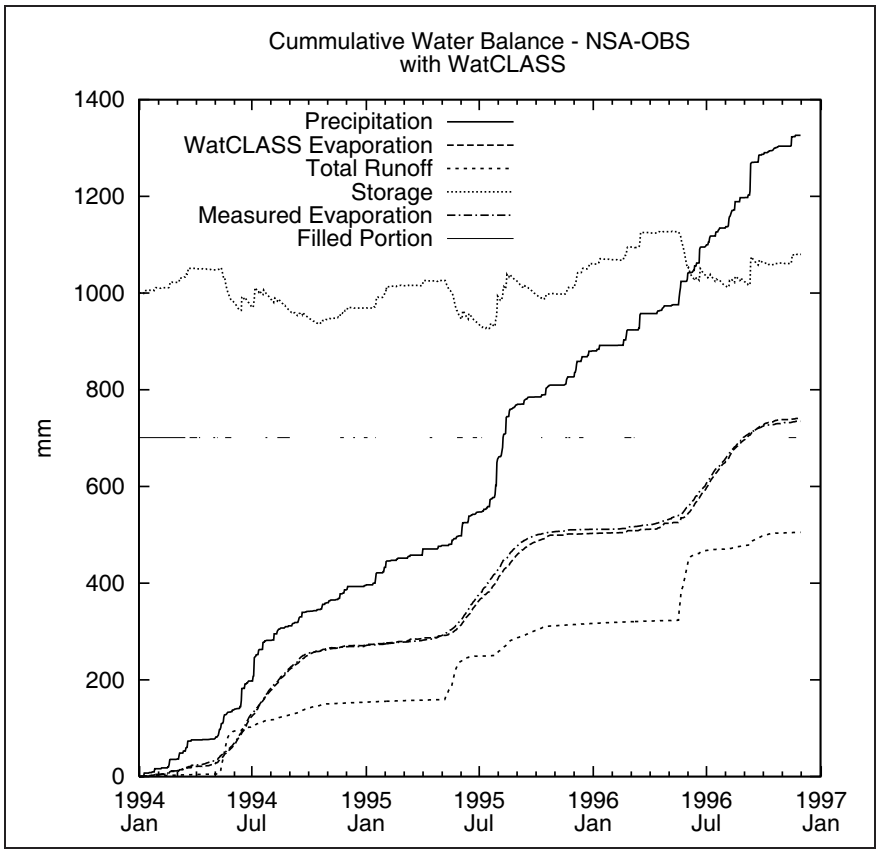

Figure 4-16 : WatCLASS run including impact of canopy resistance changes, interflow generation and restriction in rooting depth.

Runoff generation has also improved with a greater base flow amount as shown in the cumulative runoff plot in Figure 4-17 which compares WATFLOOD and WatCLASS simulations. Interflow parameters used to generate this result are $a=3.5 \times 10^{-3}$ m^2/s and b=2.5.

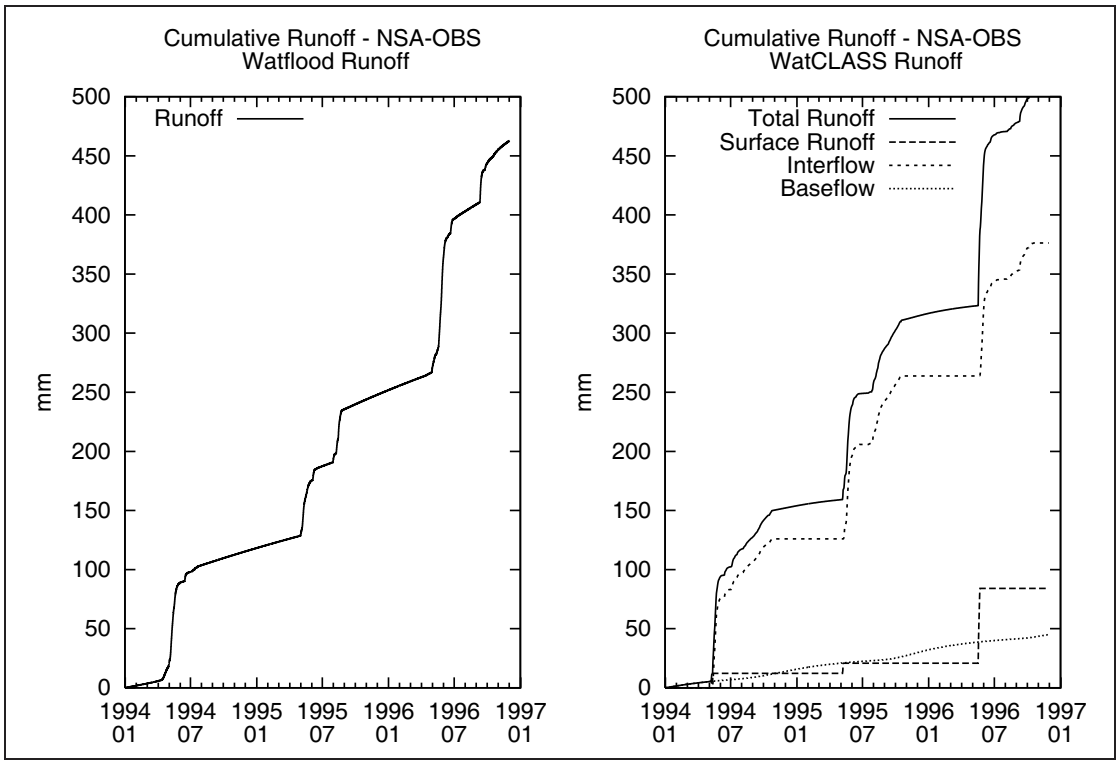

Figure 4-17 : Comparison of runoff generation between WATFLOOD and WatCLASS including impact of canopy resistance changes, interflow generation, and restriction in rooting depth.

Cumulative plots, such as the ones presented above, are important as they indicate the stability of the model over long, multi-year time periods. However, they do not reveal the change in the diurnal components of the energy balance important for atmospheric models. Figure 4-18 shows monthly average diurnal plots of net radiation, sensible, and latent heat plots (note that latent heat plots are presented in hydrologic units of mm/hr) for July 1994 which are representative of the other months. Each hourly point on these plots was created by calculating the average flux for that particular hour over the entire month in question. On the right are simulations from the original base case run with CLASS and on the left are WatCLASS runs with interflow generation, confinement of roots to two soil layers, and adjustments to the canopy resistance formulation. As expected, little sensitivity is shown to net radiation calculation as CLASS simulations of the associated canopy temperature and

albedo are not tied to changes in canopy resistance. However, the transformation and partitioning of this radiation into the turbulent fluxes of latent and sensible heat is very sensitive to the behaviour of trees in controlling transpiration. Given little resistance, as is the case with adequate third layer moisture, canopies transpire at increased rates. This is compensated by a reduction of low level warming associated with sensible heat production.

Some problems still exist with the simulation including the depression of evaporation before noon and its accentuation just following noon. This requires a rigorous examination of the canopy resistance functions. For instance, Betts *et al.* (1999) report a strong increase in canopy resistance associated with afternoon increases in relative humidity levels. While CLASS r_c does respond to changes in specific humidity, air temperature, which is an important component of relative humidity, is not currently used in r_c calculations expect for the purpose of cutting off transpiration at extreme values (i.e. $0 > T_{air} > 40^oC$).

Lhomme (2001) also presents an interesting argument for combining r_c impacts of soil moisture and atmospheric moisture into a single resistance value based on leaf water potential. The argument put forth asks whether increased atmospheric humidity is a cause or effect of canopy resistance. Certainly, it can be seen from equations 4-14 and 4-15 that atmospheric humidity is used to: (i) determine the gradient controlling transpiration, (ii) influence canopy resistance by changing stomatal response, and (iii) increase boundary layer wetness through the impact of increased latent heat release. This over-use of humidity certainly points to some greater unifying model of plant response to environmental influences. Future trends in hydrologic science toward eco-hydrology (Nuttle, 2002), which seeks to understand plant-water relations and how hydrologic processes relate to plant

growth, may well lead to improved formulations of how water, energy, and plants influence one another.

Another problem area requiring attention exists with nocturnal evaporation. This subject represents a difficult challenge for both measurement and modelling. In these simulations, CLASS over estimates night time evaporation when compared to measured values. However, Betts *et al*. (1999) cautions on the reliability of nocturnal evaporation estimates.

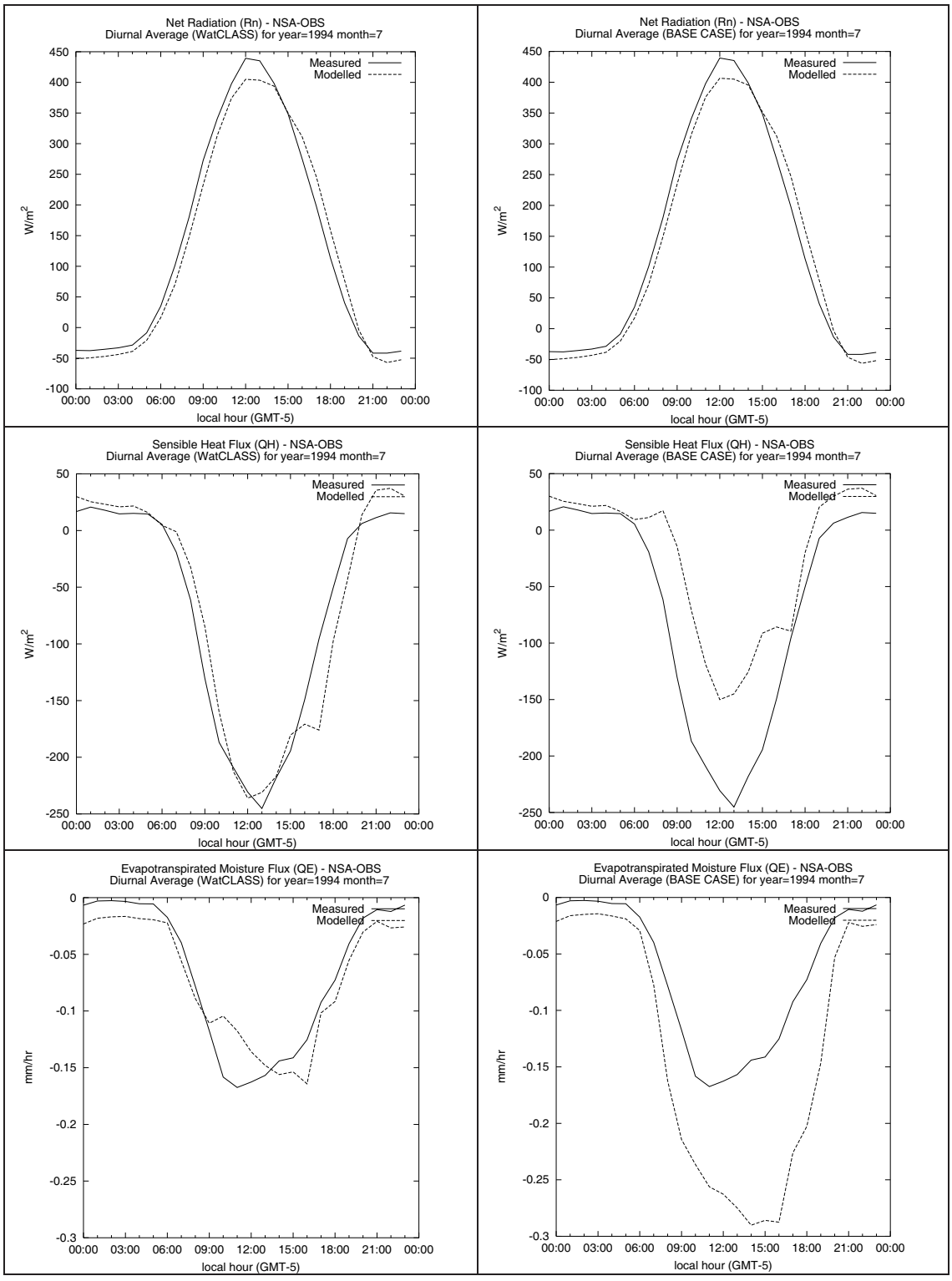

Figure 4-18 : NSA-OBS monthly average diurnal plots for WatCLASS (left side) and CLASS only (right side) simulations. Comparisons of net radiation (W/m^2), sensible heat flux (W/m^2), and evapotranspiration (mm/hr) are presented. The atmospheric sign convention of positive toward the surface is used in these plots.

Well-behaved fluxes of runoff and evaporation should translate directly to improved soil moisture results included in the storage simulation. Figure 4-19 presents the WatCLASS layer-2 soil moisture plotted against soil moisture measured by Cuenca *et al*. (1997) from a depth of 225 mm. A four month portion of the soil moisture record coincident with a large summer rainstorm that occurred in the NSA at the end of July 1995 is presented. Low soil moisture is evident prior to the start of the storm with both measured and modelled soil moisture nearing the wilting point. Rainfall onset is obvious from the plot since the timing of the rain response for measured and modelled soil moisture is similar. However, the magnitude and range of the measured soil moisture response is not reproduced by WatCLASS. Further explanation of this result should focus on the reliability TRD based soil moistures which show considerable noise and range from 20% to 80% volumetric moisture content which is well outside the description of the soil given for the site. Clay soil at 20% moisture would be extremely dry while the value of 80% is far above the soil porosity. While there is cause to question the measured data, there does appear to be a low variability in WatCLASS simulated soil moisture which suggests complexity in the natural system that is not captured by WatCLASS. Another evident discrepancy includes measured soil moisture, which shows a gradual decline following the July rainfall through to mid October while model soil moisture stays almost constant during this time.

Finally, an interesting phenomena is captured by WatCLASS in the late fall as the drop in soil moisture at the end of the period is coincident with the beginning of ice formulation in the CLASS soil layers and the associated decrease in liquid water content. It should be noted that CLASS soil moisture has not been scaled upward by the amount of the soil moisture

residual (χ_r) as indicated by Equation 4-6. This would have the effect of increasing all simulated soil moisture by 17% which would not be helpful in improving the overall fit.

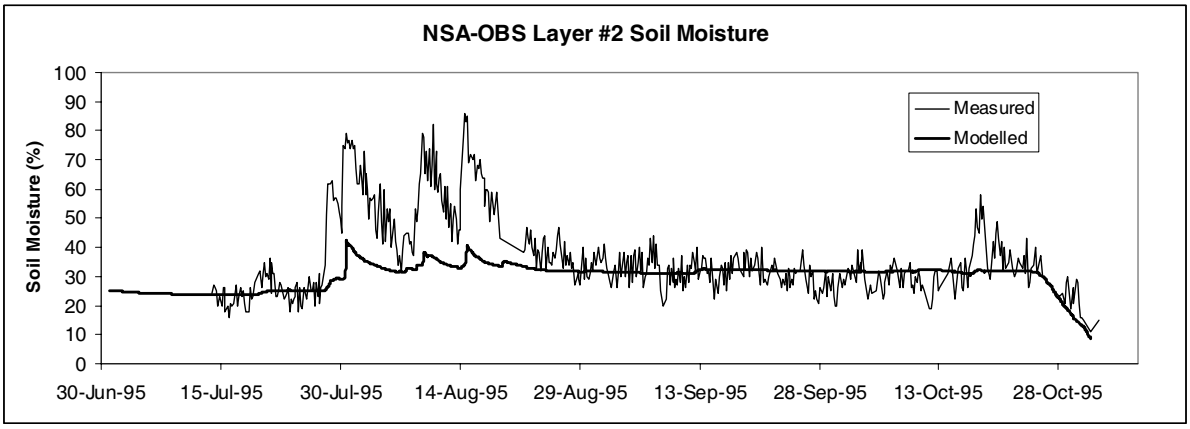

Figure 4-19 : Soil moisture from the NSA-OBS

4.3 Chapter Summary

This chapter has examined the result of adding a hydrological component to the CLASS land surface scheme. Most significant is the result obtained in Figures 4-16, 4-17 and 4-18. By manipulating the surface water balance, through control of an interflow mechanism, fluxes of heat and moisture returned to the atmosphere are altered to match flux tower observations. This confirms the hypothesis set out at the beginning of thesis.

Prior to obtaining reasonable water balance results, considerable effort was made to give CLASS a reasonable opportunity to work without WATFLOOD based runoff algorithms. BOREAS based soil and plant properties were extracted from the BOREAS data base and modified to suit CLASS requirements. Only by extending evaporation routines and adding runoff generation process was CLASS able to reproduce the components of the water and energy balance necessary to act as a reasonable atmospheric boundary for the boreal forest environment.

While the thesis hypothesis has been demonstrated for the NSA-OBS, the result represents only a single point within a small watershed. To be integrated into an atmospheric modelling context, the method must be demonstrated over larger domains with variable land surfaces. This is a much more difficult challenge and requires that the heterogeneity of the natural system be considered. Chapter 5 and 6 seek to extend the results presented here to atmospherically significant domains. This will extend the thesis hypothesis to the related objectives presented in Section 1.5.

5. BOREAS Spatial Results

5.1 Introduction

In this Chapter, WatCLASS point results, developed in Chapter 4, are extended to estimate runoff for both the NSA and SSA watersheds. This is accomplished based on the GRU concept where the areal contribution of point processes is scaled over a landscape unit. Runoff generated by each of the contributing elements will be routed through the WATFLOOD generated streamflow network to the gauging stations within the watershed, which are depicted in Figures 4-3 and 4-4.

Prior to the generation of hydrographs two issues are investigated in greater depth. The first of these is the generation of hydrologically correct digital elevation models. Many sources of digital elevation model (DEM) data exist but not all are of sufficient quality to allow automatic generation of watershed boundaries and other important hydrologic features including the channel routing network and internal slope. DEMs that cannot predict hydrologic variables of interest can be forced to reproduce the desired result by imposing drainage and will be addressed in Chapter 6. However, imposing drainage on an existing DEM leads to suspicion as to whether this DEM can generate accurate values of land surface slope, the driving gradient of hydrologic models. The second issue to be considered is the verification of the GRU concept, which is fundamental to both WATFLOOD and WatCLASS and allows the transfer of hydrologic parameters within a watershed area. Slope is important here since, together with vegetation features, it may be used to determine soil type and important hydrologic parameters.

The generation of hydrologically correct DEM data are investigated first followed by the validation of the GRU concept and these are tied together with the generation of streamflow hydrographs for the NSA and SSA.

5.2 Hydrologically Correct DEM Generation

The use of slope within hydrological models has become very important in modern hydrology. Popular models, such as the TOPMODEL, determine saturated area by the convergence of basin wetness and land surface slope, discussed in Chapter 2. WATFLOOD also makes use of DEM data to define the stream channel routing network and its properties. As well, the DEM is used to determine the driving slope gradient necessary for surface runoff and interflow generation. Land surface runoff slope is distinguished from its hydraulic stream channel counterpart using the term "internal" slope as opposed to river channel slope. Other models, including the VIC hydrologic model, do not explicitly use "internal" slope in their formulation but inherently include its impact within their parameterizations.

WATFLOOD's use of internal slope has evolved over its development period. Initially, internal slope was used only to control the velocity of overland flow generation. Parameters controlling interflow generation, as with VIC, included the land surface slope averaged over a particular land cover type within a watershed. As watershed areas became large and internal slope more variable, it was recognized that use of grid square average slope was a better predictor for interflow generation. Extending the use of land surface slope further was limited by the effort necessary to generate it. Prior to the Mackenzie GEWEX (MAGS) projects, watershed properties, including internal slope, were determined from paper maps and manual techniques. For instance, internal slope required counting the number of

contours within a grid square along the path of steepest decent. This was a laborious process suited to small watersheds that could be managed on a paper map format. Coincident with MAGS, was the availability of the GTOPO30 DEM which provided world-wide coverage of elevation data at approximately 1 kilometre resolution (30 arc seconds). These data allowed hydrological variables, including internal slope, to be determined using packaged software products such as those by Jenson and Domingue (1988) found in PCI GEOMATICA and Arc/Info GRID software. The proliferation of GIS tools and topographic data availability have revolutionized how WATFLOOD determines the elements of the drainage layer data base. Recently, WATFLOOD has moved to a specially designed tool known as ENSIM Hydrologic for pre-and-post processing.

While faster computers and useful software exist to ease the data extraction process for watershed modelling, not all sources of data have equal value. For the BOREAS project a number of DEM products are available for the extraction of hydraulic and topographic data. These include:

1. BOREAS generated DEMs for the NSA and SSA by group HYD-8 (Wang and Band, 1998). These DEMs were created from 1:50,000 scale vector topographic data (7.6 m contour intervals) from the Canadian National Topographic Data Base (NTDB). Spline interpolation of a surface through the vector topography using the TOPOG terrain analysis package resulted in a 100 m resolution data set covering both the NSA and SSA modelling sub-areas.

2. Canadian Digital Elevation Data (CDED) generated for the entire Canadian land mass. This product is derived from 1:250,000 scale vector topography (20m contour intervals) and stream channels. Elevation data are presented at a grid resolution of 3 arc seconds (100 m nominal). Topography and stream channel data are combined using ANUDEM software (Hutchinson, 1989).

3. A free product derived from the CDED product above known as CAN3D30. This DEM provides elevation data for all of Canada at a resolution of 30 arc seconds (1 km nominal) by degrading the CDED data using a 10x10 point averaging of the original elevation data.

4. GTOPO 30 DEM developed through a cooperative project lead by the United States Geological Survey (USGS) to develop a uniform global DEM at a resolution of 30 arc seconds (1 km. nominal). The origin of the topographic data differ depending on the area of the globe under consideration. For the BOREAS domain, data are derived from the 1:1,000,000 scale Digital Chart of the World where topography and river channels were combined using ANUDEM software.

Each of these data sets are contrasted with a DEM derived here using the ArcInfo implementation of ANUDEM software together with an improved procedure for facilitating the production of hydrologically correct DEMs. Figure 5-1 presents the available DEM data for the NSA. Each image has been enhanced by stretching the raw elevation data from white (low) to black (high) over the range of elevation data located within the larger NW1 watershed. Some statistics associated with each DEM for the NW1 watershed are presented in Table 5-1 and Table 5-2.

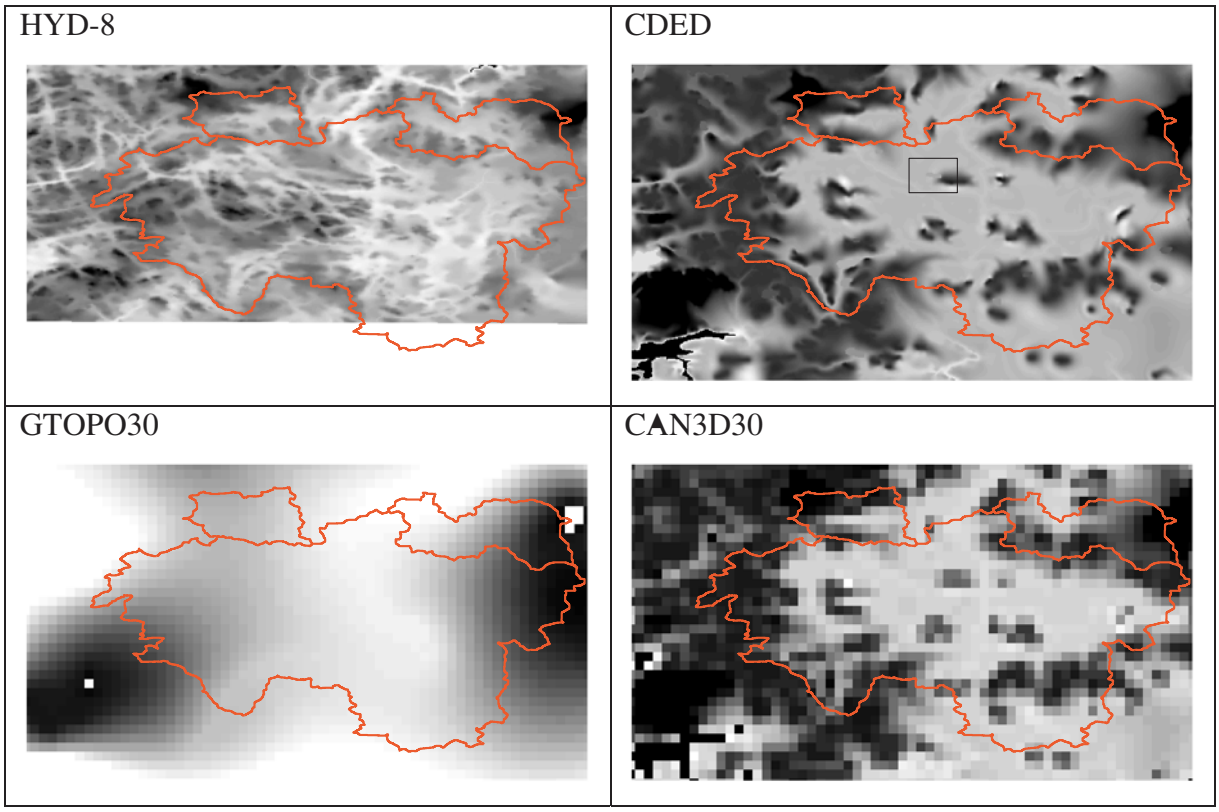

Figure 5-1 : DEM data available for BOREAS NSA Study. Lighter areas are low elevation areas. Linear watershed boundaries are shown for reference. Presented here using a geographic projection.

Table 5-1 : NSA DEM elevation statistics

DEM	*Min*	*Max*	*Range*	*Mean*
HYD-8	237	303	66	258
CDED	228	285	57	252
GTOPO30	251	309	58	266
CAN3D30	236	276	40	252
Derived DEM	236	307	71	259

Table 5-2 : NSA DEM slope statistics

DEM	*Min*	*Max*	*Mean*
HYD-8	0	11.2	1.94
CDED	0	27.2	1.68
GTOPO30	0	1.3	0.32
CAN3D30	0	2.4	0.70
Derived DEM	0	33.8	2.71

DEM data presented in Figure 5-1 show obvious differences. Both the GTOPO30 and CAN3D30 data sets are course resolution products not intended to be used at the scale of the BOREAS study area. Yet, these 1 kilometre data sets are used to derive watershed properties for large scale hydrologic models. Presentation of these coarse data products at this scale provides insight into the level of error introduced by these products. Perhaps most striking is the reduction in mean slope presented in Table 5-2 which represents approximately an order of magnitude different in value in moving from the derived DEM to the coarsest DEM product GTOPO30.

The GTOPO30 DEM is a very smooth representation of the actual surface topography. Some basic features are preserved including the higher areas surrounding the basin together with an outlet in the northern end of the basin. However, beyond general differences between high and low values, little of the internal topography is represented. This is due to the limited amount of data used to generate this DEM. The Digital Chart of the World data, on which this DEM is based, has contour intervals of 76 m (250 ft) over the BOREAS domain and a coarse representation of drainage mapped at 1:1,000,000 scale. This means

that only a single contour interval and a short section of a single stream channel are contained within the NW1 boundary.

Many more terrain features are captured in the CAN3D30 data set even though it has the same spatial resolution of the GTOPO30 product. This is due to its source data origin. CAN3D30 is derived from 1:250,000 scale CDED data set and smoothed to the same resolution of the GTOPO30. In fact, the mean of both the CDED and the CAN3D30 DEMs are the same but the range from high to low elevation is reduced from 57 to 40 m as would be expected from the operation of a 10x10 grid averaging degradation. A visual inspection of Figure 5-1 confirms that much more information was used to generate the CDED than the GTOPO-30 product. The original vector data used by the Centre for Topographic Information to derive both CDED and CAN3D30 products is shown in Figure 5-2. The contour interval for CDED source data in the NSA watershed is 20 m. This means that little more then two contour intervals define the topography of the basin.

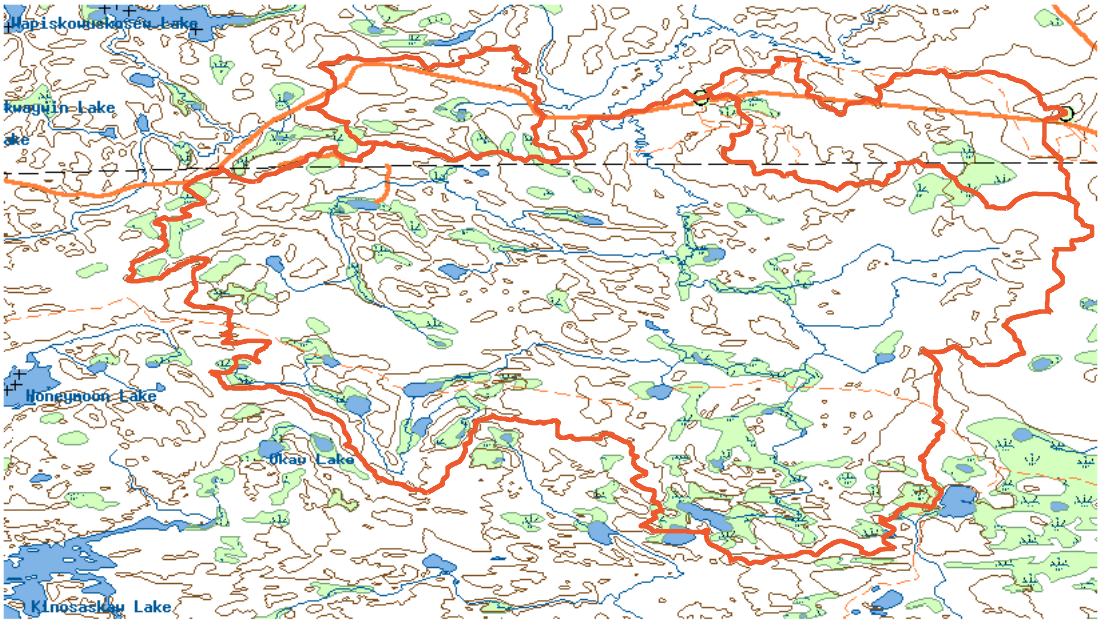

Figure 5-2 : CDED and CAN3D30 original 1:250,000vector data. Note: light shading represents wetland areas, dark shading represents lakes, and no shading represents forested area. Power line (dashed), road and watershed boundaries also presented. (raster background image from Toporama web site (http://toporama.cits.rncan.gc.ca)

Generation of DEM data from topographic maps is often done using a software package known as ANUDEM (Australian National University Digital Elevation Model) developed by Hutchinson (1989). All of the DEM data presented in Figure 5-1 were generated based on various implementations of ANUDEM software. The HYD-8 DEM was produced without drainage enforcement in the TOPOG hydrologic model's implementation of ANUDEM. This wide scale use of ANUDEM warrants a closer examination of its workings.

In ANUDEM, elevation data, in the form of contour lines and spot heights, may be combined with a hydrologic drainage network to produce a DEM that is virtually free of spurious sinks and pits. ANUDEM begins with the original, irregularly spaced elevation data and generates a coarse resolution DEM through a finite difference method. From this original data mesh,

interpolations are performed to produce progressively finer and finer resolution DEMs until the specified resolution has been achieved. As computations proceed, sinks and pits, which are systematically created by the interpolation process, are associated with adjacent saddle points bounding the sink. Saddles located near stream channel vectors are lowered by an amount necessary to provide positive drainage in the direction of stream vector. In doing so, sinks are removed and a hydrologically correct DEM is produced. There are a number of special cases in which sink removal conflicts with the original elevation data. In these cases, a number of defined 'penalty' parameters may be specified to allow adjustment to the original elevation data.

Figure 5-3 shows the implications of pit and sink removal from a small portion of the NW1 watershed. This figure compares the HYD-8 DEM which was generated without drainage enforcement with the DEM generated here which has been generated with the benefit of drainage enforcement. The HYD-8 DEM was generated by interpolating 1:50,000 scale mapping which have contour intervals of either 10 m or 7.6 m (25 ft). This interval difference is due to metric updating of a number of NTDB map sheets which make up this watershed. Three pits were spuriously created as a result of the interpolation procedures used for the HYD-8 DEM. When this same contour information is combined with vector stream channel vectors these pits are removed as shown in the derived DEM. The ArcInfo implementation of ANUDEM, known as TOPOGRID was used to produce the derived DEM.

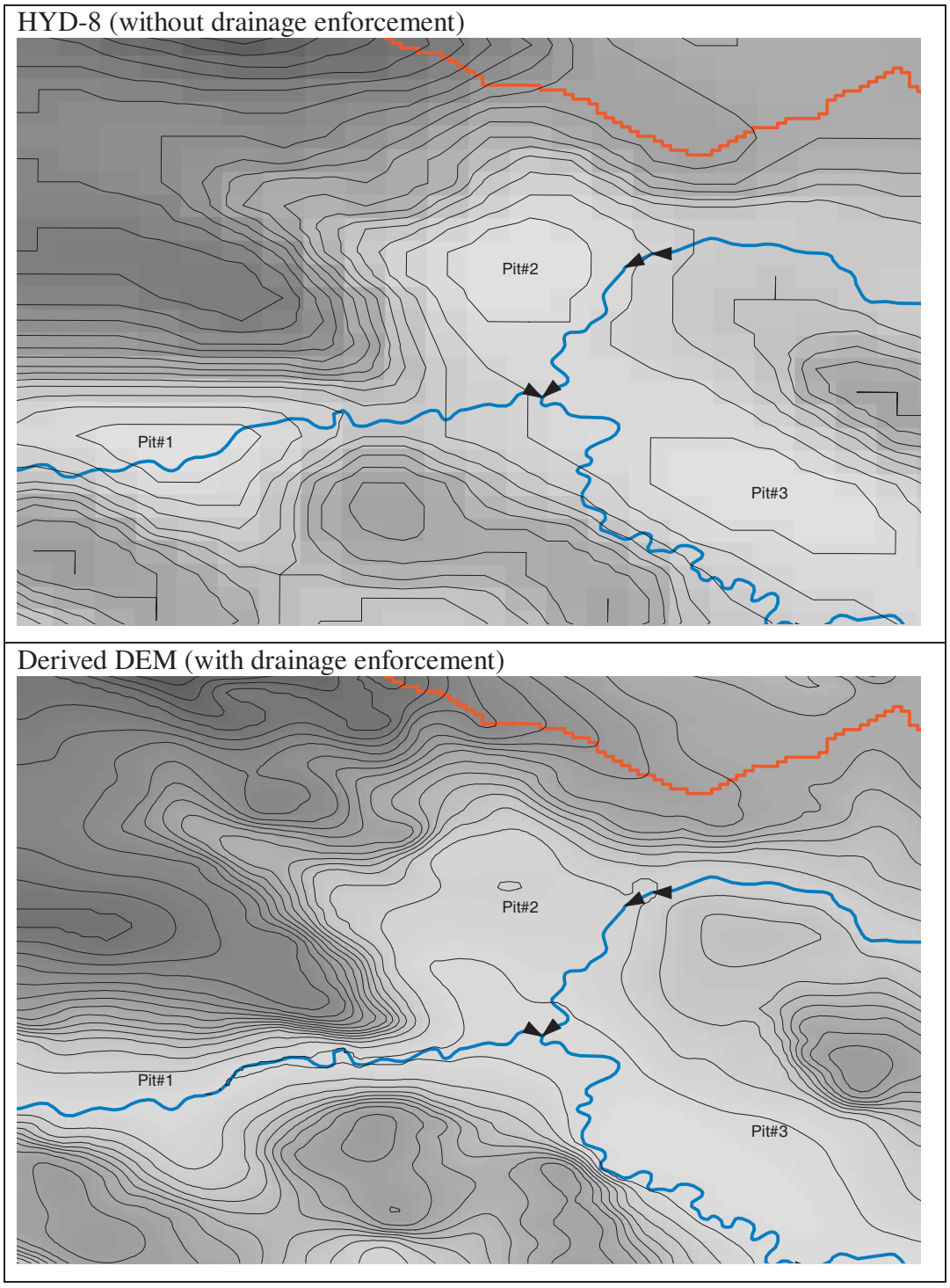

Figure 5-3 : Impact of ANUDEM drainage enforcement. The HYD-8 DEM has been prepared without drainage enforcement while the derived DEM has ANUDEM enforced drainage. Pits 1, 2 and 3, evident in the HYD-8 DEM, have been removed in the derived DEM. Contours with 2m intervals and stream channel flow direction have been added for reference.

In addition to spurious sinks and pits, the HYD-8 DEM did not completely cover the watershed area of the NSA. The original HYD-8 DEM was generated for the NSA modelling sub-area (MSA) which was defined during early BOREAS preparations and prior to the complete definition of the watershed boundary. Without a complete DEM, it was difficult to determine a complete definition of the watershed properties required for watershed modelling.

A search for alternate DEM data revealed the CDED product available for purchase from Centre for Topographic Information. These data were available at a cost of $CN250 per map sheet and covered an area of 1^{o}lat x 2^{o}lon at a resolution of 3 arc seconds (100 m nominal). Despite high expectations, many problems exist with the CDED product including large discontinuities which appear at 1^{o}x2^{o} tile boundaries, failure to reproduce watershed boundaries and poor implementation of lake elevations. Lakes, represented as polygons in the ANUDEM software, are superimposed on the completed DEM as a final step in the processing. The elevation used for the lake level pixels is calculated as the mean of the underlying DEM. There are, however, many instances in steep topography where this produces unsatisfactory results. The top portion of Figure 5-4 illustrates a situation in the CDED data where the lake level and the surrounding land surface show an instantaneous elevation change of 20 m at eastern lake shoreline. This is an artifact of superimposing lakes on the final DEM without considering lake boundaries as important sources of topographic information.

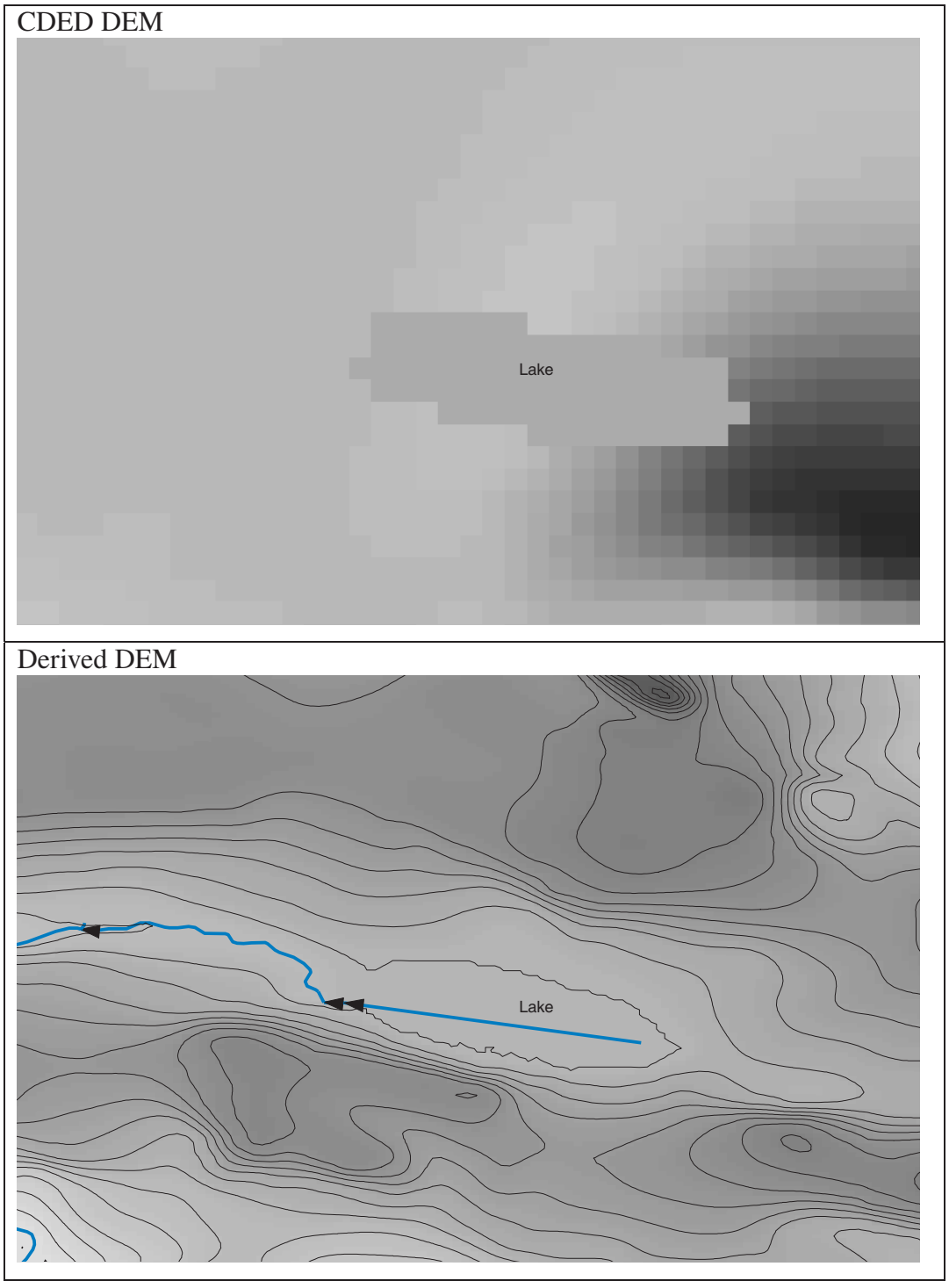

Figure 5-4 : Implications of lake polygons on DEM construction. The CDED DEM (above) uses the standard ANUDEM implementation of superimposing lakes on the completed DEM which has an elevation equal to the mean of the surrounding elevations. The derived DEM (below) uses a two stage process which first derives the water surface elevation and then assigns this elevation to the lake polygon. This is then used as additional contour data when creating the final derive DEM.

As a result of the search for DEM data, each of the four candidates were dismissed. GTOPO-30 and CAN3D30 due to coarse resolution, CDED because of coarse input data and spurious lakes, and HYD-8 because of excessive sinks and pits coupled with incomplete coverage. Having rejected all candidate products, the only remaining choice was to generate a new DEM, known here as the derived DEM.

The derived DEM is generated from the NTDB contour data supplemented by 1:50,000 scale river and lake data. The resolution of the final DEM was selected as 20 m which conforms to the standard used by the Centre for Topographic Information in generating its high resolution DEM products available in southern Canada. To alleviate some of the problems found with other DEM products, a two stage generation process was developed. First, a trial DEM was generated using topographic data and a continuous network of stream channels without lake polygons. This trial DEM was then used to determine an elevation for each lake polygon using i) the average shoreline elevation for lakes which did not have a positive stream outlet and ii) the outlet elevation for lakes with stream channel outlets. These two new sets of lake contour data were added to the original contour data set to derive the final DEM which had significantly fewer sinks and pits than the HYD-8 DEM and whose lakeshore boundaries blended into and enhanced the surrounding topography.

Improvement in the appearance of lakes is shown in Figure 5-4. This figure contrasts the appearance of lakes in the single pass approach, used in the CDED product, with the two stage approach, detailed above. Rather than simply being superimposed on the finished DEM, the lake shore boundary is used as an integral elevation data source for the generation of the final DEM. Figure 5-5 presents the final derived DEM for the NSA watershed and the watershed boundaries derived from it.

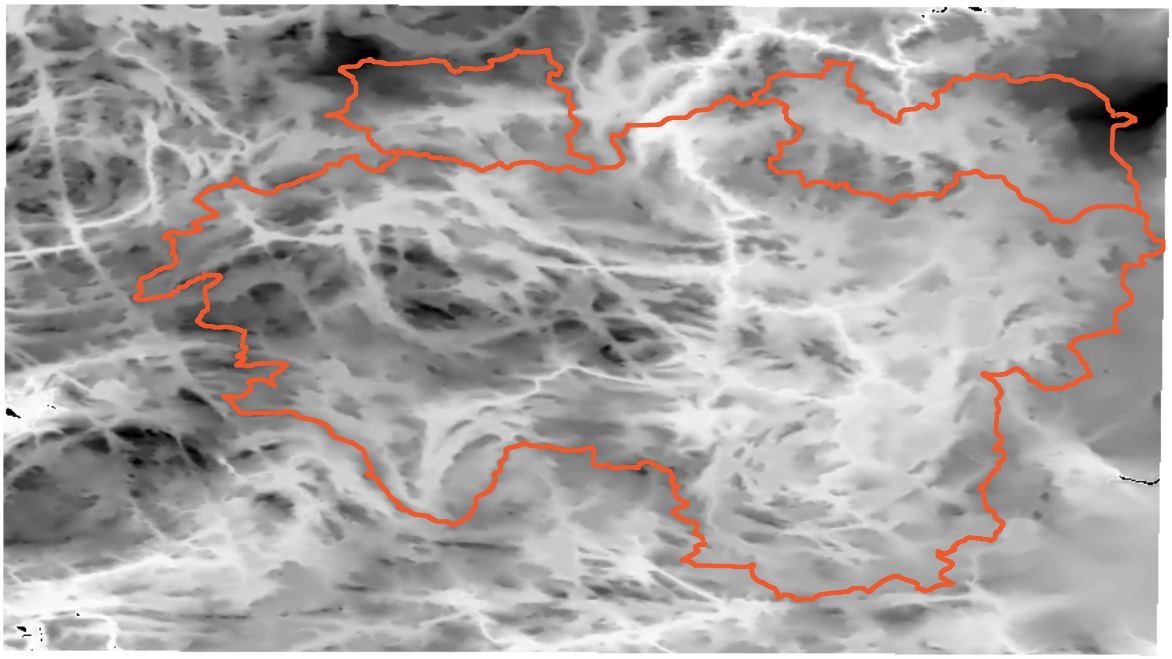

Figure 5-5 : Derived DEM for NSA Study Area.

While the derived DEM of Figure 5-5 looks very similar to the HYD-8 DEM in Figure 5-1, there are significant differences. These include the lack of lake coverage and the existence of many pits and sinks. Both Wise (2000) and Kenward *et al*. (2000) have compared DEMs from a number of different origins and generation methods. Wise (2000), in particular, points to the necessity of DEM evaluation prior to their use; even those purchased from reputable external agencies. One evaluation criteria used in both studies was the ability of the DEM to reproduce the measured watershed area. This has been problematic for WATFLOOD watershed modelling in other areas of Canada and most often requires a process of burning in stream channels to enable satisfactory terrain analysis.

Prior to the availability of DEMs for the BOREAS NSA and SSA watersheds, Neff (1996) delineated the watershed boundaries using traditional hand techniques based on topographic

map analysis supplemented with air photo stereo pairs. Figure 5-6 shows watershed boundaries prepared by Neff and those generated automatically from the DEMs derived here for NSA and SSA watersheds. These are shown on a backdrop of NTDB mapped stream and lakes polygons. In general, the automated delineation preserves many of the features in the hand drawn boundaries. Some differences do occur in flat, poorly drained areas, particularly the eastern portion of the NSA watershed and northern portion of the SSA watershed. It is difficult to speculate which of these is, in fact, correct since there is little further information on the original map with which to make a judgement. Table 5-3 gives a comparison of the numeric values of each watershed area.

Table 5-3 : Watershed area comparison for the NSA and SSA watersheds

Watershed	*Hand Delineation Area(km^2)*	*Area Derived from DEM(km^2)*	*Difference (km^2)*
NW1	398.8	397.1	1.7
NW2	29.0	28.9	0.1
NW3	42.6	50.0	-7.4
SW1	603.4	595.3	8.1
SW2	481.5	474.0	7.5
SW3	205.0	247.5	-42.5
SW4	81.6	79.8	1.8
SW5	22.7	15.7	7.0

The large area difference for the SW3 watershed indicates the need for further investigation as to the cause of the mismatch. For now the SW3 gauge should be treated as suspect since the watershed boundaries used in WATFLOOD and WatCLASS are those determined by Neff (1996). The remainder are within the reasonable ranges given that the grid squares used to define GRUs for the NSA and SSA are four square kilometres each.

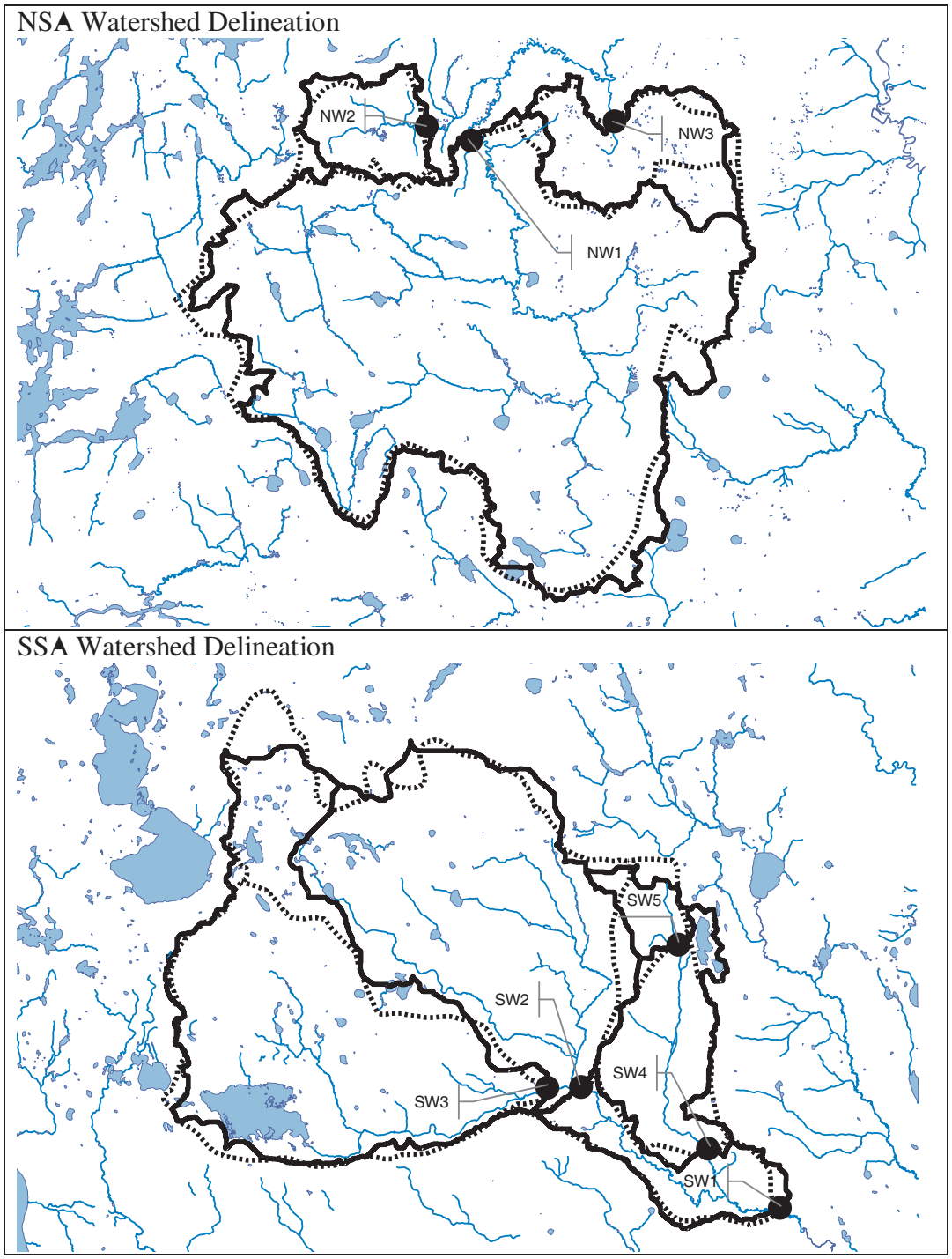

Figure 5-6 : NSA and SSA watershed delineation. Solid outline represents watersheds delineated from derived DEM and broken line derived from hand methods by Neff (1996). Stream gauge locations and 1;50,000 scale river and lake vectors from NTDB shown from reference. Note: map presented in UTM projection.

5.3 GRU Validation

Fundamental to the Grouped Response Unit (GRU) approach is the concept that watershed response can be predicted by grouping together vegetation of a similar type and treating this group as a homogeneous unit for determining runoff. Each vegetation category within a watershed is given the same parameters and is expected to behave in a similar fashion. For example, all the spruce forest in the NSA watershed would receive the same set of controlling parameters which describe its hydrologic response to forcing data inputs. These parameters are expected to be different for pine forests, which in turn would be different from wetland areas.

In WATFLOOD, the GRU approach is used to estimate a number of vegetation specific parameters including leaf interception capacity and Priestley-Taylor alpha (ζ). This latter term (ζ) controls the evaporative response of vegetation to net radiation inputs under well-watered conditions. Parameters of this type can be tied to vegetation characteristics which are the direct objects of the grouping process. However, WATFLOOD also uses vegetation type to estimate soil parameters. These soil parameters are very important to the operation of WATFLOOD and have a major impact on the partitioning of the upper zone storage (UZS) soil moisture reservoir. Three UZS partitioning functions controlled by soil functions include:

1. Infiltration capacity: This is determined by a saturated hydraulic conductivity specification, AK1, and an antecedent precipitation index decay parameter, A5, which controls the development of wetting front suction. Rainfall and snow melt inputs are partitioned into surface overland flow and soil moisture by these infiltration controls.

Infiltration increases UZS moisture content while evaporation, horizontal, and vertical drainage decrease it.

2. Horizontal drainage: also known as interflow, removes moisture from UZS by a linearly varying conductivity model. Control within this model is determined by the selection of a limiting soil water amount, RETN, and a scale factor, REC, which increases lateral conductivity as UZS moisture content increases.

3. Finally, drainage of UZS to lower zone storage (LZS) is also controlled by a linear model similar to interflow. The parameters are AK2 and RETN.

These three flow mechanisms are primarily functions of and controlled by the properties of the soils underlying the vegetation. Selection of these parameters based on vegetation cover alone presupposes that vegetation and soil type follow similar patterns. WATFLOOD relies strongly on this relationship and soil mapping is almost never used as input to the model. In practice, soil parameters are selected by an optimization process intended to match hydrograph response. This differs in WatCLASS and other land surface schemes where soil and vegetation parameters may be specified separately. This leads to the question of the applicability of soil parameter estimates from vegetation surrogates and whether this relationship can be used to derive a set of land cover based soil parameters that have universal application.

To begin to test the association of land cover and soils, the BOREAS NSA is examined in detail. Here, both land cover and soils have been mapped in detail so that the degree of spatial correlation can be examined. Input data include a detailed soils map prepared by Hugo Veldhuis (2000), vegetation classification derived by an optimal integration of the multiple source remote sensing instruments (Ranson *et al.*, 1997), and topographic information derived in Section 5.2. The goals here are to i) determine the degree of spatial

association of soils, topography and land cover and ii) to expand spatially the existing soils data base for use in future study.

Soil mapping of various domains within the BOREAS area was undertaken as part of the original study plan. For all SSA and NSA tower sites, detailed mapping was performed at a scale of 1:5000 for small ~1 km^2 areas surrounding each of the flux tower sites. These areas of detailed study are too small to derive meaningful spatial patterns about the watershed areas as a whole. Fortunately, much of the NSA watershed was mapped at a larger 1:50,000 scale and is known as the NSA-MSA (Modelling Sub Area). No equivalent mapping was performed for the SSA area and the existing 1:250,000 scale soil mapping prepared by the Province of Saskatchewan is the only data source available for the SSA watershed. Soil mapping polygons for the NSA-MSA is shown overlaid with the NSA watershed area in Figure 5-7. Polygon shapes within the soil coverage represent either an area of homogeneous soil composition or (most often) a mixture of soil associations that are intertwined to such an extent that they cannot be broken down further at the current map resolution. These mixtures of soil type are identified and characterized in a polygon attribute table according to the percentage of the polygon area that the individual soil series occupies.

This system of polygon mapping is quite different from raster-based remote sensing data that give a unique value to each pixel mapping unit. The polygon system has been adopted for mapping soil resources at various scales across Canada. The data collected for the NSA are typical of the data that have been mapped for the entire Canadian land mass with the exception of its detailed scale representation.

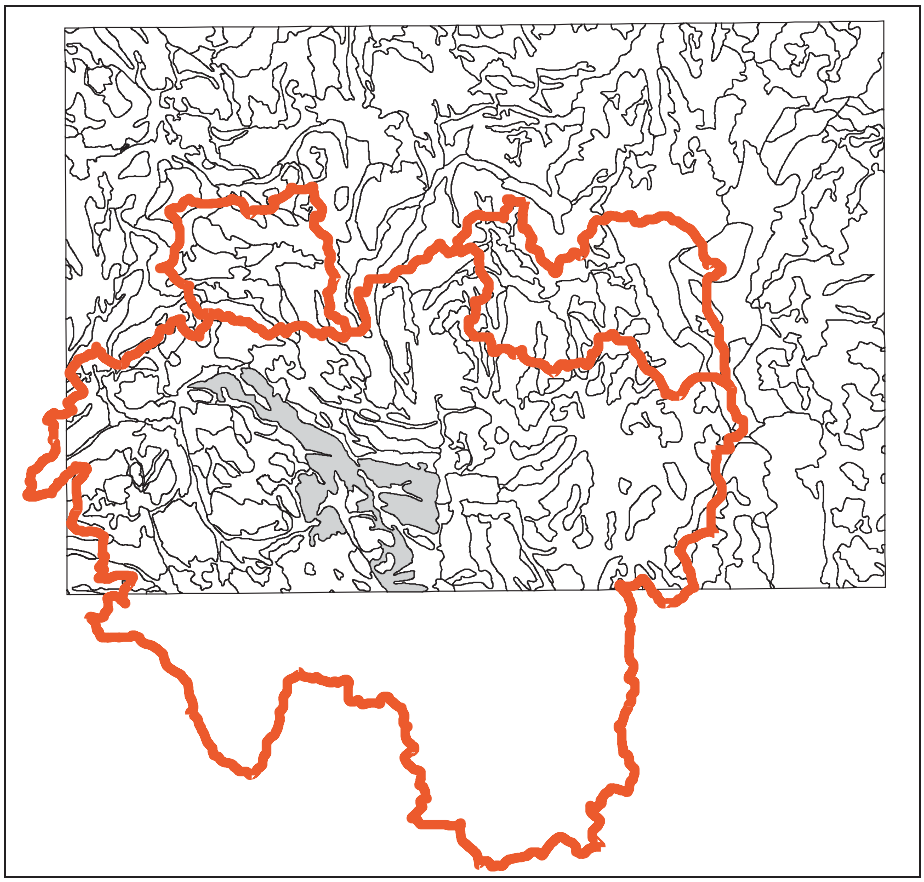

Figure 5-7 : Soil polygon coverage for the NSA from Veldhuis (2000). Shaded region is polygon number 57 discussed in the text.

The shaded area within Figure 5-7 represents a typical soil data polygon. This polygon is identified by the number 57 in the associated soil attribute table where soil properties are detailed. Table 5-4, below, shows a selection of data from the soil attribute table associated with polygon number 57. Referring to the table, this polygon has 65% (40+25) of its area composed of mineral soil (SO), with terrain that is slightly undulating to hummocky as a result of underlying bedrock topography (by), the upper soil layer is of glacio-lacustrine (deposited within a glacial lake) origin (GL) whose texture is heavy clay (HC). Information related to the second soil layer is missing (-). This mineral soil classification is further subdivided by a drainage indicator with 40% moderately well (MW) drained and 25% classed as imperfect (I) drainage. Organic soils (OR) cover 25% of the area with 15% as

veneer bog (Bv) and 10% as collapsed scar fen (Fc) both of which overlie heavy clay defined in the second soil layer. The bog (B) designation is poorly drained (P) and has a fabric (F) decomposition texture while the fen designation (FN) has a very poor (VP) drainage and a more humified mesic (M) degree of decomposition. Finally, 10% of the polygon is classes as exposed bedrock (R2) with a hummocky land form (h). Many of the soil attributes associated with rock are classed as not applicable (#).

Table 5-4 : Selected Soil Attributes for Polygon 57 of NSA-MSA vector soil data.

Percent Coverage	*Material Designation*	*Landform*	*Layer 1 Mode of Deposition*	*Layer1 Texture*	*Layer 2 Mode of Deposition*	*Layer2 Texture*	*Drainage Indicator*
40	SO	by	GL	HC	-	-	MW
25	SO	by	GL	HC	-	-	I
15	OR	Bv	B	F	GL	HC	P
10	OR	Fc	FN	M	GL	HC	VP
10	R2	h	RK	#	#	#	#

Polygon 57 is typical of the data presented in the soil attribute table. To find its relation with the overlying vegetation, the predominant hydrologic characteristic "texture" was grouped and mapped as raster images using ArcInfo software. Some grouping was performed to reduce the number of soil classes. These include the combination of fen and bog classes into an organic category, grouping of silty clay, clay, and heavy clay soil types into a clay categorization, and the creating a sand class from coarse sand and medium sand textures. These groupings, together with the differentiation of water and exposed bedrock, are mapped as raster images and represent the likelihood of encountering a given surface soil form in any one of the soil polygons. These soil maps are present in Figure 5-8 by soil and non-soil

category with darker polygons indicating a higher likelihood of encountering the feature within a polygon. Note that the NSA-MSA is dominated by the aggregate of clay and organic soils with a small area of sand in the eastern and western portions of the map.

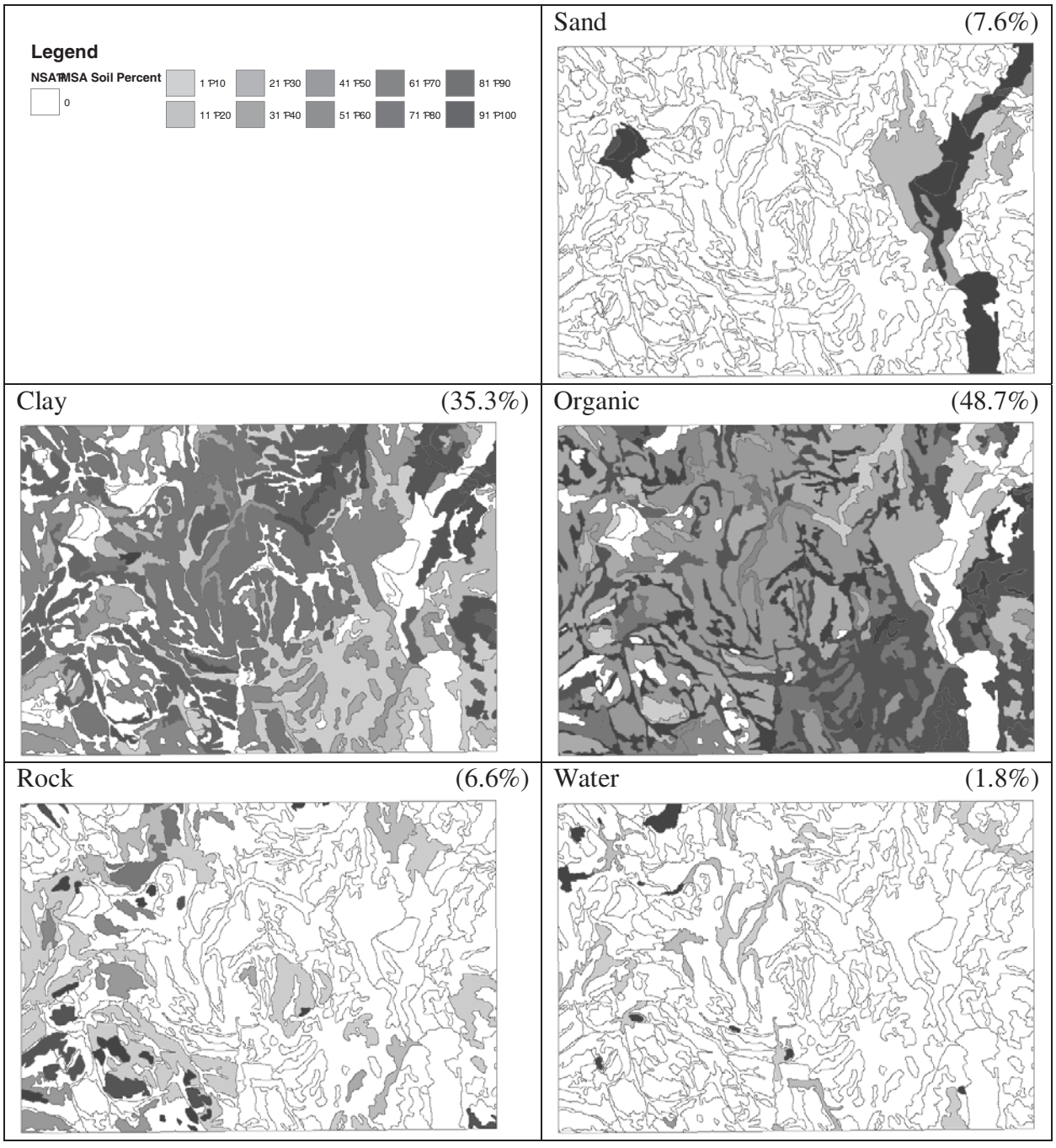

Figure 5-8 : Distribution of NSA-MSA soil information by %land cover within a polygon feature. Percentage totals for the area are given in brackets.

Land cover mapping, used in the analysis which follows, is based on the classified vegetation images prepared by Ranson *et al*. (1997). This vegetation mapping is unique in that a number of independent image sources were used to produce the final classification. Image sources used by Ranson include Landsat TM imagery together with multi-band (C, L, and X-bands) and multi-polarization (various horizontal (H) and vertical (V)) scenes from the Shuttle Imaging Radar (SIR) using imagery from both April and October. Using 20 of the original image channels as input, Ranson performed a principal component analysis to reduce the original set of 20 images to six channels that contained a majority of the scene information (i.e. scene variance). These six principal components were composed primarily (75%) of the October SIR C-band and L-band images as well as TM bands 4, 5 and 7 from the LandSat image. Providing less information (25%) were the April SIR images, SIR X-band channels and TM bands 1, 2 and 3. Ranson *et al*. (1997) state that the classification accuracy of the final image was in excess of 90% when compared to the training data set. Higher scores were obtained for pine and aspen classes and lower scores were obtained for spruce. This image is depicted in Figure 5-9. The large swath of shrub land classification in the centre of the watershed represents an area of fire damage that is in various stages of regrowth.

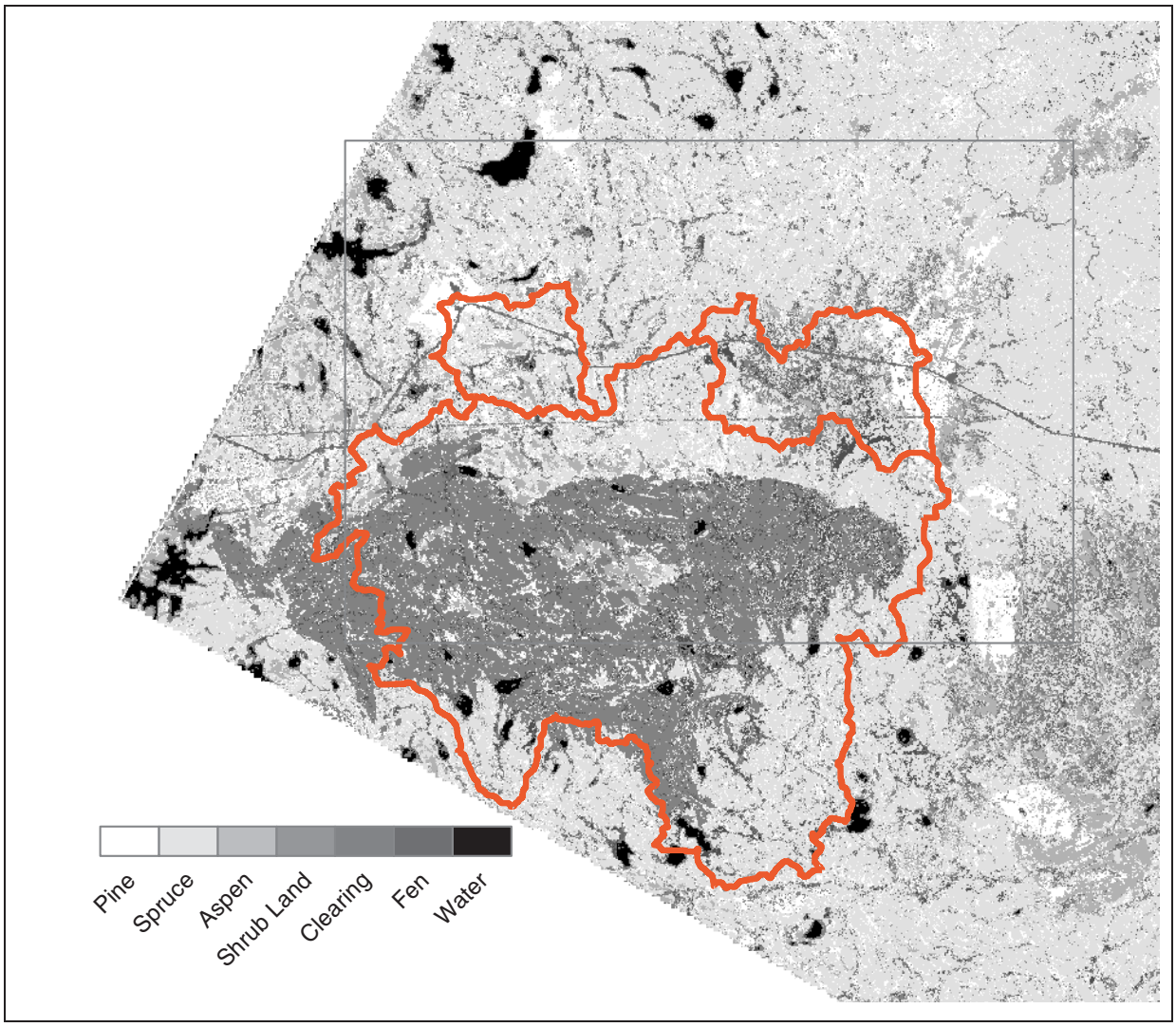

Figure 5-9 : Land cover mapping from Ranson *et al* (1997). Superimposed on the image is NSA watershed (thick line) and the extent of soil information rectangle (narrow line). Note: this is the lower left corner of a larger image in Figure 5-10.

To determine relationships with soil occurrence, the classified vegetation image was reduced to a number of binary equivalent images each containing a distinct land cover feature. Unlike the soil data, whose likelihood of occurrence range from 0-100% in a polygon, land cover data have either a 0% or 100% likelihood of occurring in any one pixel. The original land cover data are converted into pixel percentage to produce seven binary images as shown in Figure 5-10.

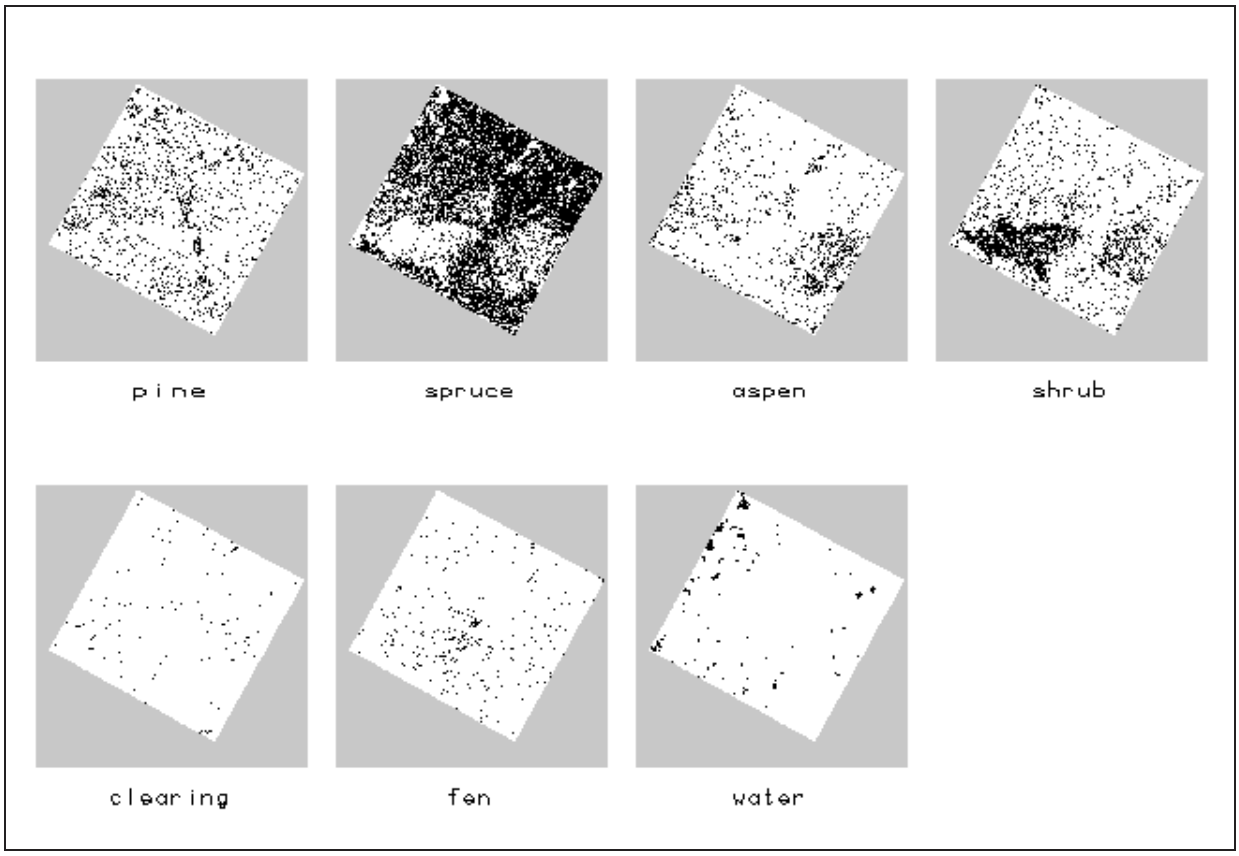

Figure 5-10 : Binary image of NSA land cover data. Note that dark regions represent the presence of a vegetation category and white areas the absence. Grey areas represent NODATA areas within the image.

A final source of input data used to predict soil occurrence was topography developed in Section 5.2. Within the NSA-MSA, sandy features occur as a result of glacial outwashes that have deposited sand over the previously deposited clay soils and are generally higher than the surrounding terrain. Additionally, wet areas such as fens and bogs are often found in lower, flatter areas which further emphasize the topographic relation to soil occurrence. To determine quantitatively if topographic relationships exist, a separate analysis was performed with and without the elevation and slope data. A final step in generating elevation inputs required the log transformation of the derived slope data set. This was required to normalize the frequency distribution because of a large skewness which existed in the slope data set.

A linear regression was performed using various combinations of the independent soil and topographic variables with the dependent soil data classifications. The results of this analysis, performed with a statistical software packaged called SPSS, are shown in Table 5-5.

Table 5-5 : Error analysis of regression analysis between soil type and land cover

Soil Type	*Percent Area*	*Vegetation Alone*		*Vegetation and Topography*	
		RMS	R^2	*RMS*	R^2
Sand	7.6	23.8	0.088	22.8	0.164
Clay	35.3	27.9	0.052	26.8	0.125
Organic	48.7	30.4	0.100	27.7	0.253
Rock	6.6	18.3	0.034	16.9	0.166
Water	1.8	6.3	0.632	6.3	0.634
	Area Average Values	***27.8***	***0.087***	***25.9***	***0.202***

Results of the regression analysis indicate that the addition of the topographic information increase the predictability of the soil type. The area averaged, root mean squared error (RMS) indicates that vegetation and topographic predictors of soil type are likely to be in error by up to 26%. This translates to area averaged values of R^2 of only 0.2 meaning that the use of vegetation and topography as surrogates for soil type only accounts for 20% of the variability within the original soils data set. In fact, it appears that topographic information explains significantly more of the variance (11.5%) in the soils data than does vegetation data alone (8.7%).

Reasons for these low scores are reinforced by looking at a contingency table of the land cover data in relation to the soil data presented in Table 5-6. In this table the soils associated

of each vegetation pixels category are shown. As expected, the water class from the land cover data are primarily associated with the water identified by soil investigation (89.3%) with a small portion classed as organic on the soils map. More surprising, however, is that pine has no clear association with either sand, clay or organic soils. This may be due to the misclassification of low density spruce trees as pine forest which Ranson *et al.* (1997) reports the most common classification error. Further study using alternate forestry data sets may reduce vegetation classification error.

Table 5-6 : Contingency Table for Vegetation Associations with Soils

	Pine	***Spruce***	***Shrub***	***Aspen***	***Fen***	***Clear***	***Water***
sand	23.0	4.9	2.1	16.8	0.5	9.9	0.0
clay	35.0	39.5	30.1	41.0	14.9	28.0	0.2
organic	34.3	51.0	54.4	34.9	80.0	48.4	10.5
rock	7.2	3.9	11.8	6.9	1.5	11.5	0.0
water	0.5	0.7	1.6	0.4	3.1	2.2	89.3
Σ	100	100	100	100	100	100	100

Another error that may be present includes the manner in which spatial soil data are collected. The pedologist (soil scientist) combines his knowledge of soil associations, with field test pits, laboratory analysis, air-photo interpretation and topographic maps to determine the distribution of soils within a polygon. The use of air-photos would undoubtedly bias the identification of soils in favour of a land cover association. This could lead to biases by associating soils in favour of an increasing the vegetation/soil relationship. However, quantifying these errors and assessing the amount of new information the pedologist adds to

the air photo interpretation is difficult to determine. Clearly this does not appear to be evident in the current data set as there is a poor vegetation/soil association.

The primary goal of this exercise was to determine quantitatively the reliability of predicting soil properties based on land cover distribution. The analysis presented above indicates that while land cover is not overwhelmingly associated with a single soil association that each land cover classification does have a distinctly different mixture of soil representation. This may help to explain the success of the GRU concept in generating soil parameters through optimization which match observed hydrographs for a watershed. It may also explain WATFLOOD's inability to match these parameters to textbook values of soil properties and transfer them successfully from one watershed to another. It should be noted that this conclusion is based only on a single very small dataset that may not be representative of the larger world. However, it does indicate the need for further research into the role of vegetation in defining hydrologic similarity.

Secondary to this study is the development of a predictive model of NSA soil type based on vegetation and topographic information. Table 5-7 gives the parameters of the regression model developed for Table 5-5. The dependent variable (DV) is estimated by summing the Y-intercept value with the values of the independent variables (ID) multiplied by their associated coefficients in Table 5-7. Land cover independent variables have values of either 0 or 100, elevation is the height above sea level in meters and the natural logarithm of the slope is in percent. Pixel maps of the five soil types were produced from the regression coefficients and a simple selection model was used to pick the highest likelihood of occurrence value amongst the five contending soil types on a pixel by pixel basis. The resulting soil classification produces a 'pixelated' or raster version of the original soil data.

This raster soil model allows the extension of the soil data base beyond the original polygon boundaries. This pixelated soil map is presented in Figure 5-11.

Table 5-7 : Regression analysis coefficients for soil texture prediction from land cover and topography.

Dependent Variable	*Y-Int*	*Independent Variable Coefficients (×10²) and t-statistic (absolute value)*								
Soil Type		*PINE*	*SPRUCE*	*SHRUB*	*ASPEN*	*FEN*	*CLEAR*	*WATER*	*ELEV*	*SLOPE*
Sand	-121.8	13.6	*	-3.6	8.2	-2.0	3.8	-4.9	48.6	37.9
t-test	*258*	*176*	*	*57*	*83*	*14*	*14*	*18*	*269*	*16*
Clay	109.8	-2.8	*	-9.6	1.9	-22.5	-10.9	-31.0	-28.2	601.5
t-test	*198*	*30*	*	*129*	*17*	*135*	*35*	*96*	*133*	*218*
Organic	215.4	-9.8	*	5.4	-9.1	21.6	-0.9	-51.4	-61.4	-863.2
t-test	*376*	*105*	*	*70*	*76*	*125*	*3*	*153*	*280*	*302*
Rock	-112.6	-1.1	*	6.8	-1.1	0.8	6.4	-1.0	44.3	252.9
t-test	*321*	*20*	*	*146*	*15*	*7*	*32*	*5*	*330*	*145*
Water	9.2	0.1	*	1.0	0.0	2.1	1.6	88.3	-3.2	-29.1
t-test	*71*	*6*	*	*57*	*2*	*55*	*22*	*1162*	*64*	*45*

This model of soil prediction is rather simple and has a number of shortcomings. Some major features evident in the original soils data are preserved in the model including the sandy areas in the north-east and north-west portions of the basin. However, there is difficulty in determining a distinction between organic and clay soils. Some of the elevated and steep portions of the basin are given clay soil covers but there is confusion in the differentiation between the shrub, spruce and fen land covers and their associations with a particular soil. This is shown in the validation results present in Table 5-8 where the soil distribution from the original polygon coverage and the soils predicted by regression analysis are compared for the original polygon coverage area.

Table 5-8 : Validation results for regression based soil estimation

Soil Type	*Original Polygon Data*	*Regression Results*
Sand	7.6	2
Clay	35.3	25
Organic	48.7	72
Rock	6.6	<1
Water	1.8	1

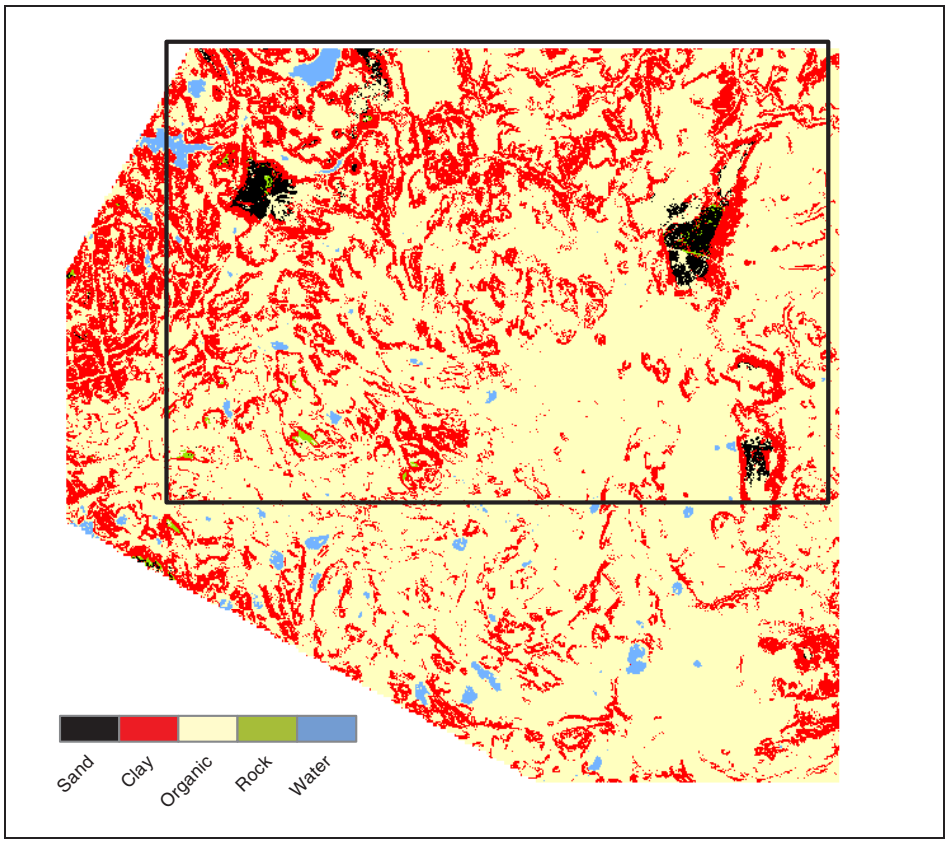

Figure 5-11 : Pixelated soil map of the NSA produced from vegetation and topographic data. Some distinct features are reproduced including the sandy areas associated with pine forest and water bodies. The NSA-MSA soil polygon boundary is shown for reference.

Clearly, much additional work remains to improve the association of soil type to physiographic elements of the landscape. Results above indicate that a linear model of vegetation and topographic inputs do not explain the majority of the variability in the underlying soil data set and errors of approximately 25% can be expected. While land cover does have a role to play in representing hydrologic similarity, it should not be expected to totally explain the variability in natural landscapes. In the NSA, for instance, vegetation is not a fixture of the environment and is constantly changing as a result of fire and timber harvesting operations which leave large portions of the landscape in various stages of regeneration.

5.4 Streamflow Generation

Previous sections in this chapter have discussed the important physiographic inputs required for watershed modelling including topographic, land cover and soil. Much of these data had been compiled previously based on the work of Neff (1996) and sections 5.2 and 5.3 have attempted to automate the tasks required for watershed delineation by DEM production and quantification of the associations between soil and land cover for parameter selection.

Drainage Layer Database

For streamflow simulation of the NSA and SSA watersheds, databases previously compiled for WATFLOOD were used. Land cover mapping was determined from LandSat imagery and classified into wet forest, dry forest, wet land and water based on maximum likelihood classification (Neff, 1996). The topography and river drainage networks were extracted from analysis of paper maps. Summary of the distribution of land cover, drainage area, and internal slope used for both NSA and SSA are given in Table 5-9.

Table 5-9 : Summary for drainage layer database for SSA and NSA watersheds

Basin	*Area (km^2)*	*Average Internal Slope (%)*	*Bare*	*Dry Forest*	*Wet Forest*	*Wetland*	*Water*
SSA (SW1)	605	1.73	1.2	27.7	60.7	7.0	3.4
NSA (NW1)	398	3.67	3.3	51.8	37.5	6.2	1.2

An analysis of 1:50,000 scale base maps was also performed to obtain the drainage density of each of the basins. Drainage density (D_D) is defined by Dingman (2002, p. 433) as the total length of streams draining in watershed divided by the watershed area. It has dimensions of L^{-1} and its inverse can be considered as the average straight line distance one would have to travel before encountering a stream channel. From a conceptual point of view, drainage density can be considered as the distance storm water must travel in the relatively 'slow' land surface system prior to concentrating into a stream routing element where travel velocities increase dramatically. Table 5-10 gives drainage density values for the NSA and SSA watersheds.

Examining the two larger watersheds, SW1 and NW1, reveal differences in their capability to generate runoff. In the conceptual model of runoff generation, presented in Chapter 3, interflow, the primary flow generation mechanism, is impacted by a soil conductivity term, $K(\chi)$, which is non-linear plus a linear component made up of drainage density and topographic slope. Considering the linear component alone, it is expected that the SSA, having a drainage density of 0.36 per kilometre and an average slope of 1.3% would be less responsive to rainfall /snow melt input than the NSA with a higher drainage density of 0.51 per kilometre and an average slope of 3.7%. Figures 4-2 and 4-3 illustrate these differences

graphically. These shaded relief maps of the watersheds are generated with exactly the same parameters and the smooth texture of the SSA image contrasts sharply with the rough NSA image. It should be noted that NW3 contains only a single mapped stream channel which results in a very low drainage density.

Table 5-10 : Drainage density values for NSA and SSA sub-watersheds

Basin	*Stream Length (km)*	*Area (km^2)*	*Drainage Density (km^{-1})*
SW1	216	595	0.363
SW2	153	473	0.323
SW3	66	248	0.266
SW4	28	80	0.350
SW5	6.2	15.7	0.395
NW1	201	397	0.507
NW2	13.2	28.9	0.486
NW3	2.4	50	0.05

This concept of drainage density, as presented, makes an assumption that 'fast' routing is only available in defined stream channels mapped at the scale of the current base map. This interpretation is essentially a static view of drainage density. Another idea of drainage density, which has yet to be explored in the WATFLOOD or WatCLASS models, is a dynamic one that is related to the natural landspace roughness and the potential of the undulating topographic surface to concentrate storm runoff and produce ephemeral stream or 'rivulets'. Clearly, with modern GIS tools, the ability to determine flow pathways through DEM analysis has become less of an obstacle. More difficult, however, is developing conceptual models relating surface wetness to a dynamic increase in drainage density. A dynamic drainage density model would effectively decrease the distance stormflow must

travel in the soil before encountering a fast routing element and change in response to basin wetness. Future research using this concept of dynamic drainage density may provide a physical basis for the non-linear nature of runoff response from natural watersheds.

Forcing Data

As with point results presented in Chapter 4, seven atmospheric forcing variables are required to drive the WatCLASS model in spatial mode. The spatial data set used for the NSA and SSA were developed by Val Pauwels as part of the BOREAS Follow-On Project (Pauwels *et al.*, 1999). This forcing data set was constructed based on the observations made at the various tower sites, mesonet sites, and other weather sites that were operated during the BOREAS project.

Included in the data used to develop the spatial precipitation field were the radar rainfall measurements made during the 1994 field campaign. These data, as with all radar rainfall data, have numerous problems that must be corrected prior to use. In keeping with previous work done at the University of Waterloo and because of the relatively large rain gauge network that was available during the project, rainfall data files prepared by Whidden (1999) will be used to override those developed as part of the BOREAS Follow-On Study.

Streamflow Hydrographs

Streamflow generated by the NSA (NW1) and SSA (SW1) watersheds are presented in Figure 5-12 and Figure 5-13, respectively. These plots represent the best runs obtained from the WatCLASS model. Major features of the hydrograph are preserved including the seasonality and watershed responsiveness to storm inputs. However, there are a number of features which will require further research to address inaccuracies.

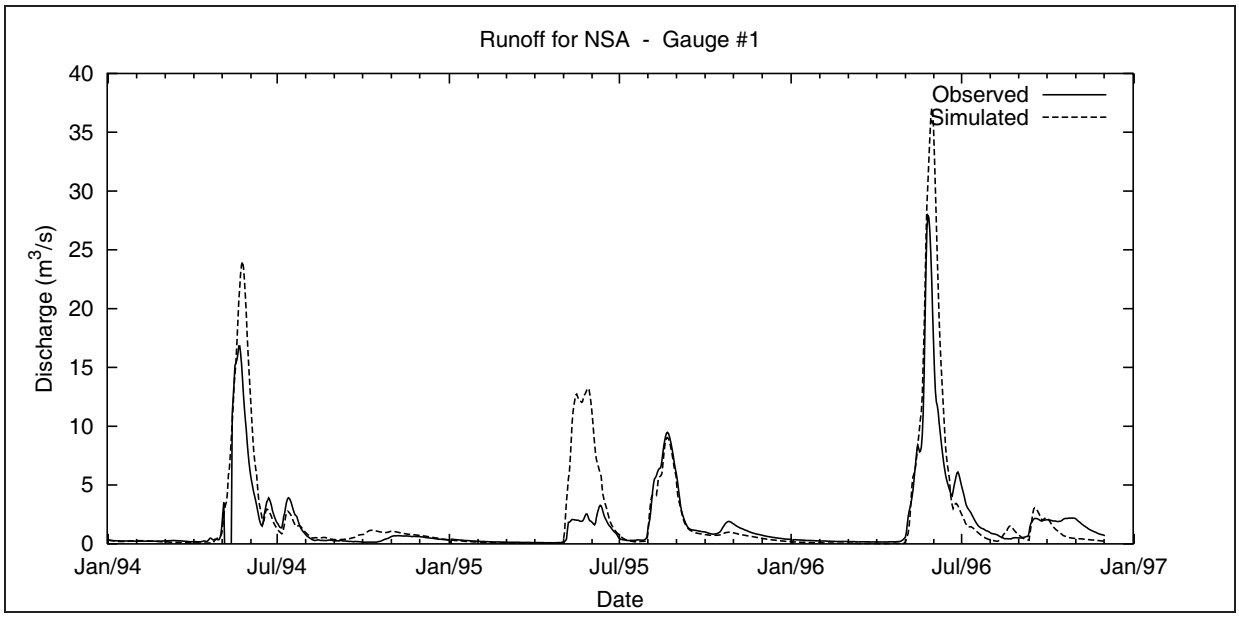

Figure 5-12 : WatCLASS runoff hydrograph for BOREAS stream gauge NW1

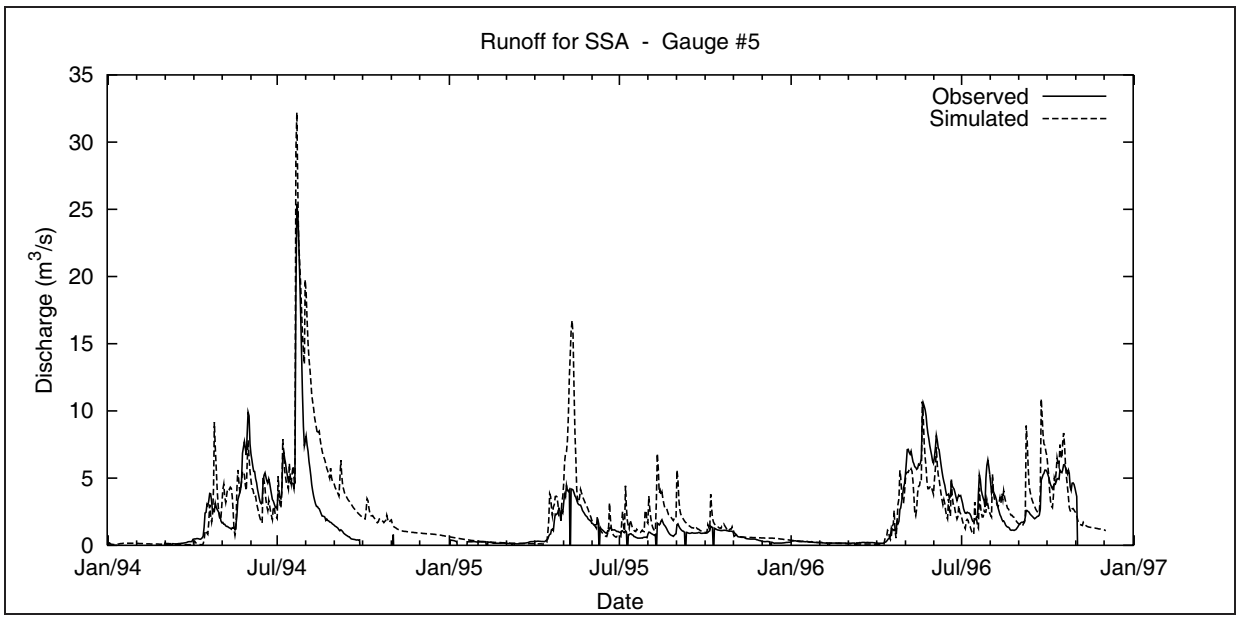

Figure 5-13 : WatCLASS runoff hydrograph for BOREAS stream gauge SW1

NSA Discussion

For the NSA, there is a consistently high spring runoff amount. This is especially prevalent in the spring of 1995 where there was a very low recorded snowmelt runoff. Initial speculation as to the cause of this large anomaly included inaccuracy in streamflow measurements due to gauge measurement errors, over estimates of snowfall measurements during the winter of 94/95, and reduced infiltration amounts due to frozen ground. Stream gauge errors were ruled out after review of other gauged basins in western Canada, including the Mackenzie River basin, many of which show anomalously low spring runoff amounts for the spring of 1995. For snowfall, there is a known issue with the quality of snow data collected during the BOREAS project. However, these should give consistently poor and scattered results that are not evident in the data. The most plausible cause of the high spring runoff may be related to how WatCLASS handles infiltration into frozen ground.

As soils freeze in WatCLASS, liquid soil moisture is reduced and converted into frozen soil moisture. All moisture is accounted for, however, the calculation of soil suction and hydraulic conductivity are based on the 'liquid' moisture portions only. Reduction in soil moisture, caused by soil freezing, has exactly the same impact as drying the soil matrix; that is an increase in soil suction and reduction in hydraulic conductivity. This effective soil 'freeze-drying' has two potentially adverse impacts on spring infiltration amounts. First, as the freezing front advances downward during the fall, upper soil layers freeze prior to lower layers. This greatly increases the suction potential of the partially frozen upper soil layers which pulls moisture from the still unfrozen lower layers into the upper soil layers in response to the induced gradient. This unnaturally increases the degree of ice saturation in

the upper soil layer and the energy required in the following spring to melt the ice and allow infiltration to occur.

A second impact, related to the first, occurs during the spring melt when soils thaw from the top down. As the topmost layer thaws, moisture from melting snow travels laterally as interflow through the top layer. As this occurs, the second layer, which remains partially frozen, severely restricts the passage of liquid moisture even though there is a large soil moisture deficit in the third layer which had developed from the previous fall. By the time the second layer thaws sufficiently to allow deeper percolation, a large portion of the spring melt water has run off as interflow through the upper soil layer.

For partially frozen soils, the question becomes whether or not freezing has the same impact as drying on the physics of water movement. The contention here is that they are not the same process and that flow in partially frozen soils has a different response mechanism than soil drying. As unsaturated soils begin to freeze, moisture is contained in the smallest pores of the soil matrix preferentially, just as they are in the unfrozen state. These pores are naturally less conductive than the larger unfilled ones. If this moisture is frozen, the larger diameter pore spaces remain available to transmit water while the smaller less conductive pores contribute no flow because they are filled with moisture and frozen. In this case, frozen moisture, residing in small pores, acts in a similar fashion to the solid soil phase and effectively reduces available void space. In calculating the suction and hydraulic conductivity values for partially frozen soil, the degree of saturation term in the Campbell / Clapp and Hornberger formulations used by CLASS should be changed to:

$$S \mid \left(\frac{\chi_{total} - \chi_{frozen}}{\lambda - \chi_{frozen}} \right) \qquad \text{Equation 5-1}$$

where λ represents the porosity of the soil and χ_{total} represents the sum of the liquid and frozen (χ_{frozen}) portions of soil moisture. Arranging the degree of saturation calculation in this way reflects the reduction in both in soil moisture and available void space and would tend to increase flow through the partially frozen soil matrix since large pores remain available to conduct moisture. Also, a decrease in the upward migration of liquid moisture during fall would result since freezing would have no net impact on soil potential calculation.

While this theory is plausible, it remains largely untested in WatCLASS and will be the subject of future research. Other issues related to thawing of the soils must be addressed as well including a determination of whether the smallest or largest ice filled pores become available first as thawing progresses. Also required is research into the impacts on soil moisture suction and conductivity on very ice rich soils and whether the simple relation proposed in Equation 5.1 is effective for all ice contents. While spring melt problems do exist for the NSA for all three years and the SSA during 1995, SSA spring melt hydrograph from 1996 shows a shortfall in runoff production.

Another method explored for reducing snowmelt runoff includes the reduction of interflow conductivity. This method corrected the NSA spring hydrographs of the 1994 and 1996 spring events but could not reduce the 1995 result to a satisfactory level. However, reducing interflow had a negative impact on other storm hydrographs. In particular, the August 1995 runoff event was much reduced. Selection of parameters was geared primarily to capture this event and allow the remaining events to evolve from these parameters.

SSA Discussion

For the SSA there are two obvious concerns from the hydrograph result. The first is the large overestimate in runoff following the rainfall event of late July 1994 and the second is the general overestimate in hydrograph peak flows. These are both the result of maintaining predictability of other features of the hydrograph. To provide a constant source of water necessary to maintain observed low flows during the spring and summer, alterations to the wet conifer land class was required. BOREAS data indicate that water table levels in this land class are maintained near the surface. However, soils in the area are generally sandy in texture which alone would not support a high water table.

To provide the necessary drainage restriction, a CLASS parameter that restricts flow from the bottom of the wet conifer land class was set to stop the flow of water and third soil layer was initialized with soil moisture content at saturation. This maintained moisture close to the surface and supported observed low summer flow values. Maintaining water close to the surface increases interflow opportunity and hence the high peak flows which occur in response to rainfall inputs. This is also true of the large runoff volume that overwhelms the hydrograph in the fall of 1994. Water close to the surface is permitted to runoff due to the interflow response mechanism. Without increased storage or increased evaporation the simulation cannot be changed.

Water Balance Summaries

Water balances for the two watersheds are shown in Table 5-11. Measured runoff data were extracted from the HYDAT CD ROM where the missing hourly streamflows in the original BOREAS data set have been filled in. Missing values in the BOREAS hourly archive are especially evident for the SSA during the fall of 1994. For both the NSA and SSA, there are

runoff amounts in excess of measurements of 44 mm and 79 mm, respectively. Reducing runoff will require increasing evaporation for both areas.

Table 5-11 : BOREAS NSA and SSA Water Balance Summaries

Basin Averages	*Precipitation*	*Evaporation*	*Runoff Model (Measured)*	*÷Storage*
NSA	1284	752	472 (428)	60
SSA	1422	1024	355 (286)	43

For the SSA, evapotranspiration for the wet forest class can be enhanced beyond the amount measured at the SSS-OBS tower site. With the current arrangement, the dense spruce forest found at that tower site is used to characterize the entire wet forest class in the SSA watershed which comprises 60% of the basin area. An alternate land cover data set, known as the Saskatchewan Environment and Resource Management (SERM) Forestry Branch - Inventory Unit (Gruszka, 2000), is comprised of vector forest cover mapped at a scale of 1:12,500. This is a large and complex data base which shows the standing masses of merchantable timber by species. Although, these data have yet to be quantitatively analysed, there are large portions of the SSA watershed which are covered with a low spruce forest which has no merchantable value. The soils underlying these forests are primarily organic and so will not support a larger stand of timber. As such, the designation of the SSA-OBS tower site vegetation as being representative of the entire wet forest classification may be erroneous.

To illustrate the sensitively of this land cover designation on evapotranspiration results, a small change in the composition of the wet forest class was undertaken. In this experiment,

the 60% wet forest class was split in a 75/25% ratio to allow 45% to maintain characteristics of the SSA-OBS forest and 15% to take on the characteristic of bare soil. For this run, the evapotranspiration of the basin as a whole increased from 1024 to 1074mm, an increase of 50 mm, and the runoff amount decreased by 45 mm from 355 to 310 mm. The appearance of the final hydrograph is not much different from that in Figure 5-13 and many of the problems still remain. However, some hydrograph peaks are slightly reduced.

This change in evapotranspiration occurs because the strong stomatal control over evaporation is reduced by removing a portion of the forest cover and allowing the atmosphere direct access to the soil surface. Under normal WatCLASS operations, wind speed below the canopy is set to zero and direct evaporation from the soil is controlled solely by the humidity gradient developed between the canopy and the soil surface. In open vegetation, which exists in the non-merchantable timber class of the SSA spruce forest, there would be a large portion of the surface which would be exposed to direct soil evaporation (or more precisely evaporation from moss). One problem with proving this solution is that there is no BOREAS tower data to support enhanced evaporation from a sparse spruce forest. There is, however, evidence based on aircraft flux measurements that suggests evapotranspiration from the larger watershed is greater than that measured by the tower sites (Desjardins *et al*, 1997). Further analysis of land cover distribution using the SERM forestry data and soil maps of the SSA is required to confirm this finding.

5.5 Calibration Methodology

The proceeding discussion in Chapters 4 and 5 have detailed the methods used to arrive at a set of hydrographs for the NSA and SSA watersheds. These have been generated together

with evaporation results that are compared with BOREAS tower based measurements. The NSA-OBS tower, presented in Chapter 4, has been selected to represent these results. A summary of the steps taken to generate WatCLASS results are as follows:

1. Obtain a calibrated WATFLOOD result for the basin of interest.
    a. For BOREAS results, much of this effort had been completed by others. From these successful WATFLOOD runs, parameters controlling streamflow routing, base flow generation and surface runoff were extracted directly.
    b. Use of WATFLOOD to obtain these parameters is essential. Optimization routines provided by WATFLOOD and speed with which each parameter sets can be tested, make its use attractive for water balance assessment. Use of WatCLASS, which takes 100 times longer to run, to select these parameters would be not be a productive use of computing resources.
2. Select CLASS based soil and vegetation parameter for each GRU designation.
    a. For BOREAS results, extensive databases exist which allow the selection of parameters based on direct measurement. Once selected, these values were not permitted to vary. This presents some degree of uncertainty since values, such as LAI, are not constant over the entire watershed. However, parameter selection criteria was based on the assumption that the measurements made by BOREAS researchers were representative of the watershed's soil and vegetation character.
    b. The BOREAS field sites represent a 'best case' scenario with respect to data availability. Selection of parameters in the absence of these measurements would require transfer of parameters from literature based look-up tables. Generally, there are far too many parameters to extract from the streamflow record alone.
3. Determine parameters 'a' and 'b' from equation 3-2.
    a. These parameters are unknown and must be estimated based on the response of watershed based evaporation and streamflow. Strategies used to determine these parameters include those developed in Chapter 4 where streamflow was

disaggregated using WATFLOOD and cumulative plots of evaporation and runoff. In this case, a value of 'b' was chosen between 2 and 3 and the value of 'a' was adjusted until both the cumulative evaporation and runoff amounts balanced. Generally, as 'a' was changed, both runoff and evaporative plots would converge on measured values. When this did not occur, 'b' adjustments were made until no long term trends in storage were evident.

b. The second method for determining 'a' and 'b' values was through comparison with measured hydrographs. The rate of change in slope of hydrographs recessional limbs provides information as to the speed of interflow depletion. The 'b' parameter has the greatest impact on this shape while the 'a' parameter impacts hydrograph peak values. Use of hydrograph results must also be considered together with tower observations of evaporation. Point output of selected watershed locations is permitted using WatCLASS. These point output allow cumulative evaporation plots to be generated that provide necessary information for differentiation between GRU land covers.

c. Values of 'a' can be disaggregated into components of i) drainage density, ii) internal slope, iii) layer thickness, and iv) lateral saturated hydraulic conductivity. Future work with the model should be geared toward determining measured values for items i, ii, and iii and lateral hydraulic conductivity based on a ratio developed from its vertical counterpart. This may lead to discovery of similarities based on land use or cover.

Parameter Sensitivity

Some WatCLASS parameters are very sensitive to change. Although no formal analysis was performed, experience with the model has provided some knowledge of important parameters. Perhaps most critical is the setting of rooting depth to contain plant roots within the top two soil layers. Specification of this depth, which is sensitive only to the crossing of the third soil layer threshold, will result in large changes evaporation amounts. Interflow

conductivity ‘a’ and its exponent ‘b’ also have a significant impact on both streamflow generation and evaporation amounts. Other vegetation and soil parameters, particularly the vertical saturated hydraulic conductivity override, provided by WatCLASS, have the potential for making large changes in WatCLASS response. However, for these simulations K_{satV} values were fixed so that the impact of this parameter is unknown. In is anticipated that increasing K_{satV} will increase the amount of moisture returned to streamflow as base flow

The model is also sensitive to initial conditions, especially third layer temperature, soil moisture and ice content. In working with the model it is important to spin-up the simulation over an annual cycle prior to use. Since high moisture contents are drained quickly in the model, it is best to start spin-up simulations near saturation. This allows relative equilibrium values to be established much faster than starting with dry conditions. Setting initial ice contents is problematic. This is due to the dramatic impact small increases in ice content have on hydraulic conductivity. The actual impact of small ice fractions on moisture flow is uncertain and as a result WatCLASS simulations for BOREAS soils were initialized at $0^{o}C$ without any ice content.

Solution Uniqueness

As mentioned in Section 3.2.1, solution uniqueness is maximized by running continuous simulations over multi-year periods. This reduces the likelihood that initial conditions will dominating results and allows model storages values and fluxes to evolve in a natural way. Long continuous simulations also test the model under a variety of conditions particularly those occurring in transitional seasons of the annual cycle. However, even with long simulations there are inherent errors in the forcing data sets, the validation data, and the drainage layer database used for land surface initialization.

These errors are difficult to quantify primarily because not enough reliable data were collected to close the water and energy balances for individual BOREAS towers or the study area watersheds. Individual towers have no measurement of runoff from the water balance equation, given previously as P-E=R+÷S, and the reliability of storage change as shown by soil moisture time series, given by Figure 4-19, are questionable. This required the use of WATFOOD runoff as a surrogate and the monitoring of storage to detect long term trends. Study area watersheds are similarly flawed with good measurements provided for runoff but poor knowledge of the other water balance components. These require spatial interpolation of point data to make measurement based comparisons. However, given these errors, the simulation of the observed response patterns gives some confidence in the models ability to simulate the natural system and future efforts may focus on quantification of errors.

5.6 Chapter Summary

Moving from a point scale to a watershed domain requires the consideration of many factors. Is the watershed area and topographic character of the basin well represented in the model? Are point observations of water and energy representative of the basin as a whole? Can the physiographic characteristics of vegetation and topography be used to define hydrologic similarity? These questions have been addressed in this chapter.

In addressing these questions, the second objective, from Section 1.5, has been examined. This objective seeks to extend runoff induced changes in evaporation to the watershed areas and use measured streamflow to quantity simulation success. While hydrograph peaks are in error, particularly those during spring melt, simulation volumes are represented well.

6 Mackenzie River Results

6.1 Introduction

The Mackenzie River basin has received considerable attention recently as a result of efforts from Global Energy and Water Balance Experiment (GEWEX) activities. The Mackenzie GEWEX Project (MAGS) has brought researchers in atmospheric and land surface process study together under a unifying umbrella to study water and energy processes in the earth / atmosphere system. Figure 6-1 shows the location and major features of the basin.

Figure 6-1 – Mackenzie River Basin (from Cohen, 1997)

Interactions between hydrologists and atmospheric scientists have been of great importance to this project. These close ties have resulted in the reconciliation of the land surface water budget with the atmospheric water budget based on the streamflow record (Strong et al., 2002). Streamflow represents a spatial integration of the land surface climate that links together water and energy processes. Fortunately, streamflow is also widely measured with a high degree of accuracy. The number of Mackenzie basin streamflow stations approaches that of climate stations. However, a problem in the use of the streamflow record for evaluation of atmospheric activity is that the pathways of water and energy through the land surface are complex and highly non-linear.

This chapter sets the stage for a larger modelling effort currently ongoing as part of the Mackenzie GEWEX Study (MAGS). One of the goals of MAGS and its follow-on, MAGS 2, is to provide integrated modelling tools that will link atmospheric, land surface and hydrological models in a unified model. Implementation of this modelling effort is following a staged approach with various groups working on particular linkages. Figure 3-2 illustrates the modelling stages that will culminate in the Level 3 coupled version of the Canadian Regional Climate Model (CRCM) (Caya and Laprise, 1999). Here, the CRCM will provide atmospheric components, the Canadian Land Surface Scheme (CLASS) (Verseghy *et al.*, 1993) will provide the land surface parameterizations and the WATFLOOD hydrological model (Kouwen *et al.*, 1993) will generate and route water excesses to produce streamflow. Currently the linkages at Level 1 - atmospheric to land surface - (CRCM to CLASS) (MacKay *et al.*, 2002) and Level 2 - land surface to hydrologic (CLASS to WATFLOOD) (Soulis *et al.*, 2000) modelling are being finalized.

MAGS activities have generated some 190 journal papers, however, only a handful of these relate to the water and/or energy balances for the basin as a whole. Various other studies having global or hemispheric context have also examined the Mackenzie in a broader focus.

Recently, Betts and Viterbo (2000) examined the water and energy balances from the European Centre for Medium Range Weather Forcasting (ECMWF) model for seven of the Mackenzie River sub-basins for the period 1 September 1996 to 31 August 1998. For this work, a special archive of the ECMWF model was used which spatially aggregates model output on large sub-basins approximated by quadrilaterals at a 1-hour time resolution. This differs from the regular N-80 (1.125^{o} x 1.125^{o}) gridded archive, which has a 6-hour temporal resolution, and allows enhanced examination of the models diurnal cycle over large hydrologic sub-basins. Because the Mackenzie basin is data sparse, the validation data for comparison to ECMWF output consisted of: i) Water Survey of Canada monthly streamflow summaries and ii) Meteorological Service of Canada's (MSC) monthly basin average precipitation from corrected station data (Louis *et al.*, 2002). Results from this study show that runoff from the basin as a whole is in general agreement with the model output (202mm (observed) verses 214mm (model)) for the 1996/97 water year. However, this result was derived from a model precipitation, which is well in excess of measured precipitation (485 mm (observed) verse 654mm (model)). This seemingly contradictory result was explained by a well known high bias in model evaporation over boreal forest areas that compensated for rainfall over-prediction. Although water year volumes were correct, timing of simulated runoff was out of phase with measured streamflow. This was attributed to the lack of a streamflow routing model. There is no mechanism for streamflow routing in the special

ECMWF archive and gauge data are compared with simple summations of gridded runoff contributions.

Kite and Haberlandt (1999) examine the use of atmospheric model archive data to force a hydrological model and expands on two previous papers. Huberlandt and Kite (1998), describe the development of a precipitation dataset, and Kite *et al*. (1994), evaluate the Canadian GCM output over the Mackenzie River basin. This former work was done in parallel with the current study except using the SLURP hydrologic model rather than WATFLOOD. While the watershed area and data sets are similar to those of Kite and Haberlandt (1999), the focus and context of this effort are unique since this effort marks the beginning of a modelling excise that will culminate in a fully linked atmospheric-hydrologic model. For the MAGS project, WATFLOOD has been chosen to be linked with the Canadian Regional Climate Model (CRCM) and the Canadian Land Surface Scheme (CLASS) to fulfill the modelling requirements for MAGS.

In keeping with the modelling strategy, this section will begin by describing WATFLOOD runs (Level 0) and ending with WatCLASS (Level 2) simulations of the basin. The objective here is to show preliminary results from WatCLASS that highlight the importance of the energy balance in watershed modelling that goes beyond the partitioning of incoming energy into latent and sensible heat fluxes.

6.2 WATFLOOD Water Balance Modelling

Mackenzie basin simulations, using WATFLOOD, represents Level 0 modelling activity. Modelling studies at this level are intended to serve as a stage to gather land surface and forcing data sets and provide analysis and quality checking for these data. At this stage, WATFLOOD is forced with various atmospheric datasets to produce basin outflow hydrographs. Acceptable runoff generation with the Level 0 model indicates that the forcing precipitation, temperature and radiation fields are sufficiently close to the truth to be used for Level 2 efforts. Other studies using WATFLOOD such as Carlaw (2000), Cranmer *et al.* (2001), and Bingeman (2001) provide validation evidence of soil moisture, snow water equivalent, base flow generation, streamflow routing, and evaporation processes within WATFLOOD.

6.2.1 Topographic Data

Running WATFLOOD over the Mackenzie requires the establishment of a drainage layer data base. This involves the creation of a river network from topographic information within the watershed, the characterization of land surface properties including vegetation type and internal slope. Much of this preliminary work is attributable to unpublished work of F. Seglenieks. Figure 6-2 shows a representation of the Mackenzie River drainage network used by WATFLOOD and WatCLASS. Each line segment represents a stream reach which routes runoff from the land surface surrounding this grid square. Stream segments widths have been enhanced in this figure to provide a visual depiction of the area drained by each stream segment.

While the process of watershed delineation seems remote in terms of the generation of fluxes for coupling of atmospheric and hydrologic models, it is an essential aspect of using streamflow data sets. Without an accurate portrait of watershed areas and streamflow networks, the comparison of simulated and measured hydrographs would introduce a bias in direct proportion to the delineation error.

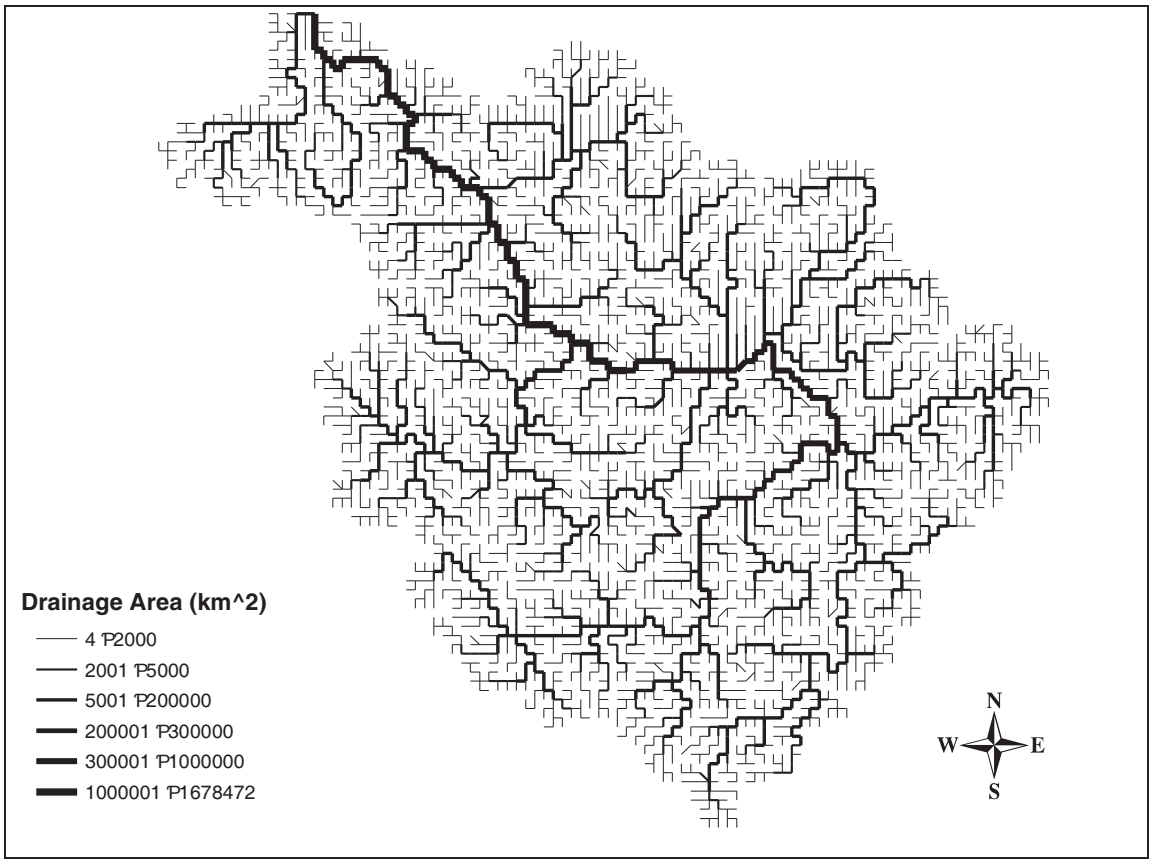

Figure 6-2 – WATFLOOD representation of Mackenzie River drainage basin. Each linear segment represent s a 50 kilometre river reach.

The Mackenzie River basin, because of its large size, required that the past practice of manual extraction of the drainage layer database information be re-examined. Initial estimates indicated that using 1:250,000 scale topographic maps, at a grid resolution of 50 kilometres, would require the handling of over 100 map sheets and the expenditure of three man-years of effort in data extraction. This was the impetus for the preparation of

geographic data through automated methods using digital elevation model (DEM) data. Coincident with the beginning of MAGS activities, a world wide DEM known as GTOPO30 became available. This data set combined a number of pre-existing DEM products into one consistent 30 arc second (1 kilometre nominal) database through a cooperative effort led by the United States Geological Survey's EROS Data Center (http://edcdaac.usgs.gov/, 1996). Although the GTOPO30 product was invaluable to the completion of this project, there are a number of limitations associated with its use that must be understood to properly use the data. These limitations include, but are not limited to, breaks in continuity between different sources of the DEM data, sink holes in the centre of large lakes, and large areas with similar elevation.

From GTOPO30, watershed properties such as drainage divides and flow directions may be obtained for large areas using pre-existing software implementations. A majority of these watershed drainage implementations are based on the work of Jensen and Domingue (1988). Because of the limitations of GTOPO30 noted above, the derived drainage divides and flow directions have resulted in significant watershed area errors. In regions where the derived flow network is incorrect, the DEM can be modified manually to encourage flow in the proper direction. This is an iterative process that requires the derived drainage network to be checked after each DEM modification. Experience has shown that this process may be improved considerably through a process of "burning in" river channels into the DEM and using this modified DEM to derive the flow network.

The “burning in” DEM modification process involves identification of pixels that coincide with existing stream channels. Once identified, a constant amount is subtracted from the elevation of corresponding stream pixels to lower them artificially. This method of DEM

modification differs from the generation of a depressionless DEM, described in section 5-2, since here a DEM is altered rather than created from scratch. This has real consequences for large area hydrologic modelling since the effort required to re-generate a hydrologically correct DEM may be prohibitive. To illustrate the method, Figure 6-3 shows a shaded relief map of the GTOPO30 DEM over southern Ontario with and without drainage imposed by "burning in" and Figure 6-4 shows the result of the automated watershed delineation algorithms before and after the DEM process.

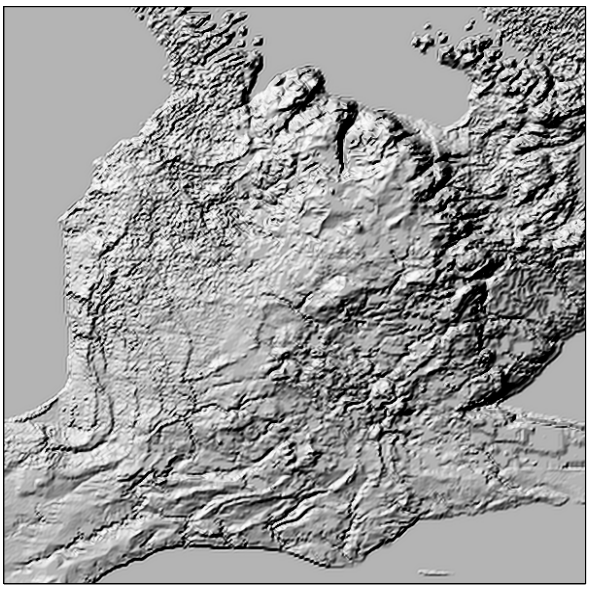

without enforcement

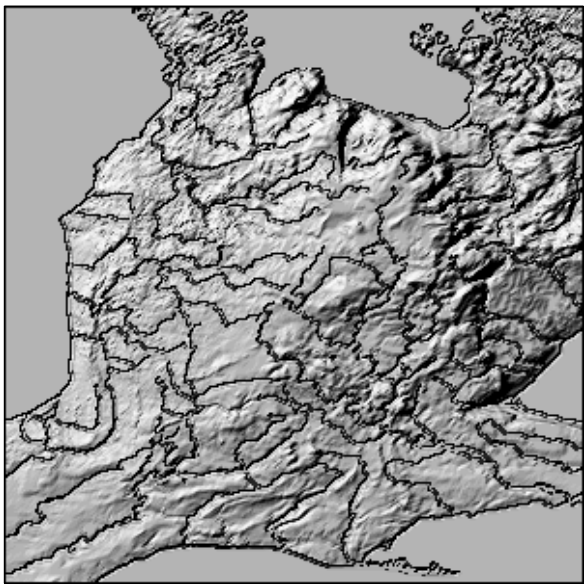

with enforcement

Figure 6-3 – GTOPO30 DEM Southern Ontario with and without drainage enforcement

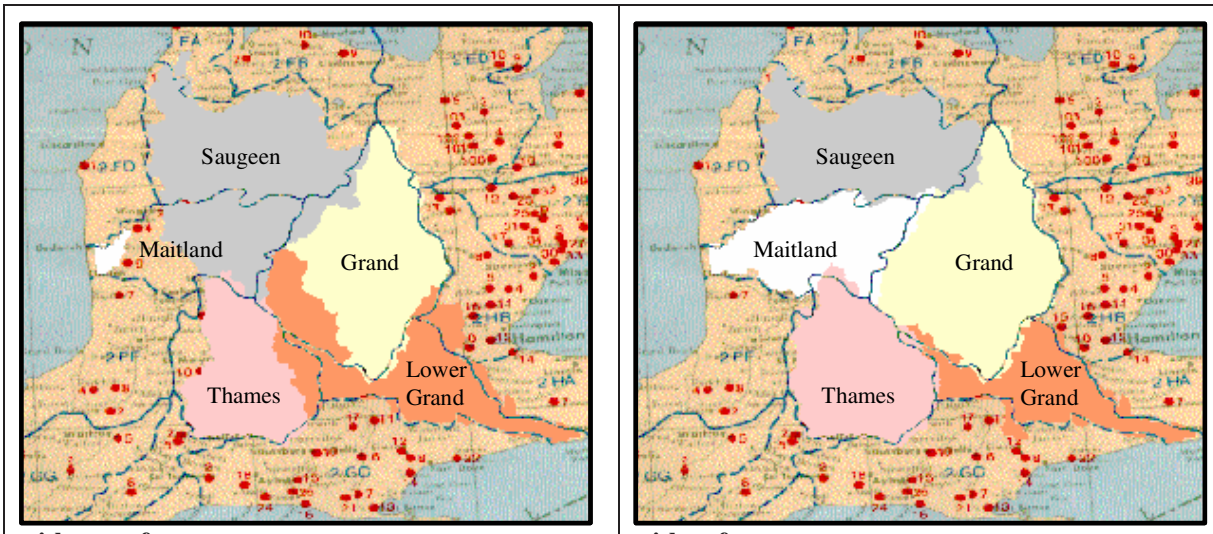

without enforcement **with enforcement**

Figure 6-4–Major Southern Ontario watersheds delineated automatically with and without drainage enforcement

Large changes in predicted watershed areas for the unaltered DEM are the result of small, localized errors in the DEM primarily related to the representation of low relief by large pixels (approximately 1km x 1km). Essentially, the "burning in" process allows the river channel network to define the majority of the watershed area and requires the DEM to interpret only those areas located between river systems. As a final check of the drainage layer database, the drainage areas of published streamflow gauges are compared to the published drainage areas of the gauges. The calculated values which fall within 5% of the published values are deemed to be acceptable.

6.2.2 Land Cover Data

Use of the GRU requires land cover information for flow calculation. This has been true for other WATFLOOD study areas including southern Ontario, and the Columbia River basin in south central British Columbia. Whidden (1999) found that areas composed of primarily boreal forest may be effectively modelled with a single land cover and those additional cover

types, while providing some refinement to the runoff calculation, do not significantly impact on the final hydrograph prediction. Although additional research is required in this area, it does indicate that size of modelling domain and heterogeneity of land cover are important in determining the optimal number of land surface types represented with the GRU.

For large domain simulation, the use of the GRU becomes less important as compared with the distribution the atmospheric forcing data and streamflow routing considerations. Here, calculations for the Mackenzie basin domain (1.68 million square kilometres) will use only one land cover type in order to capture the dominant features of the runoff hydrograph. A significant factor attributed to the success of the use of a single land cover type is the dominance of boreal forest environment (except for southern and northern extents) in the basin. (In this case, the wet forest was dominant. However, it is cautioned that this is not always the case.)

The modelling success in the Mackenzie may also be due to error reduction though the use of an area average parameter set, selected by an optimization process. Within small domains, similar land covers are likely to have distinct and separate land cover responses due to similar soil and topographic surroundings. Larger areas, such as the Mackenzie basin, are more likely to have regions of related land cover that are not hydrologically similar and have very different runoff responses. For example, the runoff response of spruce over sandy soil may be totally different from that of the same spruce over a clay soil. This is in fact the case for the black spruce forests of the north and south study areas of the BOREAS project where the interchange of calibrated WATFLOOD parameters were not readily transferable between the north and south (Whidden, 1999).

Issues related to hydrologic similarity are currently being addressed with WATFLOOD. Recently, based on the unpublished work of Kouwen, McKillop and Stadnyk, some success has been achieved in changing the conceptual view of the GRU. In this new view of hydrologic similarity, all runoff from grouped land covers is forced to enter a wetland classification before being discharged to stream channels for routing. The wetland storage unit is assumed to have a spatial structure which separates the upland areas from the grid square routing element. Moisture which enters these wetlands is controlled by a power law in an analogous fashion to the interflow model presented in Chapter 3 but with a gradient developed by head differences between the stage of stream element and wetland water level. Initial success with this new perception of watershed flow pathways has allowed this spatially structured version of WATFLOOD to achieve good agreement between measured and modelled hydrographs with the same parameter sets for NSA and SSA watersheds.

However, this agreement between NSA and SSA watershed is not achieved without a modelling cost for WATFLOOD. An extra layer of abstraction, which requires an assumption related to the spatial distribution of wetlands, has been added. This is a major departure from the original GRU concept which grouped hydrologic similarity based on a premise which required no assumption regarding the spatial structure of land cover elements. These simple ideas allowed great flexibility with respect to scaling and have been shown to be robust in many situations. Without benefit of the full implementation of the GRU concept, scale dependent assumptions regarding the distribution of wetlands in a basin will have to be made. In its current form, this non-GRU implementation of WATFLOOD effectively places all wetlands in contact with the main routing element within each grid square. This effectively denies the existence of headwater wetlands since they are forced to

occupy the lowest regions in a grid square. Also denied is the existence of first order stream channels which drain upland areas and flow, further downstream, through wetlands. Forcing all grid square runoff through a wetland implicitly removes any sub-grid routing structure since all water in a grid square must be buffered by the near stream wetland. Ivanov (1982), after extensive field studies of Russian mirelands, concluded that wetland moisture sources are primarily from direct precipitation and groundwater inputs with little or no inputs of quick flow moisture sources. WATFLOOD's non-GRU view of wetlands takes an alternate view of wetland moisture sources. Additional field work should be initiated to confirm the assumptions regarding the hydrologic function of wetlands in the natural environment.

An argument in favour of introducing a new wetland structure is the need for an evaporative moisture source during extended dry periods. This could be accomplished alternatively by reducing UZS to LZS transfers to zero and storing moisture within the original GRU based wetland class. This wetland class would have limited runoff generation capabilities as they do in the natural environment and would then make water available for evaporation. Additional moisture from the LZS could be directed upward into the base of the wetland during dry periods which would be consistent with wetland observations (Ivanov, 1982) Whidden (1999) had taken an opposite and clearly flawed approach in moving excess moisture into LZS that produced upward trends in total basin storage. Changing the structure of WATFLOOD based on these past simulations represents a major shift in modelling philosophy and the use of the new wetland option should be considered in the light of implications cited above.

6.2.3 Forcing Data Sets

WATFLOOD requires gridded surface meteorological data to drive its hydrologic calculations. Data for this purpose have traditionally been derived from a spatial interpolation of measured station data and measured weather radar, however, more recently GCM and NWP archive data have been used as well. This relatively new source of meteorological data has positive implications for both the hydrologist and the atmospheric modeller. For the atmospheric modeller, climate simulation and/or weather forecasts are evaluated against streamflow data using a hydrologic model. In these cases, the watershed acts effectively as a "large rain gauge"; although the caveats and uncertainties of hydrologic modelling must be considered. For the hydrologic modeller, a new source of data becomes available from the atmospheric archive to drive his model. This offers the opportunity to model remote watersheds for which no gauge based atmospheric data are available and to add spatial structure to atmospheric forcing data that are lost through the normal interpolation of gauge data. For this study, archives from both Canadian GCM and NWP are used together with measured station data.

GCM Data

The Global Circulation Model (GCM) data were obtained from the Canadian Centre for Climate Modelling and Analysis (CCCma) archive. Their second-generation climate model GCMII (McFarlane *et al.*, 1992) was run for a 10-year period under both 1xCO2 and 2xCO2 conditions. These simulations do not represent observed weather from specific years and as such are compared against average observed conditions. Output from this 10-year run was archived at 12 hourly time intervals on a 96x48 Gaussian grid (approximately 3.75 lat x 3.75

long). These data are available from CCCma web site (http://www.cccma.bc.ec.gc.ca/) in a monthly summary format.

For WATFLOOD runs, surface values of precipitation, temperature and net radiation where extracted from the GCM data over the Mackenzie for the $1xCO_2$ condition. This extracted data was then interpolated to a 95x90 grid (12.5' lat x 25' long) using a spline smoothing algorithm available within the commercial software package SURFER by Golden Software. Re-gridding to this fine resolution was not intended to enhance the spatial information content of the GCM data but only to match the WATFLOOD grid that was chosen for the study. The forcing fields generated from spline interpolation did not preserve the original data but rather created a new surface from which the final gridded data were generated. The interpolation process resulted in data that had larger minimum and maximum values but maintained the same trends.

Use of the GCM data in this study is limited. This is due primarily to the well-documented bias in precipitation that are associated with this data set (Kite *et al*., 1994, Arora *et al*., 2001). It is useful, however, that these results be included for qualitative comparison to show the sensitivity of the model to the forcing data set.

NWP Data

Numerical Weather Prediction (NWP) data were obtained primarily from the Canadian Meteorological Centre (CMC). Model outputs from CMC are used as the primary weather forecasting tool in Canada. For this study, data were obtained from two generations of forecast models operated by CMC i) the Regional Finite Element (RFE) model (Mailhot *et al*., 1997) and ii) the Global Environmental Multiscale (GEM) model (Côté *et al*., 1998a&b).

In addition to changes in the operational model, a new archiving system was also introduced to assist GEWEX researchers in obtaining required model outputs (Ritchie *et al*., 1999). Major changes to the model and the archive are summarized in Table 6-1. These changes reflect the continual updating and advancements of the modelling system. In addition to forecast fields, these models also produce and archive analyzed data used for model initialization and high temporal resolution time series data over selected points within CMC's GEWEX model output archive.

Table 6-1 – Significant Operational Changes for CMC Forecast Archives

Date	Change	Archive	Model
Nov 3, 1993	Increase resolution 50km / 25 level	Conventional	RFE
Oct 1, 1995	GEWEX data archive started	GEWEX	RFE
Dec 21, 1995	Increase resolution 35 km / 28 level	GEWEX	RFE
Apr 1, 1996	Increase archive content (incl. radiation)	GEWEX	RFE
Feb 24, 1997	Start GEM model (35 km / 28 level)	GEWEX	GEM
Sept 25, 1998	Increase resolution 24 km / 28 level	GEWEX	GEM

Model output from the gridded forecast archive was used as the forcing data set for WATFLOOD. As with the GCM model precipitation, temperature and net radiation where extracted from the archive. In contrast to GCM output, however, NWP model output represents particular dates and times and as such can be compared directly with measured data. Forecasts generation from NWP models involve a series of steps including the generation of initial conditions from measured data, running of a global atmospheric model, and, nested within the global model, downscaled runs used to generate regional forecasts.

Fine resolution forecasts are initialized twice daily at 00Z and 12Z and run continuously for a 24-hour period with output archived at 3 to 6-hour intervals. To minimize potential problems with spin-up of model precipitation, only data from the 00Z forecast were used.

The model archive is based only on operational runs and, as such, there are both missing time data and missing forcing fields within the 1993-1998 period of interest. This is in contrast to other atmospheric modelling agencies, such as the ECMWF, which offer reanalysis data. Reanalysis products combine previously measured data with updated measurements and rerun forecasts with the latest version of the atmospheric model to provide a complete and consistent set of atmospheric model output. On April 1, 1996, CMC operation archives were greatly expanded to include many new surface data fields and increases in their temporal resolution. Prior to this date, no surface radiation fields where archived. As a result, net radiation inputs for this study were missing. To overcome this deficiency, fields required to calculate net radiation were extracted from the National Centers for Environmental Prediction (NCEP) Medium Range Forecast (MRF) Global Flux data set (NCAR Dataset No.: ds084.5). This data set contains a variety of surface flux predictions on a 384x190 Gaussian grid at 6-hour intervals.

Calculation of net radiation, required in WATFLOOD's Priestly-Taylor evaporation routines, requires downwelling and upward components of both long and shortwave radiation. Surface downwelling radiation was extracted directly from the archive while upward components of the radiation were calculated indirectly from archived values of surface skin temperature and albedo as follows.

$$R_{net} = (K \downarrow - K \uparrow) + (L \downarrow - L \uparrow)$$

Equation 6-1

$$R_{net} = (K \downarrow (1 - \zeta)) + (L \downarrow - \kappa\omega T_s^4)$$

where T_S is skin temperature in Kelvin, κ is emissivity (assumed to be unity), ω is Stefan-Bolzmann constant, and the albedo, ζ is the surface shortwave reflectivity.

Missing forcing data amounted to 13 days for the 4-year simulations period. The strategy used to fill in these missing data included a hierarchical procedure. First, when missing data were encountered the 12Z forecast was used, then an average of the missing hours from bounding days where used, and for periods longer than one missing day (5-day maximum) fields from the next year of the same day where used. The last filling procedure was required to create a 3-hour dataset from 6-hour fields; this was accomplished by simple arithmetic averaging of the bounding 6-hour records.

The final NWP product was a complete 3-hour record of precipitation, temperature, and net radiation for the period January 1, 1994 to December 31, 1998 composed of a merging of REF, GEM, and NCEP forecast data. These data were then re-projected to a 95x90 grid (12.5' lat x 25' long) using the GRADS software package (http://grads.iges.org/).

Figure 6-5 shows a portion of the RFE archive with a precipitation event moving from west to east across the basin on September 22, 1994.

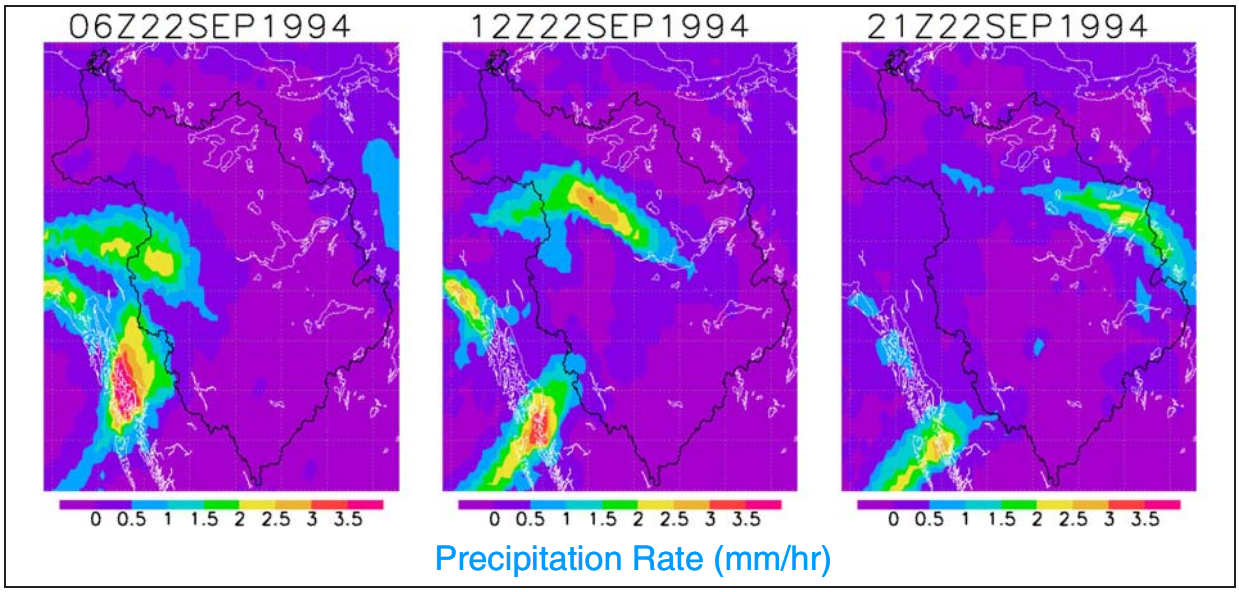

Figure 6-5 – Precipitation event over the Mackenzie River basin

Archive data at 3hr time intervals are used directly in the model and repeated for each hourly time step of the model. This results in some data loss and concentrations of precipitation due to skipping of areas. This is apparent in Figure 6-5. This is a source of modelling error especially for fast moving systems which could be corrected by a shifting and blending routine.

Measured Precipitation Data

In addition to model output data, a new source of data based on measured precipitation has also been utilized. This gridded data set represents measured precipitation from Meteorological Service of Canada (MSC) gauge sites interpolated to a 50 kilometre grid over the Mackenzie basin (Louie *et al.*, 2002). The raw daily precipitation gauge records were first corrected for under-catch using the method described by Mekis and Hogg (1999). This correction procedure includes adjustments for systematic errors due to wind, evaporation, trace observations of liquid precipitation and a density adjustment for ruler measured snow data. This corrected daily precipitation is then accumulated to obtain monthly totals.

Interpolation of the monthly gauge accumulations for a spatial coverage is accomplished by first producing station anomalies based on MSC derived climate normals. These station anomalies are then geo-statistically distributed to produce monthly spatial anomaly maps which when re-combined with normals data, produces monthly precipitation maps based only on measured data.

Monthly precipitation data are not suitable for direct input to WATFLOOD. Low temporal resolution data results in misrepresentation of rainfall partitioning into canopy interception, infiltration, depression storage and runoff which are rate dependent. To preserve both the spatial patterns from the volumetrically corrected precipitation and the temporal character of the NWP base GEWEX data archive, the two data sets were combined. This was accomplished by producing a monthly spatial multiplier to convert NWP precipitation volumes to monthly measured totals. Corrections generated were applied to the NWP precipitation which has been termed "gauge corrected NWP precipitation".

6.2.4 Level 0 Results

Each of the three forcing data sets was run with WATFLOOD to conduct Level 0 testing. The goal here was to i) provide test data to evaluate model integrity and the drainage layer database and ii) to make qualitative assessments of the forcing data in preparation for Level 2 modelling. A summary of these results and the time history of years in which they were produced are presented in Figure 6-6.

The topmost portion of Figure 6-6 shows the measured and simulated hydrograph from GCM data forcing, discussed in Section 6.2.4. Here high rainfall amounts, a well known bias for

the CCC-GCM, produces far too much runoff when compared to the 10 year average measured runoff amounts. Next, the raw NWP data produce much more reasonable simulation. However, the 1994/95 water year (1 Oct to 30 Oct) shows a much higher runoff amount when compared to the other model years. This 1994/95 water year was one of much lower than average rainfall amount and this anomaly was not captured by the NWP model during that year. When the distribution of the NWP model output is scaled to match that of the corrected monthly rainfall patterns presented in Louie *et al*. (2002), the measured and model simulations match one another much better.

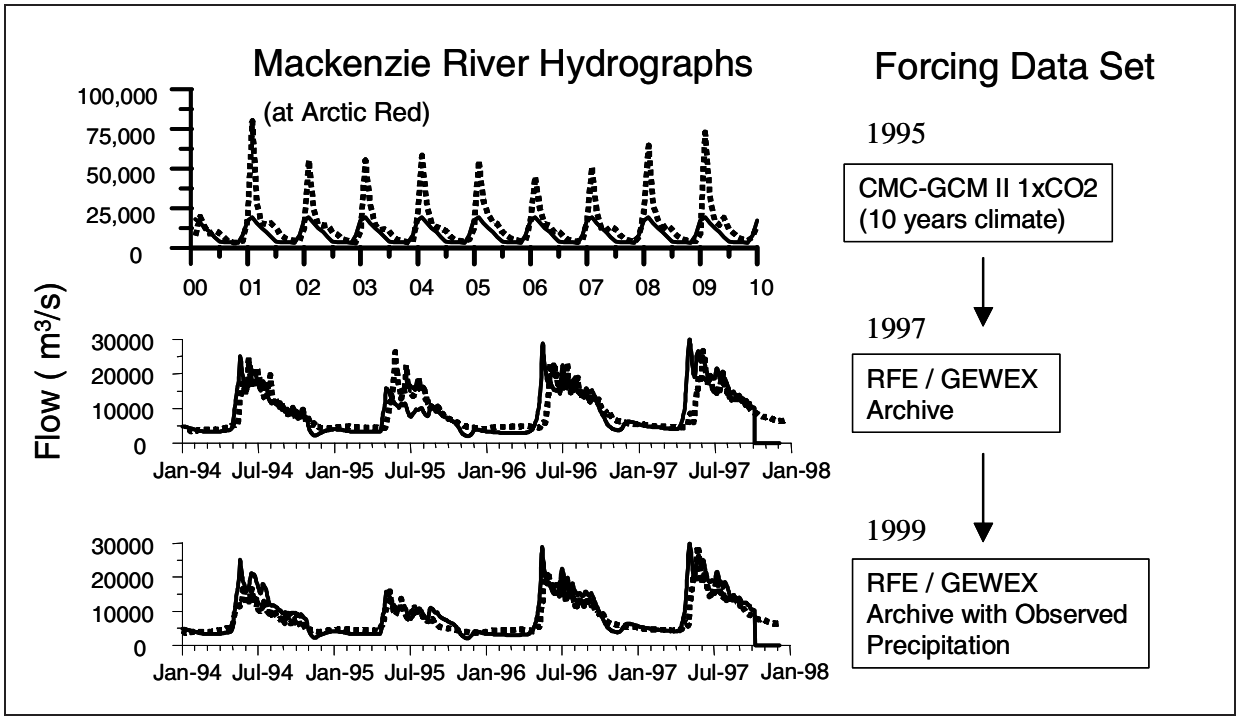

Figure 6-6 – Progress with Mackenzie River Level 0 runs. Dashed line indicates simulated data and solid line the measured streamflow

These results show the benefit of vetting competing data sets with the WATFLOOD model. Such efforts using the WatCLASS model in Level 2 runs would be very time consuming and be much more complex to decipher the root cause of difficulty.

6.2.5 Hydrologic Storage

An added benefit of the Level 0 modelling that has emerged from this study is the generation of hydrologic storage for evaluation of atmospheric water budget studies in MAGS.

Atmospheric water budget studies (Strong *et al*., 2002; Walsh *et al*., 1994), attempt to calculate the precipitation (P) [L] less the evaporation (E) [L] based on the net advection of atmospheric moisture through a closed atmospheric volume. From an atmospheric perspective this is expressed as:

$$P - E = \frac{\partial W}{\partial t} + \nabla \cdot Q \qquad \text{Equation 6-2}$$

where $\nabla \cdot$ is the horizontal divergence operator and Q [L] is the vertically integrated flux of specific humidity derived from wind and humidity measurements and W [L] is the water content in an atmospheric column. From a land surface perspective the term P-E can be expressed in a similar fashion as:

$$-(P - E) = \frac{\partial S}{\partial t} + \nabla \cdot F \qquad \text{Equation 6-3}$$

where S [L] is the water content of land surface column, and F [L] represents the lateral transport of water. If we consider a watershed as a closed system, that is, no watershed boundary leakage, then the only lateral flow across the boundary of the watershed is streamflow. This provides an effective means of evaluating the calculation of atmospheric P-E. However, the direct use of measured streamflow complicates the land surface moisture storage term, S, which has a much larger dynamic range than its atmospheric counterpart, W. Measurement of streamflow at a gauging station is a relatively simple matter when compared

to the derivation of moisture fluxes across the entire atmospheric boundary defined by the watershed area.

Hydrologists often deal with measured quantities of the water budget in terms of their time variant quantities; therefore we can express Equation 6-3 in hydrologic [L/T] units as:

$$P - E = \Delta S + R \qquad \text{Equation 6-4}$$

where ÷S is the change in water content over a given time interval, R [L/T] is runoff and P-E is as before except in hydrologic units [L/T]. To evaluate the effectiveness of atmospheric P-E calculations, runoff (R) is often used as a comparison (Walsh *et al.*, 1994). The degree of success for this comparison is often measured against a simplified continuity relation P-E = R. Using this simplified form of Equation 6-4, however, has significant limitations over large spatial domains and short time intervals. First, for time periods shorter than a decade the generalized form of the continuity Equation 6-4 must be exploited (Dingman, 2002, p.12). Components of ÷S, listed in relation to their typical time scale, include groundwater storage (> 1yr), snowpack storage (> 1mth), unsaturated soil moisture (> 1day), depression storage (< 1 day), and canopy storage (< 1 day). Depending on the time scale of interest to the study, these terms can have significant implications on results. For instance, snow cover prior to the onset of melt may comprise more than 50% of the annual precipitation. Use of the simplified continuity expression in a monthly water balance study without including snow storage would result in significant underestimation of the RHS of Equation 6-4. Secondly, the runoff term, R must be in time and space agreement with atmospheric moisture budgets scales to allow the direct use of measured streamflow. This requirement is imposed due the significant time delay between the generation of local runoff and the detection of this

signal at a downstream gauge location. In the case of the Mackenzie River basin, there may be as much as a four to six week travel time from the influence of a precipitation event at the head waters of the basin until the detection of this event at the basin's Beaufort Sea outlet.

The effects of time dependent land surface storage change and time lags due to streamflow routing can lead to serious misrepresentations of the R+÷S term in Equation 6-4. Properly accounting for these terms over the spatial domain and the accumulation of these quantities for a given time period is defined here as “estimating hydrologic storage”. In a physical sense, hydrologic storage represents the combined quantities of channel storage (unrouted streamflow) and stored land surface water within a discrete area that have accumulated over a give time period. From an atmospheric budget perspective, it represents an alternate, hydrologic view of P-E. The use of hydrologic storage for atmospheric moisture balance studies means that the complexities of land surface hydrology need not be considered by the atmospheric scientist since the observed streamflow at the basin outlet has been deconvolved into a map of storage and runoff for a given time period. For this study, the quantity hydrologic storage is determined on a monthly basis for the Mackenzie basin as a whole and each of its major sub-basins. This fulfills one of the MAGS objectives of closure of the water budget on monthly time steps.

The separation of the hydrologic system into a land surface component and a channel routing component illustrates further the difficulty of assessing the temporal gradient of the hydrologic system. Equation 6-3 can be further broken down to:

$$4\,(P\,4\,E) \mid \frac{\in S_{land}}{\in t}\,2\,R_{local}$$

where : Equation 6-5

$$R_{local} \mid \frac{\in S_{channel}}{\in t}\,2\,Q_{ba\sin}$$

where R_{local} represents runoff from the land surface tiles to the stream channels and the subscripts 'land' and 'channel' represent the storage components of land surface and the river routing network, respectively. Because there are limited spatial measurements of the land and channel storage components available, the hydrologic model WATFLOOD (Kouwen *et al.*, 1993) is employed to make assessments of these quantities.

The use of WATFLOOD in determining the storage components S_{land} and $S_{channel}$ represents a shift in emphasis for hydrologic modelling studies. Rather than the generation of stream hydrographs and the comparison of these to measured values, the objective here is the more demanding task of deconvolving a measured hydrograph into its elemental components in a physically realistic manner. This deconvolution process involves more than the breakdown of streamflow into fast and slow components at a gauge location. Rather it is a mapping of land surface processes at suitable temporal and spatial resolutions. Traditional techniques, including the tracking of precipitation inputs though various reservoirs and the simulation of evaporative and runoff losses from these reservoirs, are used. However, this is done in a fashion which attempts to constrain the solution to the measured streamflow for a given atmospheric forcing data set; in effect the inverse problem.

Use of WATFLOOD, in this way, allows Equation 6-5 to be combined in the following form:

$$P - E(L1, K1, T, S_{land}) = \frac{\partial S_{land}}{\partial t} + \frac{\partial S_{channel}}{\partial t} + Q_{basin}(S_{channel}) \qquad \text{Equation 6-6}$$

where E is derived evaporation as a function of K*, net short wave radiation, L*, net longwave radiation, T temperature, and S_{land}, and the simulated basin streamflow, Q_{basin} is determined as a function of the $S_{channel}$. Measured variables in Equation 6-6 include P, K*, L*, and T. Basin runoff, Q_{basin} is simulated by varying parameters which control $\partial S_{land}/\partial t$ (e.g. soil hydraulic conductivity) and $\partial S_{channel}/\partial t$ (e.g. Manning's roughness), as represented by WATFLOOD, within a multivariate optimization framework with the objective function set to:

$$MINIMIZE\left(\sqrt{\left|Q_{basin}(t)_{measured} - Q_{basin}(t)_{simulated}\right|}\right) \qquad \text{Equation 6-7}$$

In addition to constraints of the measured inputs P, K*, L*, and T over the four year period, the system is further constrained by features of the drainage basin including topography, the stream channel network, and model physics.

The result of this analysis is a set of monthly values of S_{land} and $S_{channel}$ which are mapped onto the basin from the 50 kilometre grid simulation area. These high resolution components are then accumulated to monthly basin totals and combined with measured streamflow to provide an independent hydrologic assessment of P-E suitable for comparison with its atmospheric counterpart. Figure 6-7 gives the results of hydrologic P-E simulations for the 1994 and 1995 water year.

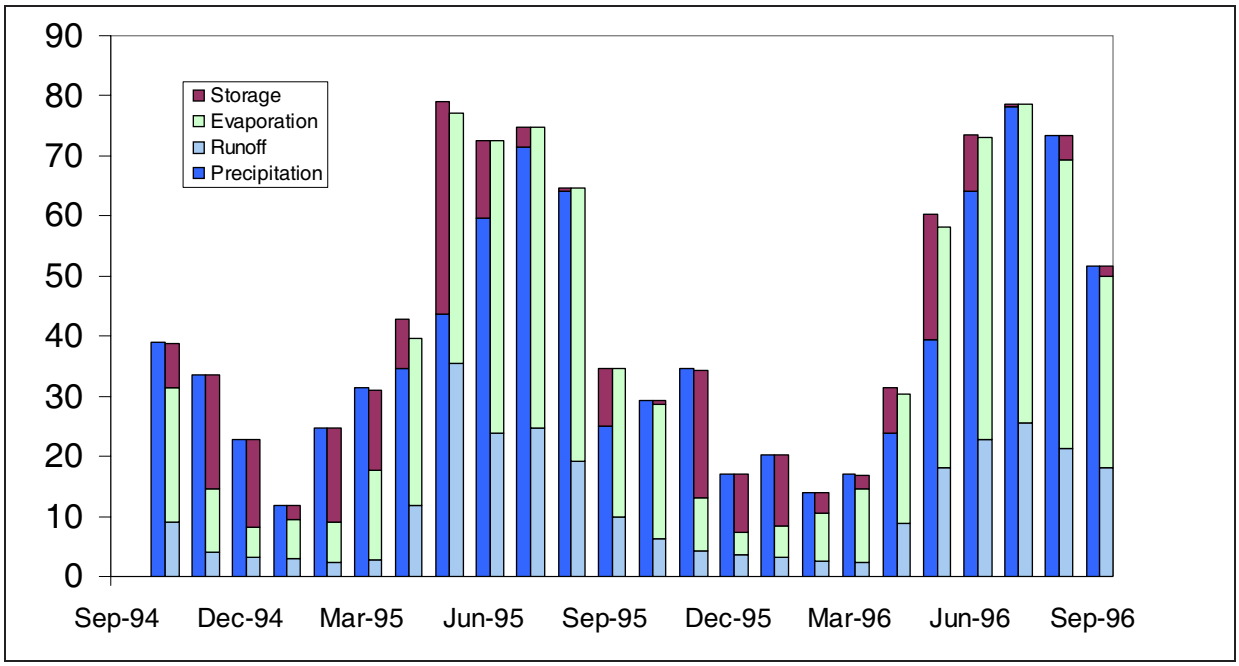

Figure 6-7 – Mackenzie River water balance for Level 0 modelling.

In Figure 6-7 negative basin storage changes are shown above precipitation and represent moisture leaving surface storage. This occurs primarily during the spring and summer when snowpack and groundwater stores are discharging. Positive values of ÷(storage) are shown above runoff and evaporation to indicate that basin storage is increasing. Net increases in basin storage occur primarily in the winter while snow packs accumulate in the model.

Strong *et al*. (2002) used the values of ÷storage from this plot to give a much more favourable validation of atmospherically derived P-E than that obtained from their simple interpretation using P-E=R.

6.3 Level 2 Modelling

WatCLASS modelling of the Mackenzie basin was undertaken to begin the process of parameter development required for Level 3 runs in which the CRCM, CLASS, and WATFLOOD would be coupled into a single model. Final parameter selection has yet to be completed, however, interesting preliminary investigations have yielded insights into the model processes and areas requiring further development in preparation for Level 3 runs.

As a consequence of Level 0 modelling of the Mackenzie basin, much of the data requirements necessary to run WatCLASS have been put in place. These include a majority of the parameters including those required to regulate i) surface runoff, ii) base flow, and iii) streamflow routing. Without prior calibration runs with WATFLOOD, which took weeks of optimization runs, it would be prohibitively time consuming to generate all these parameters separately using WatCLASS.

In addition, output from NWP models was required to provide the necessary forcing data for Level 2 runs. The additional data fields required for WatCLASS include: i) humidity, ii) wind speed, and iii) atmospheric pressure. Each of these was added to the data set discussed in Section 6.2.3 – NWP Data.

Rather than revisit water balance based calculations that were performed using WATFLOOD in Section 6.2, the focus here will be on energy balance calculations. These are beyond the capabilities of WATFLOOD. Hydrologic models are often criticized as having so many degrees of freedom that any set of inputs could be subsequently reshaped to produce the final measured hydrograph. In some respects the basis of these statement are true since, for example, temperature based snowmelt routines are not constrained by available energy and

may melt equal amounts of snow for a given temperature without consideration of wind or radiation. Certainly long periods of continuous simulation reduce the likelihood of obtaining an alternate set of parameters that might perform equally well. However, if new model constraints are added, such as full energy balance modelling and validation with additional measures of land surface data, more certainty in modelling formulations and their parameters will be gained.

Unfortunately, there are very few spatial data sets that exist to provide necessary measured evidence for validation of water and energy processes within land surface models. However, there are number of remote sensing tools being developed including evaporation based on radiative surface temperature and soil moisture based on the dielectric properties of water in soil. One method that has shown some promise is the remote sensing of snow water equivalent (SWE). This technique is based on greater absorption of microwave radiation with increasing depths of snow. Another spatial data set, that has yet to be utilized in a hydrologic study, is the extent of permafrost coverage in a landscape. Permafrost extent is related to the land surface climate, land cover and soil type of a region and the ability to reproduce this measured data set may provide some insight into the performance of the model energy processes. The following sections use remotely sensed SWE, permafrost extent and streamflow data to assess the initial performance of the WatCLASS model for the Mackenzie River basin.

6.3.1 WatCLASS Runs

Level 2 runs for the Mackenzie River basin use the same single land cover representation of the basin used for WATFLOOD as well as drainage layer data base and atmospheric forcing data sets. Parameters used to control this run are identical to the black spruce parameter set used for the BOREAS data. Early portions of the data set up until April 1, 1996 where based on a combination of NCEP and GEM data sets. Mismatches in data from these two models could conceivably result in high values of incoming longwave radiation when air temperature from the other are cool or high values of incoming solar raditation when there are clouds and rain. This, together with a known high bias in NCEP short wave radiation, favoured starting Level 2 simulation on October 1, 1996. As well, large correction factors were required for much of the NWP precipitation prior to the start of the GEWEX archive. From this point, a single source of atmospheric driver data is available.

Initialization and Permafrost Simulation

Initialization of the Level 2 model is of critical importance. The lowest layer of the CLASS soil is 2.75m thick and this represents a large heat and moisture sink that if initialized incorrectly could lead to invalid runs while the model attempts to establish some equilibrium. A model spin-up period was used to prepare these long memory components of the model. Selection of the initial temperature and moisture regimes to begin the spin up are necessary, however, of great significant importance is the selection of third layer ice content which takes a very long period of time to establish. It was decided to saturate the pore space of the soil column with ice in areas where the mean annual air temperature was less than 0^{o}C and to initialize the soil moisture at a field capacity (tension value -340 cm of water) elsewhere.

The model was run for three consecutive years of the 1996 data set and an assessment of this model run was made.

A permafrost map of Canada was compared with the ice content of the WatCLASS third soil layer. This was accomplished by comparing the five classes of permafrost in the measured database with the ice content of the third soil layer of CLASS. When ice and water exist simultaneously in any of the CLASS soil layers, the temperature of the layer remains fixed at $0^{o}C$ and net energy inputs result in either ground ice formation or melt. This amount is calculated based on the latent heat of fusion of water. Unfortunately, there is no direct conversion of CLASS ice content with either of the permafrost classes used in the measured data set (e.g. sporadic, continuous or none). Instead, ice content was binned into five groups to compare the relative spatial extent of measured and modelled permafrost. A technique known as 'natural breaks' (or Jenks method) was used to determine appropriate bin ranges (Slocum, 1999). This technique selects bin end points such that the sum of the variance calculated from within each bin group is minimized. This is reported to be the "best choice" for grouping together similar values (Slocum, 1999). Following the three year spin up, the ice content in the third layer was binned into five groups using the natural breaks method and plotted in Figure 6-8. This figure also gives the bin ranges of ice content that correspond to the groupings.

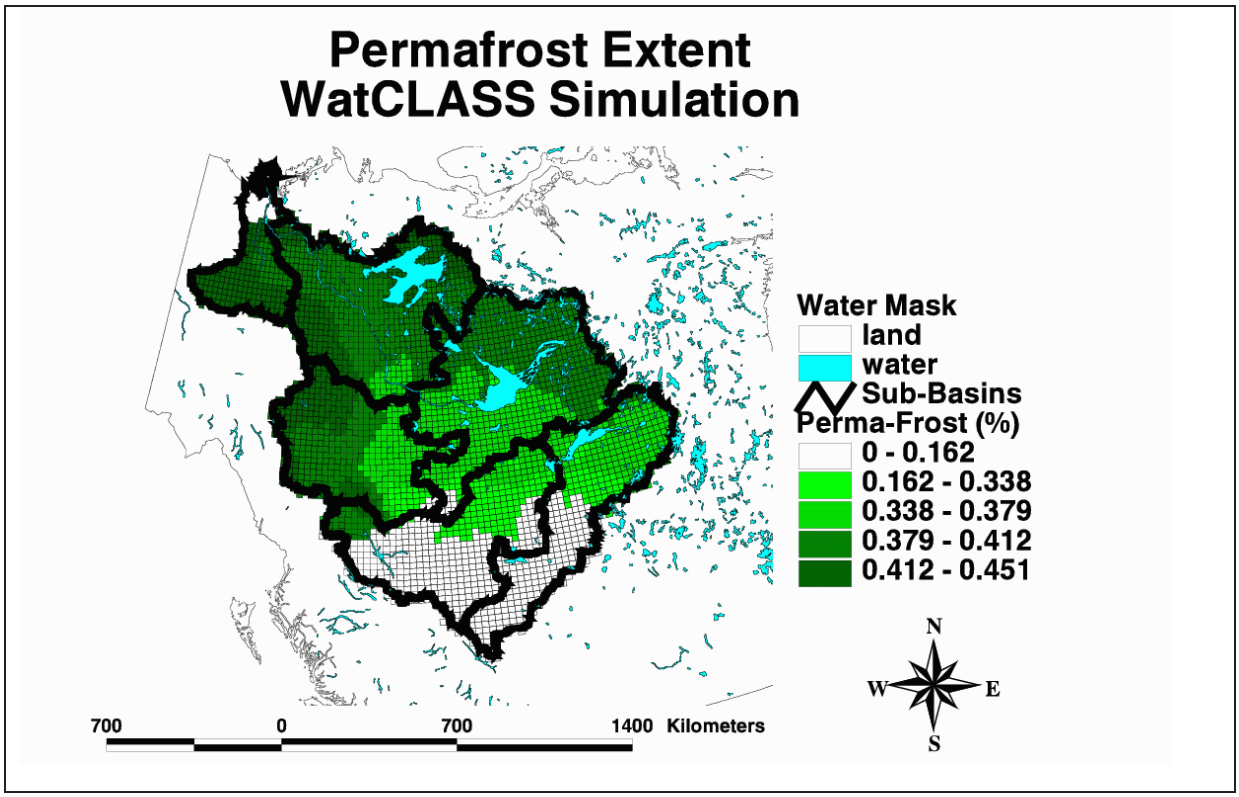

Figure 6-8 – WatCLASS derived permafrost classification

Figure 6-9 compares the spatial pattern of permafrost from the measured data, discussed previous, and the model derived from the binning technique. The similarities present are noteworthy considering that third layer ice content was initialized at 45% of the soil volume. This graphic represents an interesting coincidence for the present study and confirms that the model spin-up has moved the lowest layer ice content in the correct direction. However, it may also represent an important innovation for the assessment of environmental change under changed climate conditions. Climate change assessment and their impacts represent an area of considerable interest both for scientists and the general public. Models with the ability to assess the impact of ground ice will make a significant contribution to those who assess and plan adaptations for climate impacts.

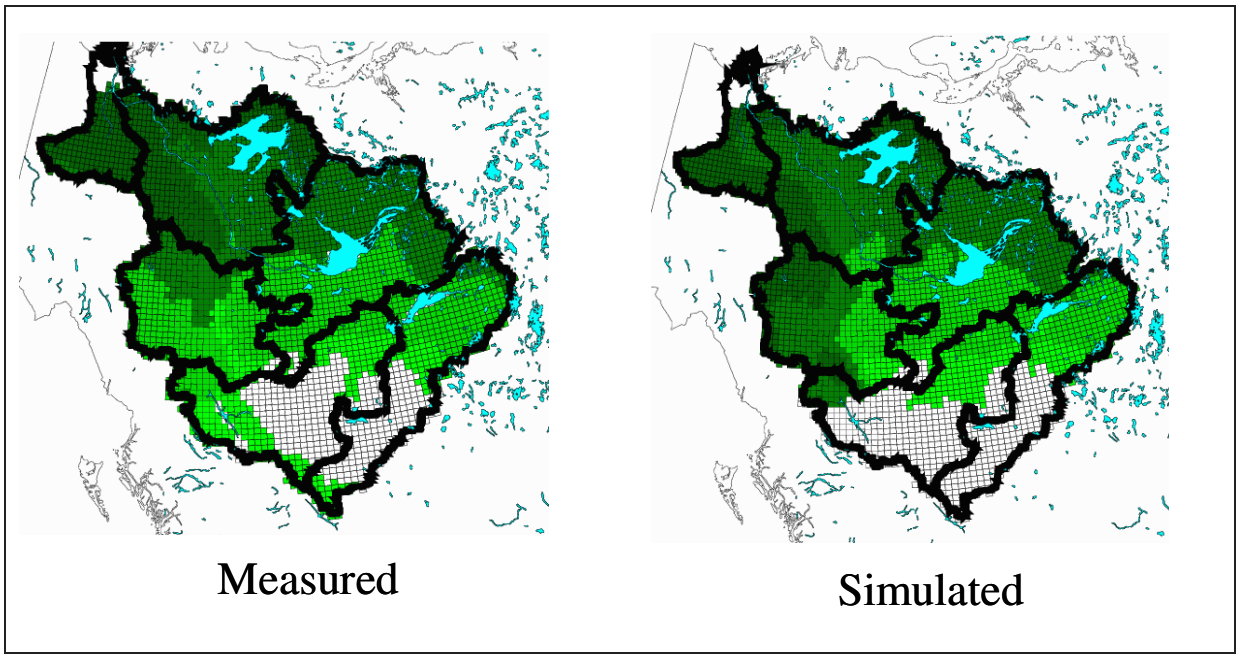

Figure 6-9 – Comparison of measured and modelled permafrost distribution.

The permafrost comparison shown in Figure 6-9 has a number of caveats which require further research to validate these findings including:

1. Extension to a greater number of land classes with more representative canopy properties such as species dependent radiation extinction coefficients. This will provide improved radiation budgets for the soil/land interface.

2. Rationalization of the meaning of ice content determined from WatCLASS with the spatially occurring definitions associated with the measured data set.

3. The impact of the frozen soil on runoff generation.

While some efforts are required before a quantitative model of permafrost distribution is available, plots such as those shown in Figure 6-9 are only available from a Level 2 model with full energy balance simulations. This shows the utility of such models for future work.

Runoff Modelling

The effect of frozen soil on moisture infiltration at point scales has been studied (Stahli *et al.*, 1996; Zhao and Gray, 1999), however, at large spatial scales the effect of frozen ground on runoff and streamflow generation has not been studied in depth. Literature on the topic is inconclusive. In fact, Shanley and Chalmers (1999) found that they could not prove the hypothesis that frozen ground increases runoff from snowmelt and rainfall inputs using 15 years of measured data in Vermont. This is contrary to the basic consensus that has emerged within land-surface process models (SVAT) community. Many SVAT models assume that ice within the soil column impedes infiltration and subsequent drainage of moisture. Implications of this practice manifest itself as enhanced generation of surface runoff and other quick runoff processes and the suppression of longer duration base flow processes.

To explicitly model permafrost and its influence on the generation of streamflow, requires highly coupled energy and water budget models. The occurrence of permafrost and frozen ground are functions of microclimate, albedo, vegetation type, snowpack condition, topography (elevation and aspect), drainage, and geothermal properties. The interactions among these factors are complex and the modification of any may lead to changes in others (Heginbottom *et al*., 1995). Perhaps most transient is the effect of snowcover, which limits the occurrence of permafrost because of its thermal properties. Add to this the changes to hydraulic conductivity and storage due the occurrence of frozen soil and the web of interactions becomes more complex for regional streamflow generation.

Pitman *et al*., (1999) have advocated suspending the influence of frozen soil for the modelling of streamflow generation in land surface models. Their paper suggests that regional effects of frozen ground are not captured well by current models and that the scaling

of point process studies to regional settings may not be appropriate. Evidence of this conclusion is offered by way of hydrograph comparisons between a number land surface process models with and without explicit influence of ice on soil hydraulic properties. In models without suppression of conductivity with frozen ground, superior runoff characteristics are observed. Most prevalent was the timing of the annual hydrograph in those models using frozen ground hydrology. For these models, larger than observed runoff amounts where simulated during spring and lower amounts generated for the remainder of the year. This characteristic indicates that spring melt of snow packs are not being stored and released over a large portion of the year but rather forced to runoff due to the suppression of infiltration and drainage resulting from frozen ground effects.

Although there is evidence to suggest that modelling of frozen ground may have negative implications for water balance calculations, the same is not true for the energy balance. A number of studies (Verseghy, 1996; Viterbo *et al*., 1999) have indicated favourable impacts on the energy balance in land surface models due to temperature buffering of the air-land surface interface. This buffering results from the change in available energy during the freezing and thawing of ice that keep soil temperatures at or near the freezing point when both ice and water phases are present in the soil matrix.

Simulation of streamflow from WatCLASS has shown mixed results for the Mackenzie River basin. In the northern portions of the basin, where continuous permafrost dominates, runoff timing and amounts were favourable. However, in the southern parts of the basin, where no or sporadic amounts of permafrost are present poorer results, similar to those described by Pitman *et al*. (1999) where observed.

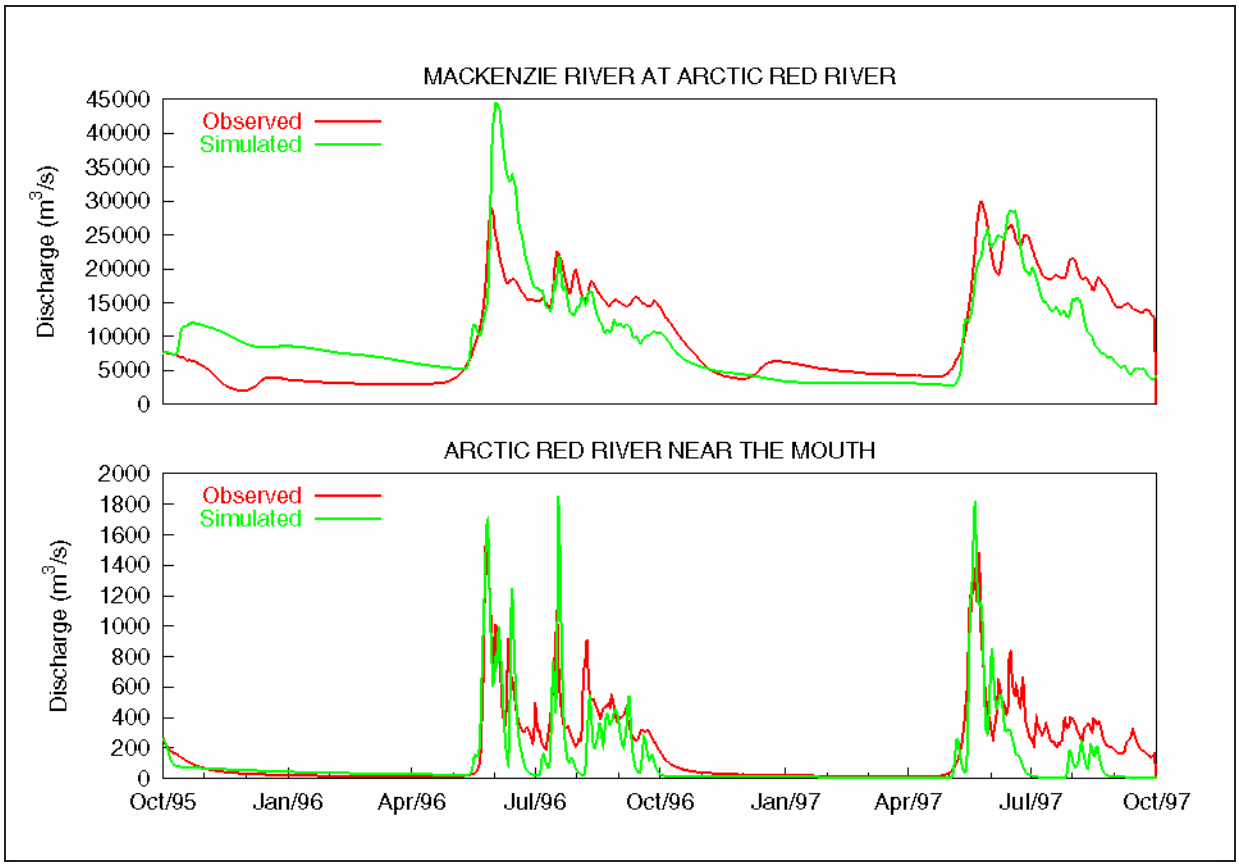

Figure 6-10 – Mackenzie River Level 2 Hydrographs

The hydrograph of the Mackenzie River at Arctic Red River shows the cumulative impact of the model runoff from the entire 1.68 million km^2 basin including those areas where frozen soils dominate runoff and those which do not. This figure also presents the results from the hydrograph that is best represented within the basin, the Arctic Red River. This much smaller watershed (18,600 km^2) is also the most northern in the basin and drains an area that is dominated by continuous permafrost. In 1996, individual rainfall and snowmelt events are captured well by the hydrographs since much of the moisture flow through the CLASS soil layers is heavily restricted by the high ice contents in the third layer. The system, in fact acts as a bucket which, when full, overflows. However, in 1997 there appears to be an overall lack of moisture to sustain summer base flow amounts.

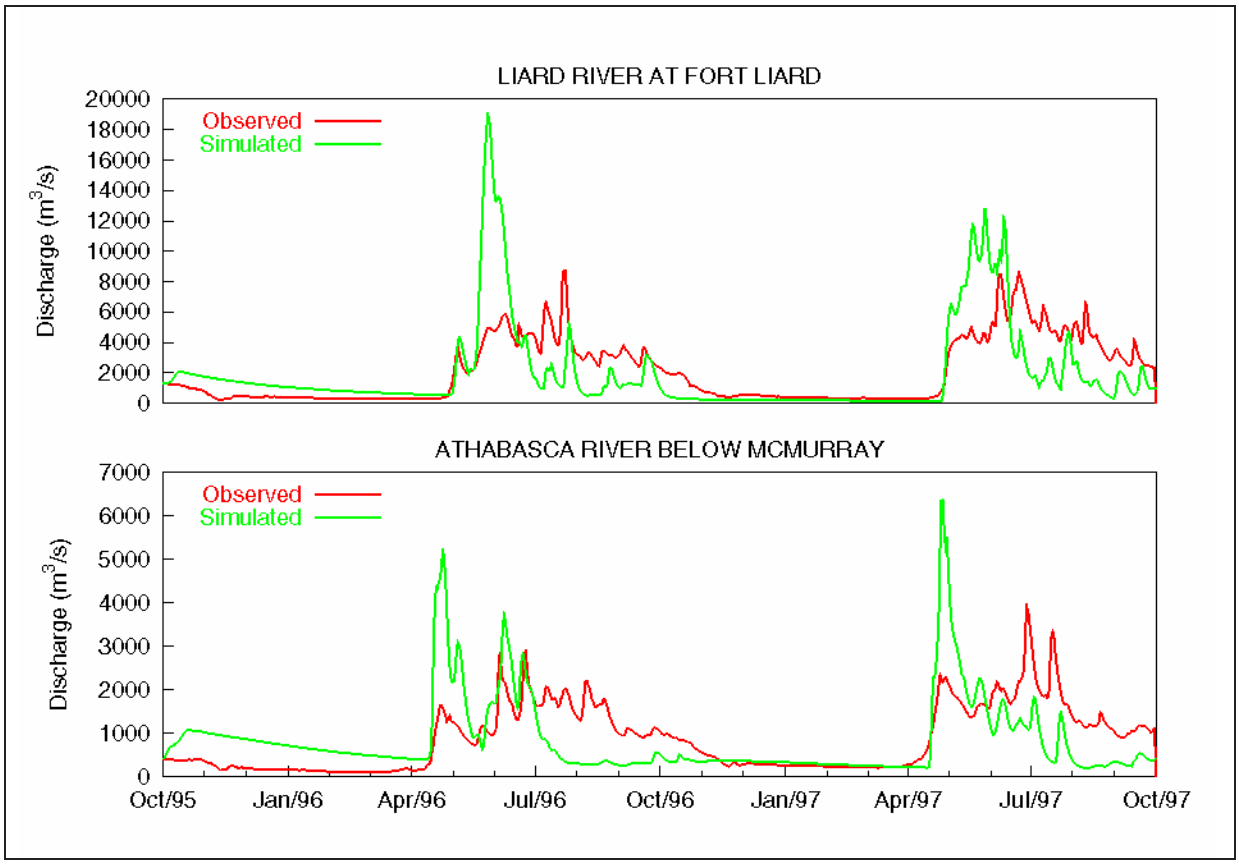

Figure 6-11 – Southern Watersheds within Mackenzie River basin

More southern basins do not reveal the same response as depicted in Figure 6-10. In these regions, hydrograph errors are dominated by high amounts of snow runoff in the spring and a lack of base flow for the remainder of the runoff season. Hydrograph volumes, from visual inspection appear to be correct, however, the distribution of runoff throughout the year is in error. This fact is more prevalent for the **A**thabasca River (133,000 km^2) which is further south than the Liard River (222,000 km^2). In all cases the timing of the spring runoff appears to be favourable with the onset of melt occurring in both measured and simulated hydrographs at the same time.

For both the Liard and **A**thabasca basins, initial snow melt produces too much runoff and not enough storage to be released later in the season. Slower rates of snowmelt from the

mountains might yield increased storage. Under these circumstances shading of snow due to aspect affects and winter drift accumulations on the leeward side of mountains lead to continued melt throughout the summer season and decreased spring melt rates.

Snowmelt Results

A factor which may be responsible for the large spring hydrograph in the southern basins is the rate of infiltration into frozen ground. Zhao and Gray (1999) have developed an empirical frozen ground infiltration model based on the behaviour of more complex, finite difference based water and energy balance soil model. One factor critical in determining the cumulative infiltration capacity of frozen ground is the "infiltration opportunity time". This input parameter is difficult to determine in practice but has been speculated to be equivalent to the cumulative time during the melt season when snowpacks are supplying moisture to the soil surface. High rates of snow melt lead to low infiltration opportunity time hence low cumulative infiltration volumes.

Remote sensing of Mackenzie River basin SWE seems to suggest model snowmelt rates which are faster than those observed. Figure 6-12 shows a comparison of snowmelt from WatCLASS and measured SWE for two dates during the 1996 snow melt season.

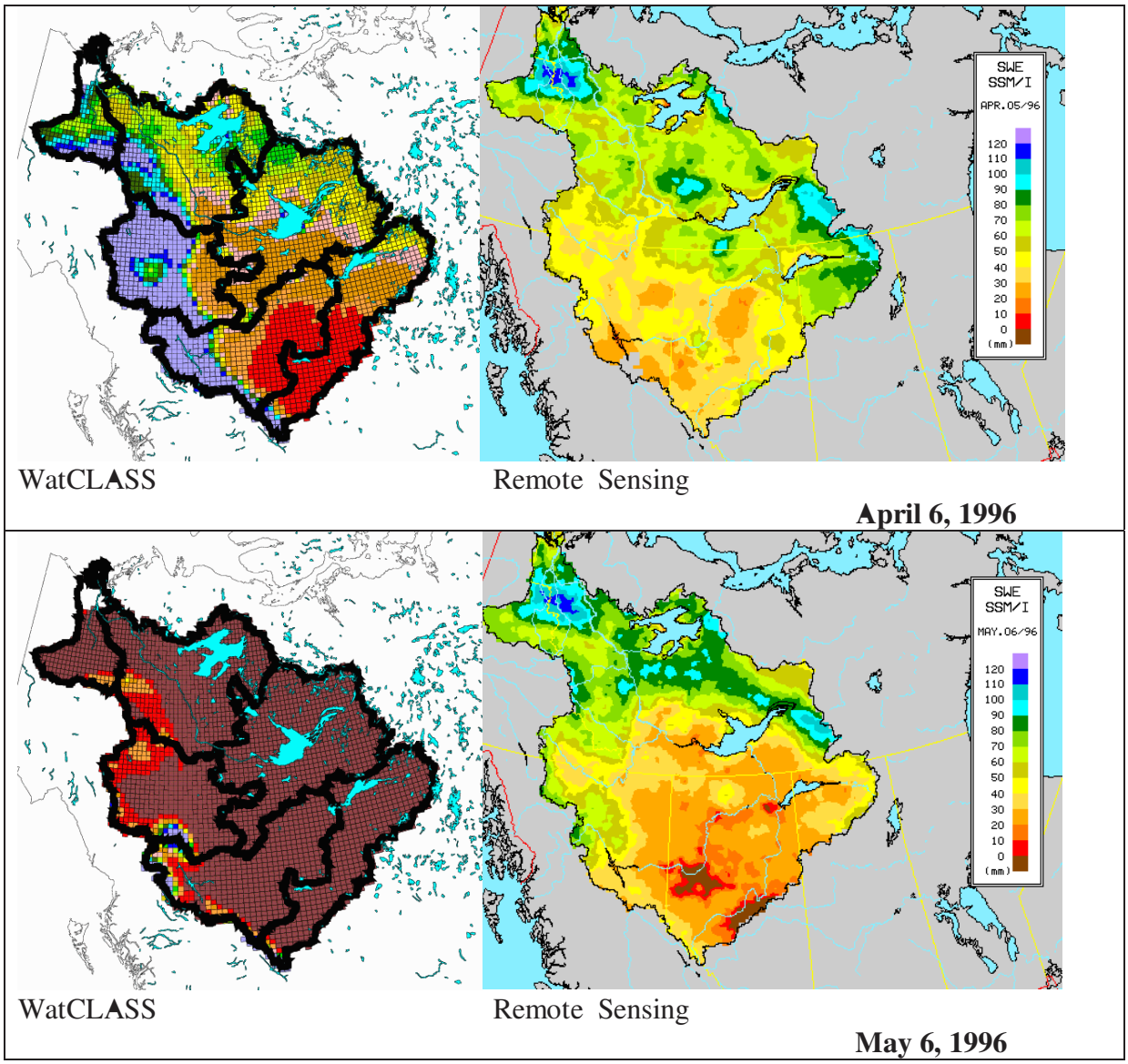

Figure 6-12 – WatCLASS vs. SSM/I derived SWE maps for two dates in 1996

This figure indicates that a majority of snow in the basin has melted in WatCLASS by May 6 1996. Remotely sensed snow depths, on the other hand, indicate that considerable snow remains with only a small area of total melt occurring in the most southern portion of the basin. This evidence suggests some problem with snowmelt parameterization in WatCLASS. Faster melt rates may not allow ample infiltration opportunity time required to infiltrate moisture to greater depths in the model. Additional research is required in this area to assess:

1. The impact of surface vegetation on the rate of snow pack evolution and melt in the model.

2. The impact of ice content on the hydraulic properties of the soil matrix.

3. The lateral flow of melt water at the snow / ground surface interface.

6.4 Chapter Summary

This chapter has shown the utility of WatCLASS at the domain of a limited area atmospheric model. This fulfills the second objective related to the thesis hypothesis, outlined in Section 1.5. In addition to WatCLASS results, WATFLOOD has been shown to function as a Level 0 model for evaluating atmospheric forcing data sets. These simulations demonstrate the utility of components of the earth/atmosphere modelling strategy presented in Chapter 3.

While simulations, particularly WatCLASS results, contain significant error, strategies and tools for improving simulations have been suggested for use in future study.

7 Discussion of Results

The hypothesis posed for this thesis in Chapter 1 indicated that the generation of runoff in a hydrologically sound fashion would improve the partitioning of turbulent energy for land surface schemes. In one respect, this would seem to be a simple task since the water balance equation, given as P-E = R + ÷S, would favour a change in evaporation (E) by simply fixing the runoff (R) to measured values. However, because inputs to the system, including precipitation (P), are dynamic and both E and R impact the change in storage (÷S) and are themselves functions of basin storage, the task becomes a more complex one of simulating the unknown storage quantity to reproduce the measured responses of streamflow and evaporation. Previous chapters have shown that when done in a consistent fashion, using physical process representations of lateral flow from the soil profile, that improvements in turbulent flux partitioning from the land surface profile can be achieved.

7.1 Model Development

A model used to generate lateral flow has been developed for CLASS based on the successful interflow implementation developed for WATFLOOD. Some modification of this theory was required for the layered soil scheme used by CLASS. Most significant is the inclusion of a non-linear term required in order to accommodate soil water movement theory used in a majority of land surface schemes. WATFLOOD is able to use a linear model of interflow by fixing a number of soil type dependent parameters and adjusting those that are most sensitive to suit the reproduction of measured hydrographs. In addition, because the parameters used by WATFLOOD are not tied to particular soil types, their values are flexible and may be adjusted using optimization procedures that allow reproduction of hydrographs

without constraints imposed by soil physics parameterizations. These parameterizations, such as Clapp and Hornberger (1978) values, impose added modelling constraints to CLASS.

The mathematics of the theory used to generate interflow in WatCLASS is not so different from that used by other researchers that are working on similar problems with slightly different modelling philosophies. These other models have been described in Chapter 2. One approach is collectively coined the Xinanjiang/ARNO/VIC approach because of their similarity (Beven, 2001, p. 48). A stormflow mechanism is introduced by relating saturated area to a non-linear description of basin storage. Zhao (1992) introduced this concept by assigning a simple two-parameter, non-linear function of saturated area to basin wetness relationship within the Xinanjiang model. However, the two parameters used in VIC-2L and Xinanjiang models have no physical description and can only be determined through streamflow calibration.

Another approach, similar to the model implemented within the GISS GCM (Rosenzweig, 1998), is based on the estimation of two parameters as well. Implemented within WatCLASS, this scheme represents a simple shallow aquifer whose conductivity and response curves are enhanced due to the presence of macropores and other conductivity enhancements present in shallow slow horizons. Soulis *et al*. (2000) have shown that this approach is equivalent with shallow aquifer schemes that provide a kinematic approximation of Richard's equation (i.e. unsaturated soil water flow) first used by Beven (1982). While the shallow aquifer and variable area models differ substantially in their perception of the dominant runoff mechanism, their underlying mathematical formulations (i.e. both have two-parameters, one a multiplier, and one an exponent) are very similar. In WatCLASS, the two model parameters are assigned values based on the topography, a soil path length scale, and

soil type. Use of these three characteristic measures of the land surface partially disaggregates the power function parameters thereby reducing, but not eliminating, the dependence on streamflow calibration. Soulis *et al*., (2000) have provided a means of estimating unknown parameters in the power law form but in doing so introduce an additional TOPMODEL based parameter, which describes the exponential decay of hydraulic conductivity with depth, for which little data are available. Although little data exist for this parameter, it does provide a physical interpretation of the flow phenomena which can be tested in future field studies.

Given that the mathematics of both the VIC/ARNO based schemes and the shallow aquifer schemes are very similar, it is expected that both are capable of hydrograph reproduction and improvements in turbulent flux partitioning. However, there are benefits in moving to a soil based approach since there is a mechanism, outlined in Soulis *et al*. (2000), for the prediction of parameters that can be accomplished without calibration. In addition, because water and soil are in contact with one another, other mass balances and processes may be included in the model structure. One area of concern in many parts of the world is the fate and transport of nutrients and pesticides from agricultural sources and their impact on aquatic ecosystems. The use of the shallow aquifer model offers an opportunity to examine the interaction between soil-water, the dominant transport mechanism, and compounds of interest. Based on the work of Leon Vizcaino (1999), WATFLOOD has had some success in modelling these fate and transport mechanisms. It would be much more difficult to model these soil based constituents within the VIC/ARNO schemes since only a surface based runoff mechanism is provided in these models. Use of WatCLASS as a water quality model has additional advantages since factors affecting the fate of pesticides and nutrients are often dependent on

the soil temperature (e.g. for reaction kinetics) and physical soil properties such as texture. These are already included in the WatCLASS structure which makes it particularly well suited to continue research in this area.

7.2 Scaling and Aggregation Issues

WatCLASS uses the GRU approach developed successfully for WATFLOOD. This approach allows for distinctly different land surface types to be modelled simultaneously so that a separate response may be generated for each. This method is often touted as being superior to parameter blending techniques because: (i) they are more physically realistic and can use measured parameters, and (ii) processes within the land surface are highly non-linear and cannot be effectively aggregated. As a result the basic choice comes down to whether parameters are blended to produce a single response or whether multiple responses are generated and simply added together to produce a single response.

Those who advocate the GRU approach rightly point to obvious cases where land surface characteristics are so blatantly different that combining their parameters would produce a composite surface whose properties would not be representative of either. An extreme example of this occurs for a parking lot and a forest land cover. For this example, it would be difficult to select a single set of parameters that would reproduce the responses of moisture and energy processes over the range of expected inputs. For parameter blending techniques, computational efficiency is often touted as a benefit. Many applications, such as atmospheric modelling, only require a single land surface response so there is little need to incur the extra expense. However, for streamflow generation the variability of soil moisture

and controlling parameters within a landscape prevents parameter blending method from capturing the essence of streamflow hydrographs.

Efforts in Chapter 5 were directed toward finding relationships between land cover and soil as a way to reinforce the concept of hydrologic similarity within land cover types. It has been hypothesised that land cover is an indicator of hydrologic similarity. However, attempts to find relationships between vegetation and soil type for the BOREAS NSA have not revealed any clear indicator that vegetation and soil type co-exist. Given they do not co-exist then there should not be any particular reason to assume that similar vegetation should be considered hydrologically similar. What was evident, however, was the fact that different land covers had distinctly different mixes of soil type and that upon grouping it could reasonably be expected that each group would yield a different response. Caveats associated with the input data to the regression analysis and the small size of the study area have been mentioned, but it would appear that grouping based on land cover would simply provide a mechanism for generating a set of blended soil parameters for each land cover designation rather than a set of parameters that could be measured directly at a partial location. If further analysis proves this representation of the GRU to be accurate, then it would appear that the essence of hydrologic similarity may in fact be best represented as statistical distribution of parameters which are divided into bin ranges for calculation.

Contrasting the GRU approach with the TOPLATS method of defining hydrologic similarity provides an interested comparison. Groupings within TOPLATS are based on the soil-topographic index where separate classifications are determined by dividing the range of index values into nominal bins. This allows soil-topography combinations to maintain distinct identities but forces the blending of vegetation characteristics. The GRU, on the

other hand, provides distinction for vegetation characteristic but may (should future results confirm NSA findings) require soil blending within each underlying vegetation type.

WatCLASS has been designed to follow the GRU approach. So far, rather than soil parameter blending, a set of measured soil characteristics associated with the various BOREAS flux towers (Cuenca *et al*., 1997) has been used to define the GRU soil characteristic. This method has yielded streamflow and energy fluxes that represent those measured during the BOREAS project. An interesting question that arises from this becomes whether the same result could be obtained through the use of a topographic-index grouping and the selection of dominant or blended vegetation type for each group. There is no reason to believe that it would not.

While WatCLASS code has been designed to accept only one set of soil properties for each vegetation type, it would be a simple matter to provide each vegetation sub-group with a distinctly different set of soil properties based on soil survey information. As spatial soil and topographic data become more prevalent and easy to use, it may be more prudent to drop the idea of hydrologic similarity and provide vegetation groupings with soil and topographic properties that are local to them. This was virtually impossible in the past since the necessary data sets did not exist in digital form and tools for manipulating and extracting such data had not matured. With improved access to physiographic data it might be timely to incorporate greater definition of the drainage layer database to capture more of its variability. Whether this will improve simulations of energy and water balance processes is yet to be seen but it does provide a direction for future research which should have as its goal to model watershed processes without calibration. Advocating greater use of data does not translate

necessarily to more complex models but rather a transfer in emphasis from model calibration to parameter selection.

Scaling of parameters will likely continue to be problematic in the future. Questions of how process parameters measured at one scale can be transferred to another have not been addressed here. Instead, streamflow generation processes in WatCLASS have been provided with scaling parameters which define the characteristic width of local first order basins. These parameters are relatively independent of scale and can continue to be used for larger grid sizes. This approach of watershed width is not a new one in hydrology. However, rather than a calibration parameter, watershed width can become part of the input data set. Scaling in WatCLASS follows that of WATFLOOD, which was designed to answer a particular problem. One model cannot be all things for all people, and the design of WATFLOOD has been geared toward prediction of streamflow from watersheds by capturing much of the land surface variability using the GRU concept and limiting grid sizes so that the dynamics of precipitation are captured. WatCLASS has followed this scaling philosophy to extend watershed processes to include energy balance methods necessary for atmospheric modelling.

7.3 Level III Modelling

Implementation of Level III modelling based on a phased implementation approach (see Figure 3-2) has been shown to be successful. Coupling of the MC2-CLASS-WATFLOOD models has been accomplished for the Saguenay Flood Study. Researchers at McGill University developed a coupling between the MC2 atmospheric model and the CLASS land surface scheme during the same time period that CLASS and WATFLOOD were coupled as

WatCLASS. Also during this same study period, MC2 was providing surface forcing data to WATFLOOD in Level 0 mode which was used to provide feedback to the atmospheric modellers with respect to the timing and spatial extent of precipitation. The final step in the process was the coupling of all the models at Level III and the simulation of runoff from the large rainfall event that occurred in the Saguenay region of Quebec in 1997. As mentioned previously, the impact of coupling CLASS and WATFLOOD within MC2 did not have a great impact on the rainfall event directly. This was likely due the limited duration of the simulation, only two days, and the dominance of initial conditions in determining the state of the land surface and atmosphere prior to the start of the simulation. While the impact on the simulated precipitation was not profound, the exercise of coupling the models has proven that the linkage strategy was sound and that models could be developed in isolation and fully coupled with moderate effort.

Continued development is underway to continue Level III modelling. This time the Mackenzie River Basin is the target watershed and the Canadian Regional Climate Model (CRCM) is the atmospheric base model. Already, the CRCM and CLASS have been linked and run over the Mackenzie as a Level I model. Surface forcing data from this model have been used to drive the WATFLOOD model in Level 0 mode. In addition, runoff generated by CLASS's original scheme inside the Level I model has been routed using the WATROUTE (Arora, 2001) streamflow routing model. These results have been reported in MacKay *et al*. (2002). During the same period, WatCLASS runs were being preformed at Level II to test the models ability to reproduce measured hydrographs. The results of Level II model testing are reported in Chapter 6. While the hydrographs generated are plausible, there are issues related to flow of moisture through frozen ground that must be addressed. In

addition, there appears to be an early snowmelt problem that was identified with the aid of remote sensing observations. Continued testing with WatCLASS over the Mackenzie basin is required. However, a benefit of the phased implementation approach allows these changes to be implemented in isolation from the CRCM so that overhead and expense of running an atmospheric model are not incurred.

It is expected that the three year simulation that will be used by the CRCM will produce a measurable impact on atmospheric model outputs as a direct result of changes made in the partitioning of land surface fluxes that runoff modelling provide. Climate model simulations such as these do not require re-initialization and are permitted to evolve for long periods based on the physical processes within the model.

Failure of the Saguenay Flood Study to provide a significant atmospheric impact does not mean that there is no place for hydrologic modelling within weather forecast simulations. On the contrary, weather prediction models can benefit greatly from both Level II and Level III modelling. Weather forecast scores compiled over many forecast cycles may begin to improve with better surface flux partitioning. Perhaps of equal importance to improved surface simulation is a data assimilation service that can be provided by a Level II model. Weather forecasts are generated based on both a predictive atmospheric model and a set of initial conditions generated at the start of each forecast which represent the measured state of the earth and atmosphere at the beginning of the forecast. Generation of these initial conditions is a difficult task especially for land surface variables such as soil temperature and moisture. These are often calculated based only on observed humidity and air temperature data measured at 2m above the surface. An alternate approach to predicting these land surface state variables might involve a parallel run of a Level II model together with the

regular Level III forecast. This parallel Level II run would use measured data to drive the land surface model and predict land surface state variables including soil moisture and temperature. These runs could be validated against measured streamflow or use measured streamflow as input data in an optimization scheme to arrive at land surface state variables. Whatever the method, these state variables could be used to initialize the land surface of the next Level III forecast.

8 Conclusions and Recommendations

The goal of this thesis has been to develop a lower boundary of an atmospheric model that is capable of providing accurate water and energy flux returns to the atmosphere and which also provides increased model realism by simulating streamflow. As it turns out, flux returns and streamflow realism are tightly coupled through a common soil moisture dependency. The WATFLOOD hydrologic model and the CLASS land surface scheme have been used to create a hybrid model known as WatCLASS which has been able to fulfill this role. Key features of the coupled model include:

1. A code base that allows WatCLASS to be incorporated into any atmospheric model that has implemented CLASS as its land surface scheme. This utility has broader implications than simply adding hydrology to an atmospheric model. It extends the usefulness of the modelling system to testing, in Level II mode, implications of new theories and/or parameter sets that can be immediately transferred to atmospheric simulations. These capabilities also provide a platform for future work that might extend modelling beyond water and energy processes and into other aspects of environmental modelling that might benefit from or have implications on atmospheric modelling.

2. Runoff and evapotranspiration endpoints that stop and start their respective influence based on a "field capacity" moisture content. Selection of this common endpoint also conforms to the natural vertical drainage threshold. This unity in modelling mimics the response of popular force-restore schemes. However, the WatCLASS implementation of the "restoring" function is based on the physical processes of drainage, evaporation and runoff rather than a specified value of decay.

3. Land surface heterogeneity modelled using the WATFLOOD GRU approach. This allows parameters developed at the point scale to be used over larger areas. While

each GRU land class does require extra parameters it allows the separation of distinctly different land surface types to be modelled independently. Care must be exercised in using many land surface types indiscriminately since within a land class grouping some degree of parameter blending must still be undertaken.

4. WATFLOOD based streamflow routing that provides a mechanism for comparison with measured data.

In addition to the generation of the WatCLASS model other conclusions can be drawn based on the results of the simulations over the BOREAS study area and the Mackenzie River basin. These conclusions include:

1. By implementing a WATFLOOD like runoff generation (i.e. lateral flow) mechanism within CLASS, evaporation from the old black spruce site of the BOREAS NSA was reduced from 1270mm to 720mm a decrease of 70%. Modifications were required to the stomatal resistance functions to provide greater realism with generated runoff. When implemented these changes had a significant impact on diurnal flux results.

2. Using results from tower observations, grouped vegetation and soil characteristics were generated the NSA and SSA watersheds. When forced with atmospheric data measured during the BOREAS project, WatCLASS was reasonably able to simulate measured streamflow. These simulations point to requirements for future research, especially those related to infiltration into frozen ground.

3. The simulations over the Mackenzie River basin have shown that modelling developed for the BOREAS project can be extended to large domains that are coincident with limited area atmospheric modelling. Issues related to snowmelt and frozen ground were identified as processes requiring additional research.

4. In addition to streamflow simulations, the Mackenzie River simulations were able to predict, in a relative sense, the distribution of permafrost in the basin. This was an unexpected result and checked only because of the problems encountered with spring hydrograph simulations. While not likely to be useful for local permafrost studies,

change studies using climate models might benefit from comparison with present day permafrost distributions.

Future work is required to bridge gaps in the current theory in order to improve simulation results. These have been identified in areas that have not yet been developed fully or have yet to be implemented. These include, in order of importance:

1. Implementation of theories for infiltration and liquid moisture flow through frozen ground that provide a consistent response with measured hydrographs. Highlighting this requirement is the 1995 BOREAS snowmelt hydrograph and the Mackenzie River spring melt simulations.

2. In light of the differences between modelled and remotely sensed snow depletion over the Mackenzie River watershed, examination of snowmelt properties within WatCLASS. Probable causes for this result are likely to be found in either: (i) the model generated forcing data provided by the numerical weather prediction model or (ii) the treatment of the Mackenzie Basin land surface with only one land class. This second cause has implications on the model radiation balance; particularly, the extinction of radiation as it penetrates the forest canopy and land surface shading resulting from topographic aspect differences.

3. Implementation of a lake surface class. Currently, water surfaces in WatCLASS are treated simply as shallow puddles over saturated soil. Lakes, on the other hand, have climates of their own with strong advective components that cannot be modelled within the current fixed land surface model structure. Lakes present a much different temperature boundary to the atmosphere than does the land surface and currently this is poorly handled in Canadian models.

4. Change the basis of the current soil physics from the Clapp and Hornberger type model to the more modern van Genuchten theory. While the work presented in Chapter 4 attempts to fit Clapp and Hornberger soil response to van Genuchten

parameters, the result is unsatisfactory, especially at the wet end of the soil moisture range which is of greatest importance to runoff production.

5. A program aimed at measuring the hydraulic conductivity of near surface soils and their influence on runoff generation. A number of hydrologic models that are finding their way into atmospheric simulations have as their basis a decreasing soil hydraulic conductivity with depth. This parameter is rarely measured and as a result, its distribution within landscapes in unknown. Highlighting this area in the future may well lead to development of functional relationships between near surface conductivity and readily measurable physiographic factors such as soil type, land use, vegetation cover, topography, and climate. The ultimate goal of such a program would be the prediction of land surface parameters for ungauged basins. This program would fit well within current, decade long emphasis of the International Association of Hydrologic Science (IAHS) (http://www.cig.ensmp.fr/~iahs, 2002) known as Prediction in Ungauged Basins (PUB).

Beyond specific changes to model physics, there is a need for continued testing of WatCLASS in other land surface environments. This will help ensure the robustness of the model in global applications. New experiments are being designed to test and develop parameters for land surface schemes. These experiments must contain a hydrologic component that examines the re-distribution of soil moisture in the landscape and its implications on both streamflow generation and evapotranspiration. A number of current experimental projects in Canada are focused primarily on the response of vegetation to atmospheric climates and virtually ignore soil climates that give rise to runoff and provide the source of moisture for transpiration. Simple monitoring of the spatial variability of soil moisture to assess storage change and measurement of runoff at headwater streams would provide closure of the surface water balance and greatly improve the utility of these data sets.

It is interesting to observe that in recent years the role of the hydrologist is changing. A trend seems to be emerging where more and more emphasis is being devoted toward using the streamflow record within atmospheric studies. Hydrologists are now filling roles in climate and weather prediction offices along side their atmospheric counterparts. Programs, such as the Mackenzie GEWEX study, are fostering communications and collaboration between these groups and the seeds planted by these ventures are beginning to bear fruit.

References

Ahuja, L. R., J. W. Naney, and R. D. Williams (1985) Estimating soil water characteristics from simpler properties or limited data, Soil Science Society of America Journal, 49(5):1100-1105.

Ahuja, L. R., J. W. Naney, R. E. Green, and D. R. Nielsen, (1984) Macroporosity to characterize spatial variability of hydraulic conductivity and effects of land management, Soil Science Society of America Journal, 48(4):699-702.

Albritton D.L., and L.G. Meira Filho (Lead Authors) (2001) Climate Change 2001: The Scientific Basis, IPCC Working Group I: IPCC Third Assessment Report, Intergovernmental Panel on Climate Change, Shanghai, 20 January 2001. Available on line at [http://www.ipcc.ch/]

Anderson, D. (1998). BOREAS TE-01 Soils Data over the SSA Tower Sites in Raster Format. Available on-line [http://www.daac.ornl.gov /] from Oak Ridge National Laboratory Distributed Active Archive Center, Oak Ridge, Tennessee, U.S.A.

Arora, V.K., and G.J. Boer (2002) An assessment of simulated global moisture budget, and the role of moisture reservoirs in processing precipitation, submitted to Climate Dynamics.

Arora, V., F. Seglenieks, N. Kouwen, and E. Soulis (2001) Scaling aspects of river flow routing, Hydrological Processes, 15(3):461-477.

Avissar, R. and R. A. Pielke (1989) A parameterization of heterogeneous land surfaces for atmospheric numerical models and its impact on regional meteorology, Monthly Weather Review, 117(10):2113-2136.

Bear, J. (1972) Dynamics of Fluids in Porous Media, American Elsevier, New York, USA.

Beljaars, A. C., P. Viterbo, M. J. Miller, and A. K. Betts (1996) The anomalous rainfall over the United States during July 1993: Sensitivity to land surface parameterization and soil moisture anomalies, Monthly Weather Review, 124(3):362–383.

Benoit, R., C. Schär, P. Binder, S. Chamberland, H. C. Davies, M. Desgagné, C. Girard, C. Keil, N. Kouwen, D. Lüthi, D. Maric, E. Müller, P. Pellerin, J. Schmidli, F. Schubiger, C. Schwierz, M. Sprenger, A. Walser, S. Willemse, W. Yu, and E. Zala (2002) The Real-Time Ultrafinescale Forecast Support during the Special Observing Period of the MAP. Bulletin of the American Meteorological Society, 83(1):85–109.

Benoit, R., P. Pellerin, N. Kouwen, H. Ritchie, N. Donaldson, P. Joe, and E. D. Soulis (2000) Toward the use of coupled atmospheric and hydrologic models at regional scale. Monthly Weather Review, 128(6):1681–1706.

Benoit, R., M. Desgagné, P. Pellerin, S. Pellerin, Y. Chartier, and S. Desjardins (1997) The Canadian MC2: A semi-Lagrangian, semi-implicit wideband atmospheric model suited for finescale process studies and simulation. Monthly Weather Review, 125:2382–2415.

Betts, A. K., and J. H. Ball (1997) Albedo over the boreal forest, Journal of Geophysical Research, 102(D24):28901-28910.

Betts, A. K., M. L. Goulden, and S. C. Wofsy, (1999) Controls on evaporation in a boreal spruce forest. Journal of Climate, 12:1601-1618.

Betts, A. K., P. Viterbo (2000) Hydrological budgets and surface energy balance of seven subbasins of the Mackenzie River from the ECMWF model. Journal of Hydrometeorology, 1(1):47–60.

Beven, K. J. (2001) Rainfall-Runoff Modelling : The Primer, John Wiley & Sons, Chichester, England.

Beven, K. J. (1986) Runoff production and flood frequency in catchments of order n: an alternate approach, In: V. K. Gupta, I. Rodriguez-Iturbe, and E. F. Wood (editors) Scale Problems in Hydrology, Reidel, Dordrecht, pp. 107-131.

Beven, K. (1982) On subsurface stormflow: Predictions with simple kinematic theory for saturated and unsaturated flows, Water Resources Research, 18(6):1627-1633.

Beven, K., and P. Germann (1982) Macropores and water flow in soils, Water Resources Research, 18(5):1311-1325.

Beven, K. J., and M. J. Kirkby (1979) A physically based variable contributing area model of basin hydrology, Hydrological Science Bulletin, 24(1):43-69.

Beven, K., R. Lamb, P. Quinn, R. Romanowicz, and J. Freer (1995) TOPMODEL, Chapter 18, In: V. P. Singh (editor) Computer Models of Watershed Hydrology, Water Resources Publications, Highlands Ranch, Colorado, USA.

Bingeman, A. K. (2001) Improving dam safety analysis by using physically-based techniques to derive estimates of atmospherically maximum precipitation, Unpublished Ph.D. thesis, University of Waterloo.

Blyth, E. (2001) Relative influence of vertical and horizontal processes in large-scale water and energy balance modeling, In: A. J. Dolman et al. (editors), Soil–Vegetation–Atmosphere Transfer Schemes and Large-Scale Hydrological Models, International Association of Hydrological Sciences, Red Book Series, No. 270:3-10.

Boussinseq, J. (1877) Essai sur la theorie des eaux courantes, Mem. PresentesDivers Savants Acad. Sci. Inst. France, 137, 5-11. As cited by: Sanford W. E. et al. (1993) Water Resourses Research, 29(7):2313-2321.

Brooks, R. H., and A. T. Corey (1964) Hydraulic properties of porous media, Hydrology Paper No. 3, Colorado State University, Fort Collins, Colorado, USA.

Brooks, R. H., and A. T. Corey (1966) Properties of porous media affecting fluid flow, Proceedings of the American Society of Civil Engineers, Journal of the Irrigation and Drainage Division, 92(IR2):61-88.

Brustsaert, W. (1967) Some methods of calculating unsaturated permeability, Transactions of the American Society of Agricultural Engineers, 10:400-404.

Burdine, N. T. (1953) Relative permeability calculations from pore size distribution data, Transactions of the American Institute of Mining and Metallurgical Engineers, 198:71-78.

Burdine, N. T., L. S. Gournay, and P. P. Reichertz (1950) Pore size distribution of petroleum reservoir rocks, Transactions of the American Institute of Mining and Metallurgical Engineers, 189:195-204.

Campbell, G. S. (1974) A simple method for determining unsaturated conductivity from moisture retention data, Soil Science, 117(6):311-314.

Carlaw, S. M. (2000) Soil Moisture Accounting in Distributed Hydrologic Modelling, Unpublished M.A.Sc. thesis, University of Waterloo.

Carman, P. C. (1956) Flow of Gases Through Porous Media, Butterworths Scientific Publications, London, United Kingdom.

Carson, D. J. (1982) Current parameterizations of land-surface processes in atmospheric general circulation models. p.67-108, In: P. S. Eagleson (editor) Land Surface Processes in Atmospheric General Circulation Models, Cambridge University Press, Cambridge, UK.

Caya, D. and R. Laprise (1999) A semi-implicit, semi-Lagrangian regional climate model: the Canadian RCM, Monthly Weather Review,127:341-362.

Childs, E. C., and N. Collis-George (1950) The permeability of porous materials, Proceedings of the Royal Society of London, Series A, 201:392-405.

Clapp, R. B. and G. M. Hornberger (1978) Empirical equations for some soil hydraulic properties, Water Resources Research, 14(4): 601-604.

Cohen, S. J., editor (1997) Mackenzie Basin Impact Study (MBIS): Final Report, Environment Canada, Environmental Adaptation Research Group, Downsview, Ontario

Cosby, B. J., G. M. Hornberger, R. B. Clapp, and T. R. Ginn (1984) Statistical exploration of the relationships of soil moisture characteristics to the physical properties of soils, Water Resources Research, 20(6): 682-690.

Côté J., S. Gravel, A. Méthot, A. Patoine, M. Roch, and A. Staniforth (1998a): The operational CMC-MRB global environmental multiscale (GEM) model. Part I : Design considerations and formulation, Monthly Weather Review, 126(6):1373-1395.

Côté J., J. Desmarais, S. Gravel, A. Méthot, A. Patoine, M. Roch, and A. Staniforth (1998b): The operational CMC-MRB global environmental multiscale (GEM) model. Part II : Results, Monthly Weather Review, 126(6):1397-1418.

Cox, P. M., R. A. Betts, C. Bunton, R. L. H. Essery, P. R. Rowntree, and J. Smith (1999) The impact of new land surface physics on the GCM simulation of climate and climate sensitivity. Climate Dynamics, 15, 183-203.

Cuenca, R. H., M. Ek, L. Mahrt (1996) Impact of soil water property parameterization on atmospheric boundary layer simulation, Journal of Geophysical Research, 101(D3): 7269-7277.

Cuenca, R. H., D. E. Stangel, and S. F. Kelly (1997) Soil water balance in a boreal forest. Journal of Geophysical Research (BOREAS Special Issue) 102(D24): 29355-29366.

Cranmer, A. J., N. Kouwen, and S. F. Mousavi (2001) Proving WATFLOOD: modelling the nonlinearities of hydrologic response to storm intensities, Canadian Journal of Civil Engineering, 28:837-855.

Deardorff J. W. (1978) Efficient prediction of ground surface temperature and moisture with inclusion of a layer of vegetation, Journal of Geophysical Research, 83(C4):1889-1903.

Delage, Y. and D. Verseghy (1995) Testing the effects of a new land surface scheme and of initial soil moisture conditions in the Canadian global forecast model. Monthly Weather Review, 123: 3305-3317.

Desjardins, R .L., J. I. MacPherson, L. Mahrt, P. Schuepp, E. Pattey, H. Neumann, D. Baldocchi, S. Wofsy, D. Fitzjarrald, H. McCaughey, and D. W. Joiner (1997) Scaling Up Flux Measurements for the Boreal Forest Using Aircraft-tower Combination. Journal of Geophysical Research, 102(D24):29125-29134.

Dickinson, R. E. (1992) Land surface, Chapter 5, In: Trenberth, K. E. (editor) Climate System Modeling, Cambridge University Press, Cambridge, UK.

Dickinson, R. E. (1984) Modeling evapotranspiration for three-dimensional global climate models, p. 58-72, In: J. E. Hanson and T. Takahashi (Editors) Climate Processes and Climate Sensitivity, Geophysical Monograph 29, Maurice Ewing Volume 5, American Geophysical Union, Washington, D.C., USA.

Dickinson R. E., A. Henderson-Sellers and P. J. Kennedy (1993) Biosphere-Atmosphere Transfer Scheme (BATS) Version 1e as Coupled to the NCAR Community Climate Model, National Center for Atmospheric Research, Boulder, Colorado, Technical Note: NCAR/TN-387+STR.

Dingman, S. L. (2002) Physical Hydrology (2end Edition), Prentice Hall, New Jersey, USA.

Dirmeyer, P. A. (1997) The global soil wetness project, GEWEX News, 7(2):3-6.

Donald, J. R., E. D. Soulis, N. Kouwen and A. Pietroniro (1995) A land cover-based snow cover representation for distributed hydrologic models, Water Resources Research, 31(4):995-1010.

Dumenil, L., and E. Todini (1992) A rainfall-runoff scheme for use in the Hamburg climate model, Chapter 9, In: P. O'Kane, (editor) Advances in Theoretical Hydrology, A Tribute to James Dooge., European Geophysical Society Series on Hydrological Sciences 1, Elsevier, Amsterdam.

Durner, W. (1994) Hydraulic conductivity estimation for soil with heterogeneous pore structure, Water Resources Research, 30(2):211-223.

Eagleson, P. S. (1970) Dynamic Hydrology, McGraw-Hill, New York, USA.

Entekhabi, D., G. R. Asrar, A. K. Betts, K. J. Beven, R. L. Bras, C. J. Duffy, T. Dunne, R. D. Koster, D. P. Lettenmaier, D. B. McLaughlin, W. J. Shuttleworth, M. T. van Genuchten,M.-Y. Wei, and E. F. Wood (1999) An agenda for land surface hydrology research and a call for the second international hydrological decade, Bulletin of the American Meteorological Society, 80(10):2043-2058.

Etchevers, P, C. Golaz, and F. Habets (2001) Simulation of the water budget and the river flows of the Rhone basin from 1981 to 1994, Journal of Hydrology, 244(1-2):60-85.

Famiglietti, J. S., and E. F. Wood (1994) Multiscale modeling of spatially variable water and energy balance processes, Water Resources Research, 30(11):3061-3078.

Fatt, I., and H. Dykstra (1951) Relative permeability studies, Transactions of the American Institute of Mining and Metallurgical Engineers, 192:249-256.

Fread, D. L. (1993) Flow Routing, Chapter 10. In: Maidment, D. R. (editor) Handbook of Hydrology, McGraw-Hill, New York, NY.

Freeze, R. A. (1974) Streamflow generation, Reviews of Geophysics and Space Physics, 12(4):627-647.

Gardner, W. R. (1974) The permeability problem, Soil Science, 117(5):243-249.

GHP (1998), Towards Carrying out the Strategy of the GEWEX Hydrometeorology Panel, Available on-line at [http://www.usask.ca/geography/MAGS/GHP].

Gruszka, F. (2000) SERM Forest Cover Data Layers of the SSA in Vector Format. Available on-line [http://www.daac.ornl.gov /] from Oak Ridge National Laboratory Distributed Active Archive Center, Oak Ridge, Tennessee, U.S.A.

Haberlandt, U. and G. W. Kite (1998) Estimation of daily space-time precipitation series for macroscale hydrological modelling, Hydrological Processes, 12(9):1419-1432.

Habets, F, J. Noilhan, C. Golaz, J. P. Goutorbe, P. Lacarrere, E. Leblois, E. Ledoux, E. Martin, C. Ottle, and D. Vidal-Madjar (1999a) The ISBA surface scheme in a macroscale hydrological model applied to the Hapex-Mobilhy area. Part I: Model and database, Part II: Simulation of streamflows and annual water budget, Journal of Hydrology, 217(1-2):75-118.

Habets, F., and G. M. Saulnier (2001) Subgrid runoff parameterization, Physics and Chemistry of the Earth, Part B: Hydrology, Oceans and Atmosphere, 26(5-6):455-459.

Habets, F., P. Etchevers, C. Golaz, E. Leblois, E. Ledoux, E. Martin, J. Noilhan, and C. Ottle (1999b) Simulation of the water budget and the river flows of the Rhone basin, Journal of Geophysical Research,104(D24):31145-31172.

Hargreaves G. H. and Z. A. Samani (1982) Estimating potential evapotranspiration, Journal Of The Irrigation & Drainage Division - Asce , 108(IR3):225-230

Hamlin, L. P. B.(1996) Snowmelt hydrologic modelling of northern wetland dominated river basins, Unpublished M.A.Sc. thesis, University of Waterloo.

Heginbottom, J. A., M. A. Dubreuil and P. T. Harker (1995) Canada-Permafrost. Map: MCR 4177. National Atlas Information Service, Canada Centre for Mapping, and the Terrain Sciences Division, Geological Survey of Canada, Natural Resources Canada. Available on-line at [http://atlas.gc.ca/site/english/archives/5th_edition/Mcrp2].

Henderson-Sellers, A, Z.-L. Yang, and R. E. Dickinson (1993) The Project for Intercomparison of Land-surface Parameterization Schemes, Bulletin of the American Meteorological Society Climate, 74(7):1335-1349.

Hewlett J. D. and A. R. Hibbert (1963) Moisture and energy conditions within a sloping mass during drainage, Journal of Geophysical Research, 68:1081-1087.

Hillel, D. (1998) Environmental soil physics, Academic Press, San Diego, CA.

Hoffmann-Riem, H., M. Th. van Genuchten, and H. Fluhler (1999) General model for the hydraulic conductivity of unsaturated soils. p 31-42. In: M. Th. van Genuchten, F. J. Leij, and L. Wu (editors) Characterization and Measurement of the Hydraulic Properties of Unsaturated Porous Media: Proceedings of the International Workshop, Riverside, California, October 2-24, 1997.

Hornberger, G. M., J. P. Raffensperger, P. L. Wiberg, and K. N. Eshleman (1998) Elements of Physical Hydrology, The John Hopkins University Press, Baltimore, Maryland, USA.

Horton, R. E. (1933) The role of infiltration in the hydrological cycle, Transactions of the American Geophysical Union, 14:446-460.

Huber, W. C., and R. E. Dickinson (1988) The USEPA SWMM4 Storm Water Management Model User's Manual, Version 4, EPA/600/3-88/001a (NTIS PB88-236641/AS) Environmental Protection Agency, Athens, Georgia, USA.

Hurley, D. G. and G. Pantelis (1985) Unsaturated and saturated flow through a thin porous layer on a hillslope, Water Resources Research, 21(6):821-824.

Hutchinson, M. F. (1989) A new method for gridding elevation and stream line data with automatic removal of pits, Journal of Hydrology, 106:211-232.

Irmay, S. (1954) On the hydraulic conductivity of unsaturated soils, Transactions / American Geophysical Union, 35(3):463-467.

Ivanov, K. E. (1982) Water Movement in Mirelands, Academic Press, New York.

Jackson R. D.(1973) Diurnal change in soil water content during drying, Chapter 3, In: R. R. Bruce et al. (editors) Field Soil Water Regimes, Soil Science Society of America special publication no. 5, Madison, Wisconsin, USA.

Jenson, S. K., and J. O. Domingue (1988) Extracting topographic structure from digital elevation data for geographic information system analysis, Photogrammetric Engineering and Remote Sensing, 54(11):1593-1600.

Kenward T., D. P. Lettenmaier, E. F. Wood, and E. Fielding (2000) Effects of digital elevation model accuracy on hydrologic predictions, Remote Sensing of Environment, 74:432-444.

Kite, G. W., A. Dalton, K. Dion (1994) Simulation of streamflow in a marcoscale watershed using general circulation model data. Water Resources Research, 30(5):1547-1559.

Kite, G. W., and U. Haberlandt (1999) Atmospheric model data for macroscale hydrology, Journal of Hydrology, 217(3-4):169-338.

Kite G. W. and N. Kouwen (1992) Watershed modeling using land classifications, Water Resources Research, 28(12):3193-3200.

Kouwen, N. (2001) WATFLOOD/SPL9: Hydrological Model & Flood Forecasting System, Computer program manual, University of Waterloo.

Kouwen, N., E. D. Soulis, A. Pietroniro, J. Donald, and R. A. Harrington (1993) Grouped response units for distributed hydrologic modeling, Journal of Water Resources Planning and Management (ASCE), 119(3):289-305.

Leon Vizcaino, L. F. (1999) Integral system for nonpoint source pollution modeling in surface waters, Unpublished Ph.D. thesis, University of Waterloo.

Letts M. G., N. T. Roulet, N. T. Comer, M. R. Skarupa, and D. L. Verseghy (2000) Parameterization of peatland hydraulic properties for the Canadian land surface scheme, Atmosphere-Ocean, 38(1):141-160.

Lhomme, J.-P. (2001) Stomatal control of transpiration: Examination of the Jarvis-type representation of canopy resistance in relation to humidity, Water Resources Research, 37(3): 689-700.

Liang, X., D. P. Lettenmaier, E. F. Wood, and S. J. Burges (1994) A simple hydrologically based model of land surface water and energy fluxes for general circulation models, Journal of Geophysical Research, 99(D7):14415-14428.

Lin, C. A., L. Wen, M. Beland, and D. Chaumont (2002) A coupled atmospheric-hydrological modeling study of the 1996 Ha! Ha! River basin flash flood in Québec, Canada, Geophysical Research Letters, 29(2):1-4.

Linsley, R. K., M. A. Kohler, and J. L. H. Paulhus (1982) Hydrology for Engineers (3rd edition). McGraw-Hill Book Co., New York, NY.

Loechel, S. E., C. L Walthall, E. Brown de Colstoun, J. Chen, B. L. Markham, and J. Miller (1997) Variability of boreal forest reflectances as measured from a helicopter platform, Journal of Geophysical Research, 102(D24):29,495-29,503.

Lohmann, D., R. Nolte-Holube, and E. Raschke (1996) A large-scale horizontal routing model to be coupled to land surface parametrization schemes, Tellus, 48A(5):708-721.

Louie, P .Y. T., W. D. Hogg, M. D. Mackay, X. Zhang, and R. F. Hopkinson (2002) The water balance climatology of the Mackenzie Basin with reference to the 1994/95 water year, Atmosphere-Ocean, 40(2):159-180.

MacKay, M. D., K. Szeto, D. Verseghy, F. Seglenieks, E. D. Soulis, K. R. Snelgrove, and A. Walker (2002) Modelling Mackenzie Basin surface water balance during CAGES with the Canadian Regional Climate Model, Journal of Hydrometeorology, submitted.

Mahfouf J.-F. and J. Noiliah (1996) Inclusion of gravitational drainage in a land surface scheme based on the force-restore method, Journal of Applied Meteorology, 34:987-992.

Mailhot, J., R. Sarrazin, B. Bilodeau, N. Brunet and G. Pellerin (1997) Development of the 35-km version of the operational regional forecast system, Atmosphere-Ocean, 35:1-28.

Manabe, S. (1969) Climate and ocean circulation: I. The atmospheric circulation and the hydrology of the earth's surface, Monthly Weather Review, 97(11):739-774.

McCord, J. T., D. B. Stephens, and J. L. Wilson (1991) Hysteresis and state-dependent anisotropy in modeling unsaturated hillslope hydrologic processes, Water Resources Research, 27(7):1501-1518.

McFarlane, N. A., G. J. Boer, J.-P. Blanchet, and M. Lazare (2001) The third generation atmospheric general circulation model, ACGMIII, Available on line at [http://www.cccma.bc.ec.gc.ca/models/gcm3.shtml]

McFarlane, N. A., G. J. Boer, J.-P. Blanchet, and M. Lazare (1992) The Canadian climate centre second-generation general circulation model and its equilibrium climate, Journal of Climate, 5(10):1013-1044.

Mein, R. G. and C. L. Larson, (1973) Modeling infiltration during a steady rain, Water Resources Research, 9(2):384-394.

Mekis, É. and W. Hogg (1999) Rehabilitation and analysis of Canadian daily precipitation time series. Atmosphere-Ocean, 37(1):53-85.

Michaud, J. D. and W. J. Shuttleworth (1996) Executive summary of the Tucson Aggregation Workshop, Journal of Hydrology, 190(3-4):176-181

Money, D. C. (1972) Climate, Soils and Vegetation, University Tutorial Press, London, UK.

Moore, K. E., D. R. Fitzjarrald, R. K. Sakai, and J. M. Freedman (2000) Growing season water balance at a boreal jack pine forest, Water Resources Research, 36(2):483-493.

Morel, P. (2001) Why GEWEX? The agenda for a global energy and water cycle research program, GEWEX News, 11(1):1, 7-11.

Mousavi and Kouwen (2002) Proving WATFLOOD: Modelling the groundwater contribution to streamflow with a simple function, Canadian Jounral of Civil Engineering (submitted).

Mualem, Y. (1976) A new method for predicting the hydraulic conductivity of unsaturated porous media, Water Resources Research 12(3): 513-522.

Mualem, Y. (1986) Hydraulic conductivity of unsaturated soils: Prediction and formulas, p. 799-824. In: A. Klute (editor) Methods of Soil Analysis, Part 1: Physical and Mineralogical Methods, 2nd edition, American Society of Agronomy and Soil Science Society of American, Madison, Wisconsin, USA.

Neff, T. M. (1996) Mesoscale water balance of the boreal forest using operational evapotranspiration approaches in a distributed hydrologic model. Unpublished M.A.Sc. thesis, University of Waterloo.

Nijssen, B., and D. P. Lettenmaier (2001) BOREAS follow-on HMET-03 hourly meteorological data at flux towers, 1994-1996 Available on-line [http://www.daac.ornl.gov/] from Oak Ridge National Laboratory Distributed Active Archive Center, Oak Ridge, Tennessee, U.S.A.

Nijssen, B., R. Schnur, and D. P. Lettenmaier (2001) Global retrospective estimation of soil moisture using the variable infiltration capacity land surface model, 1980-93, Journal of Climate, 14(8):1790-1808.

Noilhan, J., P. Lacarrere, A. J. Dolman, and E. M. Blyth (1997) Defining area-average parameters in meteorological models for land surfaces with mesoscale heterogeneity, Journal of Hydrology, 190(3-4):302-316.

Noilhan, J. and S. Plankton (1989) A simple parameterization of land surface processes for meteorological models, Monthly Weather Review, 117:536-549.

Nuttle, W. K. (2002) Eco-hydrology past and future in focus, EOS, Transactions, American Geophysical Union, 83(17):205-212.

Oke, T.R. (1987) Boundary Layer Climates, Methuen, London, UK.

Pauwels, V. R. N., J. Gu, B. Nijssen, A. K. Betts, K. R. Snelgrove, E. A.Whidden, N. Kouwen, D. P. Lettenmaier, E. A. Smith, E. D. Soulis, and E. F.Wood A multiscale surface meteorological data set for BOREAS, Water Resources Research, submitted.

Philip, J. R. (1954) An infiltration equation with physical significance, Soil Science, 77(1):153-157.

Pitman, A. J., A. G. Slater, C. E. Desborough and M. Zhao (1999) Uncertainty in the simulation of runoff due to the parameterization of frozen soil moisture using the Global Soil Wetness Project methodology, Journal of Geophysical Research, 104(D14):16,879-16,888.

Polcher J., P. Cox, P. Dirmeyer, H. Dolman, *et al*. (2001) GLASS: Global Land-Atmosphere System Study, GEWEX News, 10(2):3-5. Available on-line at: [www.gewex.org/gewex_nwsltr.html].

Priestley, C. B. H. and R. J. Taylor (1972) On the assessment of surface heat flux and evaporation using large-scale parameters. Monthly Weather Review, 100(2):81-92.

Purcell, W. R. (1949) Capillary pressures - Their measurement using mercury and the calculation of permeability therefrom, Transactions of the American Institute of Mining and Metallurgical Engineers, 186:39-48.

Quinton, W. L., D. M. Gray, and P. Marsh (2000) Subsurface drainage from hummock-covered hillslopes in the Arctic tundra, Journal of Hydrology, 237(1-2):113-125.

Raddatz, R. L. (1998) Anthropogenic vegetation transformation and the potential for deep convection on the Canadian prairies, Canadian Journal of Soil Science, (78):657-666.

Ranson, K. J., G. Sun, R. Lang, N. S. Chauhan, R. J. Cacciola, and O. Kilic (1997) Mapping of boreal forest biomass from spaceborne synthetic aperture radar, Journal of Geophysical Research, 102:29599-29610.

Rawls, W. J., and D. L. Brakensiek (1982) Estimating soil water retention from soil properties, Journal of the Irrigation and Drainage Division, Proceedings of the American Society of Civil Engineers, 108(IR2): 166-171.

Rawls, W. J., D. Gimenez, and R. Grossman (1998) Use of soil texture, bulk density, and slope of the water retention curve to predict saturated hydraulic conductivity, Transactions of the American Society of Agricultural Engineers, 41(4):983-988.

Rawls, W. J., D. L. Brakensiek, and K. E. Saxton (1982) Estimation of soil water properties, Transactions of the American Society of Agricultural Engineers, 25(5):1316-1320, 1328.

Rawls, W. J., L. R. Ahuja, D. L. Brakensiek, and A. Shormohammadi (1993) Infiltration and soil water movement, Chapter 5, In: Maidment, D. R. (editor) Handbook of Hydrology, McGraw-Hill, New York.

Richards, L. A. (1931) Capillary conduction of liquids through porous mediums, Physics, 1:318-333.

Ritchie, H., R. Hogue, L. Lefaivre, E. Radeva, R. Moffet, J. Mailhot, S. Bélair and B. Bilodeau (1999) CMC model archives and activities in support of GEWEX. MAGS 5th Scientific Workshop, Edmonton, 21-23 November 1999.

Rosenzweig, C. (1998) Representing the land surface in climate models, Appendix 3: In: Hillel, D., Environment Soil Physics, Academic Press, San Diego, California, USA.

Sanford, W. E., J.-Y. Parlange, and T. S.Steenhuis (1993) Hillslope drainage with sudden drawdown: Closed form solution and laboratory experiments, Water Resources Research, 29(7):2313-2322.

Saulnier, G. M., K. Beven, and C. Obled (1997) Including spatially variable effective soil depths in TOPMODEL, Journal of Hydrology, 202(1-4):158-172.

Saxton, K. E., W. J. Rawls, J. S. Romberger, and R. I. Papendick (1986) Estimating generalized soil-water characteristics from texture, Soil Science Society of America Journal, 50(4):1031-1036.

Schaap M. G. and F. J. Leij (1998a) Database-related accuracy and uncertainty of pedotransfer functions, Soil Science, 163(10):765-779.

Schaap M. G., F. J. Leij, M. T. van Genuchten (1998a) Neural network analysis for hierarchical prediction of soil hydraulic properties, Soil Science Society of America Journal, 62(4):847-855.

Schaap, M. G., and W. Bouten (1996) Modeling water retention curves of sandy soils using neural networks, Water Resources Research, 32(10):3033-3040.

Seglenieks, F. (1998) MapMaker Users Guide: For MapMaker Version 2.2. University of Waterloo, Department of Civil Engineering, Computer program manual, 8 pages.

Sellers, P., F. Hall, H. Margolis, B. Kelly, D. Baldocchi, G. den Hartog, J. Cihlar, M. G. Ryan, B. Goodison, P. Crill, K. J. Ranson, D. Lettenmaier, and D. E. Wickland. (1995) The boreal ecosystem-atmosphere study (BOREAS): An overview and early results from the 1994 field year. Bulletin of the American Meteorological Society. 76(9):1549-1577.

Sellers, P. J. (1992) Biophysical models of land surface processes, Chapter 14, In: Trenberth, K. E. (editor) Climate System Modeling, Cambridge University Press, Cambridge, UK.

Sellers, P. J., R. E. Dickinson, D. A. Randall, A. K. Betts, F. G. Hall, J. A. Berry, G. J. Collatz, A. S. Denning, H. A. Mooney, C. A. Nobre, N. Sato, C. B Field, and A. Henderson-Sellers (1997) Modeling the exchange of energy, water and carbon between continents and the atmosphere, Science, 275:502-509.

Sellers, P. J., Y.Mintz, Y. C. Sud, and A. Dalcher (1986) A simple biosphere model (SiB) for use within general circulation models, Journal of Atmospheric Sciences, 43(6)505-531.

Shanley, J. B. and A. Chalmers (1999) The effect of frozen soil on snowmelt runoff at SleepersRiver, Vermount, Hydrological Processes, 13(10):1843-1857.

Shuttleworth, W. J. (1993) Evaporation, Chapter 4. In: Maidment, D. R. (editor) Handbook of Hydrology, McGraw-Hill, New York, NY.

Sloan, P. G., and I. D. Moore (1984) Modeling subsurface stormflow on steeply sloping forested watersheds, Water Resources Research, 20(12):1815-1822.

Slocum, T. A. (1999) Thematic Cartography and Visualization, Prentice Hall, Upper Saddle River, New Jersey, USA.

Snelgrove, K. R. (1996) Combining WATFLOOD and CLASS - Including River Hydrology in Land Surface Process Models, Unpublished M.A. Sc. project, University of Waterloo.

Soulis, E. D., K. R. Snelgrove, N. Kouwen, F. Seglenieks, and D. L. Verseghy (2000) Towards closing the vertical water balance in Canadian atmospheric models: Coupling of the land surface scheme CLASS with the distributed hydrological model WATFLOOD, Atmosphere-Ocean, 38(1):251-269.

Stahli, M., P. E. Jansson, and L. C. Lundin (1996) Preferential water flow in frozen soil – A two-domain model approach, Hydrological Processes, 10: 1305-1316.

Stagnitti, F. , M. B. Parlange, T. S. Steenhuis ,and J. Y. Parlange (1986) Drainage from a uniform soil layer on a hillslope. Water Resources Research, 22(5):631-634.

Steenhuis, T. S., J.-Y. Parlange, W. E. Sanford, A. Heilig, F. Stagnitti, and M. F. Walter (1999) Can we distinguish Richards' and Boussinesq's equations for hillslopes?: The Coweeta experiment revisited, Water Resources Research, 35(2):589-594.

Steenhuis, T. S., J. Y. Parlange, M. B. Parlange, and F. Stagnitti (1988) A simple model for flow on hillslopes, Agricultural Water Management 14:153-168.

Stewart, J. B. (1988) Modelling surface conductance of pine forest, Agricultural and Forest Meteorology, 43:19-35.

Strong, G. S., B. Proctor, M. Wang, E. D. Soulis, C. D. Smith, F. R. Seglenieks, and K. R. Snelgrove (2002) Closing the Mackenzie basin water budget, water years 1994-95 through 1996-97, Atmosphere-Ocean, 40(2):113-124.

Tao, T., and N. Kouwen (1989) Remote sensing and fully distributed modeling for flood forecasting, Journal of Water Resources Planning and Management, 115(6):809-823.

Todini, E. (1996) The ARNO rainfall-runoff model, Journal of Hydrology, 175(1-4):339-382.

van Genuchten, M. Th. (1980) A closed-form equation for predicting the hydraulic conductivity of unsaturated soils, Soil Science Society of America Journal, 44(5):892-898.

van Genuchten, M. T., F. J. Leij and S. R. Yates (1991) The RETC Code for Quantifying the Hydraulic Functions of Unsaturated Soils, Report IAG-DW12933934, U. S. Environmental Protection Agency, Ada, Oklahoma. Available on-line at: [http://www.epa.gov/ada/download/models/retc.pdf]

van Genuchten, M. Th., and D. R. Nielsen, (1986) On describing and predicting the hydrologic properties of unsaturated soils, Annales Geophysicae, 3(5):615-627.

Veihmeyer, F. J. and A. H. Hendrickson (1950) Soil moisture in relation to plant growth, Annual Review of Plant Physiology, 1:285-304.

Veihmeyer, F. J. and A. H. Hendrickson (1952) Does transpiration decrease as soil moisture decreases?, Transactions of the American Geophysical Union, 36:425-448.

Veldhuis, H (1995) Soils of Tower Sites and Super Site, Northern Study Area, Thompson, Manitoba, Canada. BOREAS Project Soils Report for NSA.

Veldhuis, Hugo (2000) BOREAS TE-20 Soils Data over the NSA-MSA and Tower Sites in Vector Format. Available on-line [http://www.daac.ornl.gov /] from Oak Ridge National Laboratory Distributed Active Archive Center, Oak Ridge, Tennessee, U.S.A.

Venugopal, V., E. Foufoula-Georgiou, and V. Sapozhnikov (1999) A space-time downscaling model for rainfall, Journal of Geophysical Research, 104(D16):19705-19721.

Verseghy, D. L. (1996) Local climates simulated by two generations of Canadian GCM land surface schemes, Atmosphere-Ocean, 34(3):435-456.

Verseghy, D. L. (1991) CLASS--A Canadian Land Surface Scheme for GCMS, Part I: Soil Model, International Journal of Climatology,11(2):111-133.

Verseghy, D. L., N. A. McFarlane, and M. Lazare (1993) CLASS--A Canadian Land Surface Scheme for GCMS, Part II: Vegetation model and coupled runs, International Journal of Climatology, 13:347-370.

Viterbo P., A. Beljaars, J.-F. Mahfouf and J. Teixeira (1999) The representation of soil moisture freezing and its impact on the stable boundary layer, Quarterly Journal of the Royal Meteorological Society, 125(559):2401-2426.

Walter, M. T., J.-S. Kim, T. S. Steenhuis, J.-Y. Parlange, A. Heilig, R. D. Braddock, J. S. Selker, and J. Boll (2000) Funneled flow mechanisms in a sloping layered soil: Laboratory investigation, Water Resources Research, 36(4):p 841-850.

Walsh, J. E., X. Zhou, D. Portis, and M. C. Serreze (1994) Atmospheric contribution to hydrologic variations in the arctic, Atmosphere-Ocean, 32(4):733-755.

Wang, X., and L. E. Band (1998) BOREAS HYD-08 DEM Data over the NSA-MSA and SSA-MSA in UTM Projection. Data set. Available on-line [http://www.daac.ornl.gov] from Oak Ridge National Laboratory Distributed Active Archive Center, Oak Ridge, Tennessee, U.S.A.

Wetzel A. and P. J. Boone (1995) Issues related to low resolution modeling of soil moisture: experience with the PLACE model, Global and Planetary Change, 13(1-4):161-181.

Whidden, E. A. (1999) Distributed hydrological modelling in the Canadian Boreal Forests : subsurface model development, land surface model improvement and modelling results, Unpublished M.A.Sc. thesis, University of Waterloo.

Wigmosta, M. S., L. W. Vail, and D. P. Lettenmaier (1994) A distributed hydrology-vegetation model for complex terrain, Water Resources Research, 30(6):1665-1680.

Wilby, R. L., and T. M. L. Wigley (2000) Precipitation predictors for downscaling: Observed and general circulation model relationships, International Journal of Climatology, 20(6):641-661.

Wise, S. (2000) Assessing the quality for hydrological applications of digital elevation models derived from contours, Hydrological Processes, 14(11-12):1909-1929.

Wood E. F. (1997) Effects of soil moisture aggregation on surface evaporative fluxes, Journal of Hydrology, 190(3-4):397-412.

Wood E. F., D. Lettenmaier, X. Liang, B. Nijssen, and S. W. Wetzel (1997) Hydrological modeling of continental-scale basins, Annual Reviews of Earth Planetary Science, 25:279-300.

Wood, E. F., D. P. Lettenmaier, and V. G. Zartarian (1992) A land-surface hydrology parameterization with surged variability for general circulation models, Journal of Geophysical Research, 97(D3):2717-2728.

World Meteorological Organization (1970) Guide to Hydrometeorological Practices, 2end edition, WMO-No. 168 Technical Paper 82, Secretariat of the World Meteorological Organization, Geneva, Switzerland.

Wyllie, M. R. J., and G. H. F. Gardner (1958) The generalized Kozeny-Carman equation: Part 2 - A novel approach to problems of fluid flow, World Oil, 146: 210-228.

Yarnal, B., M. N. Lakhtakia, Z. Yu, R. A. White, D. Pollard, D. A. Miller, and W. M. Lapenta (2000) A linked meteorological and hydrological model system: the Susquehanna River basin experiment (SRBEX), Global and Planetary Change, 25(1-2):149-161.

Zhao, R.-J. (1992) The Xinanjiang model applied in China, Journal of Hydrology, 135:371-381.

Zhao, R. J. and X.-R. Liu, 1995 The Xinanjiang model applied in China. In Singh, V. P. (editor) Computer Models of Watershed Hydrology. Water Resource Publications, Highlands Ranch, CO, pp.215-232.

Zhoa, L. and D. M. Gray (1999) Estimating snowmelt infiltration into frozen soils, Hydrological Processes, 13(10):1827-1842.

Zobler, L. (1986) A world soil file for global climate modeling, NASA Technical Memorandum #87802, National Aeronautics and Space Administration, Greenbelt, Maryland, USA.

Appendix

Soil Physics for Hydrologic Modelling

Soil Physics for Hydrologic Modelling

The estimation of soil drainage properties in a land surface model has a key role in the determination of soil moisture evolution . Slow draining soils give rise to prolonged wet surface conditions and hence increase both future evaporation and runoff prediction. Modelling the vertical soil moisture profile and its evolution is often accomplished using Richard's equation (Richards, 1931) developed from a combination of the continuity equation and Darcey's Law for unsaturated flow:

$$\frac{\partial \chi}{\partial t} = \frac{\partial}{\partial z}\left[K(\chi)\frac{\partial \psi(\chi)}{\partial z} \right] - \frac{\partial K(\chi)}{\partial z} \qquad (1)$$

where the partial rate of change of soil moisture (χ) with respect to time (t) is dependent on a highly non-linear partial derivatives containing both conductivity (K) and soil tension (ψ) terms each of which are functions of the dependent soil moisture variable. Solution of this equation for CLASS is determined through a finite difference representation. The representation of soil conductivity and tension as functions of soil moisture make Richard's equation difficult to solve and this has received much attention in the unsaturated flow literature. The discussion that follows illustrates popularized tension/conductivity verses soil moisture relations used in land surface models.

Moisture Characteristic

The relationship between soil moisture and tension is known as the moisture-characteristic (Dingman, 2002). This curve may be measured directly from field data or estimated indirectly using quasi-empirical models. Numerous attempts have been made to developed moisture-characteristic models using more easily measured soil properties such as texture because of the difficulty in direct measurement of this quantity. Categories of these functions include results from regression analysis and those which fit continuous or piece-wise functions describing the moisture-characteristic based on estimated parameters. More recently neural network approaches have been applied which eliminate the need for function definition.

A typical moisture characteristic is shown in figure 4-5. The ordinate axis is show, as is the convention, on a log scale plotted against volumetric soil moisture content. This plot contains three major sections: 1) a steeply sloping section at low moisture contents where high values of tension hold water tightly within the soil matrix, 2) a gradually sloping section near field capacity and 3) a final steeply sloping section representing the sudden decrease in soil suction to zero found in near saturated soils. Important points along this curve include the air-entry tension beyond which significant air begins to bubble into the soil matrix , field capacity representing the point where considerable decrease in soil drainage rate s occur, and the wilting point which defines a generally accepted suction value above which plants can no longer extract soil water.

Discrete Regression Methods

Rawls et al. (1993) reports on a method from Rawls and Brakensiek (1982) for determining 12 key points along the moisture characteristic curve based on regression analysis. Three levels of information input give progressively higher correlation coefficients from the base data set which consists of 2541 soil horizons from 18 states in the United States. The first method includes particle size distribution, bulk density and organic matter data, the second method adds the wilting point tension head (1500 kPa) and the third method adds the field capacity tension head (33 kPa). Correlation coefficients (R) for the third method are highest and range from 0.99 0.77 with the lower correlations occurring for wetter values of tension head. This analysis is revised slightly and extended in Rawls et al. (1982) to include estimates of saturated hydraulic conductivity, however, it is cautioned that values may be over predicted by three or four times.

Method 3 Field Capacity and Wilting Point Tension

Tension ***kPa***	***Intercept***	***Organic Matter*** ***%Vol***	***Bulk Density*** ***g/cm³***	***Field Capacity*** ***%Vol***	***Wilting Point*** ***%Vol***	***Correlation*** ***r***
1500					1	1
1000				0.11	0.89	0.99
700				0.16	0.86	0.99
400				0.24	0.79	0.99
200				0.36	0.69	0.99
100				0.52	0.54	0.99
60	0.01		0.01	0.66	0.39	0.99
33				1		1
20	0.03			1.01	0.06	0.99
10	0.06	0.01		1.34	0.51	0.95
7	0.09	0.01		1.53	0.81	0.91
4	0.18	0.02	0.04	1.89	1.38	0.77

The table above represents the method for which the highest level of data input is required. Data requirements include volumetric soil moisture content at field capacity (33 kPa) and wilting point (1500 kPa) as well as volume organic matter content and the bulk density which have a small impact for some values of the moisture characteristic. While this method requires no sand, silt and clay contents, the methods 2 and 1 (not shown) have increasing requirements on soil texture. Ahuja et al. (1985) evaluated these methods and determined that the method 3 (33 and 1500 kPa potentials) was superior to the methods 1 and 2 for a watershed study in Oklahoma containing primarily silt loam soils.

Piecewise and Incomplete Functions

Saxton et al (1986) extends the 'texture only' method (method 1) of Rawls and Brakensiek (1982) by fitting three piecewise functions through the ordinal data and also providing hydraulic conductivity estimates as a function of soil type. A cautionary note, however, is expresses that for sand and clay contents less than 5% and clay contents greater than 60% that both the Rawls and Brakensiek (1982) and Sexton et al (1986) relations may give unreasonable results. The first piecewise segment of the model extents between wilting point tension (1500 kPa) and (1 cm H_2O = 0.09806 kPa) 10 kPa and is expressed as a power law similar to that used by Clapp and Hornberger (1978) (see below) with the multiplier and exponent parameters given as a nonPlinear function of sand and clay content. A second segment is fit to tension values between 10 kPa and the air entry tension ($\ldots_e$) using a linear relation of soil moisture alone. Estimation of the $\ldots_e$ term and its associated moisture content at saturation (χ_{sat}) is determined using a regression equation involving the sand and clay content. The final segment of the piecewise function extends from tension values of $\ldots_e$ to zero along a vertical line of constant soil moisture set to χ_{sat}, the saturated value. In addition to piecewise tension functions, Saxton et al. (1986) also produced nonPlinear functions of hydrologic conductivity with soil moisture by including sand and clay content values. Motivating the development of these functions was the assertion that the power function form used Clapp and Hornberger (1978) and Brooks and Corey (1964), did adequately fit with hydraulic conductivity curves reported by Rawls et al. (1982). Relevant formula from Saxton et al. (1986) are as follows:

Segment 1

$$\psi = A\,\theta^{B} \qquad \textit{for:} \qquad 1500 < \psi \leq 10$$

$$A = \exp[-4.396 - 0.0715(\%C) - 4.88\times10^{-4}(\%S)^2 - 4.285\times10^{-5}(\%S)^2(\%C)]\,100$$

$$B = -3.14 - 0.00222(\%C)^2 - 3.484\times10^{-5}(\%S)^2(\%C)$$

Segment 2

$$\psi = 10 - \frac{(\theta - \theta_{10})(10 - \psi_e)}{(\theta_s - \theta_{10})} \qquad \textit{for:} \qquad 10 < \psi \leq \psi_e \tag{2}$$

$$\theta_{10} = \exp\left[\frac{2.302 - \ln(A)}{B}\right] \quad ; \quad \psi_e = -10.8 + 34.1(\theta_s)$$

$$\theta_s = 0.332 - 7.251\times10^{-4}(\%S) + 0.1276\log_{10}(\%C)$$

Segment 3

$$\theta = \theta_s \qquad \textit{for:} \qquad \psi_e < \psi \leq 0$$

Prior to the work of Saxton et al. (1986), others had attempted to fit functions to the moisture characteristic and hydraulic conductivity curves. These include the well known methods of Brooks and Corey (1964) and Clapp and Hornberger (1978). These functions are given in power law form as:

$$\psi = \psi_{sat}(S)^{b} \qquad K = K_{sat}(S)^{c} \tag{3}$$

where S is a measure of effective saturation, the parameters 'b' and 'c' are related to pore space properties of the soil, and both ψ_{sat} and K_{sat} are the tension and hydraulic conductivity at some measure of soil saturation. Brooks and Corey provides physical interpretation of ψ_{sat} as the air entry suction (ψ_e) or the value of suction found at the top of the capillary fringe in saturated soils. In doing so, Brooks and Corey introduce a residual moisture content parameter (θ_r) in the S term as follows:

$$S = \frac{\theta - \theta_r}{\phi - \theta_r} \tag{4}$$

This introduces a sharp discontinuity in the function at θ_r and requires the estimation of this additional parameter. Campbell (1974) introduced a simplified formulation of Brooks and Corey which neglects the θ_r term. This simplification emphasized, however, that departures from measured tension values in the wet range (> Ƥ10 kPa) could be expended. Campbell

(1974) also introduced a relation between the exponent 'b' in the moisture characteristic and 'c' in the unsaturated hydraulic conductivity formula as c = 2b + 3 from theoretical considerations of soil pore volume distributions. However, it was added that a value of 3.5 rather than 3 in the 'c' to 'b' relation would have been more appropriate fitting parameter for their sand sample result.

The work of Campbell (1974) lead to the formulation of Clapp and Hornberger (1978) which directly uses the Campbell power law form for moisture characteristic and hydrologic conductivity. While Campbell provided analysis for only 4 soil samples, Clapp and Hornberger (1978) estimated model parameters 'b', χ_{sat} , K_{sat} and $\ldots_{sat}$ in terms of soil texture type by statistical analysis of 1446 soils. Cuenca et al. (1996) points out that this large sample base, over a wide variety of soil types, has lead to its wide spread use in atmospheric modelling including the well known SiB (Sellers et al., 1986) and BATS (Dickinson et al., 1993) land surface schemes.

In addition to the development of the parameter values, Clapp and Hornberger (1978) also devised a method for extending the model beyond that envisioned by Campbell (1974) and into wet range (< 10 kPa). This was accomplished by fitting a parabola at a point on the wet end of the moisture characteristic curve which would allow gradual air entry. This piecewise parabola segment begins at an inflection point defined as (S_i , $\ldots_i$), the 'i' designating inflection. Suggested values for the division between the power law and parabola segments lie between saturation degrees of 0.8 and 1, however, to be consistent with the power law parameters a value of $S_i = 0.92$ is suggested. The parabola describes the moisture characteristic in the range between $S=S_i$ and S=1 as follows:

$$\ldots = -m(S-n)(S-1)$$

$$m = \frac{\ldots_i}{(1-S_i)^2} - \frac{\ldots_i b}{S_i(1-S_i)} \quad ; \quad n = 2S_i - \left(\frac{\ldots_i b}{mS_i}\right) - 1 \tag{5}$$

The value of $S_i = 0.92$ is chosen to maintain the change in slope at the inflection point which requires that 'n' remain positive. This only occur if $S_i > b/(b+1)$. For the Clapp and Hornberger parameter selection, the highest value for 'b' is for clay soil with b = 11.4 giving $S_i = 11.4/(11.4 + 1) = 0.919$ which is less than 0.92 suggested for S_i. This suggests that the value chosen for S_i could vary especially for soils with values of 'b' greater than 11.4 clay value.

Clapp and Hornberger (1978) suggests values of the parameters 'b', χ_{sat} ,K_{sat} and $\ldots_{sat}$ in terms of the mid-point fractions of sand, silt and clay for each texture designation from the U.S. Department of Agriculture (USDA) texture triangle. A mid-point value was chosen since the original database used to develop the parameters gave a texture class but lacked a grain size distribution to determine the sand, silt, and clay fractions. Extending the functionality of Clapp and Hornberger (1978) parameters, Cosby et al. (1984) introduced continuous parameter estimation functions with sand, silt and clay fractions as independent variables.

Particle size fractions were chosen simply as the midPpoint values textures of the triangle classes for their 1448 soil samples. Even with the error this estimate of size fraction introduced, Cosby et al. (1984) was able to show through a series of statistical tests that the mean value of the soil parameters as well as their variances could be estimated using soil texture alone. Two formulations are given are given by Cosby et al. (1984). The first uses two components of the particle size distribution with the third deemed to be included since the sum of the three components sand, silt and clay was assumed to be unity. The second formulation is in terms of a single dominant component of sand or clay. The functional form is a simple linear model as follows:

$$Parameter = Intercept + \sum_{n=1}^{1 \text{ or } 2} (Variable * Slope)_n \qquad (6)$$

The following table gives the mean values (variances not shown) of the parameters for each of the two models

	TwoPComponent Model			***OnePComponent Model***		
Parameter	***Intercept***	***Variable***	***Slope***	***Intercept***	***Variable***	***Slope***
b	3.10	%clay	0.157	2.91	%clay	0.159
		%sand	P0.003			
log ψ_{sat}	1.54	%sand	P0.0095	1.88	%sand	P0.0131
		%silt	0.0063			
log K_{sat}	P0.60	%sand	0.0126	P0.884	%sand	0.0153
		%clay	P0.0064			
θ_{sat}	50.5	%sand	P0.142	48.9	%sand	P0.126
		%clay	P0.037			

Continuous Functions

Use of the power function form of the moisture characteristic and hydraulic conductivity relations inevitably leads to the criticism of its failure to provide realistic results for the wet conditions beyond P10 kPa tension. As described above, both Saxton et al. (1986) and Clapp and Hornberger (1978) have provided piecewise solutions to the problem by using the power law function in the dry range of soil moisture and other functions in the wet range (two linear function for Saxton and a single parabola for Clapp and Hornberger). To overcome the restrictions imposed by piecewise methods van Genuchten (1980) suggested the use of a function whose values and first derivatives where smooth and continuous. This function takes the following form:

$$S = \left[\frac{1}{1 + (\zeta \ldots)^n} \right]^m \tag{7}$$

where S is the effective saturation which in the equation 4 above, ζ, n and m are parameters with the restriction that m=1−1/n. This function matches the behavior of the moisture characteristic well with the number of parameters equal to the Brooks and Corey model. There is, however, an added degree of complexity in estimating parameter from the van Genuchten model since it cannot be simply linearized as with the power function by taking logs.

In a follow-on paper van Genuchten and Nielsen (1986) review a number of previous attempts to produce continuous functions of the moisture-characteristic. They conclude that their formulation combine both ease of use and goodness of fit which could not be advocated by the other methods. Cuenca et al. (1996) points out that the van Genuchten (1980) formulation has received considerable attention in the soil science community but is virtually unused when compared to Clapp and Hornberger (1978) methods used in land surface modelling.

Systematic deviation from van Genuchten's model have been observed which relate to multimodal size distributions in soils. The mathematical formulation of the van Genuchten model assumes of unimodal distribution of pore radii with its centoid described by the ζ parameter and its range by the n and m parameters. Durner (1994) gives examples of a number of situations where this model is not applicable including soil aggregation processes which lead to decreasing midrange pore structures and biological activity which enhance the distribution of large radii pores. For these situations Durner proposes the use of a subsystem approach where a number of moisture characteristic curves are used in a weighting scheme as follows:

$$S = \sum_{i=1}^{k} w_i \left[\frac{1}{1 + (\zeta_o \ldots)^{n_i}} \right]^{m_i} \tag{8}$$

where w_i is the weighting for each portion of the multimodal van Genuchen model. While this model maintains the continuity and differentiability of the original van Genuchen model the added number of parameters increases linearly with addition k subsystems. Its hydrologic benefit, however, may be realized in its ability to describe macropore phenomena which dominate hydrologic conductivity with only a small percentage of the total number of pores. Durner (1994) also states that the form of the model is of little consequence as long as it adequately describes the moisture-characteristic.

Neural Networks Approach

Schaap et al. (1998a, 1998b, and 1996) describe a method of estimating the moisture characteristic using a neural networks approach. Basic to this approach is the estimation of a set of weighting parameters used in a two stage logical series that transforms input data to the desired output manipulating the function:

$$H = \frac{1}{1+e^{-S}} \tag{9}$$

where H is the output from an node within a stage and S is the sum of the nodal weightings of the stage inputs. The inputs for the soil model include texture, and optionally bulk density, field capacity and wilting point soil moistures. Outputs are the parameter values the van Genuchten (1980) model plus the saturated hydraulic conductivity. The variables within the neural network are the weighting functions that link the two predictive stages. These weightings are estimated through an optimization routine that attempts to minimize the root mean square error between the model output and a set of measured values. The term 'training' is often applied to this process. An advantage of neural network parameter estimation is improved fitting to measured parameters since there is no restriction on a functional relation such as those required for linear, logarithmic or exponential regression.

The United States Salinity Laboratory, a branch of the United States Department of Agriculture has made has made the Schaap model freely available to the public under the name Rosetta. This program contains the weighting functions developed from a large cross section of field soils data and allows the user to estimate van Genuchten parameters from five neutral network models with each requiring progressively greater amounts of input data.

Hydraulic Conductivity

The hydraulic conductivity of unsaturated soil varies non-linearly with soil moisture. It maybe measured in laboratory conditions by applying a constant head gradient across a soil sample that is maintained at a pressure lower then atmospheric. The pressure differential across the sample causes moisture flow while the net pressure reduction maintains a constant moisture content. Laboratory measurement of the conductivity - soil moisture relationship is an expensive and time consuming process and has inspired the development of analytic methods for its determination.

While the models developed to describe the moisture -characteristic are for the most part empirical, unsaturated conductivity models are most often based on a physical representation of the soil-air-water system. Fundamental theory of these physical models is based on laminar flow in small diameter tubes. Description of the distribution and properties of these conduits is accomplished using the moisture-characteristic making its accurate determination essential in conductivity models. Another class of hydraulic conductivity model is based on pseudo-transfer functions using empirical relationships between soil texture and other easily measured soil properties. As with moisture-characteristic models these are most often developed from large measured data sets.

In general, hydraulic conductivity of unsaturated soil declines very rapidly with reduced soil moisture. As soil moisture is reduced below saturation, progressively smaller and smaller pores are drained with every increasing difficulty because of larger capillary forces generated between water and soil. Figure 4-5 shows typical hydraulic conductivity relationships with soil moisture.

Theoretical Models

Mualem(1986) and Brutsaert (1967) provide historical accounts of the development of these analytic methods of hydraulic conductivity of unsaturated soils all of which are based on laminar flow pipe theory. Three classifications are presents based on the assumptions regarding the distribution and arrangement of conduits. Each of these methods determines the relative conductivity of soil, K_r and must be scaled by a multiplier to product the actual conductivity K. This multiplier, often referred to as the 'matching factor', appears to have no relation to physical properties of the soil (Gardner, 1974) and as such is most often determined experimentally. Values of the matching factor are often chosen at of near saturation to allow more accurate prediction at high flow values and thus lower overall volume error.

Uniform Pore Size Models

The first classification of unsaturated conductivity theory is a simple uniform pore size model in which the porous media is given an effective pore size based on the properties of the soil particles for the determination of an average velocity,V. This pore velocity is governed by Poiseuille's equation of laminar flow as:

$$V = -\frac{R^2}{2\mu}\frac{dh}{dx} \tag{10}$$

where R is the hydraulic radius of the pore defined as the ratio flow area to its wetted perimeter,(A/P) which for a circular tube of radius, r is ($\phi r^2/2\phi r$)=r/2, and σ is the fluid viscosity. The gradient term, dh/dx is the driving pressure head along the axis of flow. Pore space geometry dictates the value of the numerical constant. While 2 is given above for a circular tube, it may also take on values of up to 3 for flow between flat plates (Eagleson, 1970, p276). Since soil pore structures are neither pipes nor plates, this value is often left as a parameter (Carmen, 1956, p12).

Irmay (1954) presents a theoretical derivation of a uniform pore size model with relative conductivity in terms of a power law relation. First, Dupuit's assumption is invoked which relates the effective discharge or flux, q to the actual pore velocities, V as $q=\lambda V$. This assumption implies that the fractional pore volume ($V_{pore}/V_{total} = \lambda$) will equal the fractional pore area (A_{pore}/A_{total}) normal to the direction of flow and has been found to be valid for random particle distributions but not valid for regularly packed particles (Carmen, 1956, p8). Second, Kozeny's assumption, that the hydraulic radius, R can be related to soil properties, is used. Since, from Dupuit's assumption, flow area ratio is equal to the porosity, hydraulic radius $R = \lambda / O$ where O is specific surface, thus equivalent to the wetted perimeter, and defined as the surface area of the particles in a unit volume of porous media. Considering only the solid volume of the soil particles, the 'particle' specific surface, defined as $O_o = O / (1-\lambda)$, can be combined with the hydraulic radius to give:

$$R = \frac{\phi}{(1-\phi)O_o}$$

where for a sphere of radius r and diameter d (11)

$$O_o = \frac{A}{V} = \frac{4\pi r^2}{4/3\pi r^3} = \frac{6}{d}$$

In addition to the use of the concept of hydraulic radius, Kozeny also introduced the concept of a tortuous flow path through the capillary tube system. This tortuosity is expressed as a ratio of increasing flow path as (L_e/L) where L is the length of the sample and L_e is the effective travel distance. Carman (1956) refined the relation by stating that the the factor should be applied to both the determination of pore velocity due to the decreased pressure

gradient in Poiseuille's equation and the overall flux due to the increase in travel distance in Dupuit's equation and so became known as the KozenyPCarmen equation:

$$q=\left(\frac{L}{L_e}\right)\phi V \qquad V=-\frac{R^2}{2\mu}\frac{dh}{dx}\left(\frac{L}{L_e}\right) \tag{12}$$

Irmay(1954) included the effect of the irreducible water content (1PS$_r$) as that portion of the pore area which does not contribute to the flow and rewrote both the Dupuit and Kozeny equations for a saturated flow condition as:

$$R=\frac{d_e\phi(1-S_r)}{6(1-\phi)} \qquad q=\left(\frac{L}{L_e}\right)^2\phi(1-S_r)V \tag{13}$$

Combining Poiseuille's law, with the equations above yields the flow through a saturated porous media assuming an equivalent pore space diameter, d_e of circular cross section as:

$$q=\left(\frac{L}{L_e}\right)^2\phi(1-S_r)\left[\frac{1}{2\mu}\left(\frac{d_e\phi(1-S_r)}{6(1-\phi)}\right)^2\frac{dh}{dx}\right]$$

by grouping tortuously and shape terms, this simplifies to

$$q=\frac{C}{\mu}d_e{}^2\frac{\phi^3}{(1-\phi)^2}(1-S_r)^3\frac{dh}{dx} \tag{14}$$

which is analogous to Darcy's law with K given as:

$$K_{sat}=\frac{C\,d_e{}^2\phi^3}{(1-\phi)^2}(1-S_r)^3$$

Irmay (1954) proposed that the constant C should be of the order 0.01 and then generalized the influence of the saturated flow analogy to the unsaturated flow case and wrote:

$$K=\frac{C\,d_e{}^2\phi^3}{(1-\phi)^2}(S-S_r)^3 \tag{15}$$

without considering the effect of soil moisture on specific surface and tortuosity calculations nor that the factors λ(1PSr) and λ(SPSr) could represent drainable porousity in the Dupuit and Kozeny equations (Brutsaert, 1967). None the less, the development of equations leads to an expression of the uniform pore sized model which makes use of a power law formulation as:

$$K_r = \frac{K}{K_{sat}} = \left[\frac{S - S_r}{1 - S_r} \right]^3 = S_e^{\,3} \qquad (16)$$

and illustrates one approach which uses fundamental relationships to derive expressions for conductivity. Other researchers have utilized the power function relation with Se using exponent values ranging from 2 to 5 (Brutsaert, 1967). Brooks and Corey (1966) state that the power function form with an exponent of 4 maybe used as a 'convenient approximation' of porous consolidated rock samples.

Parallel Tube Model

Recognizing the inherent flaws in the uniform pore size model, a second class of solutions was developed in which flow through a number of discrete size pore structures was employed. Gardner (1974) states that the first to employ this method was Childs and CollisPGeorge (1950). The basic flaw with the uniform pore size model was that it fit well for sandy soils only. Childs and CollisPGeorge (1950) where able to show that the model was not theoretically sound since summing the contributions of conductivity related to particle diameter squared was not equal to average diameter squared (ie. $(\overline{d})^2 \neq \overline{d^2}$) . The summation of contributing conductivity was known to be sound since large pores (ie. pores associated with large particles) are drained prior to smaller ones in porous media. As a result of this nonPlinearity, the CarmonPKozney model was able to perform well for closely graded materials where $(\overline{d})^2 \simeq \overline{d^2}$ but prevented from adequately representing well graded materials (Carmen, 1956, p35).

Perhaps the simplest parallel tube model is the 'Burdine' equation used by Brooks and Corey (1964). This equation stems from the petroleum industry after the work of Burdine (1953) and Wyllie and Gardner (1958). The derivation proceeds in a similar manner as in the uniform pore size model. However, rather than calculating an effective hydraulic radius based of the average particle size, one is calculated by summing over all the tube sizes. Original development provided a summation over discrete particle size ranges (Burdine, 1953 ; Childs and CollisPGeorge (1950)), however, it has become more convenient to express it as a continuous integral. Following the derivation by Fatt and Dykstra (1951), if we consider a bundle of N capillary tubes filled with water, then the total flow, Q= qA_T from the tube system will equal the sum of the individual tube flows, VA, where A is the cross sectional area of the individual tubes and A_T is the total cross sectional area of the sample:

$$qA_T = \sum_{i=1}^{i=N} V_i A_i \qquad \text{differentiating w.r.t. } N \quad \text{gives} \quad A_T \frac{dq}{dN} = VA \qquad (17)$$

use of Poiseuille's Law, defined in equation 10, gives an expression for the flux per small tube increment tube number as:

$$dq = -\frac{R^2}{2\mu}\frac{dh}{dl}\frac{\mathbf{A}}{\mathbf{A}_T}dN \tag{18}$$

where dN is the number of tubes of hydraulic radius R and length *l*. Darcy's Law can be written in a similar form as:

$$q = -K\frac{dh}{dL} \quad \text{which leads to} \quad dq = -\frac{dh}{dL}dK \tag{19}$$

where *L* is the length of the sample which differs from the length of the individual tubes, *l*. Equating these two equations by the common quantity, dq gives:

$$-\frac{dh}{dL}dK = -\frac{R^2}{2\mu}\frac{dh}{dl}\frac{\mathbf{A}}{\mathbf{A}_T}dN \tag{20}$$

Considering a fixed length of the tube system, we can define the gradients as ÷h/L and ÷h/l for the entire sample and the tubes, respectively and rewrite the equation 20 as:

$$dK = \frac{L}{l}\frac{\mathbf{A}}{\mathbf{A}_T}\frac{R^2}{2\mu}dN \tag{21}$$

The volume of water in the tube system can also be used to define a relation between the number of tubes containing water and degree of saturation. The volume of the water filled tubes can be expressed as:

$$dV = \mathbf{A}\, l\, dN \tag{22}$$

In addition, the water volume of the total sample can be determined from the degree of saturation of the sample ($S = V/V_{sat}$) where $V_{sat} = \lambda \mathbf{A}_T L$ as:

$$V = S\,\phi\,\mathbf{A}_T L \quad \text{which when differentiated gives} \quad dV = \phi\,\mathbf{A}_T L\, dS \tag{23}$$

Equating these two volume expressions and solving for dN gives:

$$dN = \phi\frac{\mathbf{A}_T}{\mathbf{A}}\frac{L}{l}dS \tag{24}$$

This expression can now be used together with the equation derived from the flow equation (equation 21) to give a new conductivity expression:

$$dK = \frac{\phi}{2\mu}\left[\frac{L}{l}\right]^2 R^2\, dS \qquad \text{or} \qquad K = \int_0^S \frac{\phi}{2\mu}\left[\frac{L}{l}\right]^2 R^2\, dS \tag{25}$$

HoffmanPRiem et al. (1999) have show that popular of the parallel tube models such as Purcell (1949), Fatt and Dykstra (1951), Burdine (1953), Wyllie and Gardner (1958) and Mualem (1976) can all be expressed in this general form. Differences between the various schemes lie in the assumptions regarding the tortuousity effect. The numeric constant 2 used above represents circular tubes and may range to a value of 3 for flow between flat plates. The value of 2.5 is often chosen after Brooks and Corey (1964). Note, that in the derivation given above, the concept of hydraulic radius, R for the tube bundle therefore assumes no particular shape, although circular tubes are most often selected.

Purcell (1949) derives his equation by referring to the tortousity effect as a constant "lithology factor" at values of saturation only as follows:

$$K_{sat} = \frac{\phi}{2\mu}\left[\frac{L}{l}\right]^2 \int_{S=0}^{S=1} R^2\, dS \qquad \text{(Purcell)} \tag{26}$$

and using the symbol F for $(L/l)^2$ stated the value could be shown theoretically to be $(2/\phi)^2$ = 0.4 for closePpacked spheres but varied from 0.1 to 0.4 for porous rock samples used during their mercury injection experiments. Results obtained indicated that samples with higher values of air permeability were associated with higher F values and approached the 0.4 maximum value given for closePpacked spheres.

Fatt and Dykstra (1951) followed closely the derivation of Purcell (1949) and extended its use into the unsaturated flow conditions. They assumed that tortuousity varied as a function of saturation and used a power law relation of the form $(L/l)^2 = aR^b$ to produce a solution of the following form:

$$K(S) = \frac{\phi a^2}{2\mu} \int_{S=0}^{S=S} R^{2+2b}\, dS \tag{27}$$

In an attempt to reduce the number of parameters requiring estimation Fatt and Dykstra (1951) normalized the equation above by the saturated conductivity. This assumes, of coarse, that the parameter "a" is more difficult to determine than K_{sat}. This normalized relative permeability is given as $K_r = K(S)/K_{sat}$ and when applied allows the constant terms in the unsaturated case to drop out yielding:

$$K_r(S) = \int_{S=0}^{S=S} R^{2+2b}\, dS \left[\int_{S=0}^{S=1} R^{2+2b}\, dS \right]^{-1}$$ Fatt and Dykstra (28)

A value of b=1/2 was suggested, however, tests on consolidated core samples indicated that the b value was not constant and varied somewhat from sample to sample. The more interesting feature of this derivation, however, is the fact that the tortuousity expression remains inside the integral and is assumed to be dependent on the degree of saturation with the system becoming more tortuous as saturation ratios decrease. While many other derivation similarly assume that tortuousity and saturation are inversely related, they are most often accomplished with less rigor then the Fatt and Dykstra derivation.

Burdine (1953) determined experimentally that tortuousity was linearly related to the degree of saturation as $S_e = L/l$ where S_e is the effective saturation reduced by the residual or irreducible moisture content. The Burdine equation in the general literature has been expressed in an integral form and differs somewhat from the original equation derived as a summation of discrete interval radii (Burdine et al., 1950). In keeping with the literature convention of the integral form of the Burdine equation is presented as:

$$K_r(S) = \frac{K(S)}{K_{sat}} = S_e^{\,2} \int_{S=0}^{S=S} R^2\, dS \left[\int_{S=0}^{S=1} R^2\, dS \right]^{-1}$$ Burdine (29)

This derivation shows that the L/l tortuousity term has been removed from its dependence on saturation in the integration. This according to the review of I. Fatt (Burdine, 1953, p. 77) renders the permeability relation as "strictly an empirical one". None the less, the Burdine formula has gained widespread use and is the foundation of the well known Brooks and Corey (1964) soil model.

In an attempt to provide a theoretical justification for the Burdine (1953) equation, Wyllie and Gardner (1958) used an approach which Burtsaert (1967) terms the "cutting and rejoining" method to derive a model from fundamental principles. The conceptual mechanism involves cutting tube bundles and then randomly rejoining them so that the newly aligned pores create intersections with both smaller and larger tubes. Those that align with smaller tubes pass the effective control of flow to the smaller tube and those that align with larger tubes retain their control. The end result is that outflow of the entire tube system is decreased which is exactly the same result as that of the tortuousity concept. Cutting and rejoining decreases the effective dynamic flow area from (λS) to $(\lambda S)^2$ while leaving the static volumetric system unchanged and following their derivation leads directly to the Burdine equation.

This concept of cutting and rejoining is an important one and underlies both the original parallel tube model of Childs and CollisPGeorge (1950) and a widely used model of today, that of Mualem (1976). Rather than considering that flow is controlled by the effective area of rejoined tubes as in Wyllie and Gardner (1958), Mualem (1976) considers that the hydraulic radius of the newly joined series is described by the mean of the two aligned radii as $R^2 = r_1 r_2$ and that these these pore spaces are completely independent giving:

$$K_r(S) = S_e^{\,n} \left[\int_{S=0}^{S=S} R \, dS \right]^2 \left[\int_{S=0}^{S=1} R \, dS \right]^{-2} \qquad \text{(Mualem) (30)}$$

Mualem (1976) used the assumption of Burdine (1953) that the tortuousity was related to the degree of saturation and added as well that the partial correlation of connectedness between the pores was embodied in the degree of saturation as well. While the Burdine equation uses a power n=2 in its derivation, Mualem (1976) pointed out that the "n" parameter could take on any value either positive or negative and as such should be determined experimentally. By analyzing 45 soil samples reported in the literature, Mualem concluded that a value of n=1/2 gave the best fit to the data. A comparison was made with the Burdine model, a KozenyPCarmen uniform pore size model by Averjanov and a modified Childs and CollisPGeorge model proposed by Millington and Quick. The Mualem model obtained the best results in the intercomparison, however, HoffmannPRiem et al. (1999) point out that the value of "n" had been calibrated for the Maulem model but that a similar luxury had been afforded to the other models.

HoffmannPRiem et al. (1999) suggest that a generalized model which encompasses the all of the models describe above can can written as:

$$K(S) = K_{sat} S_e^{\,a} \left[\int_{S=0}^{S=S_e} R^b \, dS \right]^c \qquad (31)$$

The table below shows the corresponding values of a, b, c for the various models discussed previously.

Model	***a***	***b***	***c***
Irmay(1954)	3	P	0
Purcell (1949)	0	2	1
Fatt and Dykstra (1951)	0	3	1
Burdine (1953)	2	2	1
Mualem (1976)	0.5	1	2

HoffmannPRiem et al. (1999) suggest that a nonPphysically based version of the general model can be used which provides an improved fit to the data by allowing one or more of the parameters a, b, c and K_{sat} to vary in an optimization scheme. Their results show that the K_{sat} parameter is by far the most important parameter to optimize since no acceptable fit was achieved using the measured value of K_{sat} obtained for the sand sample tested from the UNSODA data base. RMS errors where analyzed for both the Mualem and Burdine models and an improvement of ~50% was observed when K_{sat} was optimized and another ~50% when both K_{sat} and "a" were optimized. Errors remaining following these optimizations where primarily at the wet end of the saturation curve for values of S_e>~0.95. This final bias was removed by optimizing the value of K_{sat}, a and c in the generalized equation and maintaining b=1. While this optimization improved the RSME score only slightly from 0.3 to 0.24 there was a marked improvement in the result at the wet end for Se values greater than 0.95.